

**STUDIES OF THE ATMOSPHERIC CHEMISTRY OF
VOLATILE ORGANIC COMPOUNDS
AND OF THEIR ATMOSPHERIC REACTION PRODUCTS**

Final Report to the California Air Resources Board
Contract No. 99-330
for the period June 30, 2000 – October 31, 2003

Roger Atkinson and Janet Arey

Air Pollution Research Center
University of California
Riverside, CA 92521

January 2004

DISCLAIMER

The statements and conclusions in this Report are those of the contractor and not necessarily those of the California Air Resources Board. The mention of commercial products, their sources, or their use in connection with material reported herein is not to be construed as actual or implied endorsement of such products.

ACKNOWLEDGEMENTS

We thank the following for their contributions to the research described in this report:

Ms. Sara M. Aschmann
Dr. Heidi L. Bethel
Mr. William P. Harger
Mr. William D. Long
Dr. Pilar Martin
Ms. Marie V. Nguyen
Dr. Fabienne Reisen
Ms. Stephanie Wheeler
Dr. Ernesto C. Tuazon

and thank Drs. Eileen McCauley and William Vance (CARB) for their assistance and advice during this contract.

This Report was submitted in fulfillment of Contract No. 99-330, "Studies of the Atmospheric Chemistry of Volatile Organic Compounds and of their Atmospheric Reaction Products" under the sponsorship of the California Air Resources Board. Work was completed as of October 31, 2003.

TABLE OF CONTENTS

	<u>Page</u>
Disclaimer	ii
Acknowledgements	iii
List of Figures	v
List of Tables	x
Abstract	xii
Executive Summary	xiii
1. Introduction and Background	1
2. Studies of Alkane Chemistry (Including of First-Generation Products).....	9
2.1. Products and Mechanism of the OH Radical Reaction with 2,2,4-Trimethylpentane in the Presence of NO	10
2.2. Products and Mechanism of the Reaction of OH Radicals with 2,3,4,-Trimethylpentane in the Presence of NO	25
2.3. Identification of Hydroxycarbonyl Products from the OH Radical-Initiated Reactions of C ₅ -C ₈ <i>n</i> -Alkanes in the Presence of NO	40
2.4. Kinetics and Products of the Gas-Phase Reaction of OH Radicals with 5-Hydroxy-2-pentanone at 296 ± 2 K	43
2.5. Formation and Atmospheric Reactions of 4,5-Dihydro-2-methylfuran	52
3. Studies of Alkene Chemistry	75
3.1. Products of the Gas-Phase Reaction of O ₃ with Cyclohexene.....	76
3.2. OH Radical Formation from Reaction of O ₃ with Alkenes: Effects of Water Vapor and 2-Butanol	94
4. Studies of PAH Chemistry	105
4.1. Methyl- and Dimethyl-/Ethyl- Nitronaphthalenes Measured in Ambient Air in Southern California.....	106
5. Studies of the Chemistry of Oxygenated VOCs	113
5.1. Kinetics and Products of the Reactions of OH Radicals with 2-Methyl-2-pentanol and 4-Methyl-2-pentanol	114
5.2. Hydroxycarbonyl Products from the Reactions of Selected Diols with the OH Radical	133
5.3. H-Atom Abstraction from Selected C-H Bonds in 2,3-Dimethylpentanal, 1,4-Cyclohexadiene and 1,3,5-Cycloheptatriene.....	143
6. Summary and Conclusions	163
7. References	170
8. Glossary	180
9. Publications arising wholly or in part from support from this Contract.....	183

LIST OF FIGURES

	<u>page</u>
Figure 1. Schematic VOC reaction mechanism.	2
Figure 2. Reactions of the 2-hexyl radical in air in the presence of NO.	3
Figure 3. Plots of the amounts of acetone, 2-methylpropanal and 4-hydroxy-4-methyl-2-pentanone formed, corrected for reaction with the OH radical, against the amounts of 2,2,4-trimethylpentane reacted.	14
Figure 4. API-MS/MS CAD "precursor ion" spectrum (negative ion mode) of the [PFBOH·O ₂] ⁻ reagent ion in an irradiated CH ₃ ONO - NO - 2,2,4-trimethylpentane - air mixture.	17
Figure 5. Reaction scheme for the [•] OCH ₂ C(CH ₃) ₂ CH ₂ CH(CH ₃) ₂ radical.	19
Figure 6. Reaction scheme for the (CH ₃) ₃ CCH(O [•])CH(CH ₃) ₂ radical.	20
Figure 7. Reaction scheme for the (CH ₃) ₃ CCH ₂ C(O [•])(CH ₃) ₂ radical.	21
Figure 8. Reaction scheme for the (CH ₃) ₃ CCH ₂ CH(CH ₃)CH ₂ O [•] radical.	22
Figure 9. Plot of Equation (I) for the reaction of OH radicals with 2,3,4-trimethylpentane, with <i>n</i> -octane as the reference compound.	29
Figure 10. Plots of the amounts of acetaldehyde, acetone and 3-methyl-2-butanone formed, corrected for reaction with the OH radical, against the amounts of 2,3,4-trimethylpentane reacted.	30
Figure 11. Plots of the amounts of 2-propyl nitrate and 3-methyl-2-butyl nitrate formed, corrected for reaction with the OH radical (see text), against the amounts of 2,3,4-trimethylpentane reacted.	31
Figure 12. Reaction scheme for the (CH ₂) ₂ CHCH(CH ₃)CH(CH ₃)CH ₂ O [•] radical.	34
Figure 13. Reaction scheme for the (CH ₃) ₂ C(O [•])CH(CH ₃)CH(CH ₃) ₂ radical.	35
Figure 14. Reaction scheme for the (CH ₃) ₂ CHC(CH ₃)(O [•])CH(CH ₃) ₂ radical.	36
Figure 15. Plot of Equation (I) for 4-methyl-2-pentanone analyzed by on-fiber derivatization with subsequent thermal desorption and GC-FID compared to its analysis by collection onto Tenax solid adsorbent with subsequent thermal desorption and GC-FID.	47
Figure 16. Plot of Equation (I) for 5-hydroxy-2-pentanone, with 4-methyl-2-pentanone as the reference compound.	48

Figure 17. First-order plots of the decays of 5-hydroxy-2-pentanone in the 5870 liter evacuable chamber at 1.5, 16 and 740 Torr total pressure of dry N ₂ .	57
Figure 18. Plots of Equation (I) for the reaction of OH radicals with 4,5-dihydro-2-methylfuran (DHMF), with cyclohexene and 2-methylpropene as the reference compounds.	58
Figure 19. Plots of Equation (I) for the reactions of NO ₃ radicals and O ₃ with 4,5-dihydro-2-methylfuran (DHMF), with 2,3-dimethyl-2-butene as the reference compound.	59
Figure 20. Infrared spectra of products attributed to DHMF from an irradiated CH ₃ ONO – NO – DHMF – air mixture.	62
Figure 21. Reaction scheme for the reaction of OH radicals with 4,5-dihydro-2-methylfuran in the presence of NO.	63
Figure 22. Infrared spectrum of products attributed to DHMF from a reacted N ₂ O ₅ – NO ₃ – NO ₂ – DHMF – air mixture.	67
Figure 23. API-MS spectrum from a reacted N ₂ O ₅ – NO ₃ – NO ₂ – DHMF – air mixture.	68
Figure 24. Reaction scheme for the reaction of NO ₃ radicals with 4,5-dihydro-2-methylfuran.	69
Figure 25. Infrared spectrum of products from a reacted O ₃ – DHMF – air mixture.	72
Figure 26. Reaction scheme for the reaction of O ₃ with 4,5-dihydro-2-methylfuran.	73
Figure 27. Plots of the amounts of 3-hydroxy-2-butanone formed against the amounts of cyclohexene and cyclohexene-d ₁₀ reacted with O ₃ , in the presence of sufficient 2,3-butanediol to scavenge >95% of the OH radicals formed.	80
Figure 28. Plots of the amounts of pentanal and pentanal-d ₁₀ formed against the amounts of cyclohexene and cyclohexene-d ₁₀ , respectively, reacted with O ₃ , in the presence of sufficient cyclohexane or 2,3-butanediol to scavenge >95% of the OH radicals formed.	82
Figure 29. API-MS spectra of reacted O ₃ – cyclohexene – cyclohexane – air and O ₃ – cyclohexene-d ₁₀ – cyclohexane – air mixtures.	84
Figure 30. API-MS/MS CAD “product ion” spectra of the 131 and 141 u ion peaks observed in the reactions of O ₃ with cyclohexene and cyclohexene-d ₁₀ reactions, respectively.	86
Figure 31. API-MS/MS CAD “product ion” spectra of the 133 and 140 u ion peaks observed in the reactions of O ₃ with cyclohexene and cyclohexene-d ₁₀ reactions, respectively.	87

Figure 32. Reaction scheme for reaction of O ₃ with cyclohexene.	91
Figure 33. Reaction of the stabilized Criegee intermediate with water vapor.	92
Figure 34. Possible reactions of the radical co-product to the OH radical.	92
Figure 35. Plot of the sabinaketone yield from the reaction of O ₃ with sabinene against the 2-butanol concentration at ~5% and ~60% relative humidity.	98
Figure 36. Plot of the OH radical formation yield from the reaction of O ₃ with sabinene, as derived from the 2-butanone yield, against the 2-butanol concentration at ~5% and ~60% relative humidity.	100
Figure 37. Plot of the pinonaldehyde yield from the reaction of O ₃ with α -pinene against the 2-butanol concentration at ~5% and ~60% relative humidity.	101
Figure 38. Plot of the OH radical formation yield from the reaction of O ₃ with α -pinene, as derived from the 2-butanone yield, against the 2-butanol concentration at ~5% and ~60% relative humidity.	102
Figure 39. Plot of the heptanal yield from the reaction of O ₃ with 7-tetradecene against the 2-butanol concentration at ~5% relative humidity and ~60% relative humidity.	103
Figure 40. Plot of the OH radical formation yield from the reaction of O ₃ with 7-tetradecene, as derived from the 2-butanone yield, against the 2-butanol concentration at ~5% and ~60% relative humidity.	104
Figure 41. Mass chromatograms for the methylnitronaphthalenes (m/z 187) observed by GC/MS NCI-SIM analysis of: (top) Sample from the OH radical-initiated chamber reaction of the PAHs present in volatilized diesel fuel; (center) Composite of early morning (7-10:30) ambient air samples collected in Los Angeles during August 12-16, 2002; (bottom) Composite of mid-day (11-14:30) ambient air samples collected in Los Angeles during August 12-16, 2002.	109
Figure 42. Mass chromatograms for the dimethylnitronaphthalenes and/or ethylnitronaphthalenes (m/z 201) observed by GC/MS NCI-SIM analysis of: (top) Sample from the OH radical-initiated chamber reaction of the PAHs present in volatilized diesel fuel; (center) Composite of early morning (7-10:30) ambient air samples collected in Los Angeles during August 12-16, 2002; (bottom) Composite of mid-day (11-14:30) ambient air samples collected in Los Angeles during August 12-16, 2002.	110
Figure 43. Plots of Equation (I) for the gas-phase reactions of OH radicals with 2-methyl-2-pentanol and 4-methyl-2-pentanol, with <i>n</i> -octane as the reference compound.	118

Figure 44. Plots of the amounts of acetaldehyde, propanal, acetone and 2-pentanone formed, corrected for reaction with OH radicals, against the amounts of 2-methyl-2-pentanol reacted with the OH radical.	120
Figure 45. Plots of the amounts of acetaldehyde, acetone, 2-methylpropanal and 4-methyl-2-pentanone formed, corrected for reaction with OH radicals, against the amounts of 4-methyl-2-pentanol reacted with the OH radical.	121
Figure 46. API-MS negative ion spectra of irradiated CH ₃ ONO – NO – 2-methyl-2-pentanol – air and CH ₃ ONO – NO – 4-methyl-2-pentanol – air mixtures, using NO ₂ ⁻ ions – as the reagent ions.	124
Figure 47. Reactions of the $\bullet\text{OCH}_2\text{C}(\text{CH}_3)(\text{OH})\text{CH}_2\text{CH}_2\text{CH}_3$ radical.	127
Figure 48. Reactions of the $(\text{CH}_2)_2\text{C}(\text{CH}_3)(\text{OH})\text{CH}(\text{O}\bullet)\text{CH}_2\text{CH}_3$ radical.	127
Figure 49. Reactions of the $(\text{CH}_2)_2\text{C}(\text{CH}_3)(\text{OH})\text{CH}_2\text{CH}(\text{O}\bullet)\text{CH}_3$ radical.	128
Figure 50. Reactions of the $\text{CH}_3\text{CH}(\text{OH})\text{CH}(\text{O}\bullet)\text{CH}(\text{CH}_3)_2$ radical.	130
Figure 51. Reactions of the $\text{CH}_3\text{CH}(\text{OH})\text{CH}_2\text{C}(\text{O}\bullet)(\text{CH}_3)_2$ radical.	131
Figure 52. Plot of the GC-FID peak areas for the oximes of the hydroxycarbonyls observed, against the percentage of 1,3-butanediol reacted with the OH radical.	138
Figure 53. Plots of the GC peak areas of the oximes of the hydroxyaldehydes CH ₃ CH(OH)CH ₂ CHO, HOCH ₂ CHO and CH ₃ CH(OH)CHO ratioed to the peak area of the oximes of the hydroxyketone CH ₃ C(O)CH ₂ CH ₂ OH.	139
Figure 54. Plots of the amounts of benzene formed against the amounts of 1,4-cyclohexadiene reacted with the OH radical.	147
Figure 55. Plot of Equation (I) for the reaction of OH radicals with tropone, with methyl vinyl ketone as the reference compound.	148
Figure 56. Plots of Equation (I) for the reactions of OH radicals with 3-methyl-2-pentanone and 2,3-dimethylpentanal, with <i>n</i> -octane and 2-methylpropene as the reference compounds, respectively.	151
Figure 57. Infrared spectra from a CH ₃ ONO – NO – 2,3-dimethylpentanal – air irradiation (concentrations are in molecule cm ⁻³).	152
Figure 58. Plots of the amounts of acetaldehyde and 2-butanone formed (corrected for secondary reactions, see text) against the amounts of 2,3-dimethylpentanal reacted with the OH radical.	153

Figure 59. Plot of the amounts of 3-methyl-2-pentanone formed (corrected for secondary reactions) against the amounts of 2,3-dimethylpentanal reacted with the OH radical.	154
Figure 60. Reaction scheme for reaction of OH radicals with 1,4-cyclohexadiene.	156
Figure 61. Reaction scheme for the reaction of OH radicals with 1,3,5-cycloheptatriene.	157
Figure 62. Reactions expected after H-atom abstraction from the CHO group in 2,3-dimethylpentanal.	159
Figure 63. Reactions expected after H-atom abstraction from the 2-position C-H bond in 2,3-dimethylpentanal.	160
Figure 64. Reactions expected after H-atom abstraction from the 3-position C-H bond in 2,3-dimethylpentanal.	161
Figure 65. Reactions expected after H-atom abstraction from the 4-position C-H bond in 2,3-dimethylpentanal.	161

LIST OF TABLES

	<u>page</u>
Table 1. Products of reactions of the OH radical with <i>n</i> -pentane, <i>n</i> -hexane, <i>n</i> -heptane and <i>n</i> -octane in the presence of NO	4
Table 2. Products observed, and their molar formation yields, from the OH radical-initiated reaction of 2,2,4-trimethylpentane in the presence of NO	15
Table 3. The initially-formed peroxy radicals from the OH radical-initiated reaction of 2,2,4-trimethylpentane in the presence of NO and possible major observed products arising from their subsequent reactions	24
Table 4. Products observed, and their molar formation yields, from the OH radical-initiated reaction of 2,3,4-trimethylpentane in the presence of NO	32
Table 5. Fragmentation patterns observed in the MS spectra of the hydroxycarbonyls and their assignments	42
Table 6. Rate constant ratios k_1/k_2 , rate constants k_1 and estimated lifetimes for the reaction of 4,5-dihydro-2-methylfuran with OH radicals, NO ₃ radicals, and O ₃ at 298 ± 1 K	60
Table 7. Products identified and their formation yields from the gas-phase reaction of OH radicals with 4,5-dihydro-2-methylfuran	65
Table 8. Products identified and their formation yields from the gas-phase reaction of NO ₃ radicals and O ₃ with 4,5-dihydro-2-methylfuran	70
Table 9. Measured OH radical formation yields from reactions of O ₃ with selected alkenes at atmospheric pressure using 2,3-butanediol as the radical scavenger, together with recent literature data.	81
Table 10. Mass spectral evidence for products formed from the gas-phase reactions of O ₃ with cyclohexene and cyclohexene-d ₁₀ in the presence of an OH radical scavenger	85
Table 11. Volatile PAHs measured on Tenax-TA solid adsorbent tubes in Los Angeles during morning and midday sampling August 12-16, 2002. Shown for comparison is an example of a diesel fuel sample.	107
Table 12. Naphthalene and alkyl-naphthalenes concentrations and percent of <i>n</i> nitrated parent PAH for samples collected August 12-16, 2002 in Los Angeles, California, U.S.A.	111
Table 13. Rate constant ratios k_1/k_2 and rate constants k_1 for the gas-phase reactions of OH radicals with 2-methyl-2-pentanol and 4-methyl-2-pentanol at 298 ± 2 K	119

Table 14. Formation yields of selected products from the gas-phase reactions of the OH radical with 2-methyl-2-pentanol at 296 ± 2 K	122
Table 15. Formation yields of selected products from the gas-phase reactions of the OH radical with 4-methyl-2-pentanol at 296 ± 2 K	123
Table 16. Comparison of measured and calculated partial rate constants for H-atom abstraction by OH radicals from the various CH ₃ , CH ₂ and CH groups	132
Table 17. Hydroxycarbonyl products predicted and observed, and their predicted and measured yields, from the gas-phase reactions of the OH radical with diols at 296 ± 2 K	135
Table 18. Analytical relative response factors for the oximes of the products observed, and OH radical reaction rate constants for the diols and products	137
Table 19. Rate constant ratios k_2/k_3 and rate constants k_2 ($\text{cm}^3 \text{ molecule}^{-1} \text{ s}^{-1}$) for the gas-phase reactions of OH radicals with tropone, 2,3-dimethylpentanal and 3-methyl-2-pentanone at 298 ± 2 K	149
Table 20. Products observed, and their molar yields, from the reaction of OH radicals with 2,3-dimethylpentanal in the presence of NO	155
Table 21. Room temperature rate constants measured in this work for the reactions of OH radicals, NO ₃ radicals and O ₃ with selected VOCs	163
Table 22. Products identified and quantified in this work for the reactions of OH radicals, NO ₃ radicals and O ₃ with VOCs	164

ABSTRACT

During this three-year experimental program, we have used the facilities and expertise available at the Air Pollution Research Center, University of California, Riverside, to investigate the atmospheric chemistry of selected volatile organic compounds found in California's atmosphere. Experiments were carried out in large volume (5800 to ~7500 liter) chambers with analysis of reactants and products by gas chromatography (with flame ionization and mass spectrometric detection), *in situ* Fourier transform infrared spectroscopy, and *in situ* direct air sampling atmospheric pressure ionization mass spectrometry. The gas chromatographic analyses included the use of Solid Phase MicroExtraction fibers coated with derivatizing agent for on-fiber derivatization of carbonyl-containing compounds, with subsequent gas chromatographic analyses of the carbonyl-containing compounds as their oximes. This technique was especially useful for the identification and quantification of 1,4-hydroxycarbonyls and of hydroxyaldehydes which are not commercially available and do not elute from gas chromatographic columns without prior derivatization.

We have elucidated the atmospheric chemistry of alkanes and of one of their major first-generation reaction products, investigated the products of the reactions of ozone with alkenes, and studied the kinetics and products of the OH radical-initiated reactions of selected methylpentanols, diols and aldehydes. We also identified for the first time dimethyl- and ethyl-nitronaphthalenes, potentially toxic air pollutants, in the Los Angeles atmosphere and showed that these alkyl-nitronaphthalenes are formed from the OH radical-initiated reactions of their parent alkyl-naphthalenes. The data obtained in this Contract will prove important for including into chemical mechanisms for modeling photochemical air pollution and ozone-forming potentials. Additionally, the ambient concentrations and toxicity of the newly identified alkyl-nitronaphthalenes should be evaluated.

EXECUTIVE SUMMARY

During this three-year experimental program, we used the facilities and expertise available at the Air Pollution Research Center, University of California, Riverside, to investigate the atmospheric chemistry of selected volatile organic compounds found in California's atmosphere. Experiments were carried out in large volume (5800 to ~7500 liter) chambers with analysis of reactants and products by gas chromatography (with flame ionization and mass spectrometric detection), *in situ* Fourier transform infrared spectroscopy, and *in situ* direct air sampling atmospheric pressure ionization mass spectrometry. The gas chromatographic analyses included the use of Solid Phase MicroExtraction fibers coated with derivatizing agent for on-fiber derivatization of carbonyl-containing compounds, with subsequent gas chromatographic analyses of the carbonyl-containing compounds as their oximes.

The research carried out during this Contract has finally elucidated the atmospheric chemistry of alkanes, which comprise ~50% of the non-methane organic compounds observed in ambient air in urban areas, and shown that 1,4-hydroxycarbonyls are major products of the long-chain alkanes and, to a lesser extent, of branched alkanes. Our data show that isomerization of the alkoxy radicals formed after the initial OH radical reaction dominates for the larger (>C₄) *n*-alkanes, leading to formation of 1,4-hydroxycarbonyls and 1,4-hydroxynitrates. Because the rates of decomposition of branched alkoxy radicals are significantly higher than the decomposition rates of linear alkoxy radicals, alkoxy radical isomerization plays a lesser role in the chemistry of branched alkanes, and therefore more carbonyl compounds, and less hydroxycarbonyls, are formed from branched alkanes. We have investigated the atmospheric reactions of 5-hydroxy-2-pentanone, the only commercially available 1,4-hydroxycarbonyl (and the major product formed from *n*-pentane). In addition to measuring its rate constant for reaction with OH radicals and the products of that reaction, we observed that 5-hydroxy-2-pentanone cyclizes with loss of water to form the unsaturated and highly reactive compound 4,5-dihydro-2-methylfuran. For 5-hydroxy-2-pentanone, cyclization to form the dihydrofuran occurs in dry air, but the presumed equilibrium lies in favor of 5-hydroxy-2-pentanone for ~5% or higher relative humidity at room temperature. However, given the high reactivity of 4,5-dihydro-2-methylfuran towards OH radicals, NO₃ radicals and O₃ (with an estimated lifetime in the atmosphere of an hour or less, based on our measured rate constants), 4,5-dihydro-2-methylfuran may well play an important role in the atmospheric chemistry of *n*-pentane, even for the high water vapor concentrations in the typical lower atmosphere. Our initial results concerning the reactions of larger 1,4-hydroxycarbonyls formed from *n*-hexane through *n*-octane suggest that the dihydrofurans formed by cyclization and loss of water from the larger 1,4-hydroxycarbonyls are more important at higher relative humidities, and maybe up to ~50% relative humidity. This body of work on alkane chemistry both places previous predictions (for example, the formation of 1,4-hydroxycarbonyls) on a firm basis as well as discovering that a class of new and potentially important products (the dihydrofurans) are formed in the atmospheric photooxidation of alkanes. These data will need to be incorporated into chemical mechanisms used in modeling photochemical air pollution and ozone formation from alkanes.

Our work on alkene chemistry focused on the reactions of alkenes with O₃. We have shown that measurements of OH radical formation yields from the reactions of O₃ with alkenes are not affected by water vapor, and hence that laboratory studies conducted in the absence of water vapor, or at low water vapor concentrations, are applicable to atmospheric conditions. Our results on the effects of water vapor and 2-butanol (a potential scavenger of Criegee

intermediates, the key intermediate species in these O₃-alkene reactions) on these reactions aids in the elucidation of the overall reaction mechanisms, and suggests (in agreement with other recent literature data) that the formation routes to the OH radical and to other products can be viewed as parallel reaction pathways, independent of water vapor concentration. This finding is important for chemical mechanism development.

Research into the formation of volatile nitro-PAH and their presence in the Los Angeles atmosphere shows that alkylnaphthalenes are a significant fraction of the naphthalene concentrations in ambient air, and that alkyl-nitronaphthalenes are formed from the OH radical-initiated reactions of their precursor alkylnaphthalenes. Methyl-nitronaphthalenes and dimethyl- and ethyl- nitronaphthalenes were observed in ambient air samples collected in the Los Angeles air basin. This observation of dimethyl- and ethyl- nitronaphthalenes is the first report of the presence of these potentially toxic air pollutants in the atmosphere.

Our studies of the kinetics and products of selected oxygenated organic compounds (in addition to those of 1,4-hydroxycarbonyls and dihydrofurans mentioned above) have included the use of Solid Phase MicroExtraction fibers for on-fiber derivatization to identify and quantify hydroxycarbonyls (primarily hydroxyaldehydes) which otherwise cannot be readily analyzed. Our studies of the products formed from 2- and 4-methyl-2-pentanol, a series of diols, and 2,3-dimethylpentanal allow reasonably detailed reaction mechanisms for the reactions of OH radicals (the dominant atmospheric loss process for these oxygenated compounds) to be derived. These data expand the database concerning the details of VOC atmospheric reactions, which can be used to either refine present empirical estimation methods and to test new estimation and/or *ab-initio* theoretical calculational methods for the reactions of the key intermediate alkoxy radicals, and hence provide the ability to predict reaction products and their yields under atmospheric conditions.

1. INTRODUCTION AND BACKGROUND

In addition to the emissions of volatile organic compounds (VOCs) from vegetation (Guenther *et al.*, 1995, 2000), large quantities of organic compounds are emitted into the atmosphere from anthropogenic sources, largely from combustion of petroleum products such as gasoline and diesel fuels (Sawyer *et al.*, 2000) and from other sources such as solvent use and the use of consumer products. In the atmosphere organic compounds are partitioned between the gaseous and particulate phases (Pankow, 1987, 1994; Bidleman, 1988; Harner and Bidleman, 1998), with the chemicals being at least partially in the gas-phase for liquid-phase vapor pressures $>10^{-6}$ Torr at atmospheric temperature (Bidleman, 1988). In the atmosphere, these gaseous organic compounds (termed hereafter VOCs) are transformed by photolysis and/or reaction with OH radicals, NO₃ radicals and O₃ (Atkinson, 2000). Emissions of organic compounds and their subsequent *in situ* atmospheric transformations lead to a number of adverse effects, including: the formation, in the presence of NO_x, of ozone, a criteria air pollutant; the formation of secondary organic aerosol, resulting in visibility degradation and risks to human health; and the *in situ* atmospheric formation of toxic air contaminants (in addition to those directly emitted from energy usage), including, for example, formaldehyde, peroxyacetyl nitrate and nitrated aromatic species.

There is therefore a need to understand, in detail, the reactions involved in the atmospheric degradation of emitted organic compounds. This includes not only the identification and quantification of products formed from the atmospheric reactions of directly emitted chemicals, but also corresponding studies of the first- and later-generation products. Because it is likely that secondary organic aerosol is formed from second- and later-generation products of alkanes, alkenes and aromatic hydrocarbons emitted from, for example, vehicle exhaust, such comprehensive studies will provide, from the gas-phase perspective, detailed chemistry leading to secondary aerosol formation.

As a result of almost three decades of research, the rate constants and mechanisms of the **initial** reactions of OH radicals, NO₃ radicals and O₃ with VOCs are now reliably known or can be estimated (see, for example, Atkinson, 1989, 1991, 1994, 1997a; 2000). Recently significant advances have been made in our understanding of the mechanisms of the reactions subsequent to the initial OH radical, NO₃ radical, and O₃ reactions with selected VOCs and of "first-generation" products formed from these reactions (Atkinson, 2000; Arey *et al.*, 2001; Bethel *et al.*, 2000). Despite these advances however, there are still areas of significant uncertainty in our knowledge of the products and mechanisms of the atmospheric transformation reactions of VOCs, including those of the VOC atmospheric reaction products, which need to be understood if O₃ and secondary organic aerosol formation in urban and regional areas are to be quantitatively understood. Alkanes, alkenes and aromatic hydrocarbons, together with carbonyl compounds directly emitted and/or formed *in situ* in the atmosphere, are the major VOCs emitted into the atmosphere from energy usage (see, for example, Calvert *et al.*, 2000, 2002). The status, circa 2000, of our knowledge of the atmospheric photooxidations of alkanes, alkenes and aromatic hydrocarbons is briefly summarized below, and a schematic of the reactions occurring in the atmosphere is shown in Figure 1.

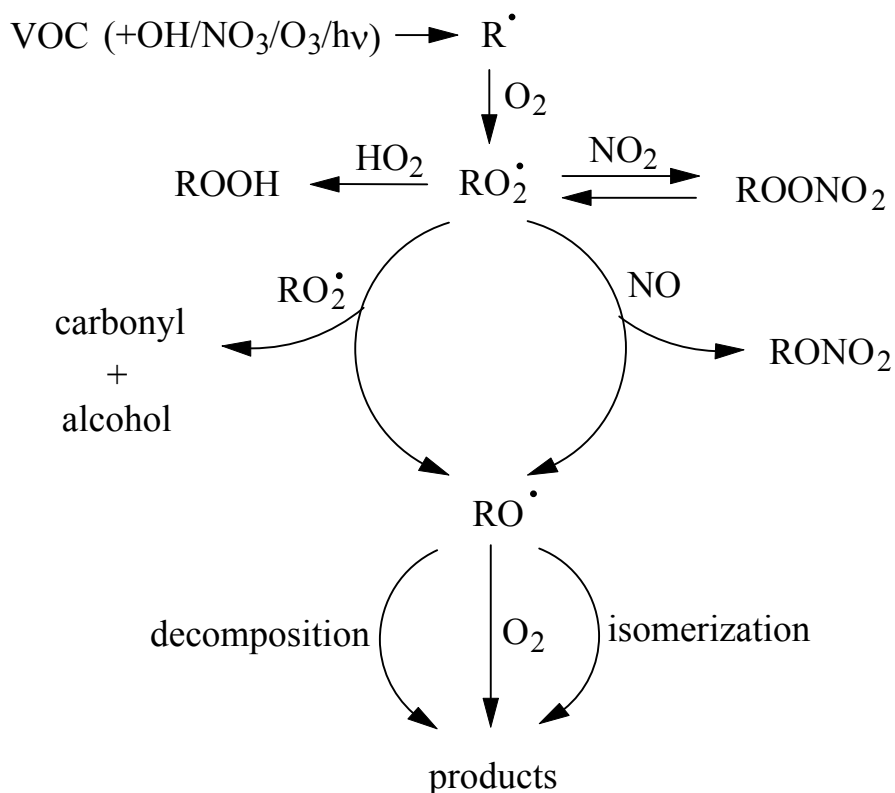


Figure 1. Schematic VOC reaction mechanism

Alkanes. The dominant loss process for alkanes in the troposphere is by reaction with the OH radical, with subsequent reactions of the initially-formed alkyl radicals leading to the formation of alkyl peroxy and alkoxy radicals (Atkinson, 2000). In the presence of NO at concentrations $\geq (2-7) \times 10^8$ molecule cm^{-3} ($\geq 10-30$ ppt), the key intermediate species are alkoxy radicals. Alkoxy radicals react with O₂, decompose, or isomerize via a 6-membered transition state (Atkinson, 1997a,b), and the relative importance of decomposition, isomerization, and reaction with O₂ of these alkoxy radicals in the troposphere appears to be able to be estimated with some reliability (Atkinson, 1997a,b; Aschmann and Atkinson, 1999). The isomerization reaction leads to the formation of 1,4-hydroxycarbonyls and (from peroxy radical + NO reactions) 1,4-hydroxynitrates (Atkinson, 2000; Arey *et al.*, 2001), as shown for the 2-hexyl radical formed from *n*-hexane in Figure 2 (note that the second isomerization of the CH₃CH(OH)CH₂CH₂CH(O•)CH₃ radical dominates over decomposition or reaction with O₂). We have recently used our PE SCIEX atmospheric pressure ionization tandem mass spectrometer with NO₂⁻ ions as the chemical ionization agent to quantify (through the use of internal standards) hydroxycarbonyls and hydroxynitrates from C₅-C₈ *n*-alkanes and obtained the product formation yields shown in Table 1.

Figure 2. Reactions of the 2-hexyl radical in the presence of NO

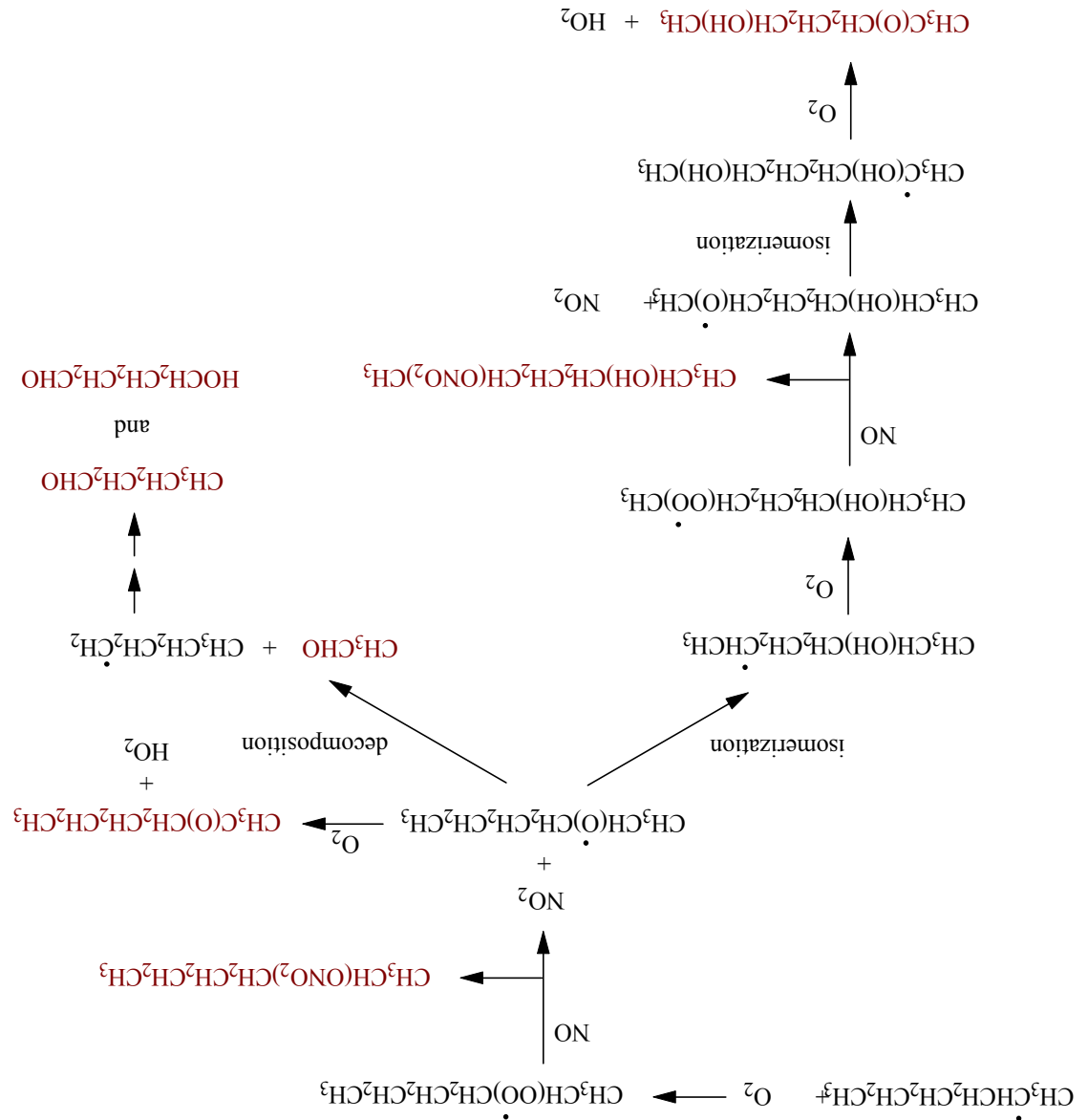


Table 1. Products of reactions of the OH radical with *n*-pentane, *n*-hexane, *n*-heptane and *n*-octane in the presence of NO [from Arey *et al.* (2001) and Section 2.3.].

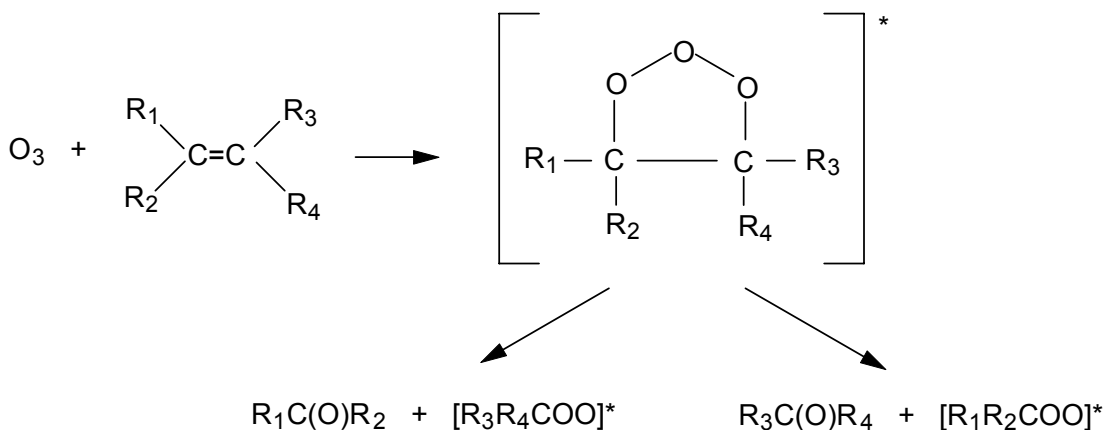
alkane	molar yield (%)			
	carbonyls	nitrates	hydroxycarbonyls	hydroxynitrates
<i>n</i> -pentane	47	10.5	36 (~59) ^a	2.5
<i>n</i> -hexane	10	14.1	53 (~57) ^a	4.5
<i>n</i> -heptane	≤1	17.8	46 (~51) ^a	4.6
<i>n</i> -octane	≤1	22.6	27 (~52) ^a	5.3

^aSee Section 2.3.

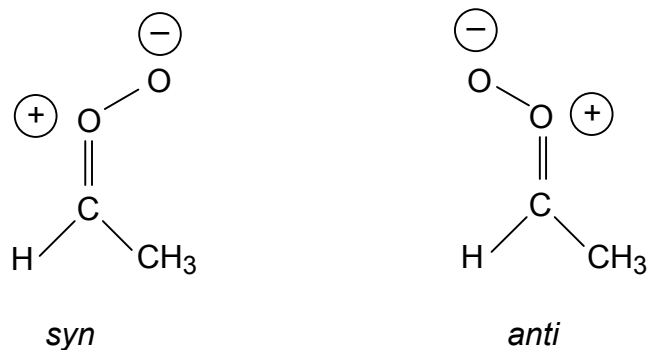
While further work is necessary to identify (on an isomer-specific basis) and quantify the hydroxycarbonyls and hydroxynitrates, the atmospheric chemistry of these two classes of organic compounds also needs to be studied. Indeed, we have made a start on that by measuring the room temperature rate constants for the reactions of a series of hydroxycarbonyls with OH radicals, NO₃ radicals and O₃ (Aschmann *et al.*, 2000a).

Alkenes (including isoprene and monoterpenes)

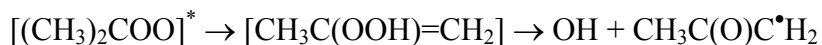
In the troposphere, alkenes react with OH radicals, NO₃ radicals and O₃ (Atkinson, 1997a). The reactions of O₃ with alkenes proceed by initial addition of O₃ across the C=C unsaturated bond to form an energy-rich primary ozonide, which then decomposes to two sets of carbonyl plus chemically-activated “Criegee” intermediate (Atkinson, 1997a), as shown below for R₁-R₄ = H or alkyl.



Theoretical calculations indicate that the Criegee intermediate is a carbonyl oxide (Cremer *et al.*, 1993; Gutbrod *et al.*, 1996, 1997), which for mono-substituted intermediates may be formed in either the *syn* or *anti* configuration (R = alkyl).



The sum of the formation yields of the two possible "primary" carbonyls is unity (Atkinson, 1997a). The initially energy-rich biradicals are collisionally stabilized or undergo decomposition or isomerization. OH radicals are formed from the isomerization/decomposition reactions of the biradicals, often in high (up to unit) yield (see, for example, Atkinson, 1997a; Paulson *et al.*, 1999a). Major uncertainties in the O₃ reactions with alkenes concern the tropospheric reactions of initially energy-rich biradicals and thermalized biradicals. The carbon-centered radical co-products to the OH radical, formed as shown below,

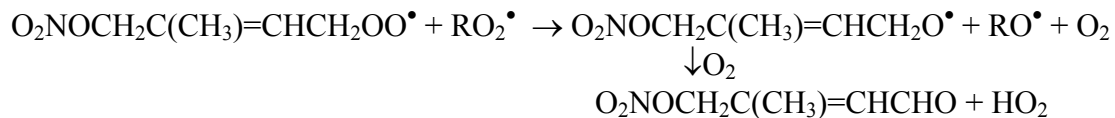
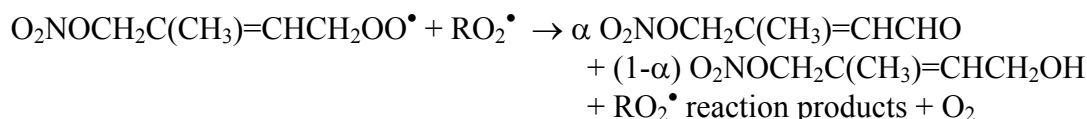


will react similarly to alkyl and substituted-alkyl radicals (see Figure 1) and thus leading to carbonyls, hydroxycarbonyls, dicarbonyls and hydroperoxycarbonyls depending on the ambient concentrations of NO, HO₂ radicals, NO₃ radicals, and organic peroxy radicals. Reactions of the thermalized biradicals with water vapor [anticipated to be the dominant reaction in the troposphere (Atkinson, 1997a)] can lead to the formation of acids and/or hydroxyhydroperoxides for biradicals of structure RCHO₂, or H₂O₂ + carbonyl for disubstituted biradicals (Alvarado *et al.*, 1998; Baker *et al.*, 2002).

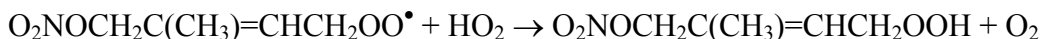
Analogous to the situation for the alkoxy radicals formed from the alkanes, the β-hydroxyalkoxy radicals formed after OH radical addition to alkenes can react with O₂, decompose, or isomerize. Recent studies indicate that a significant fraction of alkoxy radicals formed from the exothermic RO₂[•] + NO reaction appear to undergo "prompt" decomposition (Orlando *et al.*, 1998; Vereecken *et al.*, 1999). For the simple acyclic monoalkenes, the decomposition and isomerization reactions of the β-hydroxyalkoxy radicals appear to dominate [except for the HOCH₂CH₂O[•] radical formed in the OH + ethene reaction, which both reacts with O₂ and decomposes at room temperature and atmospheric pressure of air (Niki *et al.*, 1981)] (Atkinson, 1997a,b). Isomerization of the β-hydroxyalkoxy radicals formed after OH radical addition to the 1-alkenes 1-butene through 1-octene has been observed, with the isomerization reactions leading to the formation of dihydroxycarbonyls (for example, CH₃CH(OH)CH₂CH(OH)CHO and HOCH₂CH₂CH₂C(O)CH₂OH from 1-pentene) (Atkinson, 1997a), a class of products not previously considered. We have recently measured a yield of ~20% for the formation of molecular weight 184 hydroxydicarbonyl(s) from the reaction of the OH radical with α-pinene in the presence of NO and a yield of dihydroxycarbonyls from the 1-hexene reaction of ~40-50% (Aschmann *et al.*, 2002a). The 1,4-hydroxyalkoxy radicals formed

after OH radical addition to isoprene either isomerize and/or react with O₂ to form the 1,4-unsaturated hydroxyaldehydes HOCH₂C(CH₃)=CHCHO and HOCH₂CH=C(CH₃)CHO (Kwok *et al.*, 1995), and these hydroxyaldehydes probably account for the majority of the "missing" carbon observed in previous studies of the OH radical reaction with isoprene (Atkinson, 1997a).

The NO₃ radical also reacts with alkenes by initial addition to the >C=C< bond(s) (Atkinson, 1991, 2000). To date, relatively few product studies of the NO₃ radical-initiated reactions of alkenes have been carried out (see, for example Atkinson, 1997a, 2000). The reaction mechanisms and products formed from laboratory studies appear to be in accord with expectations involving reactions of nitrooxyalkyl peroxy radicals with organic peroxy radicals (including the self-reactions) and with the HO₂ radical. For example, for isoprene (Kwok *et al.*, 1996a):



where RO₂[•] is the O₂NOCH₂C(CH₃)=CHCH₂OO[•] radical or other organic peroxy radical, and



Aromatic Hydrocarbons and Polycyclic Aromatic Hydrocarbons

The dominant tropospheric reaction of benzene and the alkyl-substituted benzenes is with the OH radical, with this reaction proceeding by H-atom abstraction from the C-H bonds of the alkyl-substituent groups (minor) and by OH radical addition to the aromatic ring (major) to form a hydroxycyclohexadienyl-type radical (OH-aromatic adduct). The OH-aromatic adducts react with NO₂ and O₂ (Knispel *et al.*, 1990; Atkinson, 1994, 2000), with the O₂ reaction dominating in the troposphere but with the NO₂ reaction being important, or possibly even dominant, for certain laboratory product studies. To date, the mechanisms and products of the O₂ and NO₂ reactions with the OH-aromatic adducts are not well understood, although progress has been made on the products formed and their yields (Atkinson, 2000; Smith *et al.*, 1999; Bethel *et al.*, 2000). Recent product studies indicate that the first-generation products are comprised of: aromatic carbonyls and organic nitrates (*e.g.*, benzyl nitrate from toluene) formed after initial H-atom abstraction from the C-H bonds of the alkyl substituent group(s); phenolic compounds (*e.g.*, cresols from toluene); sets of α-dicarbonyl plus unsaturated-1,4-dicarbonyl (*e.g.*, CH₃C(O)CHO + HC(O)CH=CHCHO from toluene); di-unsaturated-1,6-dicarbonyls (*e.g.*, HC(O)CH=CHCH=CHCHO from benzene); and unsaturated-epoxy-1,6-dicarbonyls (Atkinson, 2000; Bethel *et al.*, 2000). Furthermore, the formation yields of the ring-opened products depend on the NO₂ concentration (*i.e.*, on the fraction of the OH-aromatic adduct reacting with O₂ *versus* with NO₂) with (to date) lower yields from the NO₂ + OH-aromatic adduct reaction (Atkinson and Aschmann, 1994; Bethel *et al.*, 2000). However, there is still a need to carry out

isomer-specific identification and quantification of products from the $O_2 + OH$ -aromatic adduct reaction and to delineate the detailed reaction mechanisms.

Polycyclic aromatic hydrocarbons (PAH) are ubiquitous combustion products which include known carcinogens and mutagens (IARC, 1983; 1984). Ambient atmospheric measurements of nitrated PAH (Atkinson and Arey, 1994; Arey, 1998) imply that the OH-PAH and NO_3 -PAH adducts react mainly with NO_2 in the atmosphere. This is in sharp contrast to the situation noted above for the monocyclic aromatic hydrocarbons, where reaction of the OH-aromatic adducts with O_2 dominates under atmospheric conditions. In ambient atmospheres, the nitro-PAH resulting from gas-phase OH and NO_3 radical-initiated reactions of the parent PAH have been shown to dominate over the nitro-PAH present from direct emissions such as diesel exhaust (Atkinson and Arey, 1994; Arey, 1998). Understanding the mechanisms of formation of these nitro-PAH is important because the nitro-PAH may, in some cases, be significantly more toxic than the parent PAH (IARC, 1989; Sasaki *et al.*, 1997).

Oxygen- and Nitrogen-Containing Organic Compounds

In addition to direct emissions of carbonyl compounds from combustion emissions (for example, from vehicle exhaust) and of alcohols, ethers and other oxygenates from their use in gasoline and/or as solvents, a wide variety of oxygen- and nitrogen-containing VOCs are formed in the atmosphere as a result of the photooxidations of directly emitted VOCs (see above and Atkinson, 2000). Rate constants for the initial reactions of OH radicals, NO_3 radicals and O_3 with a large number of oxygenated compounds have been measured or can be estimated (Atkinson, 1989, 1991, 1994; Atkinson, 2000). However, apart from a relatively few aldehydes, ketones, ethers, esters and alcohols, product studies have been limited and the detailed atmospheric reaction mechanisms are generally not totally understood (Atkinson, 2000). This is particularly the case for the hydroxycarbonyls and dihydroxycarbonyls formed from the OH radical-initiated reactions of alkanes and alkenes, and these products are furthermore generally not commercially available. Similarly, the products of the atmospherically-important OH radical-initiated reactions of alkyl nitrates, formed from the reactions of alkyl peroxy radicals with NO , are not known (Atkinson, 2000).

While much progress has been made, especially during the past year or two, there are still areas of uncertainty in our understanding of the tropospheric chemistry of VOCs, and of their atmospheric reaction products (Atkinson, 2000). Important uncertainties include the mechanisms and products of the OH radical-initiated reactions of aromatic hydrocarbons (including PAH) in the presence and absence of NO_x , and the detailed mechanisms and products of the reactions of energy-rich biradicals formed from the reactions of O_3 with alkenes (including isoprene and monoterpene hydrocarbons emitted from vegetation). Furthermore, while the recent research mentioned above has "firmed-up" our knowledge of the mechanisms and products of the OH and NO_3 radical-initiated reactions of alkanes and alkenes, quantitative isomer-specific measurements of the alkoxy radical isomerization products (hydroxycarbonyls and dihydroxycarbonyls, for example) remain to be made. Finally, the reactions in the troposphere of many "first-generation" products formed from alkanes, alkenes and aromatic hydrocarbons have not been studied to date (or only kinetic data for their tropospheric loss processes are known). As an example, there are presently no data concerning the atmospheric lifetimes and fates of the 1,4-hydroxycarbonyls formed from the OH radical-initiated reactions of alkanes and isoprene (the unsaturated-1,4-hydroxyaldehydes postulated to be formed from isoprene are likely to be highly reactive in the atmosphere), nor for the dihydroxycarbonyls formed from the OH radical-

initiated reactions of alkenes. There is therefore a need to investigate the atmospheric chemistry of the "first-generation" products as well as continuing *quantitative* product studies of the OH radical, NO₃ radical and O₃ reactions with alkanes, alkenes, aromatic hydrocarbons, and oxygenated compounds.

1.1. General Objectives

In this three-year experimental program, we used the array of analytical methods available at the Air Pollution Research Center (APRC) at the University of California, Riverside, to investigate the atmospherically important reactions of selected VOCs and of their reaction products (see the facilities available). In particular, we used our PE SCIEX API III MS/MS direct air sampling, atmospheric pressure ionization tandem mass spectrometer (API-MS/MS) in conjunction with *in situ* Fourier transform infrared (FT-IR) spectroscopy, gas chromatography with flame ionization detection (GC-FID), gas chromatography with FTIR detection (GC-FTIR), combined gas chromatography-mass spectrometry (GC-MS), and product derivatization with GC-FID and GC-MS analyses to identify and quantify VOC reaction products. During the past few years, we have employed these analytical methods in conjunction with our large-volume chambers and made important advances in elucidating the products and mechanisms of the gas-phase reactions of OH radicals, NO₃ radicals, and O₃ with alkanes, alkenes, aromatic compounds and oxygenated compounds (see, for example, Aschmann *et al.*, 1997, 1998; Tuazon *et al.*, 1998a,b; Arey *et al.*, 2001; Bethel *et al.*, 2000). In particular and as a result of recent developmental work, we can use the API-MS/MS (with NO₂⁻ ions as the reactant ion and with suitable internal standards) to determine the formation yields of selected compound classes (to date, hydroxycarbonyls and hydroxynitrates) which are not amenable to GC without prior derivatization.

2. STUDIES OF ALKANE CHEMISTRY (INCLUDING OF FIRST-GENERATION PRODUCTS)

2.1. Products and Mechanism of the Reaction of OH Radicals with 2,2,4-Trimethylpentane in the Presence of NO

2.1.1. Introduction

Alkanes are important constituents of gasoline fuel and vehicle exhaust (Hoekman, 1992), and account for ~50% of the non-methane organic compounds measured in ambient air in urban areas (Seila *et al.*, 1989; Lurmann and Main, 1992). In the troposphere, alkanes present in the gas phase react mainly with the OH radical (Atkinson, 1997a) to form alkyl radicals, which react rapidly with O₂ to form alkyl peroxy (RO₂[•]) radicals (Atkinson, 1997a).



In urban areas in the presence of sufficiently high concentrations of NO, alkyl peroxy radicals react with NO to form the corresponding alkoxy radical plus NO₂ or the alkyl nitrate, RONO₂ (Atkinson, 1997a).



The alkoxy radicals formed in reaction (3b) then react with O₂, decompose by C-C bond scission, or isomerize through a 6-membered ring transition state (Atkinson, 1997a). The isomerization reaction can occur for ≥C₄ alkanes and, after O₂ addition to the 1,4-hydroxyalkyl radical, results in the formation of a 1,4-hydroxyalkyl peroxy radical which then reacts further by reactions analogous to reactions (2) and (3) and leads to the formation of hydroxycarbonyls and hydroxynitrates (Atkinson *et al.*, 1995; Eberhard *et al.*, 1995; Kwok *et al.*, 1996b; Atkinson, 1997a; Arey *et al.*, 2001).

While rate constants for the reactions of the OH radical with a large number of alkanes have been measured (Atkinson, 1997a), the products and mechanisms of the OH radical-initiated reactions of alkanes have received less attention, and most of the more recent and comprehensive studies of the products and mechanisms of the OH radical reactions of alkanes have involved *n*-alkanes and cycloalkanes (Atkinson *et al.*, 1995a; Eberhard *et al.*, 1995; Kwok *et al.*, 1996b; Atkinson, 1997a,b; Aschmann *et al.*, 1997, 2001a; Arey *et al.*, 2001). However, branched alkanes are important, accounting for ~30-50% of the alkanes other than methane in urban areas (Hoekman, 1992; Seila *et al.*, 1989). Accordingly, in this work we have investigated the products and mechanism of the OH radical-initiated reaction of 2,2,4-trimethylpentane (isooctane) in the presence of NO. In addition to the use of gas chromatography for product analyses, we have used atmospheric pressure ionization tandem mass spectrometry to identify reaction products not amenable to gas chromatography. 2,2,4-Trimethylpentane-d₁₈ was also used in the experiments with API-MS analyses to aid in the interpretation of the API-MS spectra.

2.1.2. Experimental Methods

Experiments were carried out at 298 ± 2 K and 740 Torr total pressure of air (at ~5% relative humidity) in a 7900 liter Teflon chamber with analysis by gas chromatography with

flame ionization detection (GC-FID) and combined gas chromatography-mass spectrometry (GC-MS), with irradiation provided by two parallel banks of blacklamps; and in a 7300 liter Teflon chamber interfaced to a PE SCIEX API III MS/MS direct air sampling, atmospheric pressure ionization tandem mass spectrometer (API-MS), again with irradiation provided by two parallel banks of blacklamps. Both chambers are fitted with Teflon-coated fans to ensure rapid mixing of reactants during their introduction into the chamber.

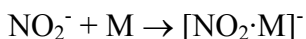
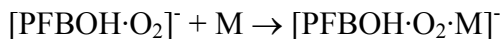
Hydroxyl radicals were generated in the presence of NO by the photolysis of methyl nitrite in air at wavelengths >300 nm (Kwok *et al.*, 1996b; Aschmann *et al.*, 1997, 2001a; Arey *et al.*, 2001), and NO was added to the reactant mixtures to suppress the formation of O₃ and hence of NO₃ radicals.

2.1.2.1. Analyses by GC-FID and GC-MS. For the reactions carried out in the 7900 liter Teflon chamber (at ~5% relative humidity), the initial reactant concentrations (in molecule cm⁻³ units) were: CH₃ONO, (2.2-2.4) x 10¹⁴; NO, (1.9-2.2) x 10¹⁴; and 2,2,4-trimethylpentane, (2.24-3.02) x 10¹³. Irradiations were carried out at 20% of the maximum light intensity for 10-45 min, resulting in up to 23% reaction of the initially present 2,2,4-trimethylpentane. The concentrations of 2,2,4-trimethylpentane and reaction products were measured during the experiments by GC-FID. Gas samples of 100 cm³ volume were collected from the chamber onto Tenax-TA solid adsorbent, with subsequent thermal desorption at ~250 °C onto a DB-1701 megabore column in a Hewlett Packard (HP) 5710 GC, initially held at -40 °C and then temperature programmed to 200 °C at 8 °C min⁻¹. In addition, gas samples were collected onto Tenax-TA solid adsorbent for GC-MS analyses, with thermal desorption onto a 60 m HP-5 fused silica capillary column in an HP 5890 GC interfaced to a HP 5970 mass selective detector operating in the scanning mode. GC-FID response factors were determined as described previously (Atkinson *et al.*, 1995b). NO and initial NO₂ concentrations were measured using a Thermo Environmental Instruments, Inc., Model 42 NO-NO₂-NO_x chemiluminescence analyzer.

2.1.2.2. Analyses by API-MS. In the experiments with API-MS analyses, the chamber contents were sampled through a 25 mm diameter x 75 cm length Pyrex tube at ~20 liter min⁻¹ directly into the API mass spectrometer source. The operation of the API-MS in the MS (scanning) and MS/MS [with collision activated dissociation (CAD)] modes has been described elsewhere (Kwok *et al.*, 1996b; Aschmann *et al.*, 1997, 2001a; Arey *et al.*, 2001). Use of the MS/MS mode with CAD allows the "product ion" or "precursor ion" spectrum of a given ion peak observed in the MS scanning mode to be obtained (Kwok *et al.*, 1996b; Aschmann *et al.*, 1997, 2001a; Arey *et al.*, 2001). Both positive and negative ion modes were used in this work.

In the positive ion mode, protonated water clusters, H₃O⁺(H₂O)_n, formed from a corona discharge in the chamber diluent air (at ~5% relative humidity) are the reagent ion and a range of oxygenated species can be observed in this mode of operation (Kwok *et al.*, 1996b; Aschmann *et al.*, 1997, 2001a; Arey *et al.*, 2001). In the negative ion mode, the superoxide ion (O₂⁻), its hydrates [O₂(H₂O)_n]⁻, and O₂ clusters [O₂(O₂)_n]⁻ are the major reagent negative ions in the chamber pure air. Other reagent ions, for example, NO₂⁻ and NO₃⁻, are formed through reactions between the primary reagent ions and neutral molecules such as NO₂, and instrument tuning and operation were designed to induce cluster formation. Two negative ions were used as reagent ions in this work; NO₂⁻ present in the irradiated CH₃ONO - NO - 2,2,4-trimethylpentane - air mixtures, and [PFBOH·O₂]⁻ (where PFBOH = pentafluorobenzyl alcohol, C₆F₅CH₂OH) generated by addition of pentafluorobenzyl alcohol to the sampled air stream from the chamber from a heated vial containing PFBOH (Arey *et al.*, 2001). Analytes were then detected as adducts formed between the neutral analyte (M) and the reagent ion (NO₂⁻ or [PFBOH·O₂]⁻),

where M can also be PFBOH when PFBOH was added to the sampled air stream.



Previous work in this laboratory (Arey *et al.*, 2001; Aschmann *et al.*, 2001a) indicates that the use of NO_2^- or $[\text{PFBOH}\cdot\text{O}_2]^-$ reagent ions allows primarily hydroxy-compounds to be detected (for example, hydroxycarbonyls and hydroxynitrates). When NO_2^- was used as the reagent ion, quantification of hydroxycarbonyls was carried out (Arey *et al.*, 2001) by adding a measured amount of 5-hydroxy-2-pentanone to the chamber after the irradiation as an internal standard and assuming that the intensities of the $[\text{NO}_2\cdot\text{M}]^-$ ion peaks were proportional to the concentrations of the hydroxycarbonyls, M, present in the chamber (including M = 5-hydroxy-2-pentanone) (Arey *et al.*, 2001).

In the positive or negative ion modes, ions are then drawn by an electric potential from the ion source through the sampling orifice into the mass-analyzing first quadrupole or third quadrupole. Neutral molecules and particles are prevented from entering the orifice by a flow of high-purity nitrogen ("curtain" gas). The initial concentrations of CH_3ONO , NO and 2,2,4-trimethylpentane (or 2,2,4-trimethylpentane- d_{18}) were $\sim(2.4\text{-}4.8) \times 10^{13}$ molecule cm^{-3} each, and irradiations were carried out at the maximum light intensity for 1-3 min (resulting in up to $\sim 15\%$ reaction of the initially present 2,2,4-trimethylpentane).

2.1.2.3. Chemicals. The chemicals used, and their stated purities, were: 4,4-dimethyl-2-pentanone (99%), 2,2-dimethylpropanal (97%), 4-hydroxy-4-methyl-2-pentanone (%), 2-methylpropanal (99+%), octanal (99%), pentafluorobenzyl alcohol (98%) and 2,2,4-trimethylpentane (99%), Aldrich Chemical Company; 5-hydroxy-2-pentanone , TCI America; 2,2,4-trimethylpentane- d_{18} (98% atom D), C/D/N Isotopes, Inc.; 3-octyl nitrate, Fluorochem, Inc.; and NO ($\geq 99.0\%$), Matheson Gas Products. Methyl nitrite was prepared and stored as described previously (Taylor *et al.*, 1980).

2.1.3. Results

2.1.3.1. GC-FID and GC-MS Analyses

GC-FID and GC-MS analyses of irradiated CH_3ONO - NO - 2,2,4-trimethylpentane - air mixtures showed the formation of acetone, 2-methylpropanal and 4-hydroxy-4-methyl-2-pentanone. As discussed below, consideration of the potential reactions involved indicated that a number of other product species could be formed, including acetaldehyde, 2,2-dimethylpropanal and 4,4-dimethyl-2-pentanone, which can be observed by gas chromatography. However, GC-FID analyses showed no evidence for the formation of these three potential products, and upper limits to their concentrations were obtained. Secondary reactions of acetone, 2-methylpropanal and 4-hydroxy-4-methyl-2-pentanone (and of the potential products acetaldehyde, 2,2-dimethylpropanal and 4,4-dimethyl-2-pentanone) with the OH radical during these experiments were taken into account as described previously (Atkinson *et al.*, 1982) using rate constants for reactions of the OH radical (in units of 10^{-12} cm^3 molecule $^{-1}$ s $^{-1}$) of: 2,2,4-trimethylpentane, 3.57 (Atkinson, 1997a); acetaldehyde, 15.8 (Atkinson, 1994), acetone, 0.219 (Atkinson, 1994); 2-methylpropanal, 26.3 (Atkinson, 1994); 4-hydroxy-4-methyl-2-pentanone, 4.0 (Atkinson and Aschmann, 1995); 2,2-dimethylpropanal, 26.5 (Atkinson, 1994); and 4,4-dimethyl-2-pentanone, 1.47 [estimated (Kwok and Atkinson, 1995)]. The multiplicative factors F to take into account the secondary reactions of OH radicals with the products increase with the rate constant ratio

$k(\text{OH} + \text{product})/k(\text{OH} + 2,2,4\text{-trimethylpentane})$ and with the extent of reaction (Atkinson *et al.*, 1982), and the maximum values of F were 1.01 for acetone, 1.74 for acetaldehyde, 2.38 for 2-methylpropanal and 2,2-dimethylpropanal, 1.16 for 4-hydroxy-4-methyl-2-pentanone, and 1.06 for 4,4-dimethyl-2-pentanone. The formation yields (or upper limits thereof) of these first-generation products obtained by least-squares analyses of the data (Figure 3) are given in Table 2. While no obvious GC peaks were observed in the GC-FID analyses which could be attributed to C₈-carbonyls or to C₈-nitrates, GC-MS analysis of an irradiated CH₃ONO - NO - 2,2,4-trimethylpentane - air mixture showed the presence of two closely eluting peaks with high-mass ions at m/z 128 (and more intense fragments at m/z 127, 109 (-HCO) and 43) and of three peaks with fragment ions at 46 u (interpreted as organic nitrates). However, no isomer-specific identifications could be made and no obvious corresponding peaks were observed in the GC-FID analyses and hence no quantifications could be made.

2.1.3.2. API-MS Analyses

A series of CH₃ONO - NO - 2,2,4-trimethylpentane (or 2,2,4-trimethylpentane-d₁₈) - air irradiations were carried out with analyses using *in situ* API-MS. In these analyses, the API-MS was operated in the positive ion mode, or in negative ion mode with NO₂⁻ or [PFBOH·O₂]⁻ ions as an ionizing agent. Using the positive ion mode, API-MS/MS "product ion" and "precursor ion" spectra were obtained for ion peaks observed in the API-MS analyses of the products of the reactions of OH radicals with 2,2,4-trimethylpentane and 2,2,4-trimethylpentane-d₁₈. Product peaks were identified based on the observation of homo- or hetero-dimers (for example, [(M_{P1})₂+H]⁺, [(M_{P2})₂+H]⁺ and [M_{P1}+M_{P2}+H]⁺, where P1 and P2 are products) in the API-MS/MS "precursor ion" spectra, and consistency of the API-MS/MS "product ion" spectrum of a homo- or hetero-dimer ion with the "precursor ion" spectra of the [M_P+H]⁺ ion peaks (Aschmann *et al.*, 1997). Water cluster ion peaks of the product ions, [M+H+H₂O]⁺, were also occasionally observed. The products observed from the OH radical-initiated reaction of 2,2,4-trimethylpentane in the presence of NO are shown in Table 2. The positive-ion API-MS and API-MS/MS analyses indicate the formation of products of molecular weight 58 (assumed to be acetone, quantified by GC-FID), 72 (assumed to be 2-methylpropanal, quantified by GC-FID), 116 [assumed to be 4-hydroxy-4-methyl-2-pentanone, quantified by GC-FID), 128, 130, 144, 177 and 191. As expected from the odd molecular weights, API-MS/MS "product ion" analyses of the [M+H]⁺ ion peaks of the two products of molecular weight 177 and 191 showed the presence of fragment ions at 46 u (NO₂⁺) and are therefore attributed to organic nitrates. API-MS and API-MS/MS analyses of irradiated CH₃ONO - NO - 2,2,4-trimethylpentane-d₁₈ - air mixtures were less conclusive, because of the lower reactivity of 2,2,4-trimethylpentane-d₁₈ relative to 2,2,4-trimethylpentane which limited the extent of reaction, but indicated the formation of products of molecular weight 64 (acetone-d₆), 80 (2-methylpropanal-d₈), 144 (which could include a protonated heterodimer of acetone-d₆ and 2-methylpropanal-d₈), 159, 191 and 207. API-MS/MS "product ion" spectra of the 145 u ion peak showed losses of HDO and D₂O, indicating that no -OH groups are present in this compound [OD groups rapidly exchange to OH groups under our experimental conditions], while API-MS/MS "product ion" spectra of the 160, 256 (protonated heterodimer of acetone-d₆ and molecular weight 191

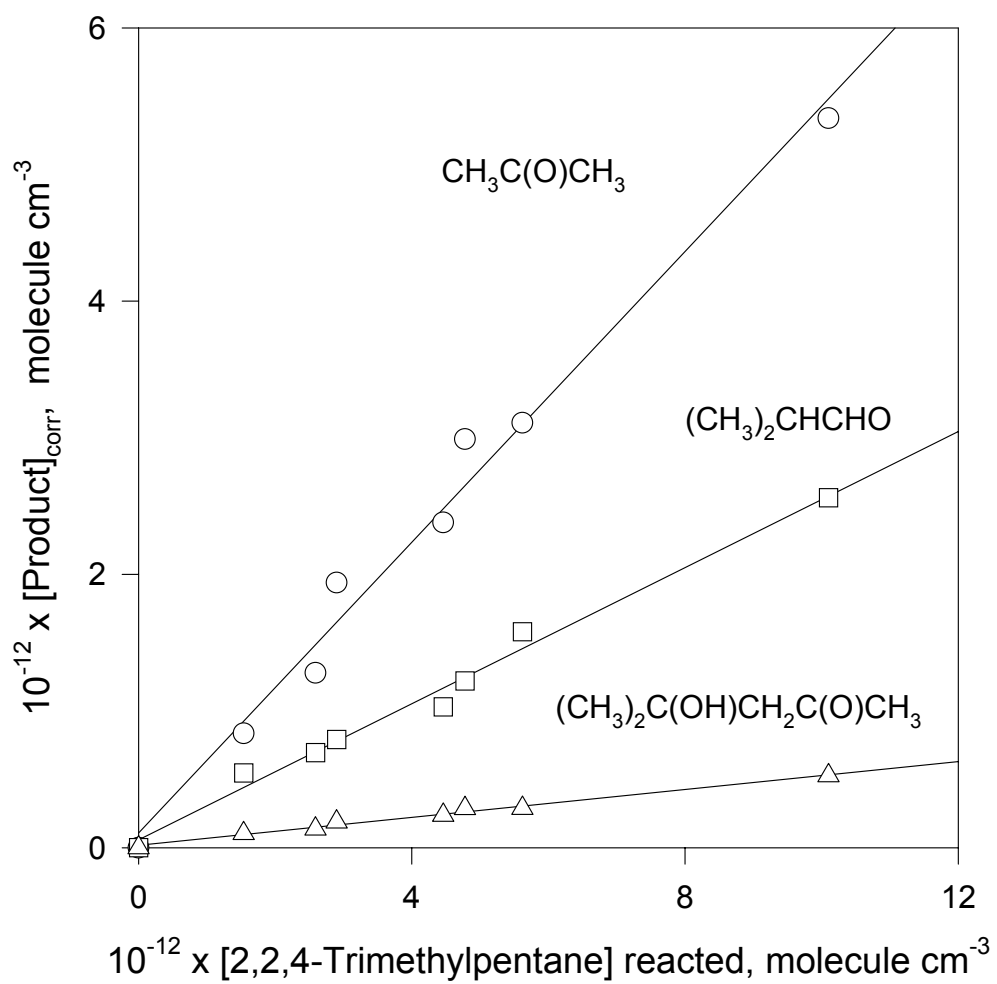


Figure 3. Plots of the amounts of acetone, 2-methylpropanal and 4-hydroxy-4-methyl-2-pentanone formed, corrected for reaction with the OH radical (see text), against the amounts of 2,2,4-trimethylpentane reacted.

Table 2. Products observed, and their molar formation yields, from the OH radical-initiated reaction of 2,2,4-trimethylpentane in the presence of NO

product	GC-FID ^a	API-MS
acetaldehyde	<0.04	
acetone	0.58 ± 0.13 ^b 0.53 ± 0.07 ^b 0.54 ± 0.07 ^c	observed ^{d,e}
2-methylpropanal	0.28 ± 0.05 ^b 0.25 ± 0.03 ^b 0.26 ± 0.03 ^c	observed ^e
4-hydroxy-4-methyl-2-pentanone (molecular weight 116)	0.051 ± 0.006	observed ^{d,f,g} yield ~0.08
2,2-dimethylpropanal	<0.013	
4,4-dimethyl-2-pentanone	<0.004	
molecular weight 128 product (CH ₃) ₃ CCH ₂ CH(CH ₃)CHO ^h		observed ^{d,e}
molecular weight 130 product HOCH ₂ C(CH ₃) ₂ CH ₂ C(O)CH ₃ ^h		observed ^{d,f,g} yield ~0.03
molecular weight 135 product C ₄ -hydroxyalkyl nitrate ^h		observed ^{f,g}
molecular weight 144 product (CH ₃) ₂ C(OH)CH ₂ C(CH ₃)CHO ^h		observed ^{d,g} yield ~0.03
molecular weight 177 species C ₇ -hydroxyalkyl nitrate ^h		observed ^{d,f,g}
molecular weight 191 species C ₈ -hydroxyalkyl nitrate ^h		observed ^{d,f,g}

^aErrors are two least-squares standard deviations combined with estimated overall uncertainties in the GC-FID response factors for 2,2,4-trimethylpentane and products, of ±5% each.

^bIndependent determinations.

^cWeighted average.

^dIn positive ion mode from the 2,2,4-trimethylpentane-h₁₈ reaction.

^eCorresponding product observed in positive ion mode from the 2,2,4-trimethylpentane-d₁₈ reaction.

^fIn negative ion mode with [PFBOH·O₂]⁻ ions from the 2,2,4-trimethylpentane-h₁₈ reaction.

^gIn negative ion mode with NO₂⁻ ions from the 2,2,4-trimethylpentane-h₁₈ reaction.

^hAttributed, see text and Table 3.

product) and 272 (protonated heterodimer of acetone-d₆ and molecular weight 207 product) u ion peaks showed losses of H₂O only, indicating the presence of -OH groups in the molecular weight 159, 191 and 207 products. exchange to -OH groups under our experimental conditions], while API-MS/MS "product ion" spectra of the 160, 256 (protonated heterodimer of acetone-d₆ and molecular weight 191 product) and 272 (protonated heterodimer of acetone-d₆ and molecular weight 207 product) u ion peaks showed losses of H₂O only, indicating the presence of -OH groups in the molecular weight 159, 191 and 207 products.

As noted in the Experimental section above, when using the negative ion mode, [PFBOH·O₂]⁻ forms trimers [PFBOH·O₂·M]⁻ with certain species M (where M includes PFBOH). API-MS/MS "product ion" spectra of the trimers [PFBOH·O₂·M]⁻ then show a fragment ion at 230 u ([PFBOH·O₂]⁻), with the difference in mass of the trimer ion and the 230 u [PFBOH·O₂]⁻ fragment ion being the molecular weight of the product M (Arey *et al.*, 2001). Additional fragment ions are also observed at [M·O₂]⁻ as well as at 165 and 193 u (the latter two from the [PFBOH·O₂]⁻ ion. API-MS and API-MS/MS analyses of irradiated CH₃ONO - NO - 2,2,4-trimethylpentane - air mixtures were carried out in the negative ion mode with PFBOH added to the sampled gas stream. API-MS/MS "precursor ion" spectra of the 230 u [PFBOH·O₂]⁻ ion showed ion peaks at 346, 360 (weak), 365 (weak), 407, 421, 428 ([PFBOH]₂·O₂]⁻), and 458 ([PFBOH]₂·O₂·NO]⁻) u (Figure 4). API-MS/MS "product ion" spectra of the ion peaks at 346, 365, 407 and 421 u showed consistency with these ion peaks being [PFBOH·O₂·M]⁻ ions and hence the presence of products of molecular weight 116, 135, 177 and 191 containing an hydroxyl group (and possibly also a product of molecular weight 130). Using NO₂⁻ as the ionizing agent, [NO₂·M]⁻ adduct ions were observed at 162, 172, 176, 181, 206, 223 and 237 u, corresponding to products of molecular weight 116, 126, 130, 135, 160, 177 and 191 (and with the most intense signals being from the products of molecular weight 116, 135, 177 and 191). A number of weaker ion peaks were also observed, including one corresponding to a molecular weight 144 product (see below).

Using 5-hydroxy-2-pentanone as an internal standard added after irradiation of a CH₃ONO - NO - 2,2,4-trimethylpentane - air mixture allowed approximate quantification of the molecular weight 116, 130 and 144 products, with formation yields of ~8%, ~3% and ~3%, respectively, after correction for secondary reactions using the measured (Atkinson and Aschmann, 1995) or estimated (Kwok and Atkinson, 1995) OH radical reaction rate constants for the products of these molecular weights predicted from the reaction mechanism [corrections for secondary reactions were only significant for the molecular weight 144 product attributed to (CH₃)C(OH)CH₂C(CH₃)₂CHO, with an estimated multiplicative correction factor of 1.76]. The negative ion mode analyses confirm the formation of the molecular weight 116, 130, 135, 144, 177 and 191 products suggested by the positive ion mode analyses and suggest that the molecular weight 116, 130 and 144 products are hydroxycarbonyls (with the molecular weight 116 product being 4-hydroxy-4-methyl-2-pentanone) and that the molecular weight 135, 177 and 191 products are hydroxynitrates.

2.1.4. Discussion

The product data given in Table 2 allow the reaction pathways to be delineated to a reasonable extent. OH radicals can react with 2,2,4-trimethylpentane at four positions; the three equivalent CH₃ groups attached to the 2-carbon (11%), the secondary CH₂ group at the 3-position (30%), the tertiary CH group at the 4-position (52%), and the two equivalent CH₃ groups attached to the 4-carbon (7%), where the numbers in parentheses are the percentages of the four reaction pathways calculated using the estimation method of Kwok and Atkinson (1995)

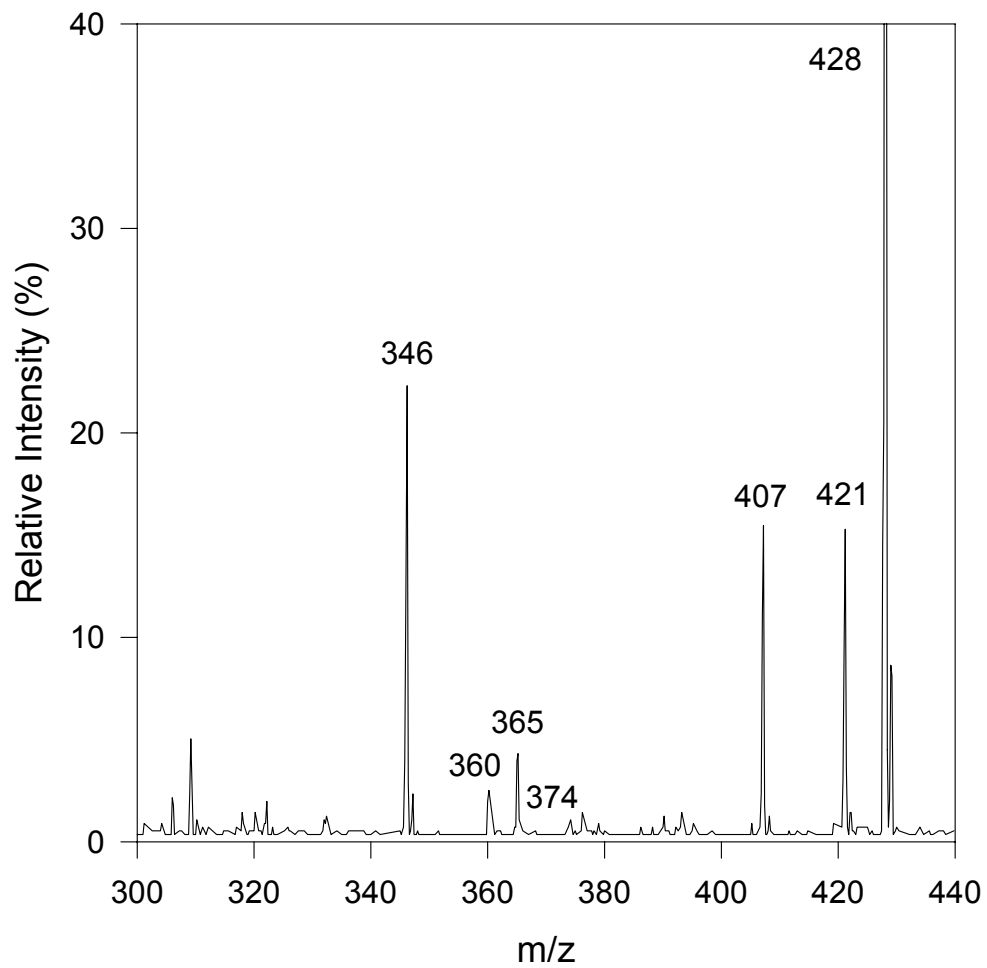


Figure 4. API-MS/MS CAD "precursor ion" spectrum (negative ion mode) of the $[\text{PFBOH}\cdot\text{O}_2]^-$ reagent ion in an irradiated $\text{CH}_3\text{ONO} - \text{NO} - 2,2,4\text{-trimethylpentane} - \text{air}$ mixture.

[these calculated percentages may be subject to significant uncertainties, especially because the total rate constant for 2,2,4-trimethylpentane is overpredicted by 30%]. After H-atom abstraction from these various C-H bonds, the resulting alkyl radicals add O₂ to form alkyl peroxy radicals which under our experimental conditions then react with NO to form the corresponding alkoxy radical (C₈H₁₇O[•]) plus NO₂ or the alkyl nitrate (C₈H₁₇ONO₂, of molecular weight 175), as shown in reactions (1) through (3) in the Introduction. As noted in the Introduction, the four C₈H₁₇O alkoxy radicals can react with O₂, unimolecularly decompose by C-C bond scission, or isomerize through a 6-membered ring transition state to form a 1,4-hydroxyalkyl radical (Atkinson, 1994, 1997a,b), with not all of these reaction pathways being possible for all four alkoxy radicals initially formed from 2,2,4-trimethylpentane.

Figures 5-8 show the potential reactions of the four C₈H₁₇O[•] alkoxy radicals leading to first-generation products. In these reaction schemes, detailed reactions are omitted for CH₃C[•]HCH₃, (CH₃)₃C[•], (CH₃)₂CHC[•]H₂, and (CH₃)₂C(OH)C[•]H₂ radicals, which are known to react in the atmosphere to form CH₃C(O)CH₃, CH₃C(O)CH₃ + HCHO, (CH₃)₂CHCHO, and CH₃C(O)CH₃ + HCHO, respectively (Atkinson, 1994, 1997a,b), and decomposition or isomerization of 1,2-hydroxyalkoxy radicals is assumed to dominate over their reaction with O₂ (Atkinson, 1997a,b). The rates of the decomposition, isomerization and reaction with O₂ of the various alkoxy and hydroxyalkoxy radicals involved in Schemes 1-4 were calculated using the estimation methods described by Atkinson (1997a,b), as revised by Aschmann and Atkinson (1999). The calculated rates of these reactions are not shown in Figures 5-8, rather the relative importance of the various reactions of a given alkoxy radical are denoted by the arrows: a dashed arrow indicates that that reaction pathway is estimated to account for ≤1% of the overall reaction rate of the alkoxy radical, and a large, boldface, arrow indicates that the reaction pathway is estimated to dominate over the other(s) by a factor of ≥10. The reactions of the four initially-formed C₈H₁₇O radicals are discussed below and compared with the products observed. It should be noted that the four expected C₈H₁₇ONO₂ nitrates formed from the reactions of the four C₈H₁₇O₂ radicals with NO [reaction (3a)] were not identified by either gas chromatographic or API-MS analyses; lack of authentic standards precluded identification by gas chromatography.

•OCH₂C(CH₃)₂CH₂CH(CH₃)₂ Radical (11%).

Figure 5 shows that this alkoxy radical can react with O₂, decompose or isomerize, with predicted reaction rates at 298 K and atmospheric pressure of air of 4.9 x 10⁴ s⁻¹, 1 x 10⁶ s⁻¹ and 5 x 10⁶ s⁻¹, respectively (Atkinson, 1997a,b; Aschmann and Atkinson, 1999). Because isomerization of the HOCH₂C(CH₃)₂CH₂C(O[•])(CH₃)₂ radical is predicted to dominate over decomposition by a factor of ~12, the dominant predicted product from the •OCH₂C(CH₃)₂CH₂CH(CH₃)₂ radical is the molecular weight 144 compound (CH₃)₂C(OH)CH₂C(CH₃)₂CHO (consistent with our API-MS analyses, including of the 2,2,4-trimethylpentane-d₁₈ reaction where a product of molecular weight 159 was observed). In addition, acetone + acetone, acetone + 2-methylpropanal, 4-hydroxy-4-methyl-2-pentanone [(CH₃)₂C(OH)CH₂C(O)CH₃], and the molecular weight 130 compound (CH₃)₂C(OH)CH₂CH(CH₃)CHO (products consistent with our GC and API-MS analyses) are predicted to be formed from more minor pathways.

(CH₃)₃CCH(O[•])CH(CH₃)₂ Radical (30%).

Figure 6 shows that this alkoxy radical can react with O₂, decompose to (CH₃)₃CCHO + CH₃C[•]HCH₃, or decompose to (CH₃)₂CHCHO + (CH₃)₃C[•], with predicted reaction rates at 298 K and atmospheric pressure of air of 4.1 x 10⁴ s⁻¹, 3.3 x 10⁵ s⁻¹ and 2.5 x 10⁷ s⁻¹, respectively

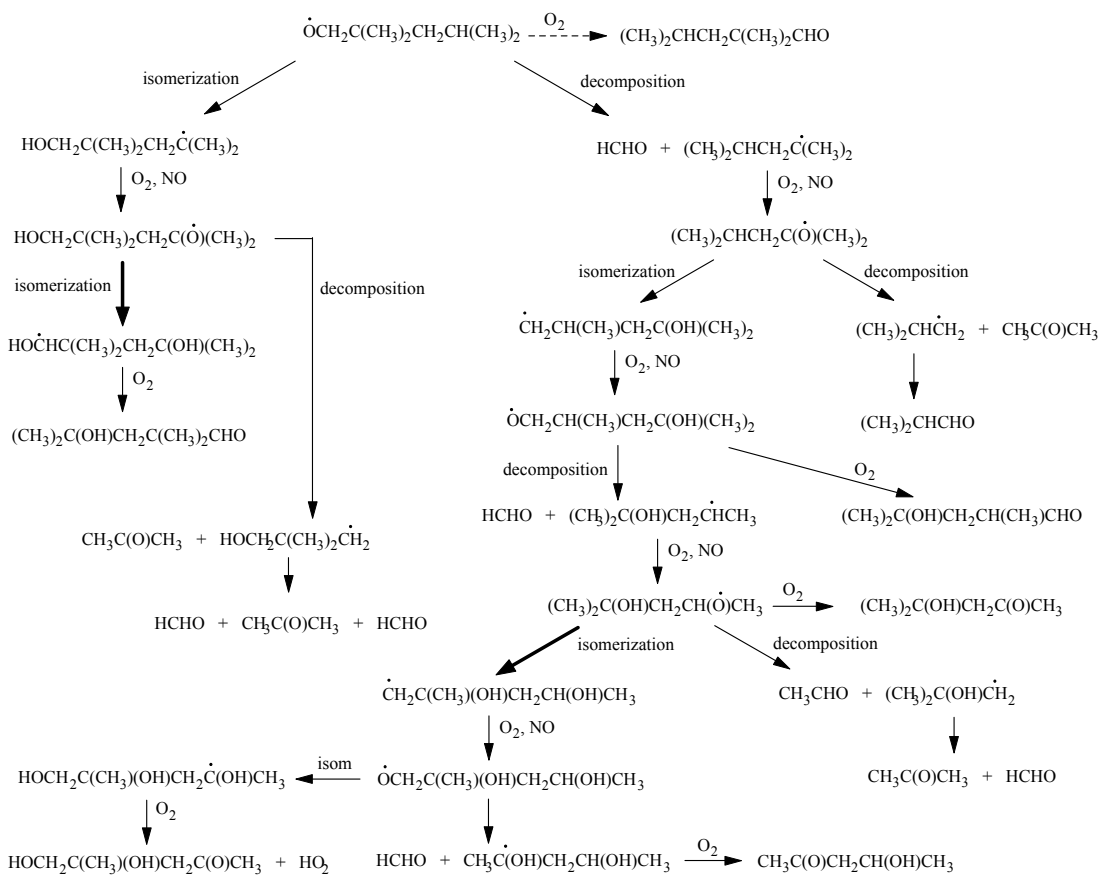


Figure 5. Reaction scheme for the $\dot{\text{O}}\text{CH}_2\text{C}(\text{CH}_3)_2\text{CH}_2\text{CH}(\text{CH}_3)_2$ radical.

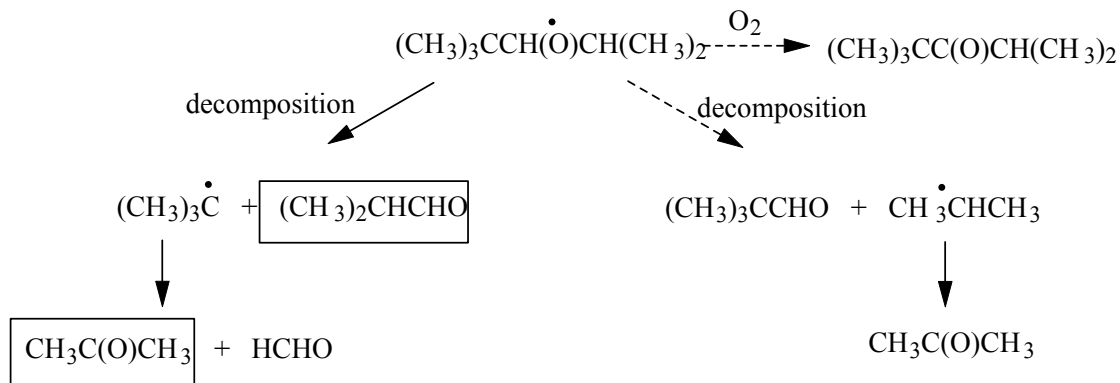


Figure 6. Reaction scheme for the $(\text{CH}_3)_3\text{CCH}(\text{O}^\bullet)\text{CH}(\text{CH}_3)_2$ radical.

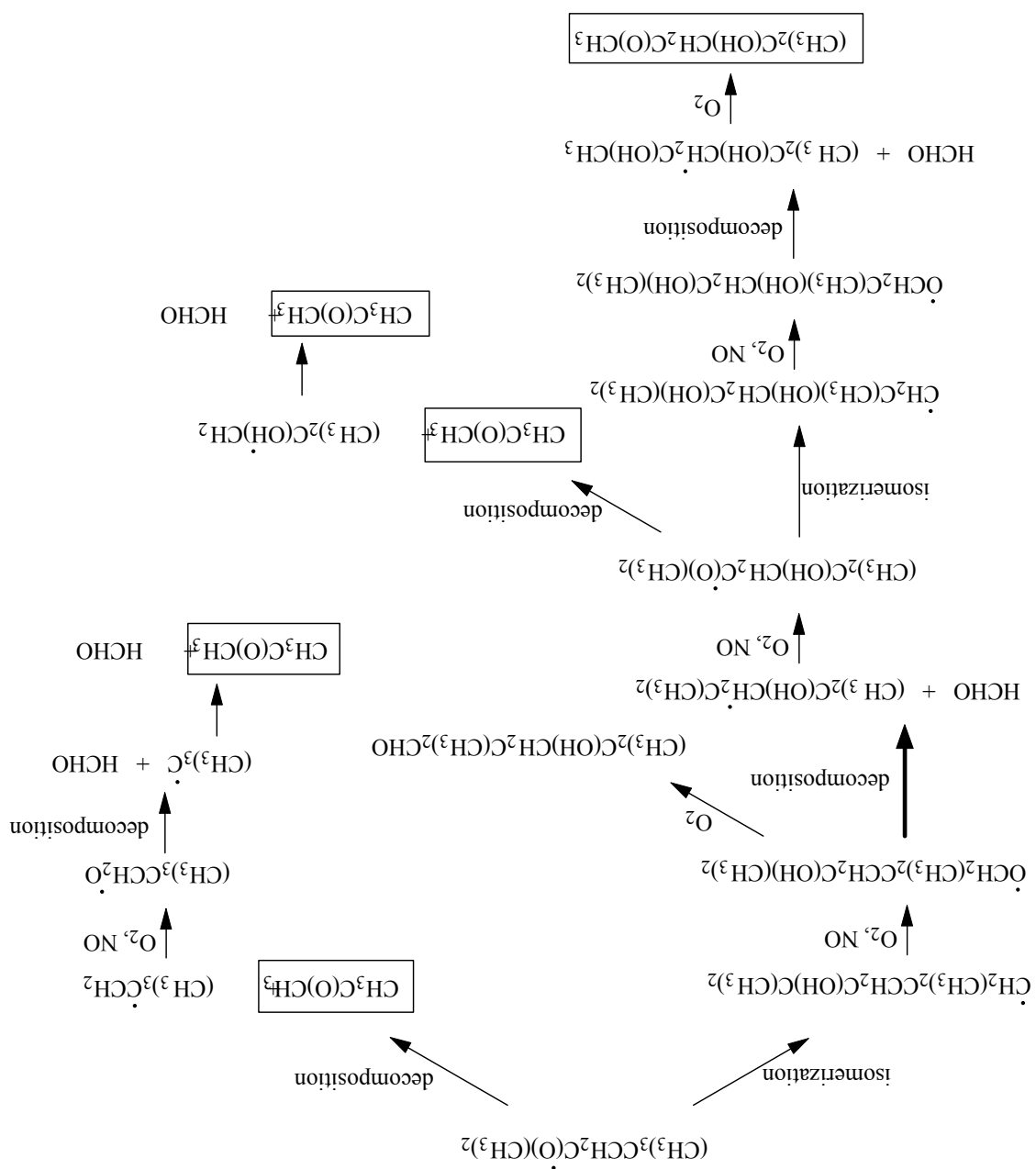
(Atkinson, 1997a,b; Aschmann and Atkinson, 1999). The formation of acetone and 2-methylpropanal as co-products is therefore anticipated to be essentially the only process for the $(\text{CH}_3)_3\text{CCH}(\text{O}^\bullet)\text{CH}(\text{CH}_3)_2$ radical, and our measured formation yield of 2-methylpropanal of $26 \pm 3\%$ is consistent with this expectation (with most or all of the 2-methylpropanal arising from this alkoxy radical decomposition). Furthermore, our lack of observation of 2,2-dimethylpropanal (with a formation yield of $<1.3\%$) confirms the prediction that decomposition of the $(\text{CH}_3)_3\text{CCH}(\text{O}^\bullet)\text{CH}(\text{CH}_3)_2$ radical to $(\text{CH}_3)_3\text{CCHO} + \text{CH}_3\text{C}^\bullet\text{HCH}_3$ is of no importance. Of the acetone observed ($54 \pm 7\%$), $\leq(26 \pm 3)\%$ must be associated with the 2-methylpropanal, leaving $\geq(28 \pm 8)\%$ acetone to be formed via other pathways.

$(\text{CH}_3)_3\text{CCH}_2\text{C}(\text{O}^\bullet)(\text{CH}_3)_2$ Radical (52%).

Figure 7 shows that this alkoxy radical can decompose or isomerize (but not react with O_2 because of the lack of an abstractable α -H atom). The decomposition and isomerization rates are calculated to be equal at $6 \times 10^6 \text{ s}^{-1}$ (Atkinson, 1997a,b; Aschmann and Atkinson, 1999). The $\text{OCH}_2\text{C}(\text{CH}_3)_2\text{CH}_2\text{C}(\text{OH})(\text{CH}_3)_2$ radical formed after the isomerization reaction cannot isomerize, and is calculated to dominantly decompose rather than react with O_2 . The anticipated major products from the $(\text{CH}_3)_3\text{CCH}_2\text{C}(\text{O}^\bullet)(\text{CH}_3)_2$ radical are therefore acetone (with two molecules of acetone formed per molecule of 2,2,4-trimethylpentane reacting) or 4-hydroxy-4-methyl-2-pentanone [$(\text{CH}_3)_2\text{C}(\text{OH})\text{CH}_2\text{C}(\text{O})\text{CH}_3$] (plus 2 HCHO). The predicted dominant decomposition of the $(\text{CH}_3)_3\text{CCH}_2\text{O}^\bullet$ radical is consistent with the observed lack of formation of the O_2 reaction product 3,3-dimethylpropanal (Table 2). Our API-MS and GC data are therefore qualitatively consistent with predictions, although the sum of the formation yields of acetone plus acetone and of 4-hydroxy-4-methyl-2-pentanone ($19 \pm 5\%$) is significantly lower than the predicted importance of H-atom abstraction from the 4-position (Kwok and Atkinson, 1995).

$(\text{CH}_3)_3\text{CCH}_2\text{CH}(\text{CH}_3)\text{CH}_2\text{O}^\bullet$ Radical (7%).

Figure 8 shows that this alkoxy radical can decompose or react with O_2 , and the reaction rates of these two processes are predicted to be essentially identical at $5 \times 10^4 \text{ s}^{-1}$ (Atkinson,

Figure 7. Reaction scheme for the $(\text{CH}_3)_3\text{CCH}_2\text{C}(\text{O})\cdot(\text{CH}_3)_2$ radical.

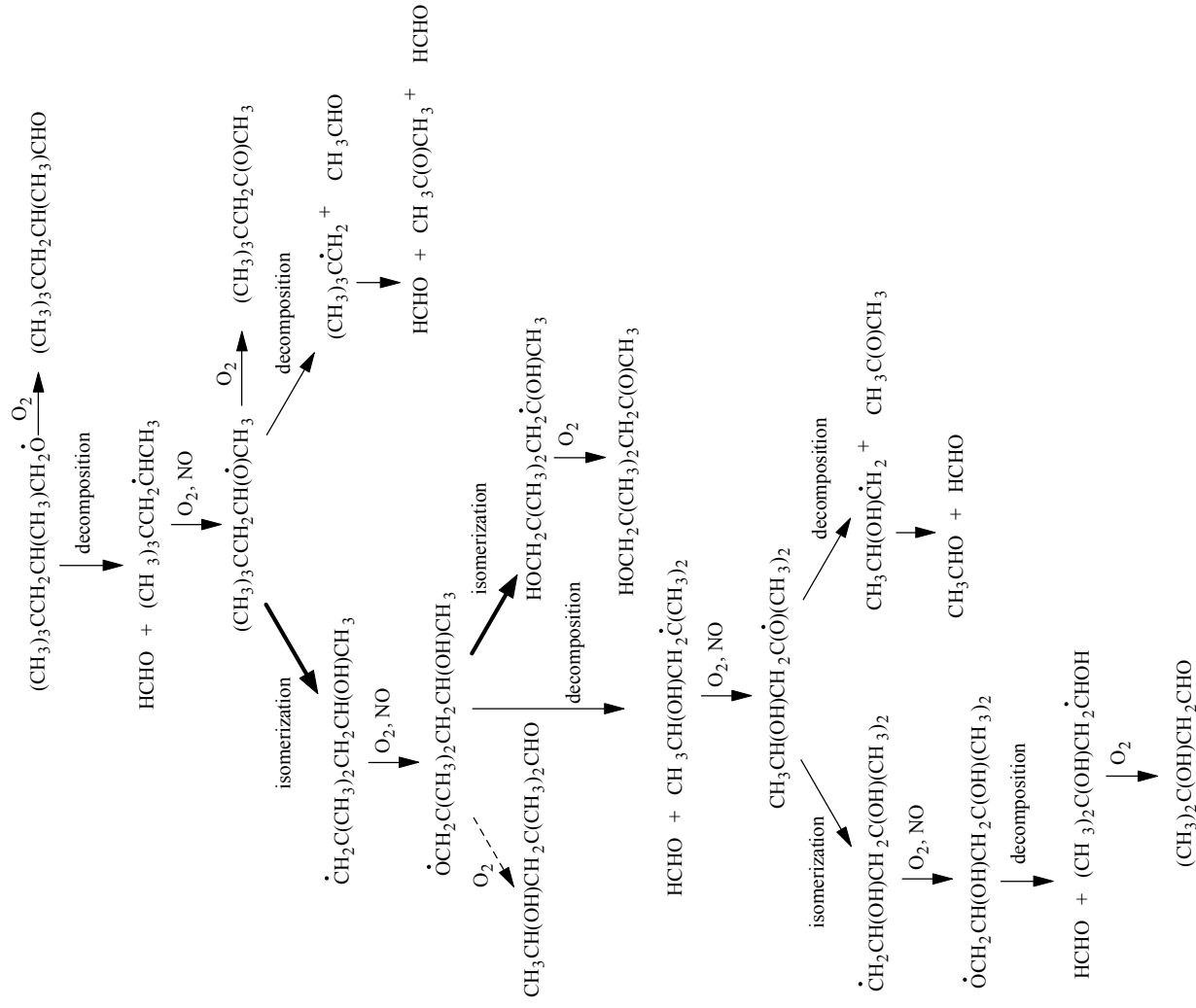


Figure 8. Reaction scheme for the $(\text{CH}_3)_3\text{CCH}_2\text{CH}(\text{CH}_3)\text{CH}_2\text{O}^\bullet$ radical.

1997a,b; Aschmann and Atkinson, 1999). The $(\text{CH}_3)_3\text{CCH}_2\text{CH}(\text{O}^\bullet)\text{CH}_3$ radical formed after the decomposition reaction can react with O_2 , decompose or isomerize with estimated rates of $4.1 \times 10^4 \text{ s}^{-1}$, $6.9 \times 10^4 \text{ s}^{-1}$ and $6 \times 10^5 \text{ s}^{-1}$, respectively (Atkinson, 1997a,b; Aschmann and Atkinson, 1999). Indeed, we observed neither 4,4-dimethyl-2-pentanone (which would be the product of the O_2 reaction) nor CH_3CHO (a product of the decomposition reaction), with formation yields of $<0.4\%$ and $<4\%$, respectively, indicating that reaction of the $(\text{CH}_3)_3\text{CCH}_2\text{CH}(\text{O}^\bullet)\text{CH}_3$ radical with O_2 is of no importance and that the decomposition of this alkoxy radical probably is not dominant. The $^\bullet\text{OCH}_2\text{C}(\text{CH}_3)_2\text{CH}_2\text{CH}(\text{OH})\text{CH}_3$ radical formed after isomerization of the $(\text{CH}_3)_3\text{CCH}_2\text{CH}(\text{O}^\bullet)\text{CH}_3$ radical is predicted to primarily decompose ($1.1 \times 10^6 \text{ s}^{-1}$) or isomerize ($\sim 2 \times 10^7 \text{ s}^{-1}$). Scheme 4 therefore predicts that the major products formed from the $(\text{CH}_3)_3\text{CCH}_2\text{CH}(\text{CH}_3)\text{CH}_2\text{O}^\bullet$ radical are the molecular weight 128 aldehyde $(\text{CH}_3)_3\text{CCH}_2\text{CH}(\text{CH}_3)\text{CHO}$ and the molecular weight 130 hydroxycarbonyl $\text{HOCH}_2\text{C}(\text{CH}_3)_2\text{CH}_2\text{C}(\text{O})\text{CH}_3$, consistent with our API-MS data.

Table 3 shows the initially formed peroxy radicals, their predicted formation yields, and the assignment of observed products. The products quantified by GC-FID and those for which approximate [to within a factor of ~ 2 (Arey *et al.*, 2001)] formation yields were obtained by API-MS analyses account for $51 \pm 10\%$ of the overall products and reaction pathways, with the remainder including alkyl nitrates, hydroxynitrates and the aldehyde $(\text{CH}_3)_3\text{CCH}_2\text{CH}(\text{CH}_3)\text{CHO}$.

In agreement with previous studies of the $\geq \text{C}_4$ alkanes (Atkinson *et al.*, 1995a; Eberhard *et al.*, 1995; Kwok *et al.*, 1996b; Atkinson, 1997; Aschmann *et al.*, 1997, 2001a; Arey *et al.*, 2001), our product data show the importance of alkoxy radical isomerization reactions leading to hydroxycarbonyls and hydroxynitrates.

Table 3. The initially-formed peroxy radicals from the OH radical-initiated reaction of 2,2,4-trimethylpentane in the presence of NO and possible major observed products arising from their subsequent reactions (note that the product yields shown in column 3 are relative to the 2,2,4-trimethylpentane reacted, and not to the peroxy radical shown in column 1)

peroxy radical	yield (%)	products formed and yield (%)	observed by
$\cdot\text{OOCH}_2\text{C}(\text{CH}_3)_2\text{CH}_2\text{CH}(\text{CH}_3)_2$	11	$(\text{CH}_3)_2\text{C}(\text{OH})\text{CH}_2\text{C}(\text{CH}_3)_2\text{CHO}$ (MW 144) (~3%) $\text{HOC}_8\text{H}_{16}\text{ONO}_2$	API-MS API-MS
$(\text{CH}_3)_3\text{CCH}(\text{OO}\cdot)\text{CH}(\text{CH}_3)_2$	30	$\text{CH}_3\text{C}(\text{O})\text{CH}_3 + (\text{CH}_3)_2\text{CHCHO}$ ($26 \pm 3\%$)	GC, API-MS
$(\text{CH}_3)_3\text{CCH}_2\text{C}(\text{OO}\cdot)(\text{CH}_3)_2$	52	2 $\text{CH}_3\text{C}(\text{O})\text{CH}_3$ ($14 \pm 4\%$) $(\text{CH}_3)_2\text{C}(\text{OH})\text{CH}_2\text{C}(\text{O})\text{CH}_3$ (MW 116) ($5.1 \pm 0.6\%$) $\text{HOC}_8\text{H}_{16}\text{ONO}_2$ $\text{HOC}_7\text{H}_{14}\text{ONO}_2$ $\text{HOC}_4\text{H}_8\text{ONO}_2$	GC, API-MS GC, API-MS API-MS API-MS API-MS
$(\text{CH}_3)_3\text{CCH}_2\text{CH}(\text{CH}_3)\text{CH}_2\text{OO}\cdot$	7	$(\text{CH}_3)_3\text{CCH}_2\text{CH}(\text{CH}_3)\text{CHO}$ (MW 128) $\text{HOCH}_2\text{C}(\text{CH}_3)_2\text{CH}_2\text{C}(\text{O})\text{CH}_3$ (MW 130) (~3%) $\text{HOC}_7\text{H}_{14}\text{ONO}_2$	API-MS API-MS API-MS

2.2. Products and Mechanism of the Reaction of OH Radicals with 2,3,4-Trimethylpentane in the Presence of NO

2.2.1. Introduction

Alkanes are important constituents of gasoline fuel, vehicle exhaust and non-methane organic compounds (NMOCs) in urban atmospheres (Hoekman, 1992), accounting for ~50% of NMOCs measured in ambient air in urban areas (Calvert *et al.*, 2002). In the troposphere, alkanes react mainly with the OH radical (Atkinson, 1997a), initiating a series of reactions which, in the presence of NO, lead to formation of alkoxy radicals and alkyl nitrates (Atkinson, 1997a).



The alkoxy radicals formed in reaction (3b) then react with O₂, decompose by C-C bond scission, or isomerize through a 6-membered ring transition state (Atkinson, 1997a). The isomerization reaction results in formation of a 1,4-hydroxyalkyl radical which then leads, after reactions analogous to reactions (2) and (3), to the formation of 1,4-hydroxycarbonyls and 1,4-hydroxynitrates (Eberhard *et al.*, 1995; Kwok *et al.*, 1996b; Arey *et al.*, 2001; Aschmann *et al.*, 2001a).

Rate constants for the reactions of the OH radical with a large number of alkanes have been measured (Atkinson and Arey, 2003). While there have been a number of studies of products formed from the OH radical-initiated reactions of alkanes, most of these have concerned *n*-alkanes and cycloalkanes and several of these studies were concerned only with the alkyl nitrate formation yields (Atkinson, 1994, 1997a). However, branched alkanes account for ~30-50% of the alkanes other than methane in urban areas (Calvert *et al.*, 2002), and comprehensive product studies have only been reported for 2,2,4-trimethylpentane [see Section 2.1 above and Aschmann *et al.* (2002b)] and 3,4-diethylhexane (Aschmann *et al.*, 2001a). In this work we have investigated the kinetics and products of the OH radical-initiated reaction of 2,3,4-trimethylpentane [(CH₃)₂CHCH(CH₃)CH(CH₃)₂] in the presence of NO. The products of this reaction and the relative importance of the three potential alkoxy radical reactions can then be compared to those for the corresponding *n*-octane (Arey *et al.*, 2001) and 2,2,4-trimethylpentane (Aschmann *et al.*, 2002b) reactions.

2.2.2. Experimental Methods

Experiments were carried out at 298 ± 2 K and 740 Torr total pressure of air at ~5% relative humidity in a ~7500 liter Teflon chamber with analysis by gas chromatography with flame ionization detection (GC-FID) and combined gas chromatography-mass spectrometry (GC-MS), with irradiation provided by two parallel banks of blacklamps; and in a ~7500 liter Teflon chamber interfaced to a PE SCIEX API III MS/MS direct air sampling, atmospheric pressure ionization tandem mass spectrometer (API-MS), again with irradiation provided by two parallel banks of blacklamps. Both chambers are fitted with Teflon-coated fans to ensure rapid

mixing of reactants during their introduction into the chamber.

Hydroxyl radicals were generated in the presence of NO by the photolysis of methyl nitrite in air at wavelengths >300 nm, and NO was added to the reactant mixtures to suppress the formation of O₃ and hence of NO₃ radicals.

2.2.2.1. Kinetic Studies

The rate constant for the reaction of OH radicals with 2,3,4-trimethylpentane was measured using a relative rate method, in which the relative decay rates of 2,3,4-trimethylpentane and a reference compound, whose OH radical reaction rate constant is reliably known, are measured in the presence of OH radicals (Aschmann *et al.*, 2001a). Providing that 2,3,4-trimethylpentane and the reference compound (*n*-octane in this case) are removed only by reaction with OH radicals, then,

$$\ln \left(\frac{[2,3,4\text{-TMP}]_{t_0}}{[2,3,4\text{-TMP}]_t} \right) = \frac{k_1}{k_4} \ln \left(\frac{[n\text{-octane}]_{t_0}}{[n\text{-octane}]_t} \right) \quad (\text{I})$$

where [2,3,4-TMP]_{t₀} and [n-octane]_{t₀} are the concentrations of 2,3,4-trimethylpentane and *n*-octane at time t₀, respectively, [2,3,4-TMP]_t and [n-octane]_t are the corresponding concentrations at time t, and k₁ and k₂ are the rate constants for reactions (1) and (4), respectively.



Hence a plot of ln([2,3,4-trimethylpentane]_{t₀}/[2,3,4-trimethylpentane]_t) against ln([n-octane]_{t₀}/[n-octane]_t) should be a straight line of slope k₁/k₄ and zero intercept.

A series of CH₃ONO – NO – 2,3,4-trimethylpentane – *n*-octane – air irradiations were carried out, with initial concentrations (molecule cm⁻³) of: CH₃ONO, ~2.4 x 10¹⁴; NO, ~2.4 x 10¹⁴; and 2,3,4-trimethylpentane and *n*-octane, ~2.4 x 10¹³ each. Irradiations were carried out at 20% of the maximum light intensity for 15–65 min. 2,3,4-Trimethylpentane and *n*-octane were analyzed by GC-FID, using two different procedures. In one, gas samples of 100 cm³ volume were collected from the chamber onto Tenax-TA solid adsorbent, with subsequent thermal desorption at ~250 °C onto a 30 m DB-5MS megabore column, initially held at -40 °C and then temperature programmed to 200 °C at 8 °C min⁻¹. In the second procedure, gas samples were collected from the chamber into 100 cm³ volume gas-tight, all-glass syringe and transferred via a 1 cm³ gas sampling valve onto a 30 m DB-5 megabore column, initially held at -25 °C and then temperature programmed to 200 °C at 8 °C min⁻¹.

2.2.2.3. Product Studies

Analyses by GC-FID and GC-MS. Products were investigated from a series of CH₃ONO – NO – 2,3,4-trimethylpentane – air irradiations, with initial reactant concentrations (in molecule cm⁻³ units) were: CH₃ONO, ~2.4 x 10¹⁴; NO, ~2.4 x 10¹⁴; and 2,3,4-trimethylpentane, (2.69-2.93) x 10¹³. Irradiations were carried out at 20% of the maximum light intensity for 10-60 min, resulting in up to 50% reaction of the initially present 2,3,4-trimethylpentane. The concentrations of 2,3,4-trimethylpentane and reaction products were measured during the

experiments by GC-FID, using the solid adsorbent/thermal desorption procedure. In addition, gas samples were collected onto Tenax-TA solid adsorbent for GC-MS analyses, with thermal desorption onto a 60 m HP-5 fused silica capillary column in an HP 5890 GC interfaced to a HP 5971 mass selective detector operating in the scanning mode. GC-FID response factors were determined as described previously (Atkinson *et al.*, 1995b). NO and initial NO₂ concentrations were measured using a Thermo Environmental Instruments, Inc., Model 42 NO-NO₂-NO_x chemiluminescence analyzer.

Analyses by API-MS. In the experiments with API-MS analyses, the chamber contents were sampled through a 25 mm diameter x 75 cm length Pyrex tube at ~20 liter min⁻¹ directly into the API mass spectrometer source. The operation of the API-MS in the MS (scanning) and MS/MS [with collision activated dissociation (CAD)] modes has been described elsewhere (Aschmann *et al.*, 1997; Arey *et al.*, 2001). Use of the MS/MS mode with CAD allows the "product ion" or "precursor ion" spectrum of a given ion peak observed in the MS scanning mode to be obtained (Aschmann *et al.*, 1997; Arey *et al.*, 2001). Both positive and negative ion modes were used in this work.

In the positive ion mode, protonated water clusters, H₃O⁺(H₂O)_n, formed from a corona discharge in the chamber diluent air (at ~5% relative humidity) are the reagent ion and a range of oxygenated species can be observed in this mode of operation (Aschmann *et al.*, 1997; Arey *et al.*, 2001). In the negative ion mode, the superoxide ion (O₂⁻), its hydrates [O₂(H₂O)_n]⁻, and O₂ clusters [O₂(O₂)_n]⁻ are the major reagent negative ions in the chamber pure air. Other reagent ions, for example, NO₂⁻ and NO₃⁻, are formed through reactions between the primary reagent ions and neutral molecules such as NO₂, and instrument tuning and operation were designed to induce cluster formation. NO₂⁻ present in the irradiated CH₃ONO - NO - 2,3,4-trimethylpentane - air mixtures was used as the reagent ion in the negative ion mode analyses (Arey *et al.*, 2001). Analytes were then detected as adducts, [NO₂⁻M]⁻, formed between the neutral analyte (M) and NO₂⁻. Previous work in this laboratory (Arey *et al.*, 2001) indicates that the use of NO₂⁻ reagent ions allows primarily hydroxy-compounds to be detected (for example, hydroxycarbonyls and hydroxynitrates).

In the positive or negative ion modes, ions are then drawn by an electric potential from the ion source through the sampling orifice into the mass-analyzing first quadrupole or third quadrupole. Neutral molecules and particles are prevented from entering the orifice by a flow of high-purity nitrogen ("curtain" gas). The initial concentrations of CH₃ONO, NO and 2,3,4-trimethylpentane were ~2.4 x 10¹³ molecule cm⁻³ each, and irradiations were carried out at 20% of the maximum light intensity for 10 min.

2.2.2.4. Chemicals. The chemicals used, and their stated purities, were: acetaldehyde (99.5+%), 3-methyl-2-butanone (99%), *n*-octane (99+%), and 2,3,4-trimethylpentane (98%), Aldrich Chemical Company; acetone (HPLC grade), Fisher Scientific; 2-propyl nitrate, Eastman Chemical Company; 3-methyl-2-butyl nitrate and 3-octyl nitrate, Fluorochem, Inc.; and NO (≥99.0%), Matheson Gas Products. Methyl nitrite was prepared and stored as described previously (Taylor *et al.*, 1980).

2.2.3. Results

2.2.3.1. Kinetics

The data obtained from a series of CH₃ONO – NO – 2,3,4-trimethylpentane – *n*-octane – air irradiations are plotted in accordance with Equation (I) in Figure 9. Independent sets of experiments were carried out using (a) collection of gas samples in gas-tight syringes with transfer to the DB-5 column through a gas sampling valve and (b) collection of gas samples onto

Tenax solid adsorbent with thermal desorption onto a DB-5MS column. As evident from Figure 9, the agreement between these data sets is excellent, and a least-squares analysis of the entire data set leads to a rate constant ratio of $k_1/k_4 = 0.844 \pm 0.014$, where the indicated error is two least-squares standard deviations. This rate constant ratio can be placed on an absolute basis by use of a rate constant for the reaction of OH radicals with *n*-octane of $k_4 = 8.11 \times 10^{-12} \text{ cm}^3 \text{ molecule}^{-1} \text{ s}^{-1}$ at 298 K (Atkinson, 2003; Atkinson and Arey, 2003), leading to

$$k_1 = (6.84 \pm 0.12) \times 10^{-12} \text{ cm}^3 \text{ molecule}^{-1} \text{ s}^{-1} \text{ at } 298 \pm 2 \text{ K}$$

where the indicated error does not include the uncertainty in the rate constant k_4 (which is expected to be in the range 10-20%).

2.2.3.2. Products

GC-FID and GC-MS Analyses. GC-FID and GC-MS analyses of irradiated CH₃ONO - NO - 2,3,4-trimethylpentane - air mixtures showed the formation of acetaldehyde, acetone, 3-methyl-2-butanone [CH₃C(O)CH(CH₃)₂], 2-propyl nitrate, 3-methyl-2-butyl nitrate, and a nitrate which eluted at around the same time as 3-octyl nitrate, and hence is presumed to be a C₈ alkyl nitrate. Secondary reactions of acetaldehyde, acetone, 3-methyl-2-butanone, 2-propyl nitrate, 3-methyl-2-butyl nitrate and the C₈-nitrate with the OH radical during these experiments were taken into account as described previously (Atkinson *et al.*, 1982) using rate constants for reactions of the OH radical (in units of 10⁻¹² cm³ molecule⁻¹ s⁻¹) of: 2,3,4-trimethylpentane, 6.84 (this work); acetaldehyde, 15 (IUPAC, 2003), acetone, 0.17 (IUPAC, 2003); 3-methyl-2-butanone, 2.87 (Le Calvé *et al.*, 1998); 2-propyl nitrate, 0.29 (IUPAC, 2003), 3-methyl-2-butyl nitrate, 1.6 (Atkinson *et al.* (1984a), re-evaluated to be consistent with the most recent rate constant (Atkinson, 2003; Atkinson and Arey, 2003) for the *n*-butane reference compound), and C₈-nitrate, ~3.6 [estimated (Kwok and Atkinson, 1995)]. The multiplicative factors *F* to take into account the secondary reactions of OH radicals with the products increase with the rate constant ratio $k(\text{OH} + \text{product})/k(\text{OH} + 2,2,4\text{-trimethylpentane})$ and with the extent of reaction (Atkinson *et al.*, 1982), and the maximum values of *F* were 1.01 for acetone, 2.10 for acetaldehyde, 1.17 for 3-methyl-2-butanone, 1.02 for 2-propyl nitrate, 1.09 for 3-methyl-2-butyl nitrate, and 1.22 for the C₈-nitrate. Plots of the amounts of products formed, corrected for secondary reactions against the amounts of 2,3,4-trimethylpentane reacted are shown in Figures 10 (acetaldehyde, acetone and 3-methyl-2-butanone) and 11 (2-propyl nitrate and 3-methyl-2-butyl nitrate). In the case of acetaldehyde, the acetaldehyde yield appears to increase as the reaction proceeds, suggesting that acetaldehyde is also a second-generation product formed from reactions of other reaction products. The formation yields of these products obtained by least-squares analyses of the data (for acetaldehyde this is the initial formation yield obtained from a second-order regression analysis) are given in Table 4. Note that the GC-FID analyses are relatively insensitive to acetaldehyde and 2-propyl nitrate because of their low GC-FID response factors and hence only small GC peaks were observed for these products, especially for 2-propyl nitrate given its low formation yield.

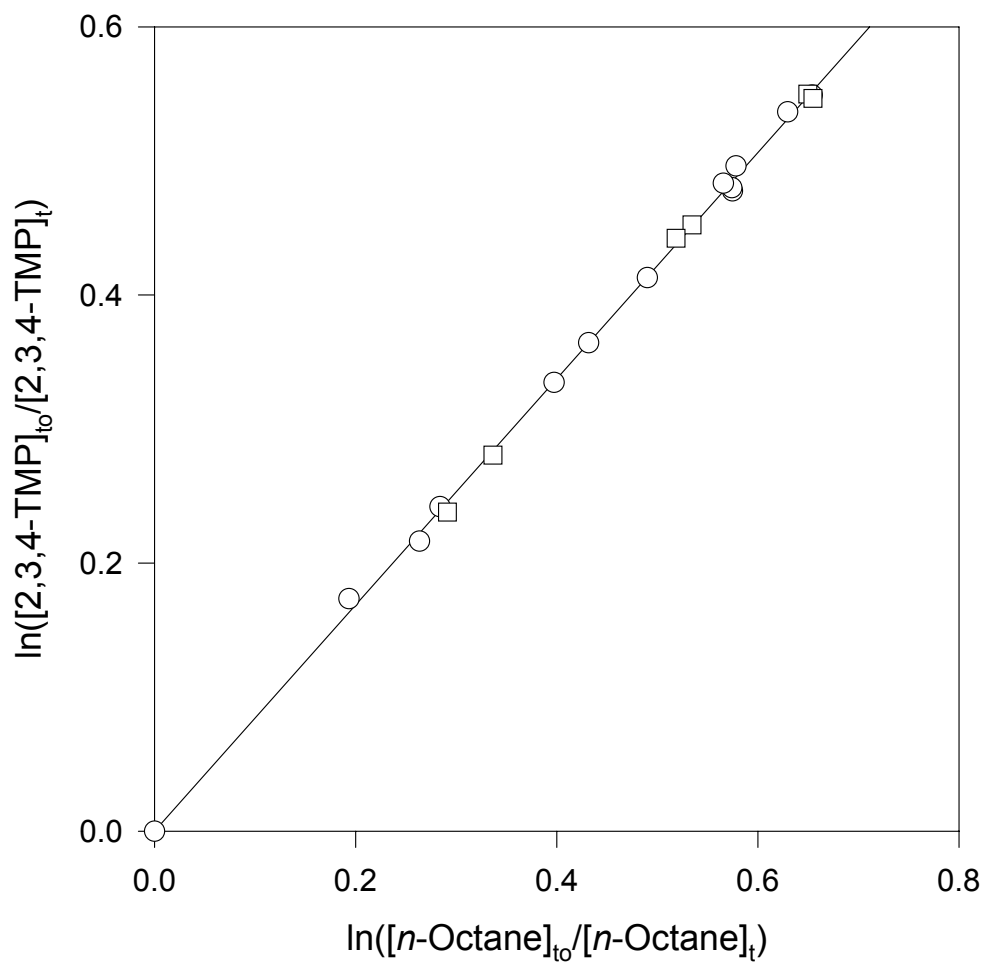


Figure 9. Plot of Equation (I) for the reaction of OH radicals with 2,3,4-trimethylpentane, with *n*-octane as the reference compound.

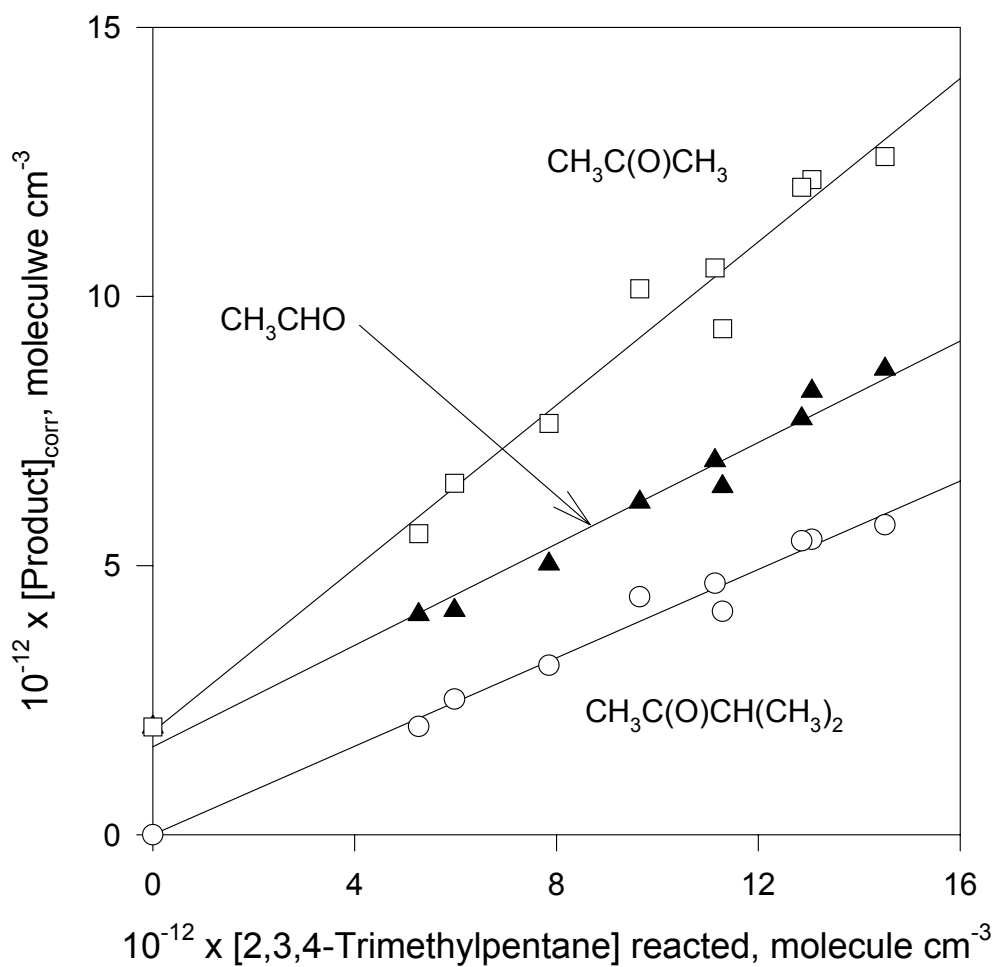


Figure 10. Plots of the amounts of acetaldehyde, acetone and 3-methyl-2-butanone formed, corrected for reaction with the OH radical (see text), against the amounts of 2,3,4-trimethylpentane reacted. The data for acetaldehyde and acetone have been displaced vertically by 2.0×10^{12} molecule cm^{-3} for clarity. The fit for the acetaldehyde data is from a second order regression.

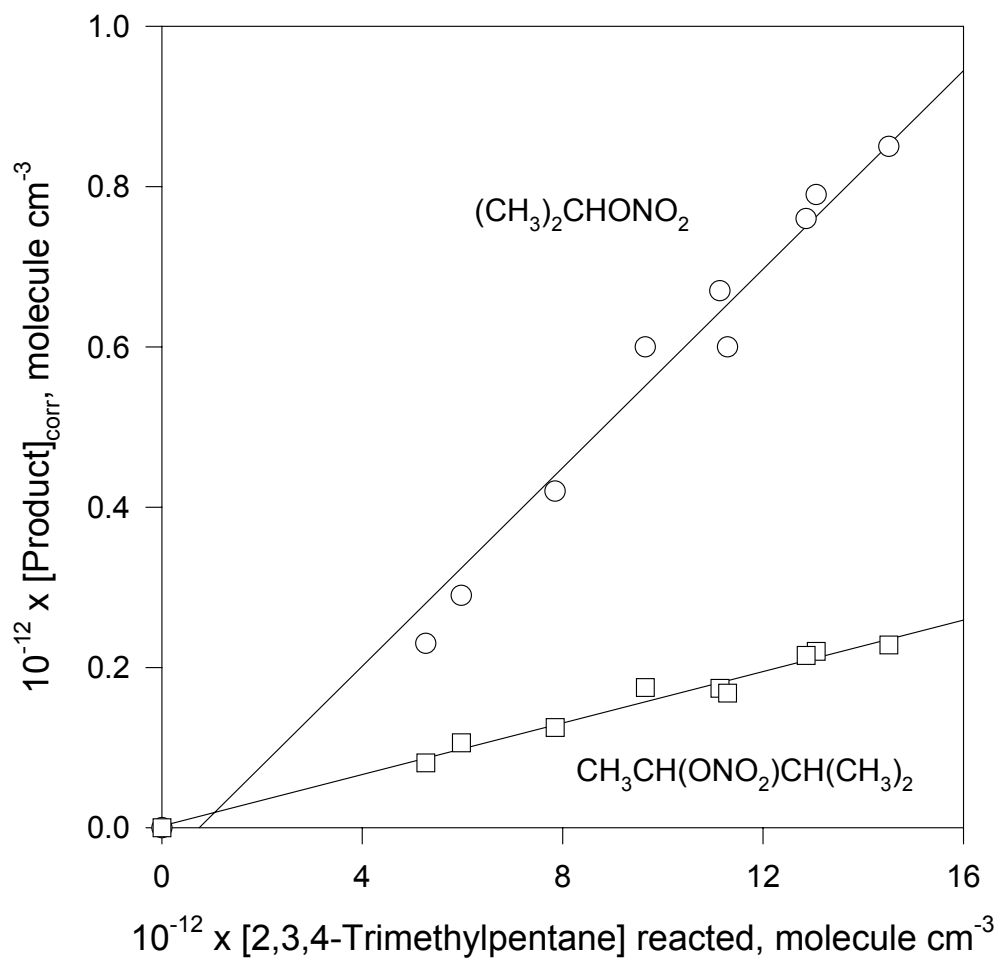


Figure 11. Plots of the amounts of 2-propyl nitrate and 3-methyl-2-butyl nitrate formed, corrected for reaction with the OH radical (see text), against the amounts of 2,3,4-trimethylpentane reacted.

Table 4. Products observed, and their molar formation yields, from the OH radical-initiated reaction of 2,3,4-trimethylpentane in the presence of NO

Product	GC-FID ^a	API-MS
Acetaldehyde	0.47 ± 0.06	
Acetone	0.76 ± 0.11	Observed ^b
3-Methyl-2-butanone	0.41 ± 0.05	Observed ^b
2-Propyl nitrate	0.062 ± 0.008	
3-Methyl-2-butyl nitrate	0.016 ± 0.002	
C ₈ -Alkyl nitrate	~0.02	
Molecular weight 149 product C ₅ -hydroxynitrate		Observed ^{b,c}
Molecular weight 191 product C ₈ -hydroxynitrate		Observed ^{b,c}

^aIndicated errors are two least-squares standard deviations combined with estimated overall uncertainties in the GC-FID response factors for 2,3,4-trimethylpentane and products, of ±5% each.

^bIn positive ion mode.

^cIn negative ion mode, as NO₂⁻ adduct.

API-MS Analyses. Analyses of an irradiated CH₃ONO - NO - 2,3,4-trimethylpentane - air mixture were carried out using *in situ* API-MS in both positive and negative ion mode. In the positive ion mode, API-MS/MS "product ion" and "precursor ion" spectra were obtained for ion peaks observed in the API-MS analyses. Product peaks were identified based on the observation of homo- or hetero-dimers (for example, [(M_{P1})₂+H]⁺, [(M_{P2})₂+H]⁺ and [M_{P1}+M_{P2}+H]⁺, where P1 and P2 are products) in the API-MS/MS "precursor ion" spectra, and consistency of the API-MS/MS "product ion" spectrum of a homo- or hetero-dimer ion with the "precursor ion" spectra of the [M_P+H]⁺ ion peaks (Aschmann *et al.*, 1997; Arey *et al.*, 2001). Water cluster ion peaks of the product ions, [M+H+H₂O]⁺, were also occasionally observed. The products observed from the OH radical-initiated reaction of 2,3,4-trimethylpentane in the presence of NO are shown in Table 4. The positive-ion API-MS and API-MS/MS analyses indicate the formation of products

of molecular weight 58 and 86, attributed to acetone and 3-methyl-2-butanone, both of which were also identified and quantified by GC-FID, and products of molecular weight 142, 147 and 191. The products of molecular weight 142, 147 and 191 were present in the API-MS spectra as their protonated hetero-dimers with acetone and 3-methyl-2-butanone at 201 u (molecular weight 142 product), 206 u (molecular weight 147 product), and 250 and 278 u (molecular weight 191 product). The API-MS/MS “product ion” spectra of the 206, 250 and 278 u ion peaks showed the presence of a 46 u fragment ion, attributed to NO_2^+ and hence indicating that the molecular weight 147 and 191 products are organic nitrates.

In the negative ion mode, the dominant ion peak was that at 237 u which was shown from API-MS/MS “product ion” and “precursor ion” spectra to be an NO_2^- adduct of a molecular weight 191 species. An order of magnitude weaker ion peak in the API-MS spectrum at 195 u was shown to be an NO_2^- adduct of a molecular weight 149 species, which is attributed (because of its odd mass) to an organic nitrate.

2.2.4. Discussion

The room temperature rate constant measured here of $(6.84 \pm 0.12) \times 10^{-12} \text{ cm}^3 \text{ molecule}^{-1} \text{ s}^{-1}$ at $298 \pm 2 \text{ K}$ is in excellent agreement with the only other reported study of Harris and Kerr (1989), in which rate constants were measured relative to those for reaction of OH radicals with *n*-hexane over the temperature range 243-313 K, with a rate constant of $k_1 = (6.46 \pm 0.21) \times 10^{-12} \text{ cm}^3 \text{ molecule}^{-1} \text{ s}^{-1}$ at 295 K (Atkinson, 2003). The 298 K rate constant calculated using the empirical estimation method of Kwok and Atkinson (1995) is $8.54 \times 10^{-12} \text{ cm}^3 \text{ molecule}^{-1} \text{ s}^{-1}$, in reasonable agreement with the measured rate constants (noting that the recommended rate constants for reaction of OH radicals with the reference compounds used here and by Harris and Kerr (1989) are now 5-7% lower than at the time of the Kwok and Atkinson (1995) study).

The product data given in Table 4 show that we have accounted for $69 \pm 6\%$ of the products (as carbon), and the GC and API-MS data allow the reaction pathways to be delineated to a reasonable extent. OH radicals can react with 2,3,4-trimethylpentane at four positions; the four equivalent CH_3 groups attached to the 2- and 4-carbon (8%), the CH_3 group attached to the 3-position carbon (2%), the two equivalent tertiary CH groups at the 2- and 4-positions (56%), and the CH group at the 3-position (34%), where the numbers in parentheses are the percentages of the four reaction pathways calculated using the estimation method of Kwok and Atkinson (1985). Note that even if the overall reaction rate constant is well predicted, these calculated percentages of reaction occurring at the various CH and CH_3 groups may be subject to significant uncertainties, and the total rate constant for 2,3,4-trimethylpentane is overpredicted by 25%.

After H-atom abstraction from these various C-H bonds, the resulting alkyl radicals add O_2 to form alkyl peroxy radicals which, under our experimental conditions, then react with NO to form the corresponding alkoxy radical ($\text{C}_8\text{H}_{17}\text{O}^\bullet$) plus NO_2 or the alkyl nitrate ($\text{C}_8\text{H}_{17}\text{ONO}_2$, of molecular weight 175), as shown in reactions (1) through (3) above. As also noted above, the four $\text{C}_8\text{H}_{17}\text{O}^\bullet$ alkoxy radicals can react with O_2 , unimolecularly decompose by C-C bond scission, or isomerize through a 6-membered ring transition state to form a 1,4-hydroxyalkyl radical, with not all of these reaction pathways being possible for all four alkoxy radicals initially formed from 2,3,4-trimethylpentane.

Figures 12-14 show the potential reactions of the three $\text{C}_8\text{H}_{17}\text{O}^\bullet$ alkoxy radicals predicted to be most important, leading to first-generation products. In these reaction schemes,

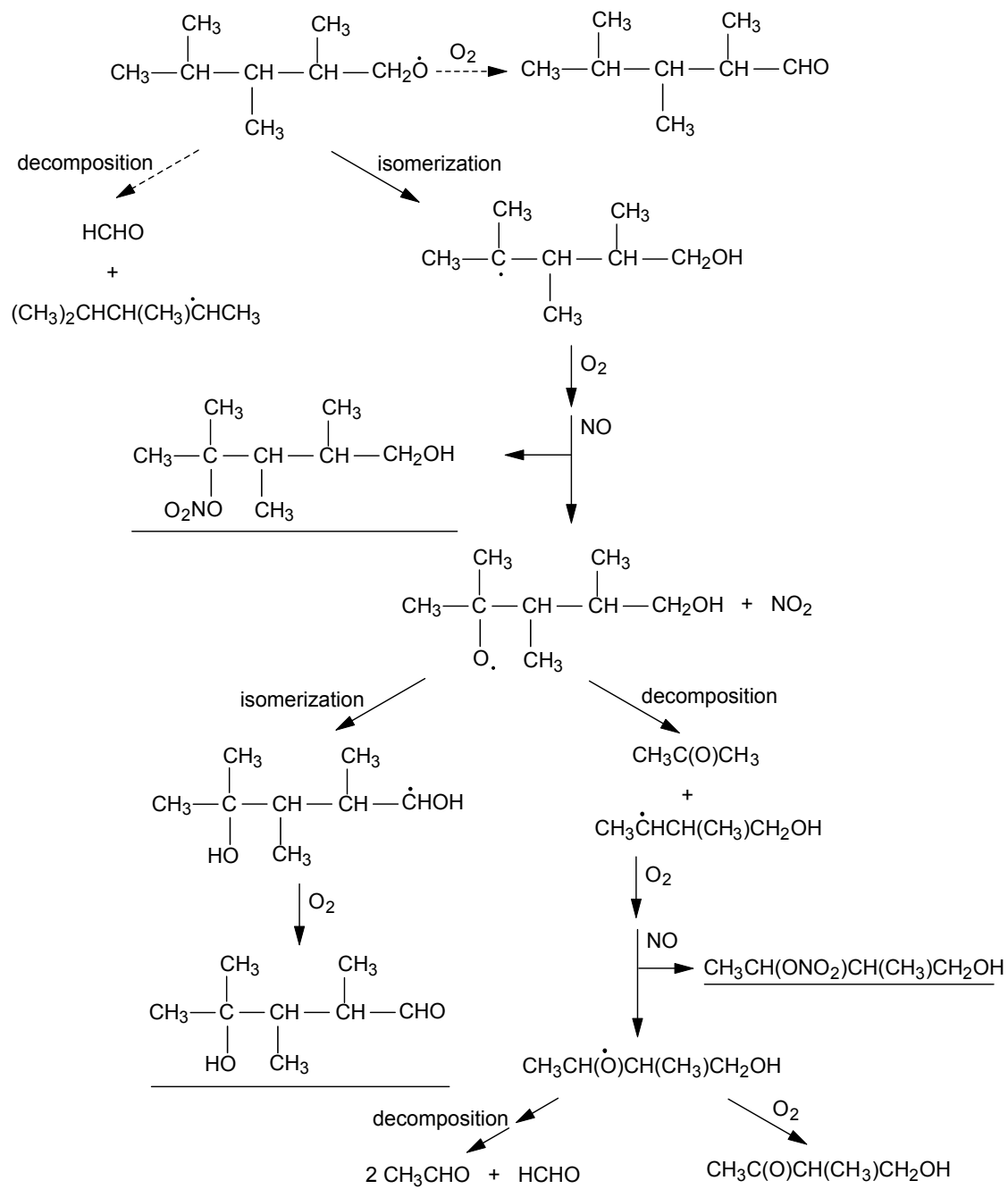


Figure 12. Reaction scheme for the $(\text{CH}_2)_2\text{CHCH}(\text{CH}_3)\text{CH}(\text{CH}_3)\text{CH}_2\text{O}^\bullet$ radical.

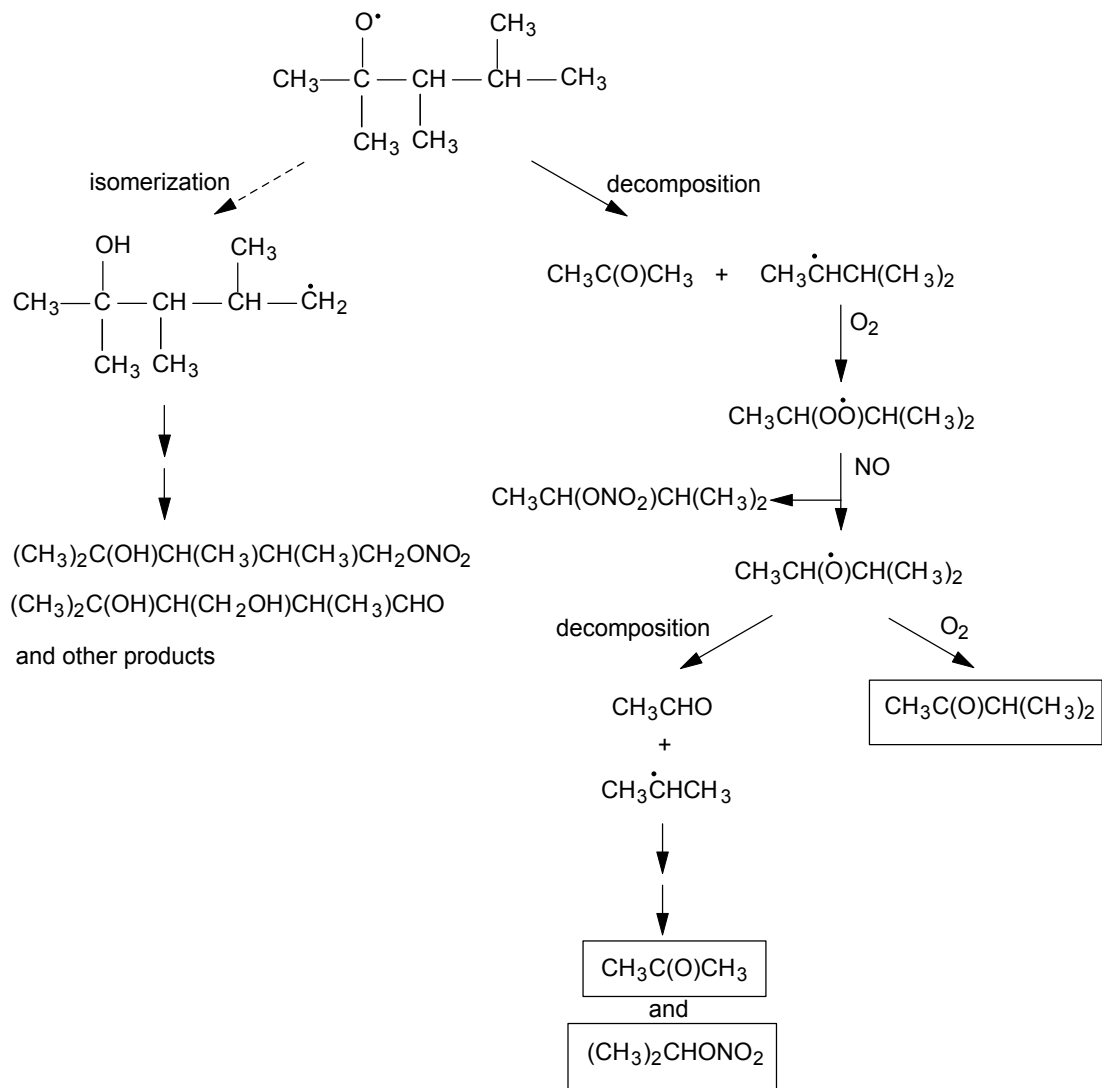


Figure 13. Reaction scheme for the $(\text{CH}_3)_2\text{C}(\text{O}^\bullet)\text{CH}(\text{CH}_3)\text{CH}(\text{CH}_3)_2$ radical.

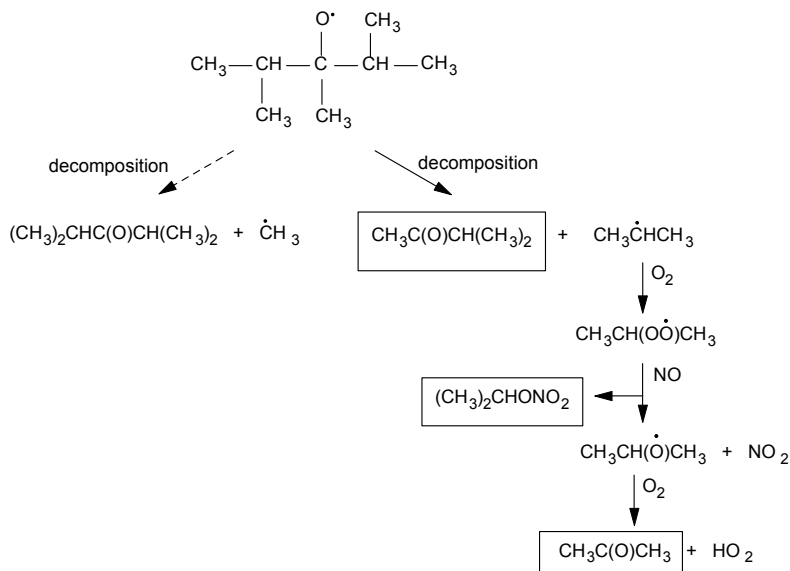


Figure 14. Reaction scheme for the $(\text{CH}_3)_2\text{CHC}(\text{CH}_3)(\text{O}^\bullet)\text{CH}(\text{CH}_3)_2$ radical.

detailed reactions are omitted for $\text{CH}_3\text{C}^\bullet\text{HCH}_3$, which are known to react in the atmosphere to form $\text{CH}_3\text{C}(\text{O})\text{CH}_3$ and 2-propyl nitrate (Atkinson, 1994, 1997a). The rates of the decomposition, isomerization and reaction with O_2 of the various alkoxy and hydroxyalkoxy radicals involved in Figures 11-13 were calculated using the estimation methods described by]. The calculated rates of these reactions are not shown in Figures 14-16, rather the relative importance of the various reactions of a given alkoxy radical are denoted by the arrows: a dashed arrow indicates that that reaction pathway is estimated to account for <10% of the overall reaction rate of the alkoxy radical. The reactions of the four initially-formed $\text{C}_8\text{H}_{17}\text{O}^\bullet$ radicals are discussed below and compared with the products observed. It should be noted that the four expected $\text{C}_8\text{H}_{17}\text{ONO}_2$ nitrates formed from the reactions of the four $\text{C}_8\text{H}_{17}\text{O}_2^\bullet$ radicals with NO [reaction (3a)] were not identified by API-MS analyses and only one of these nitrates was observed by GC-FID and GC-MS; due in large part to a lack of authentic standards.

(CH₂)₂CHCH(CH₃)CH(CH₃)CH₂O[•] Radical.

Figure 12 shows that this alkoxy radical can react with O_2 , decompose or isomerize, with predicted reaction rates at 298 K and atmospheric pressure of air of $4.7 \times 10^4 \text{ s}^{-1}$, $6.5 \times 10^4 \text{ s}^{-1}$ and $5 \times 10^6 \text{ s}^{-1}$, respectively (Atkinson, 1997a,b; Aschmann and Atkinson, 1999; Aschmann *et al.*, 2001b). Decomposition of the $(\text{CH}_3)_2\text{C}(\text{O}^\bullet)\text{CH}(\text{CH}_3)\text{CH}(\text{CH}_3)\text{CH}_2\text{OH}$ radical formed after the first isomerization is predicted to dominate over isomerization by a factor of ~ 1.6 , and the ensuing alkoxy radical $\text{CH}_3\text{CH}(\text{O}^\bullet)\text{CH}(\text{CH}_3)\text{CH}_2\text{OH}$ is predicted to dominantly decompose

rather than react with O₂. The predicted products from the (CH₂)₂CHCH(CH₃)CH(CH₃)CH₂O[•] radical then include the molecular weight 191 hydroxynitrate (CH₃)₂C(ONO₂)CH(CH₃)CH(CH₃)CH₂OH, the molecular weight 144 hydroxycarbonyl (CH₃)₂C(OH)CH(CH₃)CH(CH₃)CHO, the molecular weight 149 hydroxynitrate CH₃CH(ONO₂)CH(CH₃)CH₂OH, acetone, acetaldehyde and HCHO. Our observation of molecular weight 149 and 191 organic nitrates is consistent with these predictions, and the molecular weight 149 and 191 organic nitrates can be attributed to C₅- and C₈-hydroxynitrates, respectively.

(CH₃)₂C(O[•])CH(CH₃)CH(CH₃)₂ Radical.

Figure 13 shows that this alkoxy radical can only decompose or isomerize, with calculated reaction rates at 298 K of 1.3 x 10⁷ s⁻¹ and 4 x 10⁵ s⁻¹, respectively (Atkinson, 1997a,b; Aschmann and Atkinson, 1999; Aschmann *et al.*, 2001b). The CH₃CH(O[•])CH(CH₃)₂ alkoxy radical formed after the decomposition is predicted to dominantly decompose (1.1 x 10⁶ s⁻¹) rather than react with O₂ (4.7 x 10⁴ s⁻¹). Using the previously measured yields of 3-methyl-2-butyl nitrate from the CH₃CH(O[•])CH(CH₃)₂ + NO reaction of 13.4% [data of Atkinson *et al.* (1984) re-evaluated (Kwok and Atkinson, 1995)] and of 2-propyl nitrate from the CH₃CH(O[•])CH₃ + NO reaction of 3.9% (8), then neglecting the minor isomerization channel the major products are expected to be CH₃C(O)CH₃ (180%) + CH₃C(ONO₂)CH(CH₃)₂ (13.4%) + CH₃C(O)CH(CH₃)₂ (3.5%) + CH₃CHO (83%) + (CH₃)₂CHONO₂ (3.2%), where the percentages are the predicted molar yields from the precursor (CH₃)₂C(O[•])CH(CH₃)CH(CH₃)₂ alkoxy radical.

(CH₃)₂CHC(CH₃)(O[•])CH(CH₃)₂ Radical.

As shown in Figure 14, decomposition is the only process which can occur. Decomposition to CH₃C(O)CH(CH₃)₂ + CH₃C[•]HCH₃ is predicted to dominate, by a factor of ~2 x 10⁴, over decomposition to [•]CH₃ + (CH₃)₂CHC(O)CH(CH₃)₂ (Atkinson, 1997a,b; Aschmann and Atkinson, 1999; Aschmann *et al.*, 2001b). The expected products are therefore 3-methyl-2-butanone + acetone (or 2-propyl nitrate).

(CH₃)₂CHCH(CH₂O[•])CH(CH₃)₂ Radical.

The precursor alkyl (and peroxy) radical is predicted to account for only 2% of the overall reaction (Kwok and Atkinson, 1995) and hence no reaction scheme is shown for this alkoxy radical. Isomerization is predicted to dominate over decomposition and reaction with O₂, leading to the molecular weight 191 hydroxynitrate

(CH₃)₂CHCH(CH₂OH)CH(CH₃)CH₂OONO₂, the hydroxycarbonyl (CH₃)₂CHCH(CHO)CH(CH₃)CH₂OH, and other products.

Formation of 3-methyl-2-butanone is predicted to occur almost entirely from the (CH₃)₂CHC(CH₃)(O[•])CH(CH₃)₂ radical. That this is the case is supported by the low yield of 3-methyl-2-butyl nitrate (1.6%), which is predicted to arise only from the (CH₃)₂C(O[•])CH(CH₃)CH(CH₃)₂ radical and implies that formation of 3-methyl-2-butanone from the (CH₃)₂C(O[•])CH(CH₃)CH(CH₃)₂ radical is minor (<1%). Therefore, the yield of 3-methyl-2-butanone (41 ± 5%) corresponds to the formation yield of the (CH₃)₂CHC(CH₃)(O[•])CH(CH₃)₂ radical. Accounting for some formation of the C₈-alkyl nitrate (CH₃)₂CHC(CH₃)(ONO₂)CH(CH₃)₂ from the RO₂[•] + NO reaction, H-atom abstraction from the 3-position CH group must account for ~45%, and at a minimum for 40 ± 5% of the overall OH radical reaction. This is somewhat higher than the predicted importance of H-atom abstraction from the 3-position CH group (34%).

Delineation of the remaining pathways is rendered difficult because the same products (acetone, 2-propyl nitrate and acetaldehyde), are formed from both the $(\text{CH}_3)_2\text{C}(\text{O}^\bullet)\text{CH}(\text{CH}_3)\text{CH}(\text{CH}_3)_2$ and $(\text{CH}_3)_2\text{CHCH}(\text{CH}_3)\text{CH}(\text{CH}_3)\text{CH}_2\text{O}^\bullet$ radicals. Lumping 2-propyl nitrate in with acetone (since the $\text{CH}_3\text{CH}(\text{OO}^\bullet)\text{CH}_3$ radical forms either acetone or 2-propyl nitrate), then our observed products arising from the $(\text{CH}_3)_2\text{C}(\text{O}^\bullet)\text{CH}(\text{CH}_3)\text{CH}(\text{CH}_3)_2$, $(\text{CH}_3)_2\text{CHCH}(\text{CH}_3)\text{CH}(\text{CH}_3)\text{CH}_2\text{O}^\bullet$ and $(\text{CH}_3)_2\text{CHCH}(\text{CH}_2\text{O}^\bullet)\text{CH}(\text{CH}_3)_2$ radicals are acetone + 2-propyl nitrate ($41 \pm 13\%$), 3-methyl-2-butanone ($1.6 \pm 0.2\%$) and acetaldehyde ($47 \pm 6\%$). These correspond to 28% (as carbon) of the reaction products. While some C_8 -alkyl nitrate will be formed from the $(\text{CH}_3)_2\text{C}(\text{OO}^\bullet)\text{CH}(\text{CH}_3)\text{CH}(\text{CH}_3)_2 + \text{NO}$ reaction, this acetone + 2-propyl nitrate (other than that formed as a co-product to 3-methyl-2-butanone) yield indicates that H-atom abstraction from the 2- and 4-position CH groups cannot account for more than 25-30% of the overall reaction, significantly less than the predicted value of 56% (Kwok and Atkinson, 1995).

A plausible product distribution is: C_8 -alkyl nitrates, ~15% based on data for alkanes, including branched alkanes (Carter and Atkinson, 1989); 3-methyl-2-butanone + acetone/2-propyl nitrate from the $(\text{CH}_3)_2\text{CHC}(\text{CH}_3)(\text{O}^\bullet)\text{CH}(\text{CH}_3)_2$ radical, 40%; acetone, acetaldehyde, 3-methyl-2-butyl nitrate, 3-methyl-2-butanone and 2-propyl nitrate (in predicted ratio 1.80: 0.83: 0.134: 0.035: 0.032) from the $(\text{CH}_3)_2\text{C}(\text{O}^\bullet)\text{CH}(\text{CH}_3)\text{CH}(\text{CH}_3)_2$ radical, 15%; acetone and acetaldehyde (in approximate ratio 1:2) from the $(\text{CH}_3)_2\text{CHCH}(\text{CH}_3)\text{CH}(\text{CH}_3)\text{CH}_2\text{O}^\bullet$ radical, 15%; with alternate reactions of the $(\text{CH}_3)_2\text{CHCH}(\text{CH}_3)\text{CH}(\text{CH}_3)\text{CH}_2\text{O}^\bullet$ radical and the reactions of the $(\text{CH}_3)_2\text{CHCH}(\text{CH}_2\text{O}^\bullet)\text{CH}(\text{CH}_3)_2$ radical accounting for the remaining ~15% products (and including hydroxynitrates and hydroxycarbonyls). An alternative product distribution which fits the data about as well is: C_8 -alkyl nitrates, ~15%; 3-methyl-2-butanone + acetone/2-propyl nitrate from the $(\text{CH}_3)_2\text{CHC}(\text{CH}_3)(\text{O}^\bullet)\text{CH}(\text{CH}_3)_2$ radical, 40%; acetone, acetaldehyde, 3-methyl-2-butyl nitrate, 3-methyl-2-butanone and 2-propyl nitrate (in predicted ratio 1.80: 0.83: 0.134: 0.035: 0.032) from the $(\text{CH}_3)_2\text{C}(\text{O}^\bullet)\text{CH}(\text{CH}_3)\text{CH}(\text{CH}_3)_2$ radical, 20%; acetone and acetaldehyde (in approximate ratio 1:2) from the $(\text{CH}_3)_2\text{CHCH}(\text{CH}_3)\text{CH}(\text{CH}_3)\text{CH}_2\text{O}^\bullet$ radical, 10%; with alternate reactions of the $(\text{CH}_3)_2\text{CHCH}(\text{CH}_3)\text{CH}(\text{CH}_3)\text{CH}_2\text{O}^\bullet$ radical and the reactions of the $(\text{CH}_3)_2\text{CHCH}(\text{CH}_2\text{O}^\bullet)\text{CH}(\text{CH}_3)_2$ radical accounting for the remaining ~15% products (and including hydroxynitrates and hydroxycarbonyls).

These two alternative scenarios account for all of the reaction pathways, with yields of acetone (80 or 84%), 3-methyl-2-butanone (41%), acetaldehyde (42 or 37%), 3-methyl-2-butyl nitrate (2.0 or 2.7%) and 2-propyl nitrate (2.0 or 2.2%) [where the two yields refer to the two scenarios listed above. The predicted product yields are consistent with our measured values, except that our measured 2-propyl nitrate yield is a factor of 3 higher than that predicted. With these scenarios, H-atom abstraction from the CH groups at the 2- and 4-positions accounts for 15-20% plus the percentage formation of the C_8 -alkyl nitrate $(\text{CH}_3)_2\text{C}(\text{ONO}_2)\text{CH}(\text{CH}_3)\text{CH}(\text{CH}_3)_2$; hence expected (Carter and Atkinson, 1989) to be $\leq 25\%$ and a factor of 2 lower than predicted from the Kwok and Atkinson (Kwok and Atkinson, 1995) estimation method. This discrepancy can be attributed to steric hindrance at the 2- and 4-position CH groups towards OH radical reaction, similar to the conclusion drawn for reaction of OH radicals with 2,2,4-trimethylpentane (Aschmann *et al.*, 2002b; Section 2.1.). An alternative explanation is that isomerization of the $(\text{CH}_3)_2\text{C}(\text{O}^\bullet)\text{CH}(\text{CH}_3)\text{CH}(\text{CH}_3)_2$ radical is much more important than predicted and accounts for ~25-30% of the overall reaction and leading to hydroxycarbonyl and hydroxynitrate products which were not quantified. However, the API-MS

analyses showed no evidence for molecular weight 144 C₈-hydroxycarbonyls (API-MS/MS positive ion “product ion” spectra of the 145 u ion peak observed in the API-MS spectra showed no appreciable fragment ion due to expected loss of H₂O; rather the fragment ions were those expected for a protonated hetero-dimer of acetone and 3-methyl-2-butanone), but only showed the presence of C₈-hydroxynitrate(s) of molecular weight 191.

The reaction of OH radicals with 2,3,4-trimethylpentane therefore leads to ~70% of the product carbon being formed from alkoxy radical decomposition reactions. This can be compared to the 2,2,4-trimethylpentane reaction (Aschmann *et al.*, 2002b), where ~40% of the products were readily observed by GC methods and attributed to alkoxy radical decomposition or reaction with O₂ and to the *n*-octane reaction (Arey *et al.*, 2001) where none of the products formed arose from alkoxy radical decomposition (rather all of the first-generation alkoxy radicals appeared to undergo isomeriation to form hydroxycarbonyls and hydroxynitrates (in addition to the octyl nitrates formed from the RO₂[•] + NO reactions). Clearly, the higher the degree of branching, the higher the yields of carbonyl compounds with less carbon atoms than the parent alkane.

2.3. Identification of Hydroxycarbonyl Products from the OH Radical-Initiated Reactions of C₅-C₈ *n*-Alkanes in the Presence of NO

2.3.1. Introduction

Alkanes are important constituents of gasoline and vehicle exhaust (Hoekman, 1992) and comprise ~50% of the non-methane organic compounds observed in ambient air in urban areas (Calvert *et al.*, 2002). In the atmosphere, alkanes react primarily with OH radicals, leading to the formation of alkyl nitrates, carbonyl, hydroxyalkyl nitrates, and hydroxycarbonyls (Atkinson, 1997a, 2000; Arey *et al.*, 2001; Atkinson and Arey, 2003), with the formation of 1,4-hydroxycarbonyls appearing to account for the majority of the products for the $\geq C_6$ *n*-alkanes (Kwok *et al.*, 1996; Arey *et al.*, 2001; Aschmann *et al.*, 2001a). However, this class of carbonyl-containing compounds does not appear to elute from gas chromatography columns without prior derivatization (Eberhard *et al.*, 1995; Kwok *et al.*, 1996b; Arey *et al.*, 2001; Aschmann *et al.*, 2001a).

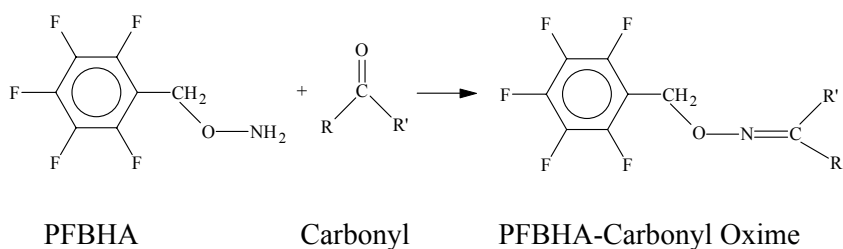
In this work, we have used Solid Phase MicroExtraction (SPME) fibers coated with *O*-(2,3,4,5,6-pentafluorobenzyl)hydroxylamine hydrochloride to allow *in situ* derivatization of hydroxycarbonyls for analysis as their oxime derivatives by gas chromatography with flame ionization detection (GC-FID) and combined gas chromatography-mass spectrometry (GC-MS). We have identified the hydroxycarbonyl products formed from the gas-phase reactions of OH radicals with *n*-pentane through *n*-octane in the presence of NO. Apart from 5-hydroxy-2-pentanone, the 1,4-hydroxycarbonyls observed as reaction products are not commercially available. Under funding from the National Science Foundation (Grant No. ATM-0234586), we have continued this work to quantify the individual 1,4-hydroxycarbonyls identified here, using estimated relative GC-FID response factors for the *in situ* analysis (as the oxime derivatives) of the hydroxycarbonyls for quantification (at both ~5% and ~50% relative humidity) and with 3-pentanone being added as an internal standard.

2.3.2. Experimental Methods

Experiments were carried out in ~7000 liter Teflon chambers at 296 ± 2 K and 740 Torr total pressure of purified air at ~5% and ~50% relative humidity. The chamber is equipped with a Teflon-coated fan to ensure rapid mixing of the reactants during their introduction into the chamber, and has two parallel banks of blacklamps for irradiation. Hydroxyl (OH) radicals were generated by the photolysis of methyl nitrite (CH₃ONO) in air at wavelengths >300 nm and NO was added to the reactant mixtures to suppress the formation of O₃ and NO₃ radicals.

The initial reactant concentrations (in molecule cm⁻³) were: CH₃ONO and NO, $\sim 2.4 \times 10^{13}$ each for the *n*-pentane and *n*-hexane reactions and $\sim 1.7 \times 10^{13}$ each for the *n*-heptane and *n*-octane reactions; and the *n*-alkane, $\sim (1-3) \times 10^{13}$. For each experiment, a single irradiation was carried out at 20% of the maximum light intensity for 10-20 min, resulting in consumption of the initial alkane of 9-30%. For the analysis of the *n*-alkanes, 100 cm³ gas samples were collected from the chamber onto Tenax-TA solid adsorbent with subsequent thermal desorption at ~250 °C onto a 30 m DB-1701 megabore column held at -40 °C and then temperature programmed to 200 °C at 8 °C min⁻¹. Analyses of the *n*-alkanes was also carried out with gas samples being collected in a 100 cm³ all-glass, gas-tight syringe and introduced via a gas sampling loop onto a 30 m DB-5 megabore column initially held at -25 °C and then temperature programmed to 200 °C at 8 °C min⁻¹.

Carbonyl-containing products were identified by using on-fiber derivatization with SPME as described by Koziel *et al.* (2001). A 65 μm polydimethylsiloxane/ divinylbenzene PDMS/DVB fiber was coated with *O*-(2,3,4,5,6-pentafluorobenzyl)-hydroxylamine hydrochloride (PFBHA). This involved headspace extraction from 4 ml of an aqueous solution (~ 40 mg of PFBHA per 100 ml of water) in a 20 ml vial over a 60 min period, with agitation using a magnetic stirrer. The PFBHA coating of the fiber was carried out under nitrogen gas to minimize any acetone contamination from laboratory air. The coated fiber was then exposed to the reactants in the chamber for 5 min to form a PFBHA-carbonyl oxime according to the following equation



For GC-FID analyses, the exposed fiber was then removed from the chamber and thermally desorbed in the injection port of the GC at 250 °C onto a 30 m DB-1701 megabore column held at 40 °C and then temperature programmed at 8 °C min⁻¹ to 260 °C. Typically, two analyses were carried out. GC-MS analyses of the exposed fibers were carried out in a similar manner, using a Varian 2000 GC/MS/MS with isobutane chemical ionization.

The following chemicals, with their stated purities, were purchased from Aldrich Chemical Co.: *n*-pentane (99+%), *n*-hexane (99+%), *n*-octane (99+%). *n*-Heptane (99+%) was from Mallinckrodt. Methyl nitrite was prepared and stored as described previously (Taylor *et al.*, 1980).

2.3.3. Results

A series of irradiated CH₃ONO – NO – *n*-alkane – air irradiations were carried out to identify the hydroxycarbonyls formed. The GC-MS analyses of coated SPME fibers exposed to irradiated CH₃ONO – NO – *n*-alkane – air mixtures showed the presence of oxime products with characteristic losses of 45 (CH₂CH₂OH), 59 (CH₂CH(OH)CH₃), 73 (CH₂CH(OH)CH₂CH₃) and 87 (CH₂CH(OH)CH₂CH₂CH₃). These fragmentation patterns allowed the specific isomers of the hydroxycarbonyl-oxime derivatives from each *n*-alkane to be determined (Table 5), noting that an authentic standard of 5-hydroxy-2-pentanone was available for its identification from the *n*-pentane reaction. In this manner, the GC-MS analyses showed the presence of the oximes of 5-hydroxy-2-pentanone and 4-hydroxypentanal from the *n*-pentane reaction; 5-hydroxy-2-hexanone, 6-hydroxy-3-hexanone and 4-hydroxyhexanal from the *n*-hexane reaction; 5-hydroxy-2-heptanone, 6-hydroxy-3-heptanone, 1-hydroxy-4-heptanone and 4-hydroxyheptanal from the

n-heptane reaction; and 5-hydroxy-2-octanone, 6-hydroxy-3-octanone, 7-hydroxy-4-octanone and 4-hydroxyoctanal from the *n*-octane reaction.

As noted in the Introduction to this section, we have continued this area of research, through funding from the National Science Foundation (Grant No. ATM-0234586), to quantify the individual 1,4-hydroxycarbonyls identified here. Because the 1,4-hydroxycarbonyls formed are (apart from 5-hydroxy-2-pentanone) not commercially available, we used estimated relative GC-FID response factors for the *in situ* analysis (as the oxime derivatives) of the hydroxycarbonyls at both ~5% and ~50% relative humidity with 3-pentanone being added as an internal standard. Our data indicate that the larger 1,4-hydroxycarbonyls cyclize and lose water at ~5% relative humidity (at room temperature), but not (or at least less) at ~50% relative humidity. Therefore, the 1,4-hydroxycarbonyl yields at ~50% relative humidity are expected to be the formation yields from the OH radical-initiated reactions, and account for ~59% of the reaction products from the *n*-pentane reaction, ~57% of the reaction products from the *n*-hexane reaction, ~51% of the reaction products from the *n*-heptane reaction, and ~52% of the reaction products from the *n*-octane reaction. Combined with the previously measured (Arey *et al.*, 2001) formation yields of alkyl nitrates, carbonyls (from the alkoxy radical decompositions and reaction with O₂) and hydroxyalkyl nitrates, we can now account for essentially all of the reaction products and pathways (~120%, ~82%, ~74% and ~80%, respectively, from *n*-pentane, *n*-hexane, *n*-heptane and *n*-octane).

Table 5. Fragmentation patterns observed in the MS spectra of the hydroxycarbonyls and their assignments.

alkane	product	M+H	M+H -H ₂ O	M+H -45	M+H -59	M+H -73	M+H -87	M+H -101
<i>n</i> -pentane	CH ₃ C(O)CH ₂ CH ₂ CH ₂ OH	X	X	X				
	CH ₃ CH(OH)CH ₂ CH ₂ CHO	X	X		X			
<i>n</i> -hexane	CH ₃ C(O)CH ₂ CH ₂ CH(OH)CH ₃	X	X		X			
	CH ₃ CH ₂ C(O)CH ₂ CH ₂ CH ₂ OH	X	X	X				
	CH ₃ CH ₂ CH(OH)CH ₂ CH ₂ CHO	X	X			X		
<i>n</i> -heptane	CH ₃ C(O)CH ₂ CH ₂ CH(OH)CH ₂ CH ₃	X	X			X		
	CH ₃ CH ₂ C(O)CH ₂ CH ₂ CH(OH)CH ₃	X	X		X			
	CH ₃ CH ₂ CH ₂ C(O)CH ₂ CH ₂ CH ₂ OH	X	X	X				
	CH ₃ CH ₂ CH ₂ CH(OH)CH ₂ CH ₂ CHO	X	X				X	
<i>n</i> -octane	CH ₃ C(O)CH ₂ CH ₂ CH(OH)CH ₂ CH ₂ CH ₃	X	X				X	
	CH ₃ CH ₂ C(O)CH ₂ CH ₂ CH(OH)CH ₂ CH ₃	X	X			X		
	CH ₃ CH ₂ CH ₂ C(O)CH ₂ CH ₂ CH(OH)CH ₃	X	X		X			
	CH ₃ CH ₂ CH ₂ CH ₂ CH(OH)CH ₂ CH ₂ CHO	X	X					X

2.4. Kinetics and Products of the Gas-Phase Reaction of OH Radicals with 5-Hydroxy-2-pentanone at 296 ± 2 K

2.4.1. Introduction

As discussed in Section 2.3. above, 1,4-hydroxycarbonyls are important products of the gas-phase reactions of OH radicals with alkanes occurring in the presence of sufficient NO that organic peroxy radicals react dominantly with NO (Eberhard *et al.*, 1995; Kwok *et al.*, 1996b; Arey *et al.*, 2001; Aschmann *et al.*, 2001a). 1,4-Hydroxycarbonyls do not elute from gas chromatographic columns without prior derivatization (Eberhard *et al.*, 1995; Martin *et al.*, 2002), and they can cyclize to a hemiacetal (Streitwieser and Heathcock, 1976; Martin *et al.*, 2002). We have recently shown that in the absence of water vapor 5-hydroxy-2-pentanone, the only commercially available 1,4-hydroxycarbonyl, cyclizes and loses water to form 4,5-dihydro-2-methylfuran, but that this process reverses in the presence of water vapor (Martin *et al.*, 2002; see also Section 2.5. below). While the atmospherically important reactions of 1,4-hydroxycarbonyls are expected to be with OH radicals and, to a much lesser extent, with NO₃ radicals (Atkinson, 1994, 2000; Chew *et al.*, 1998), no kinetic or product data have been reported for these reactions to date.

Because 5-hydroxy-2-pentanone does not elute from gas chromatographic columns unless it is derivatized prior to introduction onto the column, an obvious approach for determining its rate constant for reaction with OH radicals would be to use *in situ* Fourier transform infrared (FT-IR) spectroscopy to monitor 5-hydroxy-2-pentanone, using dry synthetic air as the diluent gas to avoid interferences due to IR absorption by water vapor (Martin *et al.*, 2002). However, in dry air 5-hydroxy-2-pentanone converts to the highly reactive 4,5-dihydro-2-methylfuran on a time-scale of ~ 1 hr (Martin *et al.*, 2002), greatly complicating such an experimental approach. While the interconversion between 5-hydroxy-2-pentanone and 4,5-dihydro-2-methylfuran is reversed in the presence of water vapor (Martin *et al.*, 2002), experiments utilizing FT-IR spectroscopy in the presence of significant concentrations of water vapor are complicated by the IR absorptions of water vapor. Furthermore, analysis by FT-IR spectroscopy is rendered difficult because carbonyl-containing products of the reaction of OH radicals with 5-hydroxy-2-pentanone will interfere with its analysis, as previously observed for OH radical-initiated reactions of the dibasic ester dimethyl glutarate (Tuazon *et al.*, 1999) and the ketones 2-pentanone and 2-heptanone (Atkinson *et al.*, 2000a).

Recently, a carbonyl analysis method employing gas chromatography (GC) following sampling by Solid Phase Micro Extraction (SPME) with on-fiber derivatization has been developed and utilized (Martos and Pawliszyn, 1998; Koziel *et al.*, 2001; Reisen *et al.*, 2003). In this work we have determined a rate constant for the reaction of OH radicals with 5-hydroxy-2-pentanone and have investigated the products formed, by conducting experiments in moist air ($\sim 5\%$ relative humidity) with GC analyses of 5-hydroxy-2-pentanone and its products as their oxime derivatives.

2.4.2. Experimental Methods

Experiments were carried out at 296 ± 2 K and 740 Torr of purified air (at $\sim 5\%$ relative humidity) in two ~ 7000 liter Teflon chambers, each equipped with two parallel banks of blacklamps and with a Teflon-coated fan to ensure rapid mixing of reactants during their introduction into the chamber. One of the Teflon chambers was interfaced to a PE SCIEX API III MS/MS direct air sampling, atmospheric pressure ionization tandem mass spectrometer (API-MS).

Kinetic Measurements

The rate constant for the reaction of OH radicals with 5-hydroxy-2-pentanone was measured using a relative rate method, in which the relative decay rates of 5-hydroxy-2-pentanone and a reference compound, whose OH radical reaction rate constant is reliably known, are measured in the presence of OH radicals (Atkinson *et al.*, 2000a; Bethel *et al.*, 2001). Providing that 5-hydroxy-2-pentanone and the reference compound (4-methyl-2-pentanone in this case) are removed only by reaction with OH radicals, then,

$$\ln \left(\frac{[5\text{-hydroxy-2-pentanone}]_{t_0}}{[5\text{-hydroxy-2-pentanone}]_t} \right) = \frac{k_1}{k_2} \ln \left(\frac{[4\text{-methyl-2-pentanone}]_{t_0}}{[4\text{-methyl-2-pentanone}]_t} \right) \quad (I)$$

where $[5\text{-hydroxy-2-pentanone}]_{t_0}$ and $[4\text{-methyl-2-pentanone}]_{t_0}$ are the concentrations of 5-hydroxy-2-pentanone and 4-methyl-2-pentanone at time t_0 , respectively, $[5\text{-hydroxy-2-pentanone}]_t$ and $[4\text{-methyl-2-pentanone}]_t$ are the corresponding concentrations at time t , and k_1 and k_2 are the rate constants for reactions (1) and (2), respectively.



Hence a plot of $\ln([5\text{-hydroxy-2-pentanone}]_{t_0}/[5\text{-hydroxy-2-pentanone}]_t)$ against $\ln([4\text{-methyl-2-pentanone}]_{t_0}/[4\text{-methyl-2-pentanone}]_t)$ should be a straight line of slope k_1/k_2 and zero intercept.

OH radicals were generated by the photolysis of methyl nitrite in air at wavelengths >300 nm (Atkinson *et al.*, 2000), and NO was included in the reactant mixtures to suppress the formation of O_3 and hence of NO_3 radicals. 4-Methyl-2-pentanone was chosen as the reference compound because its OH radical reaction rate constant (Atkinson, 1994) is similar to that estimated (Bethel *et al.*, 2001) for 5-hydroxy-2-pentanone. Additionally, 4-methyl-2-pentanone can be analyzed by gas chromatography with flame ionization detection (GC-FID) both without prior derivatization (Atkinson and Aschmann, 1995) and after derivatization as its oxime derivative (see below), thus allowing verification of the on-fiber derivitization SPME sampling method. The initial CH_3ONO , NO, 5-hydroxy-2-pentanone and 4-methyl-2-pentanone concentrations (molecule cm^{-3}) were 4.8×10^{13} , 4.8×10^{13} , 2.4×10^{12} and 1.2×10^{13} , or alternately 2.4×10^{13} , 2.4×10^{13} , 1.2×10^{12} and 6.0×10^{12} , respectively, and irradiations were carried out for 7-23 mins at 20% of the maximum light intensity. The 5-hydroxy-2-pentanone and 4-methyl-2-pentanone concentrations were chosen to provide adequate sensitivity for the Tenax/thermal desorption GC-FID measurements of 4-methyl-2-pentanone while remaining in the linear range for the derivatization/SPME measurements of 5-hydroxy-2-pentanone and 4-methyl-2-pentanone [note that the on-fiber derivitization SPME sampling procedure is, on a molar basis, over an order of magnitude more sensitive to 5-hydroxy-2-pentanone than to 4-methyl-2-pentanone (Reisen *et al.*, 2003)].

In control experiments the concentrations of 5-hydroxy-2-pentanone were monitored in a 5-hydroxy-2-pentanone – air mixture in the dark over a period of 6 hr and in a 5-hydroxy-2-pentanone – cyclohexane (to scavenge any OH radicals formed) – air mixture which was irradiated at 20% of the maximum light intensity for up to 30 mins.

5-Hydroxy-2-pentanone and 4-methyl-2-pentanone were analyzed during the experiments by GC-FID. 4-Methyl-2-pentanone was analyzed by collecting 100 cm³ volume gas samples from the chamber onto Tenax-TA solid adsorbent, with subsequent thermal desorption at ~250 °C onto a 30 m DB-1701 megabore column held at -40 °C and then temperature programmed at 8 °C min⁻¹ to 200 °C. 4-Methyl-2-pentanone and 5-hydroxy-2-pentanone were analyzed by exposing a 65 µm PDMS/DVB SPME fiber pre-coated with *O*-(2,3,4,5,6-pentafluorobenzyl)hydroxylamine (PFBHA) hydrochloride (Martos and Pawliszyn, 1998; Koziel *et al.*, 2001; Reisen *et al.*, 2003) to the chamber contents (with the mixing fan on) for 5 min, with subsequent thermal desorption at 250 °C onto a 30 m DB-1701 megabore column held at 40 °C and then temperature programmed to 260 °C at 8 °C min⁻¹. 4-Methyl-2-pentanone was therefore analyzed with and without derivatization, and comparison of these concurrent analysis methods provided a check on the on-fiber derivatization, collection and desorption procedure.

Product Investigation

Investigations of the reaction products were carried out using *in situ* API-MS analyses and combined gas chromatography-mass spectrometry (GC-MS) analyses of coated SPME fiber samples. The experiments with GC-MS analyses were as described above for the kinetic experiments, except that 4-methyl-2-pentanone was not included in the reactant mixture. In this experiment, a 65 µm SPME fiber coated with PFBHA hydrochloride was exposed to the chamber reaction products and then analyzed by GC-MS, with thermal desorption onto a 30 m DB-1701 fused silica capillary column in a Varian 2000 GC/MS/MS with analysis by isobutane chemical ionization (CI).

In the experiments with API-MS analyses, the chamber contents were sampled through a 25 mm diameter x 75 cm length Pyrex tube at ~20 L min⁻¹ directly into the API mass spectrometer source. The operation of the API-MS in the MS (scanning) and MS/MS [with collision activated dissociation (CAD)] modes has been described previously (Aschmann *et al.*, 1997). Use of the MS/MS mode with CAD allows the “product ion” or “precursor ion” spectrum of a given ion peak observed in the MS scanning mode to be obtained (Aschmann *et al.*, 1997).

The positive ion mode was used in this work, in which protonated water hydrates (H₃O⁺ (H₂O)_n) generated by the corona discharge in the chamber diluent air were responsible for the protonation of analytes (Aschmann *et al.*, 1997; Arey *et al.*, 2001). Ions are drawn by an electric potential from the ion source through the sampling orifice into the mass-analyzing first quadrupole or third quadrupole. In these experiments the API-MS instrument was operated under conditions that favored the formation of dimer ions in the ion source region (Aschmann *et al.*, 1997). Neutral molecules and particles are prevented from entering the orifice by a flow of high-purity nitrogen (“curtain gas”), and as a result of the declustering action of the curtain gas on the hydrated ions, the ions that are mass analyzed are mainly protonated molecules ([M + H]⁺) and their protonated homo- and hetero-dimers (Aschmann *et al.*, 1997).

The initial reactant concentrations (molecule cm⁻³) were: CH₃ONO, ~2.4 x 10¹³; NO, ~2.4 x 10¹³; and 5-hydroxy-2-pentanone, (0.48-2.4) x 10¹²; and irradiations were carried out for 5-10 mins at 20% of the maximum light intensity, or for 5 mins at the maximum light intensity.

Chemicals

The chemicals used and their stated purities were as follows: 5-hydroxy-2-pentanone (95%), TCI America; 4-methyl-2-pentanone (99+%), and *O*-(2,3,4,5,6-pentafluorobenzyl)hydroxylamine hydrochloride (98+%), Aldrich Chemical Company; cyclohexane (HPLC grade), American Burdick & Jackson; and NO (≥99%), Matheson Gas Products. Methyl nitrite was prepared as described by Taylor *et al.* (1980) and stored at 77 K under vacuum.

2.4.3. Results

Dark Decays and Photolysis of 5-Hydroxy-2-pentanone

The measured gas-phase concentration of 5-hydroxy-2-pentanone in the chamber in the dark showed no significant change over a period of 6.0 hr. A least-squares analysis of $\ln([5\text{-hydroxy-2-pentanone}])$ against time led to a slope of $(4.8 \pm 5.7) \times 10^{-4} \text{ min}^{-1}$, where (as elsewhere in this article) the indicated error is two standard deviations. Hence the measured 5-hydroxy-2-pentanone concentration remained constant to within $\pm 20\%$, which we assume to be the analytical uncertainty of the on-fiber derivatization procedure. The observed lack of any significant decay of the 5-hydroxy-2-pentanone concentration over this 6-hr time period shows that under our experimental conditions no observable conversion of 5-hydroxy-2-pentanone to 4,5-dihydro-2-methylfuran occurred.

In a photolyzed 5-hydroxy-2-pentanone – cyclohexane (in excess) – air mixture, the concentration of 5-hydroxy-2-pentanone remained constant to within $\pm 17\%$ over 30 min of irradiation (two 15-min irradiations occurring over 4.7 hr) at the same light intensity as used during the rate constant determinations. Least-squares analysis of the data resulted in a photolysis rate of $-(1.1 \pm 8.3) \times 10^{-3} \text{ min}^{-1}$; *i.e.*, zero within the experimental uncertainties. Alternatively, these data correspond to an overall decay rate of $-(2.1 \pm 8.3) \times 10^{-4} \text{ min}^{-1}$ over the 4.7 hr duration of the experiment. Hence within the analytical uncertainties of $\pm 20\%$, no photolysis or dark decay of 5-hydroxy-2-pentanone occurred during the rate constant determination experiments. The results of these experiments indicate that the overall uncertainty in the measured 5-hydroxy-2-pentanone concentrations is approximately $\pm 20\%$ using the on-fiber derivatization procedure, and this is also assumed to be the case for the on-fiber derivatization measurements of 4-methyl-2-pentanone.

Measurement of the OH Radical Reaction Rate Constant

A series of $\text{CH}_3\text{ONO} - \text{NO} - 5\text{-hydroxy-2-pentanone} - 4\text{-methyl-2-pentanone} - \text{air}$ irradiations were carried out with analysis of 4-methyl-2-pentanone by both Tenax/thermal desorption and on-fiber derivatization and of 5-hydroxy-2-pentanone by on-fiber derivatization. Based on pre-irradiation analyses of 4-methyl-2-pentanone using the Tenax/thermal desorption system, the reproducibility of these analyses was within $\leq 3\%$, consistent with previous experience in this laboratory for similar analyses. We therefore used a comparison of the Tenax/thermal desorption and on-fiber derivatization analyses for 4-methyl-2-pentanone as a check on the on-fiber derivatization analysis method. For one experiment (out of 5 conducted) the on-fiber derivatization analyses disagreed with the Tenax/thermal desorption analyses of 4-methyl-2-pentanone (on a relative basis) by more than 20%, and the results of this experiment were therefore not used in the data analysis.

The data obtained for 4-methyl-2-pentanone using the SPME sampling method vs the Tenax sampling method are plotted in accordance with Equation (I) in Figure 15, allowing comparison of the two analysis methods. Figure 16 shows a plot of Equation (I) for 5-hydroxy-2-pentanone with the Tenax data for 4-methyl-2-pentanone as the reference. The regression slope of the data shown in Figure 15 (with the fit being constrained to pass through the origin) is 1.01 ± 0.30 (an unconstrained fit resulted in a slope of 1.03 ± 0.30), showing that within the

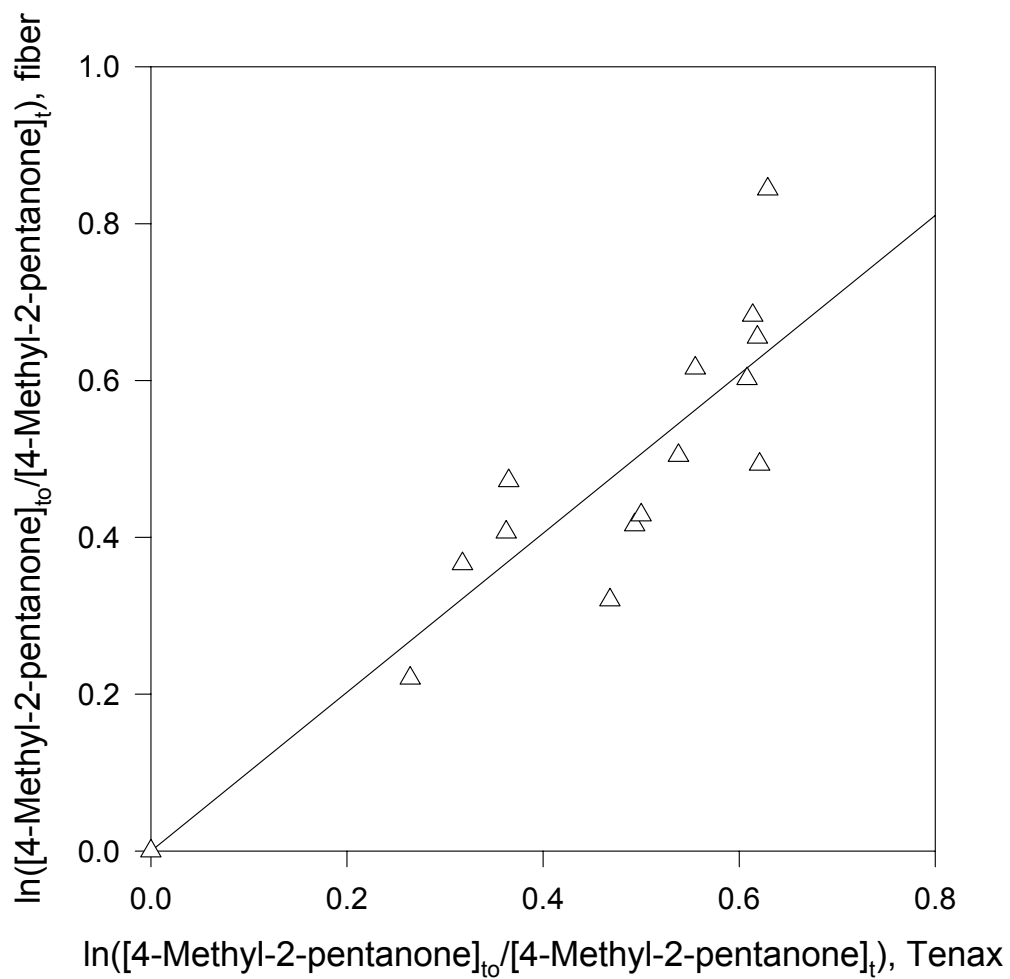


Figure 15. Plot of Equation (I) for 4-methyl-2-pentanone analyzed by on-fiber derivatization with subsequent thermal desorption and GC-FID compared to its analysis by collection onto Tenax solid adsorbent with subsequent thermal desorption and GC-FID. The line is the regression line constrained to pass through the origin.

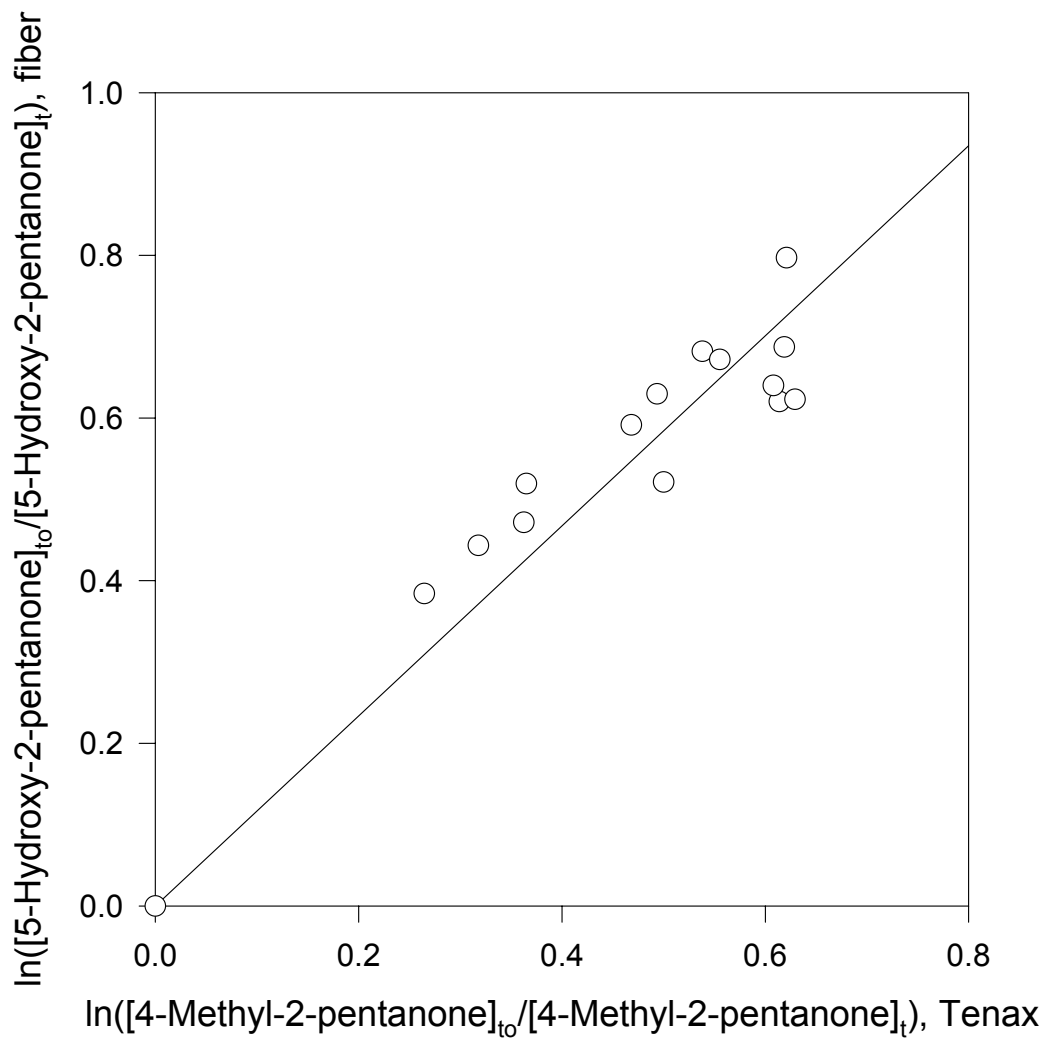


Figure 16. Plot of Equation (I) for 5-hydroxy-2-pentanone (analyzed by on-fiber derivatization with subsequent thermal desorption and GC-FID), with 4-methyl-2-pentanone (analyzed by collection onto Tenax solid adsorbent with subsequent thermal desorption and GC-FID) as the reference compound. The line is the regression line constrained to pass through the origin.

rather large) uncertainties the on-fiber derivatization analyses tracked the much more precise Tenax/thermal desorption analyses and, therefore, the on-fiber derivatization analyses for 5-hydroxy-2-pentanone could be used to obtain the rate constant for its reaction with OH radicals. Regression analysis of the data shown in Figure 16, with the fit being constrained to pass through the origin, leads to the rate constant ratio,

$$k_1(5\text{-hydroxy-2-pentanone})/k_2(4\text{-methyl-2-pentanone}) = 1.17 \pm 0.22$$

with an unconstrained fit having a slope of 1.00 ± 0.20 .

Reaction Products

GC-MS analyses of SPME fibers pre-coated with derivatizing agent and exposed to the chamber contents were carried out before and after irradiation of a $\text{CH}_3\text{ONO} - \text{NO} - 5\text{-hydroxy-2-pentanone} - \text{air}$ mixture. Using isobutane CI, molecular weight information is obtained from the protonated molecule with a smaller adduct generally appearing at 40 mass units higher. Thus, for a carbonyl-containing compound of molecular weight M , its oximes (*Z*- and *E*- oximes are possible) show spectra with strong $[\text{M}+196]^+$ and less intense $[\text{M}+236]^+$ ions. Compounds with two carbonyl moieties will have pseudo-molecular ions at $[\text{M}+391]^+$, again with a less intense ion at 40 mass units higher. In addition to the oximes of 5-hydroxy-2-pentanone, the GC-MS analyses of the reacted mixture showed the presence of di-oximes of two dicarbonyl products with molecular weights of 86 and 100.

In addition to the two dicarbonyl products, the oxime of a carbonyl-containing product of molecular weight 116 and exhibiting a characteristic intense fragment ion resulting from loss of 60 ($\text{CH}_3\text{C}(\text{O})\text{OH}$) from the molecular ion was present. The retention time and mass spectrum of this product were identical to that of the product observed from the OH radical-initiated reaction of 4,5-dihydro-2-methylfuran and identified as $\text{CH}_3\text{C}(\text{O})\text{OCH}_2\text{CH}_2\text{CHO}$ (Martin *et al.*, 2002). While the GC-MS peak areas of the di-oximes of molecular weight 86 and 100 were much larger than that of the oxime of molecular weight 116, no quantifications could be carried out in the absence of appropriate GC-MS response factors.

API-MS analyses of irradiated $\text{CH}_3\text{ONO} - \text{NO} - 5\text{-hydroxy-2-pentanone} - \text{air}$ mixtures showed (in addition to those at 85, 103, 169, 187 and 205 u arising from protonated 5-hydroxy-2-pentanone (molecular weight 102) and its dimer and losses of H_2O and $2\text{H}_2\text{O}$ from these) the presence of ion peaks at 87, 101, 189 and 201 u. API-MS/MS “product ion” spectra of these ion peaks in the API-MS spectra showed that these ion peaks were: 87 $[\text{86}+\text{H}]^+$; 101, $[\text{100}+\text{H}]^+$; 189, $[\text{86}+\text{102}+\text{H}]^+$; and 201, $[\text{100}+\text{100}+\text{H}]^+$ u, indicating the formation of products of molecular weight 86 and 100. Additional ion peaks in the API-MS spectra at 171 and 185 u are attributed to $[\text{86}+\text{102}+\text{H}-\text{H}_2\text{O}]^+$ and $[\text{100}+\text{102}+\text{H}-\text{H}_2\text{O}]^+$, respectively. An additional ion peak was observed in 2 out of the 3 experiments at 117 u, with its API-MS/MS “product ion” spectrum being identical to that of the product formed from the reaction of OH radicals with 4,5-dihydro-2-methylfuran and attributed to $\text{CH}_3\text{C}(\text{O})\text{OCH}_2\text{CH}_2\text{CHO}$ (Martin *et al.*, 2002).

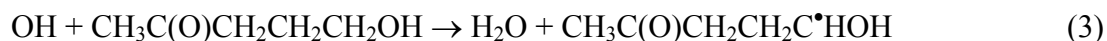
2.4.4. Discussion

The measured rate constant ratio k_1/k_2 can be placed on an absolute basis by use of a rate constant k_2 for the reaction of OH radicals with 4-methyl-2-pentanone of $1.41 \times 10^{-11} \text{ cm}^3 \text{ molecule}^{-1} \text{ s}^{-1}$ at room temperature (Atkinson, 1994), resulting in

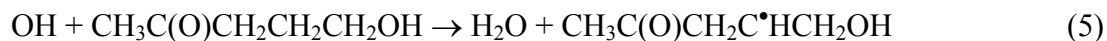
$$k_1(5\text{-hydroxy-2-pentanone}) = (1.6 \pm 0.4) \times 10^{-11} \text{ cm}^3 \text{ molecule}^{-1} \text{ s}^{-1}$$

at 298 ± 2 K, where the indicated error includes the estimated overall uncertainty of $\sim \pm 10\%$ (Kramp and Paulson, 1998) in the rate constant k_2 . The 298 K rate constant calculated using the estimation method of Kwok and Atkinson (1995), as revised by Bethel *et al.* (2001), is $1.39 \times 10^{11} \text{ cm}^3 \text{ molecule}^{-1} \text{ s}^{-1}$, in excellent agreement with the measured value.

The reaction of OH radicals with 5-hydroxy-2-pentanone proceeds by H-atom abstraction from the various C-H and O-H bonds, with predicted (Kwok and Atkinson, 1995; Bethel *et al.*, 2001) percentages of the overall reaction being: from the 1-position CH_3 group, 1%; from the 3-position CH_2 group, 6%; from the 4-position CH_2 group, 68%; from the 5-position CH_2 group, 24%; and from the OH group, 1%. H-atom abstraction from the 5-position CH_2 group leads to formation of the molecular weight 100 dicarbonyl $\text{CH}_3\text{C}(\text{O})\text{CH}_2\text{CH}_2\text{CHO}$.



H-atom abstraction from the 4-position CH_2 group leads to formation of the molecular weight 86 dicarbonyl $\text{CH}_3\text{C}(\text{O})\text{CH}_2\text{CHO}$,



with the 1,2-hydroxyalkoxy radical $\text{CH}_3\text{C}(\text{O})\text{CH}_2\text{CH}(\text{O}^*)\text{CH}_2\text{OH}$ being predicted to dominantly decompose rather than isomerize or react with O_2 at 298 K and atmospheric pressure of air (Atkinson, 1997a,b; Aschmann and Atkinson, 1999),



followed by reaction of the $\text{C}^*\text{H}_2\text{OH}$ radical with O_2 to form HCHO plus the HO_2 radical. H-atom abstraction from the 3-position CH_2 group is predicted to lead to the formation of 3-hydroxypropanal plus the acetyl radical.

Hence the observed molecular weight 86 and 100 dicarbonyls are predicted and are attributed to $\text{CH}_3\text{C}(\text{O})\text{CH}_2\text{CHO}$ and $\text{CH}_3\text{C}(\text{O})\text{CH}_2\text{CH}_2\text{CHO}$, respectively. The observation of the molecular weight 116 carbonyl-containing product $\text{CH}_3\text{C}(\text{O})\text{OCH}_2\text{CH}_2\text{CHO}$ formed from the reaction of OH radicals with 4,5-dihydro-2-methylfuran indicates that some conversion of 5-hydroxy-2-pentanone to 4,5-dihydro-2-methylfuran occurs under the experimental conditions employed, noting that the 4,5-dihydro-2-methylfuran reaction product was not observed in all of the experiments utilizing *in situ* API-MS analyses.

Atmospheric Implications

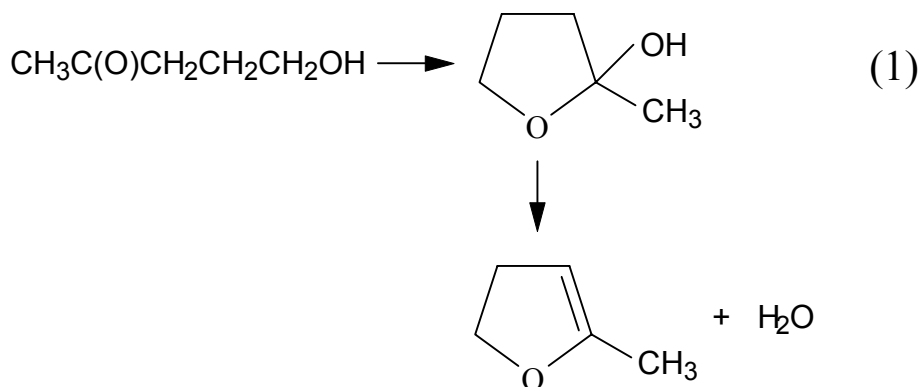
The present study indicates that for relative humidity >5% at room temperature, 5-hydroxy-2-pentanone does not convert to any significant extent to 4,5-dihydro-2-methylfuran, and that the lifetime of 5-hydroxy-2-pentanone is determined by its reaction with OH radicals (and presumably to a much lesser extent with NO₃ radicals). The calculated lifetime of 5-hydroxy-2-pentanone in the atmosphere is 9 hr for an assumed average daytime OH radical concentration of 2.0×10^6 molecule cm⁻³ (Krol *et al.*, 1998; Prinn *et al.* 2001), and the reaction products include the dicarbonyl compounds CH₃C(O)CH₂CH₂CHO and CH₃C(O)CH₂CHO.

2.5. Formation and Atmospheric Reactions of 4,5-Dihydro-2-methylfuran

2.5.1. Introduction

In the troposphere, the dominant loss process for alkanes is by reaction with the hydroxyl (OH) radical (Atkinson, 1997a). In the presence of NO, the OH radical-initiated reactions of alkanes lead to formation of alkoxy (RO[•]) radical intermediates which subsequently decompose, react with O₂, and isomerize (Atkinson, 1997a,b), with the isomerization reactions being predicted to generally result in the formation of 1,4-hydroxycarbonyls (Atkinson, 1997a,b, 2000). Consistent with these predictions, product studies of the reactions of C₄-C₈ *n*-alkanes with the OH radical in the presence of NO show that hydroxycarbonyls account for a significant fraction of the overall reaction products (Eberhard *et al.*, 1995; Atkinson *et al.*, 1995a; Kwok *et al.*, 1996b; Arey *et al.*, 2001; Aschmann *et al.*, 2001a, 2002b; Section 2.4. above). As discussed in Section 2.3. above, we have shown that these hydroxycarbonyls are indeed 1,4-hydroxycarbonyls, and that they account for significant, and often dominant, fractions of the total products formed from >C₄ *n*-alkanes, with the remaining products being alkyl nitrates, 1,4-hydroxyalkyl nitrates, and carbonyl compounds (Arey *et al.*, 2001; Aschmann *et al.*, 2001a; Reisen *et al.*, 2004; Section 2.3. above). For example, 1,4-hydroxycarbonyls account for ~50-60% of the products formed from the OH radical-initiated reactions of *n*-pentane through *n*-octane (Arey *et al.*, 2001; Reisen *et al.*, 2004; Section 2.3. above).

The only commercially available 1,4-hydroxycarbonyl is 5-hydroxy-2-pentanone, which in the liquid phase is reported to be in equilibrium with its cyclic hemiacetal form (Aelterman *et al.*, 1997). Formation of 4,5-dihydro-2-methylfuran from 5-hydroxy-2-pentanone by thermal dehydration in the liquid phase (Mikhlina *et al.*, 1970; Markevich *et al.*, 1981) and by catalytic dehydration in the gas-phase has been reported. In previous studies, both in this laboratory and by Cavalli *et al.* (2000), vapor-phase samples of 5-hydroxy-2-pentanone introduced into environmental chambers have been observed to convert at an appreciable rate at room temperature to 4,5-dihydro-2-methylfuran, most likely via loss of a water molecule from the cyclic hemiacetal.



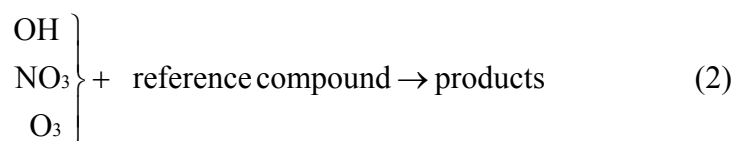
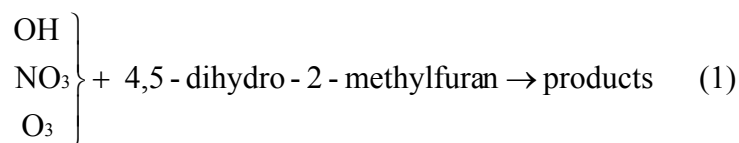
In this work we have investigated the conversion of 5-hydroxy-2-pentanone to 4,5-dihydro-2-methylfuran (DHMF) and studied the atmospherically-relevant reactions of DHMF with OH radicals, NO₃ radicals, and O₃.

2.5.2. Experimental Methods

Kinetic Studies

Experiments were carried out at 298 ± 2 K in a 5870 liter evacuable, Teflon-coated chamber equipped with an *in situ* multiple-reflection optical system interfaced to a Nicolet 7199 FT-IR spectrometer. Irradiation was provided by a 24-kW xenon arc lamp, with the light being filtered through a 6 mm thick Pyrex pane to remove wavelengths <300 nm. The chamber is fitted with two Teflon-coated fans to ensure rapid mixing of reactants during their introduction into the chamber. IR spectra were recorded with 64 scans per spectrum (corresponding to 2.0 min averaging time), a full-width-at-half-maximum resolution of 0.7 cm^{-1} and a path length of 62.9 m.

Rates of conversion of 5-hydroxy-2-pentanone to 4,5-dihydro-2-methylfuran were measured at 298 ± 2 K and at ~ 1.5 , 16 and 740 Torr total pressure of dry N_2 . Rate constants for the reactions of OH and NO_3 radicals and O_3 with 4,5-dihydro-2-methylfuran were measured at 298 ± 2 K and 740 Torr total pressure of dry synthetic air (80% N_2 + 20% O_2), using relative rate techniques in which the reactions of 4,5-dihydro-2-methylfuran and a reference compound were monitored in the presence of OH radicals, NO_3 radicals, or O_3 .



Providing that 4,5-dihydro-2-methylfuran (DHMF) and the reference compound react only with OH radicals, NO_3 radicals, or O_3 , then,

$$\ln \left(\frac{[\text{DHMF}]_{t_0}}{[\text{DHMF}]_t} \right) = \frac{k_1}{k_2} \ln \left(\frac{[\text{reference compound}]_{t_0}}{[\text{reference compound}]_t} \right) \quad (I)$$

where $[\text{DHMF}]_{t_0}$ and $[\text{reference compound}]_{t_0}$ are the concentrations of 4,5-dihydro-2-methylfuran and reference compound at time t_0 , $[\text{DHMF}]_t$ and $[\text{reference compound}]_t$ are the corresponding concentrations at time t , and k_1 and k_2 are the rate constants for reactions (1) and (2), respectively.

Hydroxyl radicals were generated in the presence of NO by the photolysis of CH_3ONO in air (Atkinson *et al.*, 1981) at wavelengths >300 nm. The initial reactant concentrations

employed for the OH radical reaction were 2.5×10^{14} molecule cm^{-3} each of DHMF, the reference compound (cyclohexene or 2-methylpropene), CH_3ONO , and NO. Irradiations were carried out intermittently, with IR spectra being recorded during the dark periods and with total irradiation times of 7-8 min. NO_3 radicals were generated *in situ* in the dark by the thermal decomposition of N_2O_5 (Atkinson *et al.*, 1984b, 1988) and O_3 was produced as O_3/O_2 mixtures of known concentrations by an ozone generator. For both the NO_3 radical and O_3 reactions, the initial reactant concentrations (molecule cm^{-3}) were: DHMF, 2.5×10^{14} ; and 2,3-dimethyl-2-butene (the reference compound), 4.9×10^{14} ; with successive additions of aliquots of N_2O_5 [3-4 additions of $(0.93\text{-}1.2) \times 10^{14}$ molecule cm^{-3} of N_2O_5 in the chamber] or O_3 [3-4 additions of $(0.79\text{-}1.1) \times 10^{14}$ molecule cm^{-3} of O_3 in the chamber] and with the aliquots being added after complete consumption of the previously added N_2O_5 or O_3 . The O_3 experiments were carried out in the presence of 1.6×10^{17} molecule cm^{-3} of cyclohexane, sufficient to scavenge $\geq 90\%$ of the OH radicals formed (Atkinson, 1997a, 2000).

In addition, DHMF concentrations were monitored in DHMF – air mixtures, both in the dark under dry conditions ($\ll 1\%$ relative humidity) and in the presence of 4.0×10^{16} molecule cm^{-3} of water vapor (5% relative humidity), and during irradiation. The initial DHMF concentrations were the same as those used in the kinetic experiments.

Product Studies

Experiments were carried out at 298 ± 2 K and 740 Torr total pressure of air in three reaction chambers: in the 5870 liter evacuable chamber with *in situ* FT-IR analysis, in a 7900 liter Teflon chamber equipped with two parallel banks of black lamps and interfaced to a PE SCIEX API III MS/MS direct air sampling, atmospheric pressure ionization tandem mass spectrometer (API-MS); and in a 7500 liter Teflon chamber equipped with blacklamps and with provision for sampling onto a Solid Phase Micro Extraction (SPME) fiber (Pawliszyn, 1997).

The majority of experiments carried out to identify the products of the reactions of DHMF were carried out in the 5870 liter evacuable chamber with *in situ* FT-IR analyses. For the OH radical reactions, the initial concentrations (in units of 10^{14} molecule cm^{-3}) were: CH_3ONO , 2.46; NO, 2.46; and DHMF, 0.74-2.46. In order to measure the yield of HCHO, one experiment employed 2-propyl nitrite instead of methyl nitrite as the OH radical precursor (Aschmann *et al.*, 2001b) [photolysis of 2-propyl nitrite forms acetone (Aschmann *et al.*, 2001b), in contrast to the photolysis of methyl nitrite which forms HCHO], with initial concentrations (in units of 10^{14} molecule cm^{-3}) of: $(\text{CH}_3)_2\text{CHONO}$, 1.47; NO, 2.46; and DHMF, 2.46.

One experiment was also carried out in the 7500 liter all-Teflon chamber (at $\sim 1\%$ relative humidity) with initial reactant concentrations (molecule cm^{-3}) of: CH_3ONO , 2.4×10^{14} ; NO, 1.9×10^{14} ; and DHMF, 2.40×10^{13} . After irradiation for 1 min (corresponding to 15-20% reaction of DHMF based on similar experiments with other organic compounds), a 65 μm PDMS/DVB SPME fiber coated with *O*-(2,3,4,5,6-pentafluorobenzyl)hydroxylamine hydrochloride (Koziel *et al.*, 2001) was exposed to the chamber contents for 3 min, and then analyzed by GC-MS with thermal desorption onto a 30 m DB-1701 fused silica capillary column in a Varian 2000 GC/MS with analysis by isobutane chemical ionization.

For the reaction with NO_3 radicals, one experiment was carried out in which 1.23×10^{14} molecule cm^{-3} of N_2O_5 was added to 2.46×10^{14} molecule cm^{-3} of DHMF in air. Two experiments were carried out for the reaction with O_3 , with 8.5×10^{16} molecule cm^{-3} of cyclohexane being present as an OH radical scavenger in one of the experiments. In each of these experiments, two separate aliquots of 1.29×10^{14} molecule cm^{-3} of O_3 were added to the DHMF (2.46×10^{14} molecule cm^{-3}) - air mixture.

Reactions of DHMF with OH radicals, NO₃ radicals and O₃ were also carried out in the 7900 liter Teflon chamber at 740 Torr of purified air at ~5% relative humidity with API-MS and API-MS/MS analyses. The operation of the API-MS in the MS (scanning) and MS/MS [with collision activated dissociation (CAD)] modes has been described elsewhere (Aschmann *et al.*, 1997). The positive ion mode was used in these analyses, with protonated water hydrates [H₂O⁺(H₂O)_n] acting as the ionizing agent and resulting in the ions that were mass-analyzed being mainly protonated molecules ([M+H]⁺) and their protonated homo- and hetero-dimers (Aschmann *et al.*, 1997). For the OH radical reactions, the initial reactant concentrations (in molecule cm⁻³) were: CH₃ONO and NO, (4.4-4.7) x 10¹³ each; and DHMF, 2.3 x 10¹³; and the mixtures were irradiated for 0.17-5.67 min at 20% of the maximum light intensity, with API-MS spectra being recorded prior to irradiation and after each irradiation. For the NO₃ reactions, the initial concentrations (molecule cm⁻³) were: DHMF, 2.3 x 10¹³; NO₂ (added to slow down the N₂O₅ decomposition), 2.2 x 10¹³; and N₂O₅, 1.4 x 10¹³. For the O₃ experiments, the initial concentrations (molecule cm⁻³) were: DHMF, 2.3 x 10¹³; cyclohexane, 1.4 x 10¹⁶; and with 2 additions of O₃, each addition corresponding to an initial O₃ concentration of ~5 x 10¹² molecule cm⁻³ in the chamber.

Chemicals

The chemicals used and their stated purities were as follows: 5-hydroxy-2-pentanone (95%), TCI America; 4,5-dihydro-2-methylfuran [DHMF] (97%), 2-methylpropene (99%), 2,3-dimethyl-2-butene (99+%), Aldrich Chemical Company; cyclohexene (99%), Chem Samples Co.; and NO (≥99%) and NO₂ (≥99.0%), Matheson Gas Products. Methyl nitrite was prepared as described by Taylor *et al.* (1980) and an analogous method was employed for the synthesis of 2-propyl nitrite. N₂O₅ was prepared by reacting NO₂ with O₃ as described by Atkinson *et al.* (1984b). Methyl nitrite, 2-propyl nitrite and N₂O₅ were all stored at 77K under vacuum prior to use. Partial pressures of all the above chemicals were measured in calibrated 2 liter and 5 liter Pyrex bulbs with a 100-Torr MKS Baratron sensor, except for 5-hydroxy-2-pentanone which was introduced into the bulbs with a microliter syringe, and flushed into the chambers with a stream of N₂ gas. Ozone was produced in a Welsbach T-408 ozone generator at pre-calibrated settings of voltage and input flow of high-purity O₂ (Puritan-Bennett Corp., 99.994%).

2.5.3. Results and Discussion

Kinetic Studies

5-Hydroxy-2-pentanone Decays in Dry N₂

In situ FT-IR analyses of mixtures of 2.48 x 10¹⁴ molecule cm⁻³ of 5-hydroxy-2-pentanone in dry N₂ (<<1% relative humidity) at total pressures of 1.5-740 Torr in the 5870 liter evacuable chamber showed the formation of DHMF (8-18% of the 5-hydroxy-2-pentanone introduced) after the 12-20 min introduction and mixing period. For the experiment at ~1.5 Torr total pressure in which 5-hydroxy-2-pentanone was introduced (with a flow of N₂) into the evacuated chamber, the measured gas-phase concentration of 5-hydroxy-2-pentanone after the 12-min introduction period was only 40% of that introduced into the chamber, suggesting a significant loss of 5-hydroxy-2-pentanone (presumably to the walls). As shown in Figure 17, after the introduction and mixing periods the measured decays of 5-hydroxy-2-pentanone followed first-order behavior. In all three experiments, the sum of the concentrations of gas-phase 5-hydroxy-2-pentanone remaining and DHMF formed after ~100 min accounted for only 75-80 % of the initial 5-hydroxy-2-pentanone (as measured after the introduction and mixing period).

Based upon these three experiments conducted over a period of several months, the 5-hydroxy-2-pentanone decay rate in dry N₂ was independent of the total pressure with a first-order rate constant of $1.5 \times 10^{-2} \text{ min}^{-1}$. The lifetime of 5-hydroxy-2-pentanone in this chamber at low water vapor concentrations ($<8 \times 10^{15} \text{ molecule cm}^{-3}$) is therefore 1.1 hr. A very similar decay rate ($1.3 \times 10^{-2} \text{ min}^{-1}$) and hence lifetime was reported by Cavalli *et al* (2000) [as revised by Barnes, University of Wuppertal, private communication, 2002] for conversion of 5-hydroxy-2-pentanone to DHMF in a 480 liter glass chamber in dry synthetic air.

Photolysis and Dark Decays of 4,5-Dihydro-2-methylfuran

Photolysis of DHMF in dry air showed ~1% loss of DHMF after 30 min irradiation, indicating that photolysis of DHMF during the OH radical reactions was negligible (<1%) and also that there was no significant decay of DHMF in dry air ($\leq 3 \times 10^{-4} \text{ min}^{-1}$). However, in the presence of $4.0 \times 10^{16} \text{ molecule cm}^{-3}$ of water vapor (5% relative humidity), DHMF was observed to decay in the dark at a rate of $(4.8 \pm 0.2) \times 10^{-3} \text{ min}^{-1}$ (as elsewhere here, the indicated error is two least-squares standard deviations), with a measured 58% loss of the initial DHMF over a period of 185 mins and concurrent formation of 5-hydroxy-2-pentanone in ~92% yield (only an approximate quantification of 5-hydroxy-2-pentanone by FT-IR in the presence of water vapor could be obtained). No evidence for attainment of an equilibrium between DHMF and 5-hydroxy-2-pentanone was observed over this time scale.

Clearly, the kinetic and product studies conducted in dry air (<<1% relative humidity) were for the reactions of OH radicals, NO₃ radicals, and O₃ with DHMF without interference from 5-hydroxy-2-pentanone. In contrast, in the presence of water vapor DHMF decays to form 5-hydroxy-2-pentanone with a measured DHMF lifetime at 5% relative humidity of 3.5 hr. The forward and backward reactions shown above therefore occur, leading in the presence of water vapor to interconversion of 5-hydroxy-2-pentanone and DHMF to some equilibrium ratio. While the reactions of DHMF can be studied in dry air, it appears that the reactions of DHMF in the presence of water vapor are complicated by this interconversion, making unambiguous kinetic and product studies difficult. Indeed, it is possible that the API-MS analyses of the reaction of DHMF with OH radicals conducted at ~5% relative humidity involved the participation of 5-hydroxy-2-pentanone and/or its cyclized form [5-hydroxy-2-pentanone is not anticipated to react with O₃ at a measurable rate and the reaction of NO₃ radicals with 5-hydroxy-2-pentanone is expected to be approximately 5 orders of magnitude slower than with DHMF (Aschmann *et al.*, 2003)].

Rate Constants for Reactions of 4,5-Dihydro-2-methylfuran

The data obtained from irradiations of CH₃ONO - NO - DHMF - cyclohexene - air and CH₃ONO - NO - DHMF - 2-methylpropene - air mixtures are plotted in accordance with Equation (I) in Figure 18, and the data from reacting N₂O₅ - NO₃ - NO₂ - DHMF - 2,3-dimethyl-2-butene - air and O₃ - DHMF - 2,3-dimethyl-2-butene - cyclohexane (in excess) - air mixtures are shown in analogous plots in Figure 19. Good straight-line plots are observed and the rate constant ratios k_1/k_2 obtained from least-squares analyses are given in Table 6. These rate constant ratios k_1/k_2 are placed on an absolute basis using the recommended rate constants k_2 for

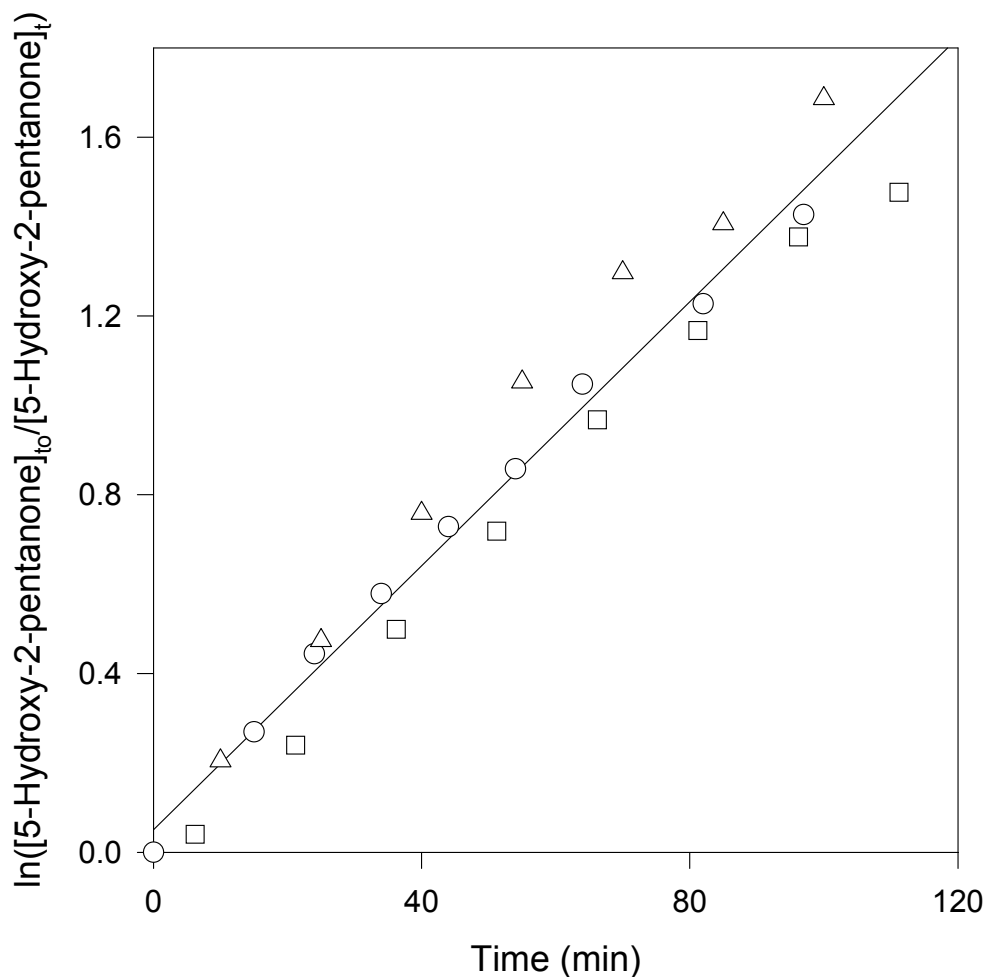


Figure 17. First-order plots of the decays of 5-hydroxy-2-pentanone in the 5870 liter evacuable chamber at 1.5 (\square), 16 (Δ) and 740 (o) Torr total pressure of dry N_2 . The decay rates for the three experiments are, in chronological order, $(1.45 \pm 0.09) \times 10^{-2} \text{ min}^{-1}$ at 740 Torr (the indicated errors are two least-squares standard deviations), $(1.48 \pm 0.05) \times 10^{-2} \text{ min}^{-1}$ at 1.5 Torr, and (5 months later after numerous other types of reactions had been conducted in the chamber) $(1.68 \pm 0.13) \times 10^{-2} \text{ min}^{-1}$ at 16 Torr. The line shown is from a least-squares analysis of the entire data set.

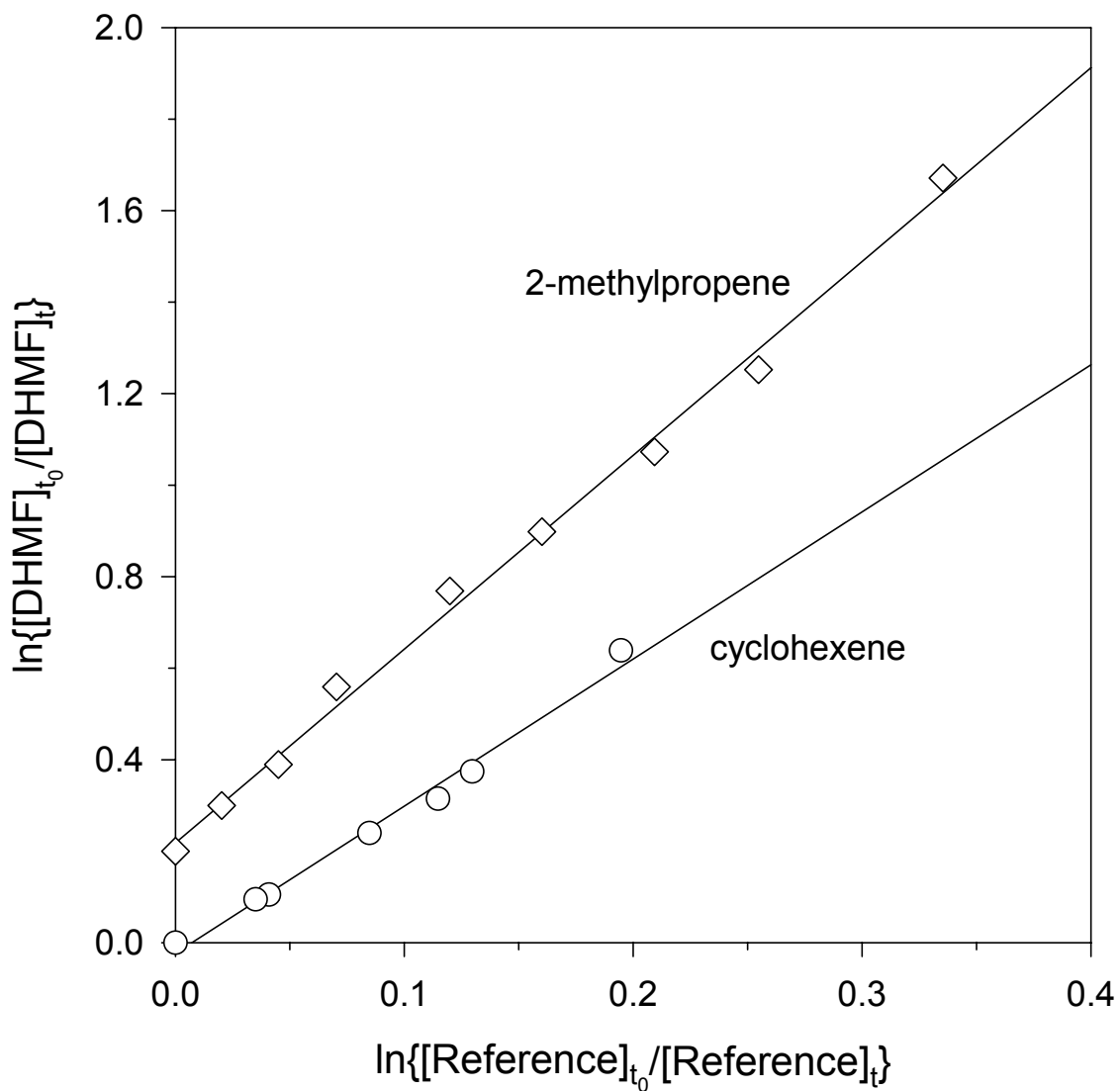


Figure 18. Plots of Equation (I) for the reaction of OH radicals with 4,5-dihydro-2-methylfuran (DHMF), with cyclohexene and 2-methylpropene as the reference compounds. Note that for clarity the data with cyclohexene as the reference compound has been shifted vertically on the y-axis by 0.2 units.

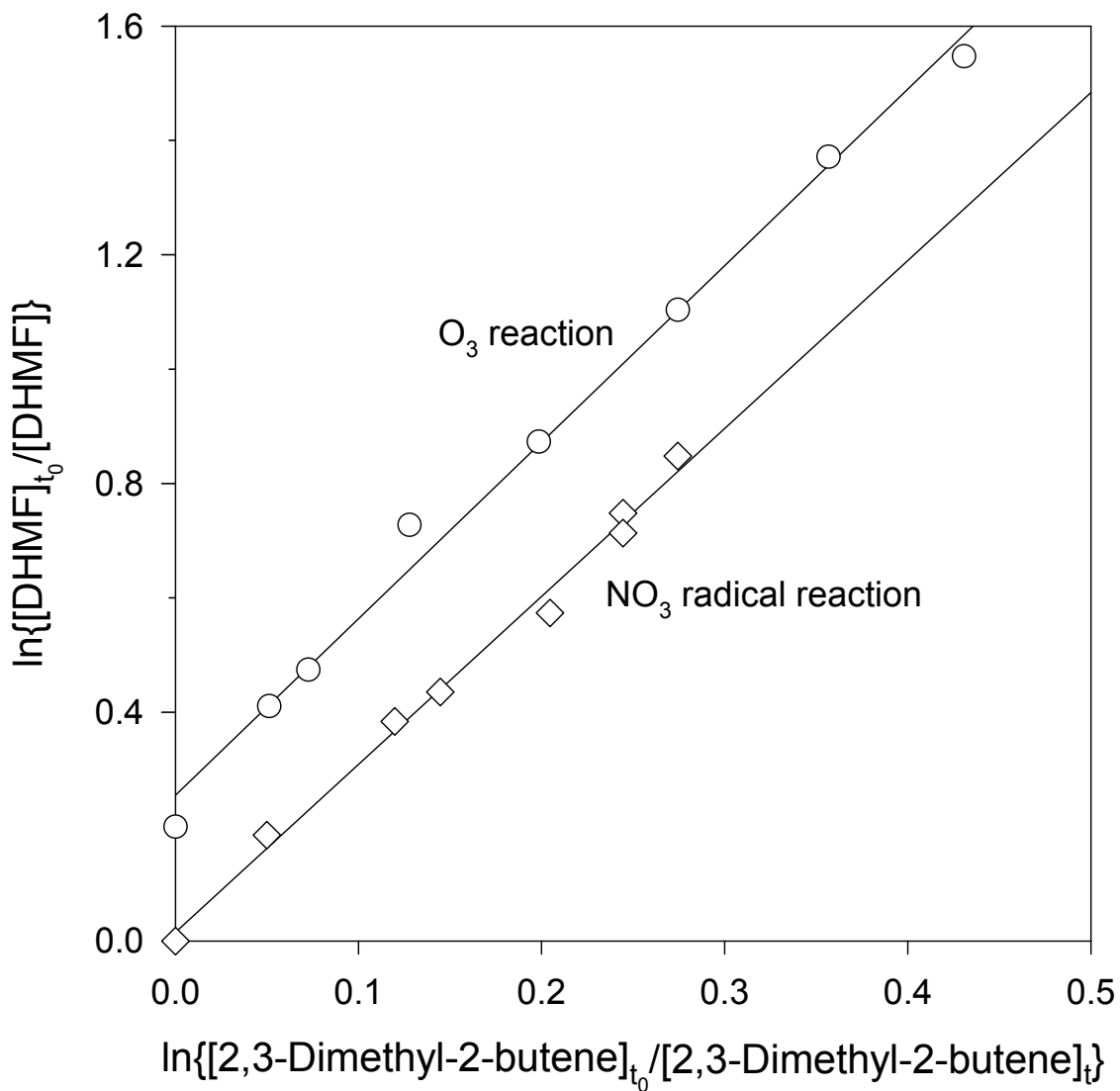


Figure 19. Plots of Equation (I) for the reactions of NO₃ radicals and O₃ with 4,5-dihydro-2-methylfuran (DHMF), with 2,3-dimethyl-2-butene as the reference compound. Note that for clarity the data for the O₃ reaction has been shifted vertically on the y-axis by 0.2 units.

Table 6. Rate constant ratios k_1/k_2 , rate constants k_1 and estimated lifetimes for the reaction of 4,5-dihydro-2-methylfuran with OH radicals, NO_3 radicals, and O_3 at 298 ± 1 K

Reaction and reference compound	k_1/k_2^a	k_1 ($\text{cm}^3 \text{ molecule}^{-1} \text{ s}^{-1}$) ^b	Lifetime ^d
OH Radical Reaction Cyclohexene 2-Methylpropene	3.22 ± 0.32 4.24 ± 0.22	$(2.18 \pm 0.22) \times 10^{-10}$ $(2.17 \pm 0.12) \times 10^{-10}$ $(2.18 \pm 0.11) \times 10^{-10}$ ^c	1.3 hr
NO_3 Radical Reaction 2,3-Dimethyl-2-butene	2.94 ± 0.20	$(1.68 \pm 0.12) \times 10^{-10}$	24 s
O_3 Reaction 2,3-Dimethyl-2-butene	3.09 ± 0.21	$(3.49 \pm 0.24) \times 10^{-15}$	7 min

^aIndicated errors are two least-squares standard deviations.

^bPlaced on an absolute basis by use of rate constants k_2 for the reactions of OH radicals with cyclohexene and 2-methylpropene at 298 K of $6.77 \times 10^{-11} \text{ cm}^3 \text{ molecule}^{-1} \text{ s}^{-1}$ and $5.14 \times 10^{-11} \text{ cm}^3 \text{ molecule}^{-1} \text{ s}^{-1}$, respectively; ¹a rate constant k_2 for the reaction of NO_3 radicals with 2,3-dimethyl-2-butene of $5.72 \times 10^{-11} \text{ cm}^3 \text{ molecule}^{-1} \text{ s}^{-1}$; ¹ and a rate constant k_2 for the reaction of O_3 with 2,3-dimethyl-2-butene of $1.13 \times 10^{-15} \text{ cm}^3 \text{ molecule}^{-1} \text{ s}^{-1}$ (Atkinson, 1997a). The indicated errors in k_1 do not include the uncertainties in the values of k_2 .

^cWeighted average.

^dEstimated on the basis of 24-hour average tropospheric concentrations (molecule cm^{-3}) of: OH radicals, 1.0×10^6 ; NO_3 radicals, 2.5×10^8 ; and O_3 , 7.4×10^{11} .

the reference compounds (Atkinson, 1997a; see footnotes to Table 6), and are also included in Table 6.

These are the first reported rate constants for these reactions of 4,5-dihydro-2-methylfuran. These OH radical, NO_3 radical and O_3 reaction rate constants are all high, comparable to what may be expected for an alkene containing dialkyl and ether substituents, $\text{R}_2\text{C}=\text{CHOR}$ (Atkinson, 1989, 1991, 1994; Kwok and Atkinson, 1995), and proceed mainly or solely by initial addition of OH radicals, NO_3 radicals and O_3 to the C=C bond (Atkinson, 1989, 1991, 1994; Kwok and Atkinson, 1995). Grosjean and Grosjean (1999) have reported a rate constant at 288 ± 1 K for the reaction of O_3 with ethyl 1-propenyl ether [$\text{CH}_3\text{CH}=\text{CHOCH}_2\text{CH}_3$] of $\geq (5.85 \pm 1.32) \times 10^{-16} \text{ cm}^3 \text{ molecule}^{-1} \text{ s}^{-1}$, reasonably consistent with the rate constant measured here for DHMF considering the additional substituent group attached to the C=C bond in DHMF. As shown in Table 6, the calculated lifetimes of DHMF are short during both daytime and nighttime.

Products of the DHMF Reactions

Reaction with the OH radical

Figures 20A and 20B show the FT-IR spectra of products formed from DHMF during the irradiation of a $\text{CH}_3\text{ONO} - \text{NO} - \text{DHMF} - \text{air}$ mixture, corresponding to 33% and 67%, respectively, of the initial $2.46 \times 10^{14} \text{ molecule cm}^{-3}$ of DHMF being consumed by reaction. In

both Figures 20A and 20B, the absorption bands of the remaining DHMF and the products arising from CH_3ONO and NO (HCHO , HCOOH , CH_3ONO_2 , HNO_3 , HONO , HOONO_2 , and NO_2) have been subtracted. The set of prominent bands at 1769, 1236, and 1057 cm^{-1} indicate the presence of an ester as a major product (Pouchert, 1975, 1989). The $\text{C}=\text{O}$ stretch region also shows the likely presence of an overlapped band at $\sim 1744\text{ cm}^{-1}$ which can be attributed to another carbonyl group. The relative intensities of the overlapped $\text{C}=\text{O}$ stretch bands and the 1236 and 1057 cm^{-1} bands remained constant during the reaction, indicating that all of these absorption bands could belong to the same product. The major product expected from a consideration of the chemical mechanism involved (see Figure 21) and which is consistent with the infrared spectrum is $\text{CH}_3\text{C}(\text{O})\text{OCH}_2\text{CH}_2\text{CHO}$ (molecular weight 116). The formation of increasing but minor amounts of $\text{CH}_2=\text{CH}_2$, as indicated by the Q-branch feature at 950 cm^{-1} , can also be seen in Figure 20.

A subtraction of the spectrum of Figure 20A, with the appropriate scale factor, from the spectrum of Figure 20B to cancel out the absorption bands of $\text{CH}_3\text{C}(\text{O})\text{OCH}_2\text{CH}_2\text{CHO}$ resulted in Figure 20C, which shows absorption bands of a minor product(s) formed during the latter part of the reaction. The residual bands at approximately 1835, 1730, 1290 and 790 cm^{-1} (Figure 20C) are characteristic of acyl peroxy nitrates, $\text{RC}(\text{O})\text{OONO}_2$, (Stephens, 1964) although minor amounts of alkyl peroxy nitrates, ROONO_2 , may also be contributing to the three lower-frequency band positions. A possible product is $\text{CH}_3\text{C}(\text{O})\text{OCH}_2\text{CH}_2\text{C}(\text{O})\text{OONO}_2$, which is expected to be formed as a second-generation product from $\text{CH}_3\text{C}(\text{O})\text{OCH}_2\text{CH}_2\text{CHO}$ (Atkinson, 1994, 2000).

FT-IR analysis of an irradiated $(\text{CH}_3)_2\text{CHONO} - \text{NO} - \text{DHMF} - \text{air}$ mixture showed the formation of HCHO , with the measured yield increasing with the extent of reaction, being 5.4% after 1 min and 12% after 4 min of irradiation (corresponding to 13% and 59% consumption, respectively, of the initial 2.46×10^{14} molecule cm^{-3} of DHMF). It was verified from a separate $(\text{CH}_3)_2\text{CHONO} - \text{NO} - \text{air}$ irradiation, employing the same light intensity and initial concentrations as in the run with DHMF present, that the major product formed from $(\text{CH}_3)_2\text{CHONO}$ is acetone, with negligible formation of HCHO at irradiation times of 1 and 4 min. The increase of HCHO yield with irradiation time in the DHMF experiment is therefore attributed to HCHO formation from secondary reactions.

The results of GC-MS and API-MS analyses of irradiated $\text{CH}_3\text{ONO} - \text{NO} - \text{DHMF}$ mixtures demonstrated the formation of a major product of molecular weight 116 from DHMF. GC-MS analyses of the *O*-(2,3,4,5,6-pentafluoro)benzyl hydroxylamine coated SPME fiber exposed to the reaction products showed a large product peak whose mass spectrum had an $[\text{M}+\text{H}]^+$ base ion corresponding to the oxime of a molecular weight 116 carbonyl product at $[\text{M}+\text{H}]^+ = 312\text{ u}$. The mass spectrum also exhibited an intense fragment ion resulting from a loss of 60 ($\text{CH}_3\text{C}(\text{O})\text{OH}$) from the molecular ion. The compound therefore contained a carbonyl group and an ester $\text{CH}_3\text{C}(\text{O})\text{O}$ - group, consistent with this product being $\text{CH}_3\text{C}(\text{O})\text{OCH}_2\text{CH}_2\text{CHO}$. It should be noted that the oxime of 5-hydroxy-2-pentanone was also observed in both the pre- and post reaction SPME analyses.

API-MS spectra of non-reacted $\text{CH}_3\text{ONO} - \text{NO} - \text{DHMF} - \text{air}$ mixtures (in air at $\sim 5\%$ relative humidity) consist of ion peaks at 85, 169, 187, 205 and 253 u which are attributed to the

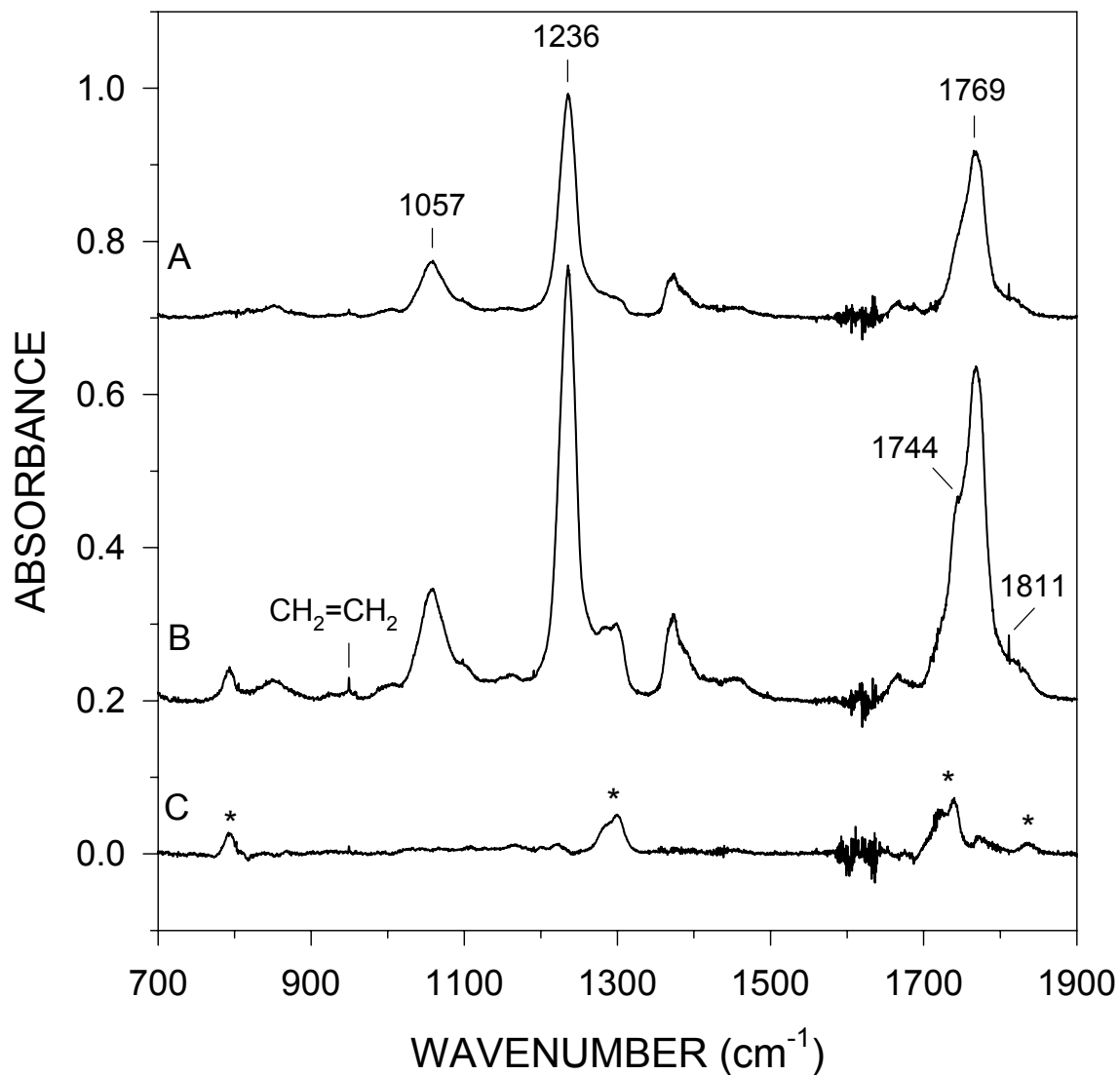
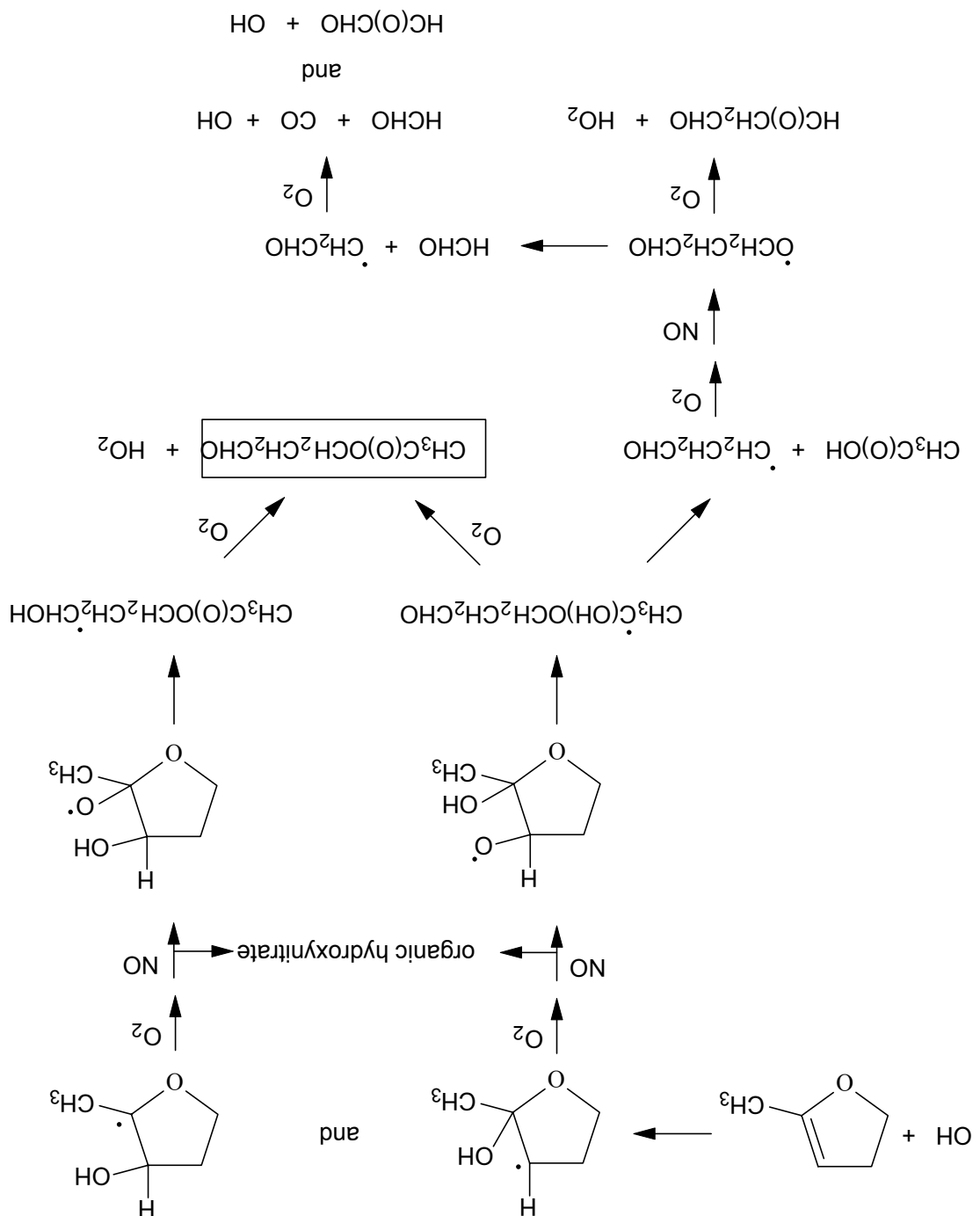


Figure 20. Infrared spectra of products attributed to DHMF from an irradiated CH₃ONO – NO - DHMF - air mixture corresponding to (A) 33% consumption and (B) 67% consumption of the initial 2.46×10^{14} molecule cm⁻³ of DHMF (see text). (C) Residual spectrum resulting from a scaled subtraction of (A) from (B) to cancel the absorption bands of the major product CH₃C(O)OCH₂CH₂CHO. Asterisks denote absorption bands attributed to RC(O)OONO₂.

Figure 21. Reaction scheme for the reaction of OH radicals with 4,5-dihydro-2-methylfuran in the presence of NO. Product in box is observed (see text).



protonated DHMF, the protonated dimer, the mono- and dihydrated protonated dimer, and the protonated trimer, respectively. Note that the presence or absence of 5-hydroxy-2-pentanone cannot be discerned in the API-MS spectra, since ion peaks at 187 and 85 u are also expected from 5-hydroxy-2-pentanone. API-MS spectra of irradiated CH₃ONO - NO - DHMF - air mixtures showed, at total irradiation times of 10, 30 and 40 s, an additional ion at 201 u which API-MS/MS “fragment ion” spectrum showed to be a protonated heterodimer of DHMF and a molecular weight 116 product. After longer irradiation times, product ion peaks due to additional products of molecular weight 86, 100 and 132 were observed. It is possible that these 86, 100 and 132 molecular weight products arise from secondary reactions and/or formation and reaction of 5-hydroxy-2-pentanone from the hydrolysis of DHMF in these experiments. Reaction of OH radicals with 5-hydroxy-2-pentanone is expected to proceed largely by H-atom abstraction from the C-H bonds of the CH₂ groups at the 4- and 5-positions (Kwok and Atkinson, 1995), leading in the presence of NO to the formation of CH₃C(O)CH₂CHO (molecular weight 86) and CH₃C(O)CH₂CH₂CHO (molecular weight 100), respectively (Atkinson, 1994, 1997a). API-MS analyses of irradiated CH₃ONO – NO – 5-hydroxy-2-pentanone –air mixtures (~5% relative humidity) in our laboratory showed the formation of products of molecular weight 100 and 86 (see Section 2.4).

While CH₃C(O)OCH₂CH₂CHO was identified by GC-MS as its oxime, quantitative measurements could not be made by GC-MS because of the lack of an authentic standard. Quantification of CH₃C(O)OCH₂CH₂CHO was therefore carried out using an average absorption coefficient obtained from the ~1240 cm⁻¹ IR bands of CH₃C(O)OCH₂CH₃, CH₃C(O)OCH₂CH₂=CH₂ and CH₃C(O)OCH₂Cl, with an average peak-to-baseline absorption coefficient of (7.89 ± 0.50) x 10⁻¹⁹ cm² molecule⁻¹ and an average integrated (baseline-corrected) absorption coefficient of (2.27 ± 0.11) x 10⁻¹⁷ cm molecule⁻¹. CH₃C(O)OCH₂CH₂CHO concentrations derived from spectra such as those shown in Figures 20A and 20B using these two absorption coefficients agreed to within 5% and the average value was adopted for each spectral record. These estimated CH₃C(O)OCH₂CH₂CHO concentrations were then corrected for secondary reaction with the OH radical (Atkinson *et al.*, 1982), using the rate constant measured here for the reaction of OH radicals with DHMF and an estimated rate constant of 2.7 x 10⁻¹¹ cm³ molecule⁻¹ s⁻¹ for reaction of OH radicals with CH₃C(O)OCH₂CH₂CHO (Kwok and Atkinson, 1995). The corrections for secondary reaction were ≤8%. The formation yield of CH₃C(O)OCH₂CH₂CHO, determined from a least-squares analysis of a plot of the corrected CH₃C(O)OCH₂CH₂CHO concentrations against the amounts of DHMF reacted, is given in Table 7 together with the range of observed yields for the minor products HCHO and ethene.

As noted above, the magnitude of the rate constant measured for DHMF indicates that the reaction proceeds by initial addition of the OH radical at the C=C bond. Subsequent addition of O₂ to form a peroxy radical, followed by reaction of the peroxy radical with NO leads to formation of an organic nitrate or an alkoxy radical plus NO₂ (Atkinson, 2000).



The alkoxy radicals can then react with O₂, decompose by C-C bond scission, or isomerize through (typically) a 6-membered transition state (Atkinson, 1997a,b, 2000). A possible reaction

Table 7. Products identified and their formation yields from the gas-phase reaction of OH radicals with 4,5-dihydro-2-methylfuran

Product	Molar yield		
	FT-IR	API-MS	GC-MS
CH ₃ C(O)OCH ₂ CH ₂ CHO	0.74 ± 0.19 ^a	Major product observed of MW 116	Carbonyl product of MW 116 observed
HCHO	0.054-0.12 ^b		
CH ₂ =CH ₂	0.034-0.048 ^b		
CH ₃ C(O)OH	<0.02		
RC(O)OONO ₂	Observed, secondary product		

^aEstimated using an average absorption coefficient from a series of organic esters (see text).

^bIncreased in yield with extent of reaction.

sequence following initial OH radical addition to the double bond is given in Figure 21 (in this scheme and those that follow, products that were observed are shown in boxes). The expected products are the molecular weight 163 organic nitrates, CH₃C(O)OCH₂CH₂CHO (molecular weight 116), and possibly acetic acid plus co-product (HC(O)CH₂CHO, HCHO and/or glyoxal).

However, acetic acid was not observed, with an upper limit to its formation yield of 2% being determined based on its well-isolated “Q-branch” at 642 cm⁻¹. The expected major product arising after H-atom abstraction from the C-H bonds at the 4- and 5-positions of DHMF (abstraction is expected to be minor given the magnitude of the rate constant) is the unsaturated dicarbonyl HC(O)CH=C(CH₃)OCHO, for which no evidence was seen in the API-MS analyses.

Thus, the main product observed in the GC-MS, API-MS and FT-IR analyses is attributed to the molecular weight 116 aldehyde-ester CH₃C(O)OCH₂CH₂CHO. The appearance of the weak but distinct 1811 cm⁻¹ absorption feature (Figure 20), which grew in proportion with the absorption bands of the ester during the reaction, indicates the formation of an additional minor primary product from DHMF. Although the sharp peak observed at 1811 cm⁻¹ (Figure 20) is generally consistent with the C=O stretch of lactones (Pouchert, 1975, 1989), the vapor-phase infrared spectrum of an authentic sample of α-angelicalactone (4-hydroxy-3-pentenoic acid γ-lactone), a potential product of the H-atom abstraction route, showed the corresponding Q-branch absorption to be at 1834 cm⁻¹. The estimated yield of CH₃C(O)OCH₂CH₂CHO of 74 ± 19%, together with the expected formation of organic nitrates in small yield from the RO₂[•] + NO reactions, accounts for most of the reaction products. Given the high reactivity of DHMF towards O₃, it is possible that some contribution of O₃ reaction to DHMF removal occurred in the experiments with FT-IR analyses, and this could account for the observation of small amounts of HCHO and ethene observed in the FT-IR analyses and possibly also of the molecular weight 132 product observed in the API-MS analyses at longer reaction times (see below).

Subsequent reaction of CH₃C(O)OCH₂CH₂CHO with OH radicals will lead (in the presence of O₂) to the formation of the peroxyacyl radical CH₃C(O)OCH₂CH₂C(O)OO[•].^{1,25} Reaction of CH₃C(O)OCH₂CH₂C(O)OO[•] with NO₂ will result in formation of the peroxyacyl nitrate CH₃C(O)OCH₂CH₂C(O)OONO₂ (Atkinson, 1994), which is presumably responsible for the acyl nitrate absorption bands observed in the FT-IR analyses.

Reaction with the NO₃ Radical

Figure 22A shows an infrared spectrum of the major products from a mixture of 1.23×10^{14} molecule cm⁻³ of N₂O₅ and 2.46×10^{14} molecule cm⁻³ of DHMF after ~3 min of mixing time, corresponding to 100% consumption of N₂O₅ and a 46% loss of DHMF. The absorption bands of the remaining DHMF and the other products NO₂, HNO₃ and HONO have been subtracted. Two sets of characteristic absorption bands are easily seen in Figure 22A: one set at 1674, 1285 and 846 cm⁻¹ indicating the presence of an -ONO₂ group, while the second set at 1724, 1301 and 792 cm⁻¹ is an absorption pattern attributed to an -OONO₂ group. The simultaneous presence of these two sets of bands suggests the formation of an R(ONO₂)(OONO₂)-type compound, an expected initial and thermally-labile product (Atkinson, 1997a). A similar product spectrum obtained after the mixture was left for 1 hour in the chamber is shown in Figure 22B, where a decrease in the intensity of the bands attributed to the R(ONO₂)(OONO₂) product is seen along with the possible growth of absorption bands by other products. Figure 22C resulted from a scaled subtraction of the spectrum of Figure 22A from that of Figure 22B, revealing that one product which increased in concentration has the same characteristic absorption bands as the ester product CH₃C(O)OCH₂CH₂CHO formed during the reaction of DHMF with the OH radical (see Figure 20A). CH₃C(O)OCH₂CH₂CHO concentrations were derived using the quantified spectra obtained from the OH + DHMF experiment, with the specific use of the isolated 1236 cm⁻¹ band (Figure 22). The R(ONO₂)(OONO₂) concentrations were estimated from the intensities of the 1674 cm⁻¹ band, using the average integrated absorption coefficient of $(2.5 \pm 0.3) \times 10^{-17}$ cm molecule⁻¹ derived from corresponding absorption bands of a series of organic nitrates (Aschmann *et al.*, 2001b). The ranges of yields obtained for CH₃C(O)OCH₂CH₂CHO and R(ONO₂)(OONO₂) are given in Table 8. Two weaker but distinct absorption features also appear in Figure 22A, at 1047 and 820 cm⁻¹, which are consistent with a C-O bond stretch and ring vibration of an epoxy group (Pouchert, 1975, 1989). These absorptions decreased markedly with time (see Figure 22B), thus indicating that the possible epoxy compound formed in the DHMF + NO₃ reaction is thermally unstable. An authentic sample of the suspected epoxide product is not available.

An API-MS spectrum recorded from a reacted NO₃ – N₂O₅ – NO₂ - DHMF – air mixture in the 7900 liter Teflon chamber is shown in Figure 23. As noted above, the ion peaks at 85, 169, 187 and 203 u are attributed to protonated DHMF, the protonated dimer, and water adducts of the protonated dimer, and these were the only ion peaks present in the pre-reaction spectrum. API-MS/MS “product ion” spectra indicated that the ion peaks at 101, 185, 201, 269, 285, 301 and 385 u arising from reaction products were the protonated molecule and dimers of a product of molecular weight 100. The API-MS/MS “product ion” spectrum of the 201 u ion peak was significantly different to that of the 201 u ion peak observed in the OH radical-initiated reaction and attributed to a protonated hetero-dimer of DHMF and CH₃C(O)OCH₂CH₂CHO. The API-MS analyses showed no significant evidence for the formation of a product of molecular weight 116, and no ion peaks were observed which correspond to the R(ONO₂)(OONO₂) product(s) whose absorption bands dominated the FT-IR product spectra.

The expected reactions occurring during the reaction of NO₃ radicals with DHMF are shown in Figure 24. The initial reaction involves addition of the NO₃ radical to the carbon-carbon double bond at the 2- and/or 3- positions, to form nitrooxyalkyl radicals which can decompose to the epoxide plus NO₂ (with this process typically decreasing in importance as the

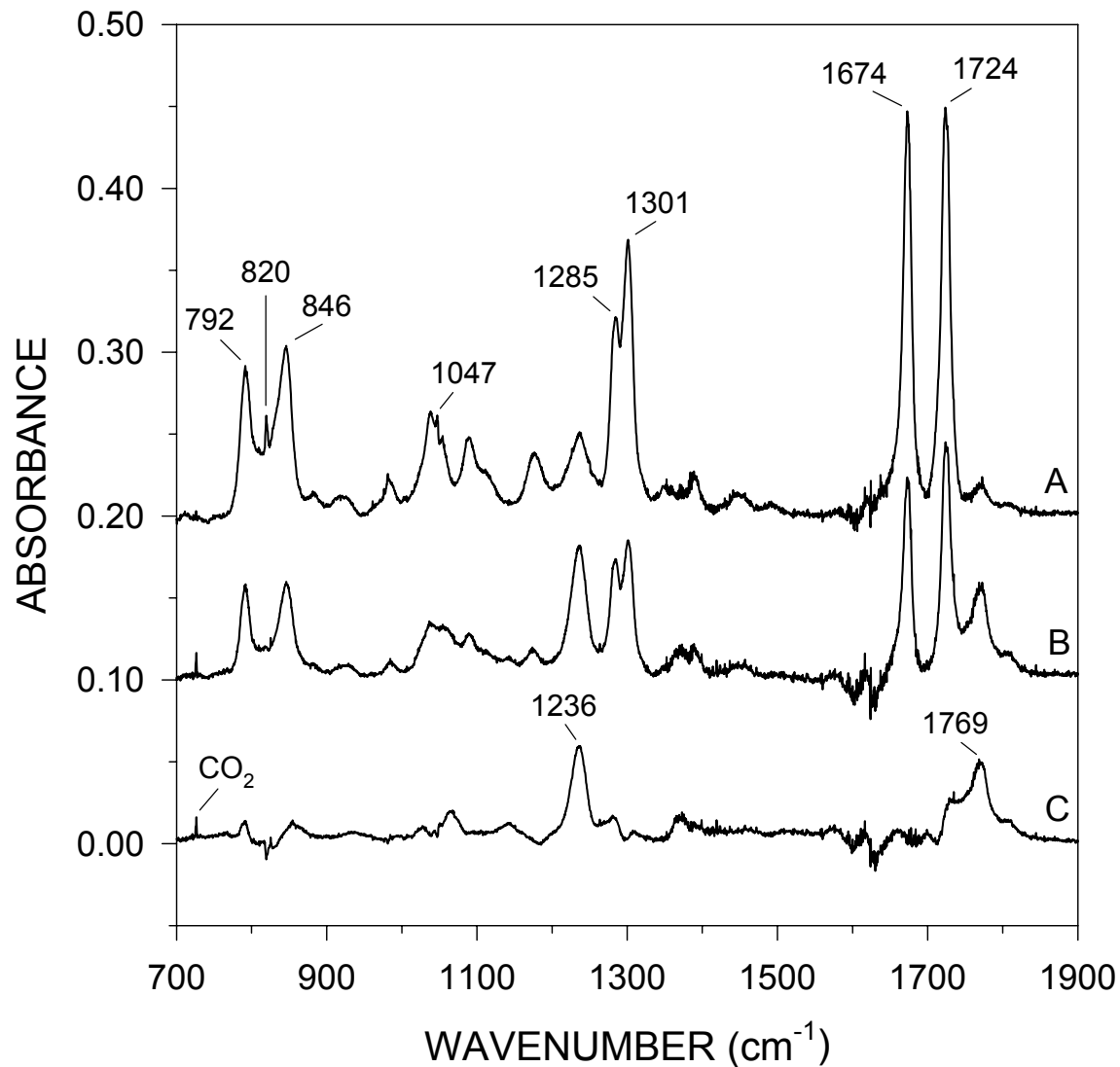


Figure 22. (A) Infrared spectrum of products attributed to DHMF from a reacted $\text{N}_2\text{O}_5 - \text{NO}_3 - \text{NO}_2 - \text{DHMF} - \text{air}$ mixture, corresponding to a 46% consumption of the initial 2.46×10^{14} molecule cm^{-3} of DHMF after 3 min of mixing time (see text). (B) Infrared spectrum of the same mixture after 1 hr. (C) Residual spectrum from a scaled subtraction of (A) from (B) to cancel the bands due to the product(s) $\text{R}(\text{ONO}_2)(\text{OONO}_2)$.

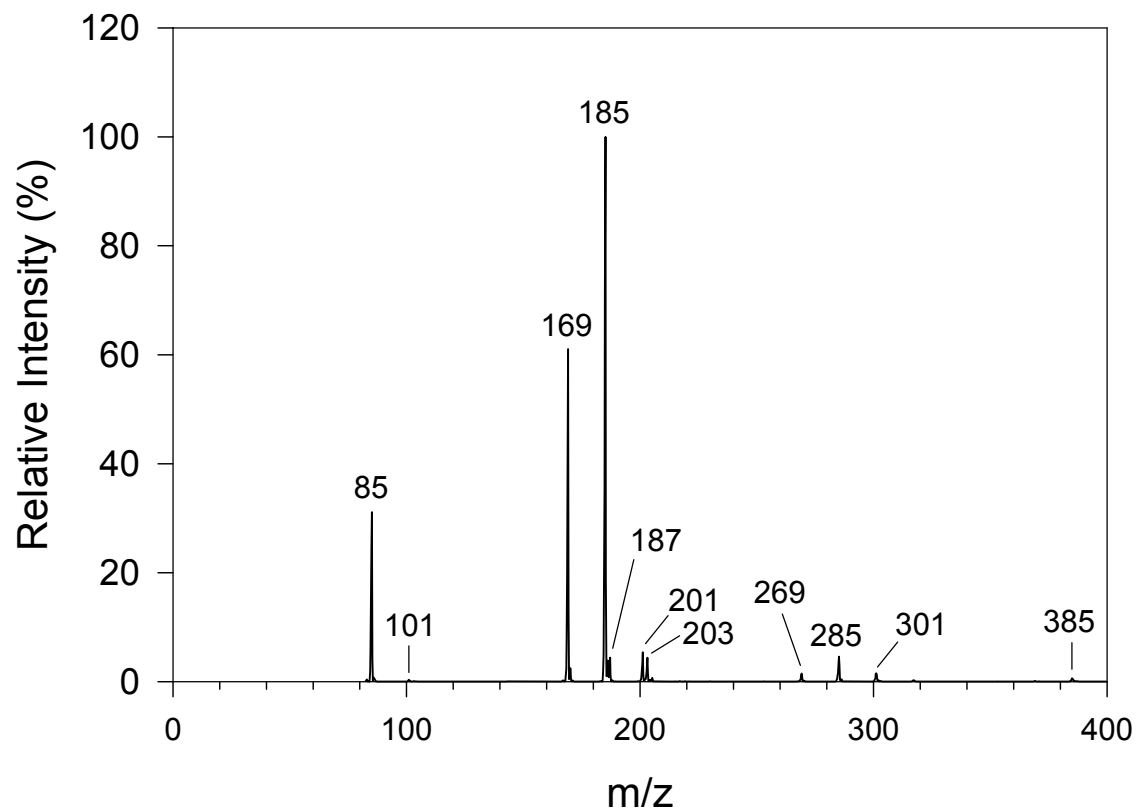


Figure 23. API-MS spectrum from a reacted $\text{N}_2\text{O}_5 - \text{NO}_3 - \text{NO}_2 - \text{DHMF} - \text{air}$ mixture.

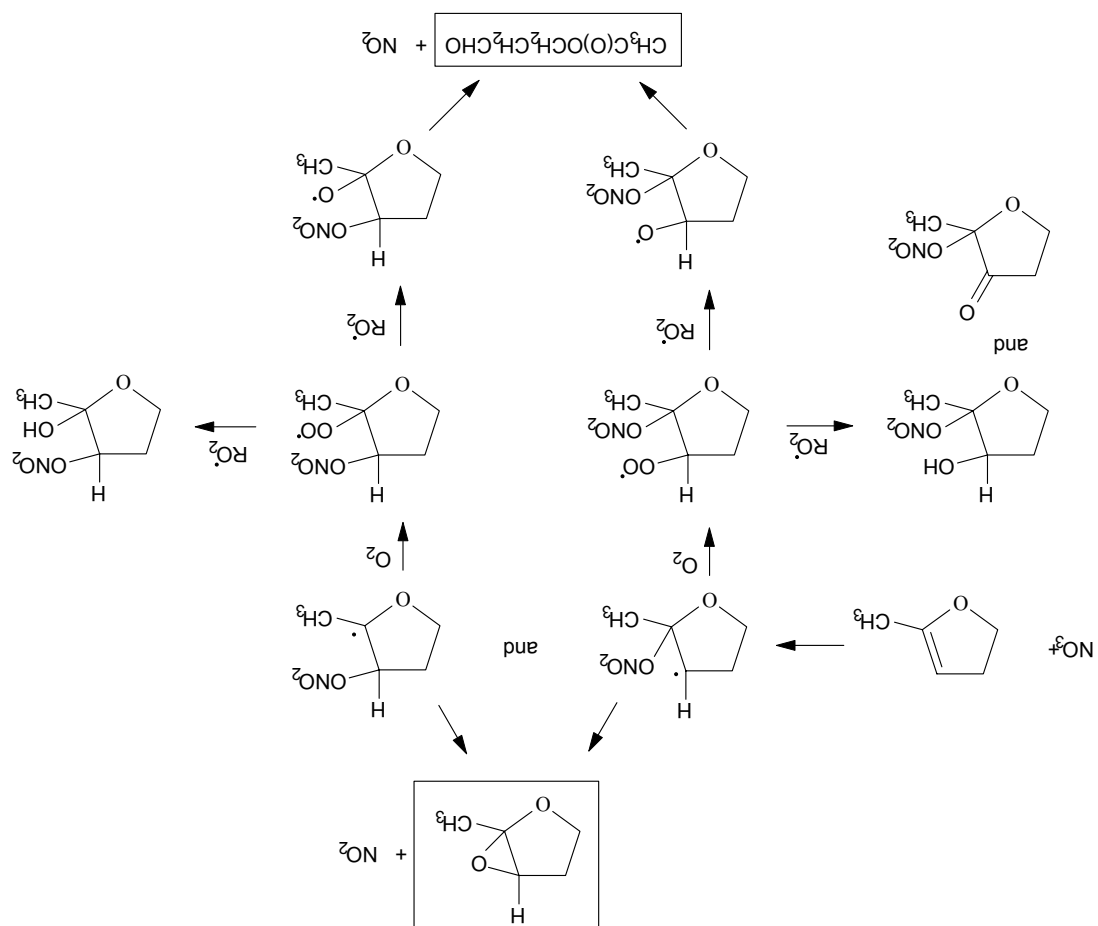
Figure 24. Reaction scheme for the reaction of NO_3 radicals with 4,5-dihydro-2-methylfuran.

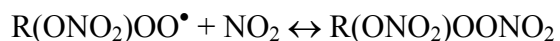
Table 8. Products identified and their formation yields from the gas-phase reaction of NO₃ radicals and O₃ with 4,5-dihydro-2-methylfuran

Product and reaction	Molar yield	
	FT-IR	API-MS
NO ₃ Radical Reaction		
CH ₃ C(O)OCH ₂ CH ₂ CHO	0.054-0.12 ^a	
R(ONO ₂)(OONO ₂)	0.19-0.10 ^a	
Epoxide of MW 100	Epoxide bands observed	MW 100 product observed
O ₃ Reaction		
CH ₃ C(O)OCH ₂ CH ₂ CHO	0.23 (0.22) ^b	MW 116 product observed
HCHO	0.28 (0.36) ^b	
CH ₃ OH	0.095 (0.14) ^b	
HC(O)OH	0.021 (0.013) ^b	
CH ₂ =C=O	0.021 (0.020) ^b	
CH ₂ =CH ₂	0.066 (0.076) ^b	
CO	0.20 (0.17) ^b	
CO ₂	0.47 (0.51) ^b	
CH ₃ C(O)OCH ₂ CH ₃	<0.03	

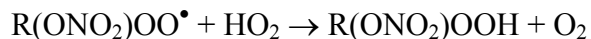
^aRange of yields shown is for the analysis upon immediate consumption of N₂O₅ and the analysis obtained after the reaction mixture stood for 1 hr (see text).

^bValues in parentheses were obtained in the absence of an OH radical scavenger.

total pressure and O₂ content increases) or add O₂ to form nitrooxyalkyl peroxy radicals (Atkinson, 1991, 1997a). The nitrooxyalkyl peroxy radicals can react with NO₂ to form thermally unstable peroxy nitrates,



with HO₂ radicals to form nitrooxy-hydroperoxides,



and, as shown in Figure 24, with organic peroxy (RO₂[•]) radicals. The reactions with organic peroxy radicals (including the self-reaction) proceed through a “molecular” channel, forming a nitrooxy-alcohol and/or (if feasible) a nitrooxy-carbonyl, and through a “radical” channel to form the nitrooxy-alkoxy radical which, as shown in Figure 24, is expected to decompose to form CH₃C(O)OCH₂CH₂CHO. Our FT-IR and API-MS analyses are consistent with Figure 24, with formation of the molecular weight 100 epoxide and CH₃C(O)OCH₂CH₂CHO (plus the thermally labile R(ONO₂)OONO₂ species) being observed and with nitrooxy-alcohol, nitrooxy-carbonyl and nitrooxy-hydroperoxide species accounting for the remainder of the products.

Reaction with O₃

The reaction of DHMF with O₃ occurred rapidly and was complete during the <3 min period of O₃ addition and mixing of the reactants. The FT-IR spectrum of the products from the reaction of 2.46 x 10¹⁴ molecule cm⁻³ of DHMF with a total of 2.6 x 10¹⁴ molecule cm⁻³ of O₃ (added in two equal aliquots) is presented in Figure 25A, where the absorption features of the low-molecular weight products HCHO, CH₃OH, CH₂=CH₂, CO and CO₂ are clearly seen. Subtraction of the absorptions by these compounds (except CO₂) from Figure 25A results in the spectrum of Figure 25B, which shows more clearly the presence of CH₂=C=O (ketene) as a product, as well as the bands at 1769, 1236 and 1057 cm⁻¹ assigned to CH₃C(O)OCH₂CH₂CHO, an expected major product. Subtraction of the absorption bands of CH₃C(O)OCH₂CH₂CHO from Figure 25B using its IR spectrum derived from the OH radical reaction of DHMF (e.g., Figure 20A) resulted in Figure 25C, which shows distinct residual bands of unidentified products at 1283, 1725 and 1770 cm⁻¹. The comparison of CH₃C(O)OCH₂CH₂CHO band intensities with those of the quantified spectra obtained from the OH radical experiment allowed the yields of CH₃C(O)OCH₂CH₂CHO to be estimated. The same products were observed, with very similar yields (defined as the amount of product formed/the amount of DHMF reacted), from an experiment conducted in the presence of sufficient cyclohexane to scavenge ≥90% of any OH radicals formed. The yields of the identified products from both experiments are listed in Table 8.

API-MS and API-MS/MS spectra of a reacted O₃ - DHMF - cyclohexane - air mixture, with sufficient cyclohexane to scavenge >95% of any OH radicals formed, provided evidence for the formation of the same molecular weight 116 and 132 products observed in the OH radical-initiated reaction (see above, noting that the molecular weight 132 product was observed in the OH radical-initiated reaction at longer reaction times).

As shown in Figure 26, the reaction of O₃ with DHMF involves initial addition of O₃ to the C=C bond to form an energy-rich primary ozonide, which rapidly decomposes to form two excited Criegee intermediates [theoretical calculations show these to be carbonyl oxides (Gutbrod *et al.*, 1996, 1997)]. As shown in Figure 26, these Criegee intermediates can decompose (through formation of a hydroperoxide) to an OH radical plus an organic radical co-product, or be collisionally thermalized (Atkinson, 1997a). The [CH₃C(OO)OCH₂CH₂CHO]^{*} intermediate is expected to primarily decompose to an OH radical plus [•]CH₂C(O)OCH₂CH₂CHO or be thermalized (Atkinson, 1997a), with the thermalized intermediate also decomposing to an OH radical plus [•]CH₂C(O)OCH₂CH₂CHO (Fenske *et al.*, 2000a; Kroll *et al.*, 2001a). The [CH₃C(O)OCH₂CH₂CHOO]^{*} intermediate is expected to primarily decompose to an OH radical plus CH₃C(O)OCH₂C[•]HCHO (if in the *syn*-configuration), decompose (through the “ester” channel) to CO₂ plus CH₃C(O)OCH₂CH₃, or be thermalized, with the thermalized *syn*-intermediate also decomposing to an OH radical plus CH₃C(O)OCH₂C[•]HCHO (Fenske *et al.*, 2000a; Kroll *et al.*, 2001a). The thermalized intermediates can also react with water vapor to form CH₃C(O)OCH₂CH₂CHO and/or CH₃C(O)OCH₂CH₂C(O)OH (Sauer *et al.*, 1999; Winterhalter *et al.*, 2000; Baker *et al.*, 2002).

The organic radical co-products to the OH radical [[•]CH₂C(O)OCH₂CH₂CHO and CH₃C(O)OCH₂C[•]HCHO] then react as do alkyl or substituted alkyl radicals in the absence of NO (Atkinson, 2000). The products potentially formed from these [•]CH₂C(O)OCH₂CH₂CHO and CH₃C(O)OCH₂C[•]HCHO radicals include the molecular weight 132 species HOCH₂C(O)OCH₂CH₂CHO and CH₃C(O)OCH₂CH(OH)CHO, which may account for the

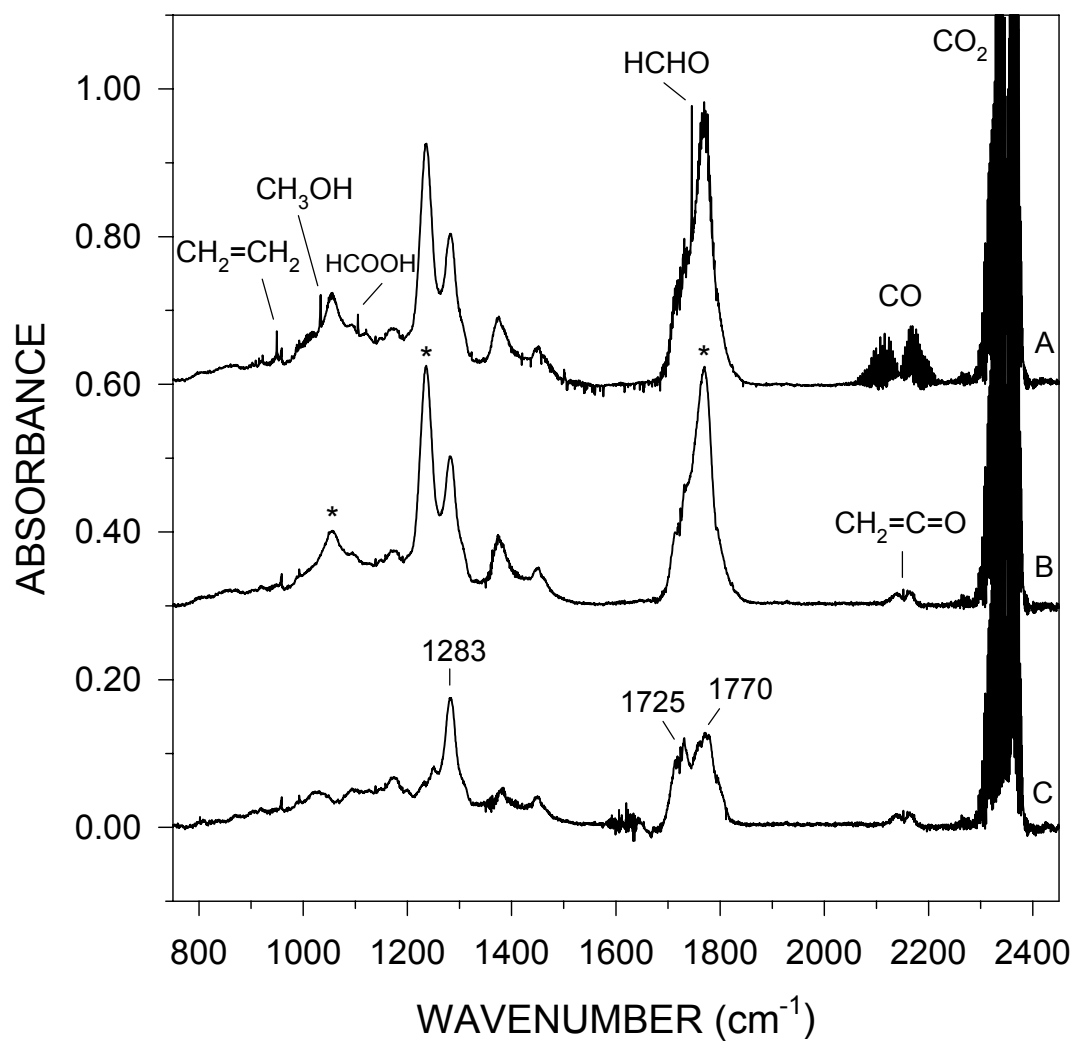


Figure 25. (A) Infrared spectrum of products from a reacted O₃ - DHMF – air mixture. (B) Spectrum after subtraction of the absorption bands of HCHO, CH₃OH, CH₂=CH₂, and CO from (A). (C) Residual spectrum after subtraction of absorption bands (marked by asterisks in (B)) attributed to the product CH₃C(O)OCH₂CHO (see text).

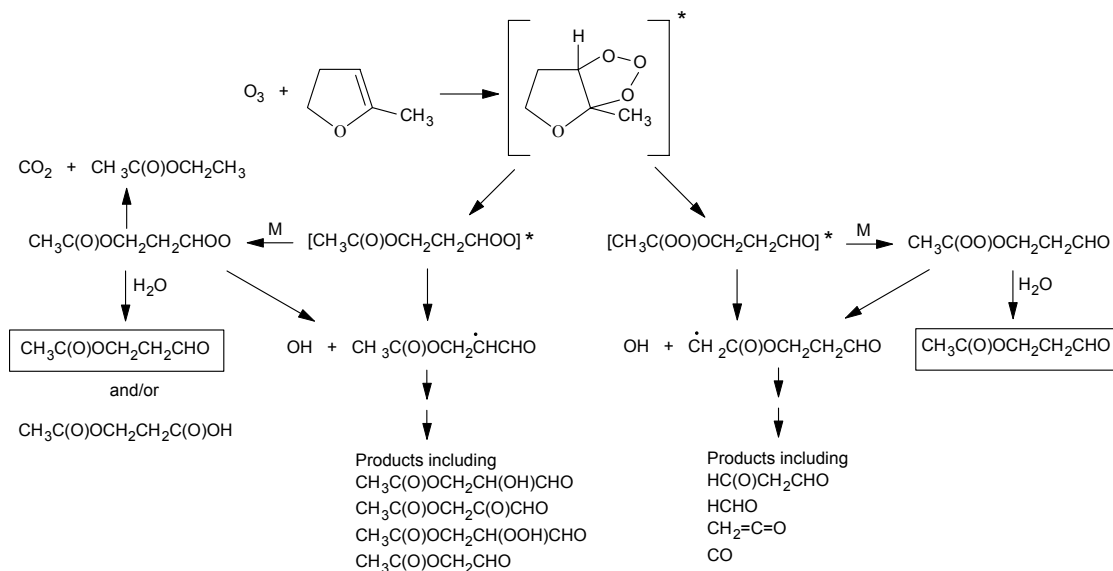


Figure 26. Reaction scheme for the reaction of O_3 with 4,5-dihydro-2-methylfuran.

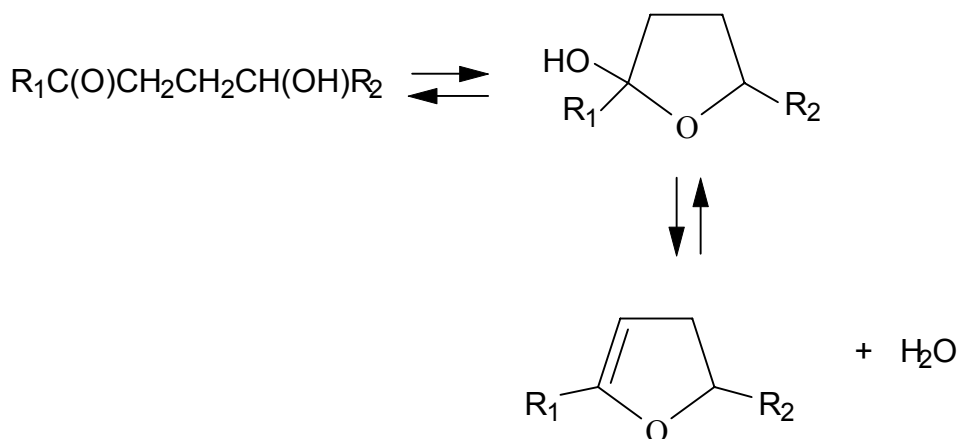
molecular weight 132 product(s) observed in the API-MS analyses. Formation of $CH_2=C=O$ may arise from decomposition of the $\dot{C}H_2C(O)OCH_2CH_2CHO$ radical. Although the high yield of CO_2 (~50%) could indicate that the ester channel is important in the decomposition of the $[CH_3C(O)OCH_2CH_2CHOO]^*$ intermediate, an upper limit to the formation yield of ethyl acetate of 3% was estimated from residual spectra such as that shown in Figure 26C. The similar yield of $CH_3C(O)OCH_2CH_2CHO$ (relative to DHMF reacted) in the presence and absence of the OH radical scavenger suggests that either the OH radical yield from the reaction of O_3 with DHMF is low or (more likely) that the OH radical reaction with DHMF in the absence of NO_x also leads to formation of $CH_3C(O)OCH_2CH_2CHO$.

Atmospheric Implications

Our experiments and those of Cavalli *et al.* (2000) show that 5-hydroxy-2-pentanone is converted to DHMF in dry diluent air or N_2 , with a 5-hydroxy-2-pentanone lifetime of ~1.1 hr in our chamber. Under dry conditions DHMF is not converted to 5-hydroxy-2-pentanone and DHMF is one of the most reactive volatile organic compounds studied to date with respect to reactions with OH and NO_3 radicals and O_3 . Based on 24-hour average tropospheric concentrations (molecule cm^{-3}) of 1.0×10^6 for the OH radical (Prinn *et al.*, 1995; Hein *et al.*, 1997), 2.5×10^8 for the NO_3 radical (Atkinson, 1991), and 7.2×10^{11} for O_3 (Logan, 1985), the calculated lifetimes for DHMF are 1.3 hr for reaction with OH radicals (38 min for a 12-hr average daytime OH radical concentration of 2.0×10^6 molecule cm^{-3}), 24 s for reaction with NO_3 radicals, and 7 min for reaction with O_3 .

However, in moist air, DHMF converts to 5-hydroxy-2-pentanone (with a DHMF lifetime of ~3.5 hr at 5% relative humidity in our chamber). The OH radical reaction rate constant for 5-hydroxy-2-pentanone is $1.6 \times 10^{-11} \text{ cm}^3 \text{ molecule}^{-1} \text{ s}^{-1}$ (see Section 2.4) which corresponds to an estimated tropospheric lifetime of 0.7 days. Furthermore, 5-hydroxy-2-pentanone is not expected to react with O_3 and its reaction with NO_3 radicals is likely to be several orders of magnitude slower than that of DHMF. Therefore, in the atmosphere the reactive species (DHMF vs 5-hydroxy-2-pentanone) depends critically on the equilibrium ratio of DHMF and 5-hydroxy-2-pentanone resulting from their interconversion and may be different at nighttime from daytime. It is possible that in the lower troposphere the dominant species is 5-hydroxy-2-pentanone, although even a small fraction of DHMF could lead to removal of DHMF/5-hydroxy-2-pentanone through reaction of DHMF with OH radicals, NO_3 radicals and/or O_3 . Clearly further work is needed to investigate the interconversion of these two species as a function of water vapor content and the effect of surfaces on the rates of interconversion should also be examined.

Finally, the atmospheric behavior of larger 1,4-hydroxycarbonyls formed from alkane photooxidations, and of their corresponding dihydrofuran interconversion products



may be similar to those of 5-hydroxy-2-pentanone and 4,5-dihydro-2-methylfuran.

3. STUDIES OF ALKENE CHEMISTRY

3.1. Products of the Gas-Phase Reaction of O₃ with Cyclohexene

3.1.1. Introduction

Alkenes are emitted into the atmosphere from anthropogenic and biogenic sources (Calvert *et al.*, 2000). In the troposphere, alkenes react with OH radicals, NO₃ radicals and O₃ (Atkinson, 1997a, 2000; Calvert *et al.*, 2000), with the O₃ reactions often being an important transformation process during both daytime and nighttime (Atkinson, 1997a, 2000; Calvert *et al.*, 2000). The reactions of O₃ with alkenes lead to the production of OH radicals, often in high yield (Atkinson, 1997a, 2000, and these reactions also lead to the formation of secondary organic aerosol (Yokouchi and Ambe, 1985; Hatakeyama *et al.*, 1985; Hoffmann *et al.*, 1997; Kalberer *et al.*, 2000; Ziemann, 2002). While the initial steps involved in the reactions of O₃ with alkenes are understood (Atkinson, 1997a, 2000; Calvert *et al.*, 2000), there are many details of the complete reaction schemes which require investigation, and these include the identity of the reaction products which initiate formation of secondary organic aerosol, and the reactions of the stabilized Criegee intermediates. For example, it has been reported that the reaction of O₃ with cyclohexene (a symmetrical cycloalkene which can serve as a model compound for several monoterpenes emitted from vegetation) forms C₅- and C₆-dicarboxylic acids which nucleate and/or partition into seed particles and are important components of secondary organic aerosol (Hatakeyama *et al.*, 1985; Kalberer *et al.*, 2000; Ziemann, 2002). However, the routes leading to formation of these dicarboxylic acids are at present speculative.

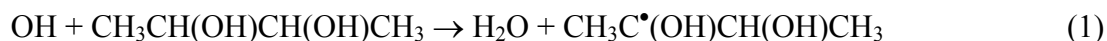
To complement a recent study by Ziemann (2002) of the aerosol-phase products formed from the reaction of O₃ with cyclohexene, in this work we have used gas chromatography with flame ionization detection (GC-FID), combined gas chromatography-mass spectrometry (GC-MS), *in situ* Fourier transform infrared spectroscopy (FT-IR) and *in situ* atmospheric pressure ionization tandem mass spectrometry (API-MS) to investigate the gas-phase products formed from the reactions of cyclohexene and cyclohexene-d₁₀ in the presence of OH radical scavengers. The use of cyclohexane and cyclohexane-d₁₂ as OH radical scavengers in the experiments with API-MS analyses allowed the products arising from the reactions of O₃ with cyclohexene to be differentiated from those formed from the OH radical reaction with cyclohexane, and investigation of the cyclohexene-d₁₀ reaction further aided in the elucidation of products using API-MS. As part of this work, the use of 2,3-butanediol as a radical scavenger to determine OH radical formation from the reactions of O₃ with cyclohexene and cyclohexene-d₁₀ was validated.

3.1.2. Experimental

Experiments were carried out at atmospheric pressure of air and at 296-298 K in a 5800 liter evacuable, Teflon-coated chamber equipped with a multiple-reflection optical system interfaced to a Nicolet 7199 FT-IR spectrometer, in a ~8000 liter Teflon chamber with off-line analyses by GC-FID, and in a ~7000 liter Teflon chamber interfaced to a PE SCIEX API III MS/MS direct air sampling, atmospheric pressure ionization tandem mass spectrometer (API-MS). The experiments with GC-FID, GC-MS and API-MS analyses were carried out at ~5% relative humidity (~3.4 x 10¹⁶ molecule cm⁻³ of water).

GC-FID Analyses. Two series of O₃ – cyclohexene (or cyclohexene-d₁₀) – scavenger – air reactions were carried out, with analysis by gas chromatography with flame ionization detection (GC-FID) and with the scavenger being present to (a) react with the OH radicals formed in the reactions of O₃ with cyclohexene (Atkinson and Aschmann, 1993; Fenske *et al.*, 2000b) or cyclohexene-d₁₀ and (b) to enable the OH radical formation yields from the O₃ reactions to be derived from measurements of a product(s) of the OH radical reaction with the scavenger

compound (Atkinson and Aschmann, 1993; Chew and Atkinson, 1996). Previously cyclohexane was employed as a radical scavenger (Atkinson and Aschmann, 1993), but because of uncertainties in the yields of the products measured to quantify the amount of OH radical formation, 2-butanol has more recently been employed with measurements of the amounts of 2-butanone formed (Chew and Atkinson, 1996; Aschmann *et al.*, 2002c). However, on the DB-1701 column used to separate 2-butanone from a large excess of 2-butanol, cyclohexene and 2-butanone co-eluted. Therefore, a number of other diol and hydroxycarbonyl scavengers were investigated, with the goal being to measure the amounts of hydroxycarbonyl or dicarbonyl products formed, respectively. For example, when 2,3-butanediol was used as an OH radical scavenger the product monitored was 3-hydroxy-2-butanone (Bethel *et al.*, 2001).



The OH radical scavengers investigated were 1,2-, 1,3- and 2,3-butanediol, for which the rate constants for their reactions with OH radicals and the formation yields of the corresponding hydroxyketone have been measured (Bethel *et al.*, 2001). Another potential scavenger, 4-hydroxy-3-hexanone, had as an impurity ~0.7% of 3,4-hexanedione, its OH radical reaction product. Hence in the presence of $\sim 1.5 \times 10^{15}$ molecule cm^{-3} of 4-hydroxy-3-hexanone, the level required for efficient scavenging of OH radicals, formation of 3,4-hexanedione during the O_3 reactions would have been relatively small compared to its initial concentration. As in our previous study using 2-butanol as the OH radical scavenger (Chew and Atkinson, 1996), in preliminary experiments we investigated formation of the hydroxycarbonyls from the diols in the presence of O_3 , with the diol and O_3 concentrations being $\sim 1.7 \times 10^{15}$ molecule cm^{-3} and $(4-5) \times 10^{12}$ molecule cm^{-3} , respectively. Based on the concentrations of the hydroxycarbonyls initially present and the amounts formed in the presence of O_3 , we decided to use 2,3-butanediol as the OH radical scavenger, with formation of 3-hydroxy-2-butanone in $89 \pm 9\%$ yield from the OH radical-initiated reaction (Bethel *et al.*, 2001). To test the use of 2,3-butanediol as a radical scavenger to measure OH radical yields, OH radical formation yields from the reactions of O_3 with propene (and propene- d_6), α -pinene and 2,3-dimethyl-2-butene were also measured.

The initial reactant concentrations (molecule cm^{-3} units) were: cyclohexene or cyclohexene- d_{10} , $(2.20-2.47) \times 10^{13}$; 2,3-butanediol, 1.7×10^{15} , or cyclohexane (used as the OH radical scavenger in certain of the experiments to measure the yields of pentanal or pentanal- d_{10}), 4.9×10^{15} ; and 4 additions of 50 cm^3 volume O_3/O_2 aliquots were made to the chamber during an experiment, with each O_3/O_2 addition corresponding to an initial concentration of O_3 in the chamber of $\sim 5 \times 10^{12}$ molecule cm^{-3} . The water vapor concentration was $\sim 3.4 \times 10^{16}$ molecule cm^{-3} (~5% relative humidity). The concentrations of cyclohexene and cyclohexene- d_{10} and of selected products were measured during the experiments by GC-FID. For the analyses of cyclohexene and cyclohexene- d_{10} , gas samples were collected from the chamber into 100 cm^3 volume all-glass gas-tight syringes and transferred via a 1 cm^3 gas sampling loop onto a 30 m DB-5 megabore column held at -25 $^\circ\text{C}$ and then temperature programmed at 8 $^\circ\text{C min}^{-1}$ to 200 $^\circ\text{C}$. For the analysis of pentanal (or pentanal- d_{10}) and 3-hydroxy-2-butanone, 100 cm^3 volume gas samples were collected from the chamber onto Tenax-TA solid adsorbent, with subsequent thermal desorption at ~ 250 $^\circ\text{C}$ onto a 30 m DB-1701 megabore column held at -40 $^\circ\text{C}$ and then temperature programmed to 200 $^\circ\text{C}$ at 8 $^\circ\text{C min}^{-1}$. GC-FID response factors were determined by

introducing measured amounts of the chemicals into the chamber and conducting several replicate GC-FID analyses.

GC-MS Analyses. To identify carbonyls as their oxime derivatives, experiments were also carried out in which a 65 μm PDMS/DVB Solid Phase Micro Extraction (SPME) fiber (Pawliszyn, 1997) coated with *O*-(2,3,4,5,6-pentafluorobenzyl)hydroxylamine (PFBHA) hydrochloride (Koziel *et al.*, 2001) was exposed to the chamber reaction products and then analyzed by combined gas chromatography-mass spectrometry (GC-MS) with thermal desorption onto a 30 m DB-1701 fused silica capillary column in a Varian 2000 GC/MS/MS with analysis by isobutane chemical ionization. Carbonyl-containing products were examined from cyclohexene and cyclohexene- d_{10} reactions in which cyclohexane was used as the OH radical scavenger. Standards of pentanal and glutaraldehyde were analyzed to confirm the retention times and mass spectra of their oxime derivatives.

API-MS Analyses. In these experiments, the chamber contents were sampled through a 25 mm diameter x 75 cm length Pyrex tube at $\sim 20 \text{ L min}^{-1}$ directly into the API mass spectrometer source. The operation of the API-MS in the MS (scanning) and MS/MS [with collision activated dissociation (CAD)] modes has been described previously (Aschmann *et al.*, 1997). Use of the MS/MS mode with CAD allows the “product ion” or “precursor ion” spectrum of a given ion peak observed in the MS scanning mode to be obtained (Aschmann *et al.*, 1997).

The majority of the data obtained used the positive ion mode, in which protonated water hydrates ($\text{H}_3\text{O}^+(\text{H}_2\text{O})_n$) generated by the corona discharge in the chamber diluent air were responsible for the protonation of analytes (Aschmann *et al.*, 1997; Arey *et al.*, 2001). Ions are drawn by an electric potential from the ion source through the sampling orifice into the mass-analyzing first quadrupole or third quadrupole. In these experiments the API-MS instrument was operated under conditions that favored the formation of dimer ions in the ion source region (Aschmann *et al.*, 1997). Neutral molecules and particles are prevented from entering the orifice by a flow of high-purity nitrogen (“curtain gas”), and as a result of the declustering action of the curtain gas on the hydrated ions, the ions that are mass analyzed are mainly protonated molecular ions ($[\text{M} + \text{H}]^+$) and their protonated homo- and hetero-dimers (Aschmann *et al.*, 1997).

Experiments were carried out with cyclohexene + cyclohexane, cyclohexene- d_{10} + cyclohexane, cyclohexene + cyclohexane- d_{12} , and cyclohexene- d_{10} + cyclohexane- d_{12} . The initial reactant concentrations (in molecule cm^{-3} units) were: cyclohexene or cyclohexene- d_{10} , $\sim 2.4 \times 10^{13}$; cyclohexane, $\sim 2.4 \times 10^{15}$ or cyclohexane- d_{12} , $\sim 3.6 \times 10^{15}$; and 2 additions of 50 cm^3 volume of O_3 in O_2 diluent were made to the chamber. The water vapor concentration was $\sim 3.4 \times 10^{16}$ molecule cm^{-3} ($\sim 5\%$ relative humidity). In additional experiments, $\sim 2.4 \times 10^{13}$ molecule cm^{-3} of butanal was added to the cyclohexene (or cyclohexene- d_{10}) – cyclohexane – air mixture (at $\sim 5\%$ relative humidity) prior to reaction to investigate whether or not the butanal intercepted the Criegee intermediate.

FT-IR Analyses. Experiments were carried out in which cyclohexene and cyclohexene- d_{10} were reacted with O_3 , both in the presence and absence of cyclohexane as an OH radical scavenger, with analyses by *in situ* FT-IR spectroscopy. The initial concentrations (in units of molecule cm^{-3}) were: cyclohexene or cyclohexene- d_{10} , $(4.77 - 4.92) \times 10^{14}$; O_3 , 1.47×10^{14} ; and in certain experiments, cyclohexane, 9.5×10^{16} . The reactants were mixed for 3 min using two magnetically-coupled Teflon-coated fans, including an ~ 0.5 min injection time for O_3 . FT-IR spectra were recorded every 2.5 min with a pathlength of 62.9 m and a full width at half-maximum resolution of 0.7 cm^{-1} .

The following IR absorption bands with sharp Q branches (cm^{-1}) were used for quantitative measurements: cyclohexene, 1140; cyclohexene- d_{10} , 1082; HC(O)OH, 1105; and DC(O)OH, 1143. Calibrated reference spectra of DC(O)OH were obtained by introducing 0.241 g of DC(O)OH into air at atmospheric pressure in the 5800 liter chamber, recording the spectra at a pathlength of 5.59 m for 30 min with 5-min intervals, and correcting the concentrations based on the measured decay rate of $1.90 \times 10^{-3} \text{ min}^{-1}$. A similar procedure was used for the calibration for anhydrous HC(O)OH, obtained from a sample of 90.6% HC(O)OH solution in H_2O which was dried over anhydrous CaSO_4 .

Chemicals. The chemicals used and their stated purities were: cyclohexane (HPLC grade), Fisher Scientific; 1,2-butanediol (99%), 2,3-butanediol (98%), 1,3-butanediol (99+%), cyclohexane- d_{12} (99.5 atom % D), glutaraldehyde (50 wt%), 1-hydroxy-2-butanone (95%), 3-hydroxy-2-butanone, *O*-(2,3,4,5,6-pentafluorobenzyl)hydroxylamine hydrochloride (98+%), and pentanal (99%), Aldrich Chemical Company; cyclohexene (99%), Chem Samples; cyclohexene- d_{10} (98 atom % D), Isotec Inc; 4-hydroxy-2-butanone (95+%), TCI America; HC(O)OH (90.6%), Baker Analyzed Reagent; and DC(O)OH (95% wt. in water), Aldrich/Isotec. O_3 in O_2 diluent was prepared as needed using a Welsbach T-408 ozone generator.

3.1.3. Results

Measurement of OH Radical Yields. In addition to investigating the formation of OH radicals from the reactions of O_3 with cyclohexene and cyclohexene- d_{10} , we also studied the reactions of O_3 with propene, propene- d_6 , α -pinene and 2,3-dimethyl-2-butene to investigate the effect of deuteration on the propene reaction and compare the measured OH radical formation yields for propene, α -pinene and 2,3-dimethyl-2-butene with previous literature data (Chew and Atkinson, 1996; Paulson *et al.*, 1998, 1999; Rickard *et al.*, 1999; Neeb and Moortgat, 1999; Fenske *et al.*, 2000b,c; Siese *et al.*, 2001; Orzechowska and Paulson, 2002). Plots of the amounts of 3-hydroxy-2-butanone formed against the amounts of cyclohexene and cyclohexene- d_{10} reacted are shown in Figure 27, and the OH (or OD) radical formation yields obtained for the alkenes studied are given in Table 9.

GC-FID and FT-IR Analyses. In agreement with the previous studies of Hatakeyama *et al.* (1985), Grosjean *et al.* (1996) and Kalberer *et al.* (2000), pentanal was observed from the O_3 reaction with cyclohexene. Plots of the amounts of pentanal and pentanal- d_{10} formed against the amounts of cyclohexene and cyclohexene- d_{10} reacted are shown in Figure 28. Least-squares analyses of these data lead to formation yields of pentanal from cyclohexene and pentanal- d_{10} from cyclohexene- d_{10} of 0.236 ± 0.018 and 0.164 ± 0.014 , respectively, where the indicated errors are two least-squares standard deviations combined with estimated uncertainties in the GC-FID response factors for cyclohexene and pentanal (or their deuterated analogs) of $\pm 5\%$ each. *In situ* FT-IR analyses of reacted O_3 – cyclohexene – cyclohexane – air and O_3 – cyclohexene- d_{10} – cyclohexane – air mixtures showed total consumption of the O_3 introduced within 4 min of mixing in all cases. In the cyclohexene reaction in the absence of added cyclohexane, $1.47 \times 10^{14} \text{ molecule cm}^{-3}$ of O_3 consumed $2.18 \times 10^{14} \text{ molecule cm}^{-3}$ of cyclohexene, with a 2.5% yield of HC(O)OH which gradually increased to 3.2% after a period of 34 min. HCHO was not detected as a product. In the cyclohexene reaction in the presence of sufficient cyclohexane to scavenge $>95\%$ of the OH radicals formed, $1.47 \times 10^{14} \text{ molecule cm}^{-3}$ of O_3 consumed $1.62 \times 10^{14} \text{ molecule cm}^{-3}$ of cyclohexene, with a 3.5% yield of HC(O)OH which increased to 4.4% after 17 min. In the cyclohexene- d_{10} reaction in the absence of an OH

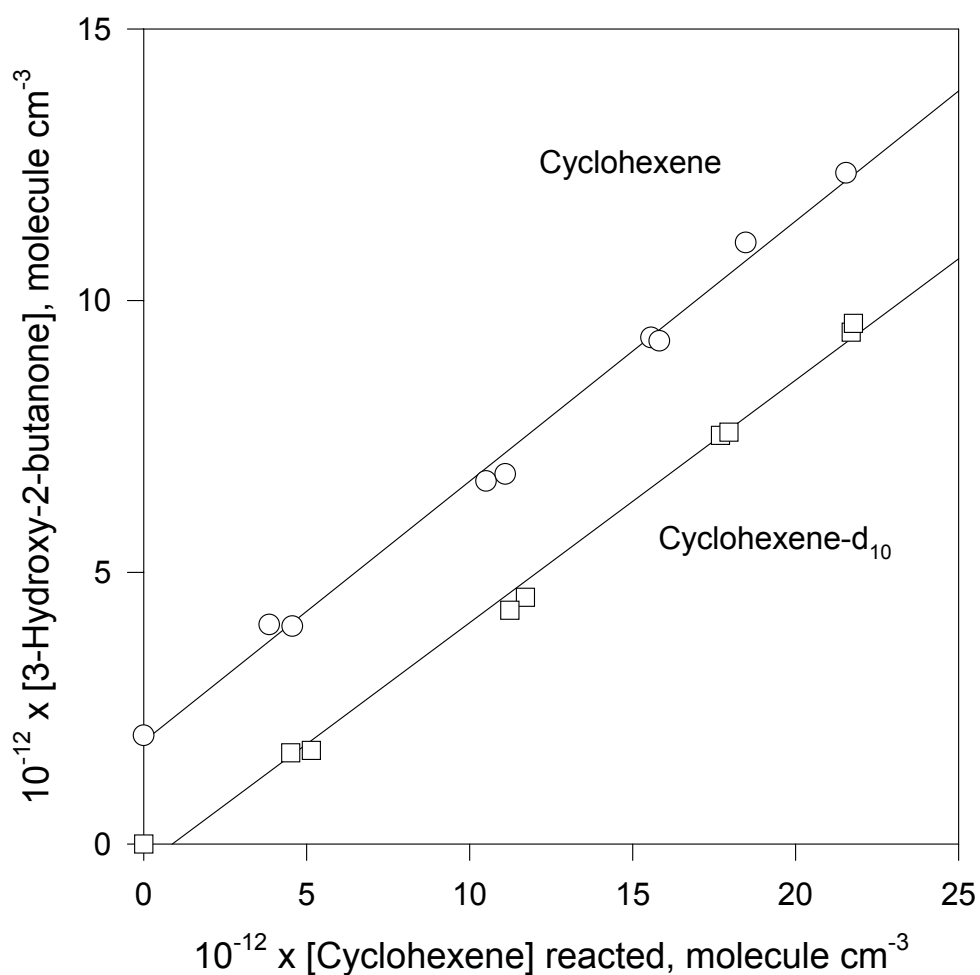


Figure 27. Plots of the amounts of 3-hydroxy-2-butanone formed against the amounts of cyclohexene and cyclohexene-d₁₀ reacted with O₃, in the presence of sufficient 2,3-butanediol to scavenge >95% of the OH radicals formed. The 3-hydroxy-2-butanone data from the cyclohexene reaction have been displaced vertically by 2.0 x 10¹² molecule cm⁻³ for clarity.

Table 9. Measured OH radical formation yields from reactions of O₃ with selected alkenes at atmospheric pressure using 2,3-butanediol as the radical scavenger, together with recent literature data.

Alkene	OH radical formation yield		
	This work ^a	Literature	Reference
Cyclohexene	0.54 ± 0.08	0.54 ± 0.13	Fenske <i>et al.</i> (2000b)
Cyclohexene-d ₁₀	0.50 ± 0.07		
Propene	0.40 ± 0.06	0.35 ± 0.07 0.32 ± 0.08 0.34 ^{+0.03} _{-0.06} 0.33 ± 0.07 0.37 ± 0.08	Paulson <i>et al.</i> (1999b) Rickard <i>et al.</i> (1999) Neeb and Moortgat (1999) Fenske <i>et al.</i> (2000c) Fenske <i>et al.</i> (2000c)
Propene-d ₆	0.27 ± 0.04		
α-Pinene	0.86 ± 0.13	0.76 ± 0.11 0.70 ± 0.17 0.83 ± 0.21 0.91 ± 0.23	Chew and Atkinson (1996) Paulson <i>et al.</i> (1998) Rickard <i>et al.</i> (1999) Siese <i>et al.</i> (2001)
2,3-Dimethyl-2-butene	1.07 ± 0.16	0.80 ± 0.12 0.89 ± 0.22 0.99 ± 0.18 1.00 ± 0.25 0.91 ± 0.14	Chew and Atkinson (1996) Rickard <i>et al.</i> (1999) Fenske <i>et al.</i> (2000c) Siese <i>et al.</i> (2001) Orzechowska and Paulson (2002)

^aIndicated errors are two least squares standard deviations combined with estimated uncertainties in the GC-FID response factors for the alkene and 3-hydroxy-2-butanone of ±5% each.

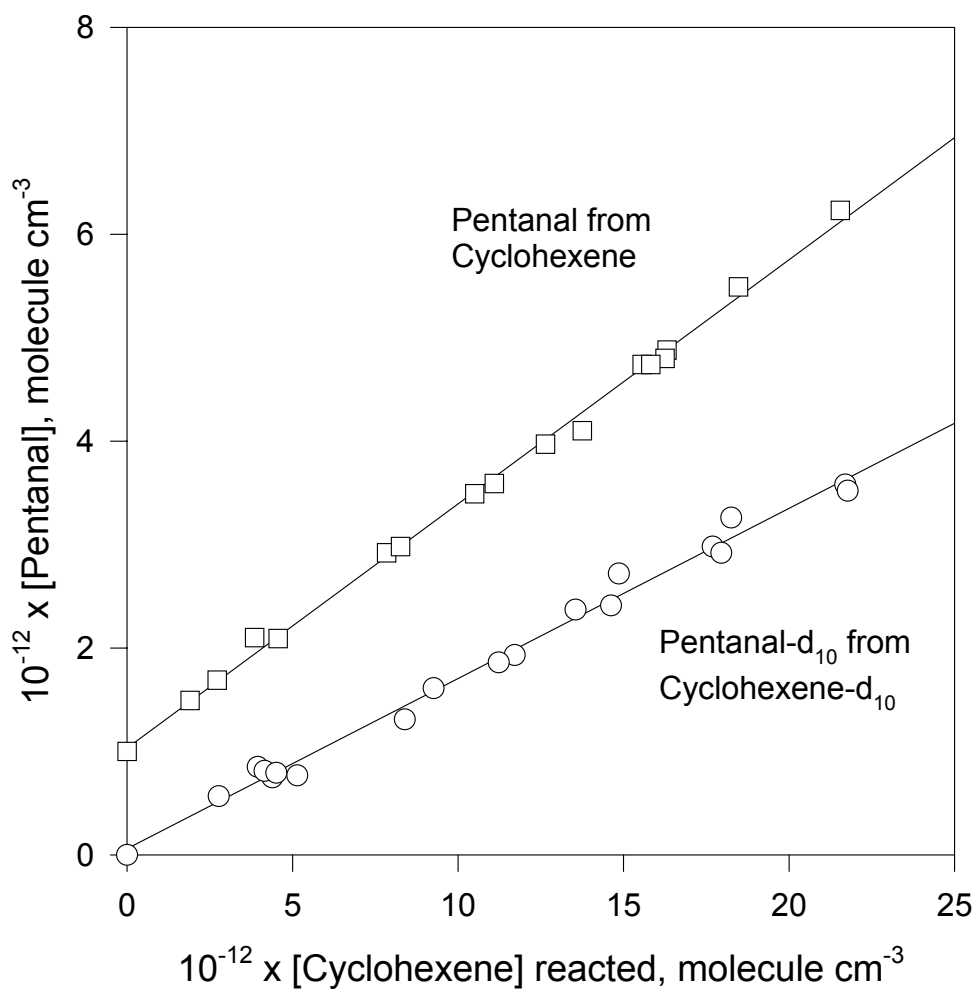


Figure 28. Plots of the amounts of pentanal and pentanal-d₁₀ formed against the amounts of cyclohexene and cyclohexene-d₁₀, respectively, reacted with O₃, in the presence of sufficient cyclohexane or 2,3-butanediol to scavenge >95% of the OH radicals formed. The pentanal data from the cyclohexene reaction have been displaced vertically by 1.0×10^{12} molecule cm⁻³ for clarity.

radical scavenger, 1.47×10^{14} molecule cm^{-3} of O_3 consumed 2.19×10^{14} molecule cm^{-3} of cyclohexene- d_{10} and showed a 0.8% yield of DC(O)OH which increased to 1.0% after 10 min. DC(O)OD, which has a sharp Q-branch absorption at 1171 cm^{-1} [the equivalent of the 1143 cm^{-1} absorption of DC(O)OH (Millikan and Pitzer, 1957)] was not observed; it is expected that the labile D atom of DC(O)OD rapidly undergoes D/H exchange with the water vapor present in the chamber (Wine *et al.*, 1985). In the cyclohexene- d_{10} reaction with added cyclohexane, 1.47×10^{14} molecule cm^{-3} of O_3 consumed 1.80×10^{14} molecule cm^{-3} of cyclohexene- d_{10} , and resulted in a 1.6% yield of DC(O)OH which increased to 2.2% after 10 min.

API-MS Analyses. API-MS spectra were obtained from the reactions of O_3 with cyclohexene and cyclohexene- d_{10} , each in the presence of sufficient cyclohexane and cyclohexane- d_{12} to scavenge >91% (added cyclohexane) or >86% (added cyclohexane- d_{12}) of the OH radicals formed from the O_3 reactions. The use of cyclohexane and cyclohexane- d_{12} as OH radical scavengers allowed the products formed from the O_3 reactions with cyclohexene and cyclohexene- d_{10} to be differentiated from those formed from the reactions of OH radicals with cyclohexane and cyclohexane- d_{12} . Thus, Figure 29 shows API-MS spectra from reacted O_3 – cyclohexene – cyclohexane – air and O_3 – cyclohexene- d_{10} – cyclohexane – air mixtures using protonated water clusters as the reagent ion, with the ion peaks arising from the reaction of OH radicals with cyclohexane being noted by asterisks. Analysis of the API-MS spectra from the various combinations of reactions showed the products listed in Table 10 from the reactions of O_3 with cyclohexene and cyclohexene- d_{10} .

The most intense ion peaks from pentanal and pentanal- d_{10} were those at $[\text{M}+\text{H}+\text{H}_2\text{O}]^+$ at 105 and 115 u, respectively, and an API-MS/MS CAD “product ion” spectrum of the weak 87 u ion peak from the cyclohexene reaction was identical to that of an authentic standard of pentanal. An API-MS/MS CAD “product ion” spectrum of the 101 u ion peak in the cyclohexene reaction in the presence of cyclohexane- d_{12} (the reaction of O_3 with cyclohexene in the presence of cyclohexane leads to a 101 u ion peak from cyclohexanol formed from cyclohexane⁹) was identical to that of an authentic standard of glutaraldehyde. The ion peaks at 115 and 125 u in the cyclohexene and cyclohexene- d_{10} reactions, respectively, are attributed to adipaldehyde (see Table 10).

An API-MS/MS CAD “product ion” spectra of the protonated molecular weight 130 and 140 products from the cyclohexene and cyclohexene- d_{10} reactions, respectively are shown in Figure 30. The CAD spectra reveal that these are analogous products, with the 131 u ion peak from the cyclohexene reaction showing losses of H_2O , $2\text{H}_2\text{O}$, $\text{H}_2\text{O}+\text{CO}$ and $2\text{H}_2\text{O}+\text{CO}$ while the 141 u ion peak from the cyclohexene- d_{10} reaction shows losses of $\text{HDO}+\text{CO}$ and $\text{HDO}+\text{D}_2\text{O}+\text{CO}$. These fragmentation patterns suggest the presence of three oxygens, and the presence of ten deuteriums in the cyclohexene- d_{10} reaction product is consistent with a secondary ozonide.

Figure 31 shows that the 133 u ion peak from the cyclohexene reaction has losses of H_2O , 34 (H_2O_2) and $\text{H}_2\text{O}+\text{CO}$, while the 140 u ion peak from the cyclohexene- d_{10} reaction has losses of H_2O , H_2O_2 , and $\text{H}_2\text{O}/\text{HDO}+\text{CO}$. Particularly interesting (and allowing identification of the 140 u ion peak in the cyclohexene- d_{10} reaction as the analog to the 133 u ion peak in the cyclohexene reaction) is the loss of a 34 mass unit fragment (H_2O_2) in both cases. Loss of H_2O_2 is indicative of the presence of an OOH group and, because OD (and OOD) groups undergo rapid D/H exchange (Atkinson *et al.*, 1995a; Vaghjiani and Ravishankara, 1989), these losses of H_2O and H_2O_2 are indicative of products containing OOH and OOD groups. Therefore, the products of molecular weight 132 and 139 from the cyclohexene and cyclohexene- d_{10} reactions, respectively,

Figure 29. API-MS spectra (using $\text{H}_3\text{O}^+(\text{H}_2\text{O})_n$ as the reagent ion) of reacted O_3 - cyclohexene peaks arising from the reaction of OH radical with cyclohexene are noted by asterisks. For the identities of the major ion peaks see Table 10.

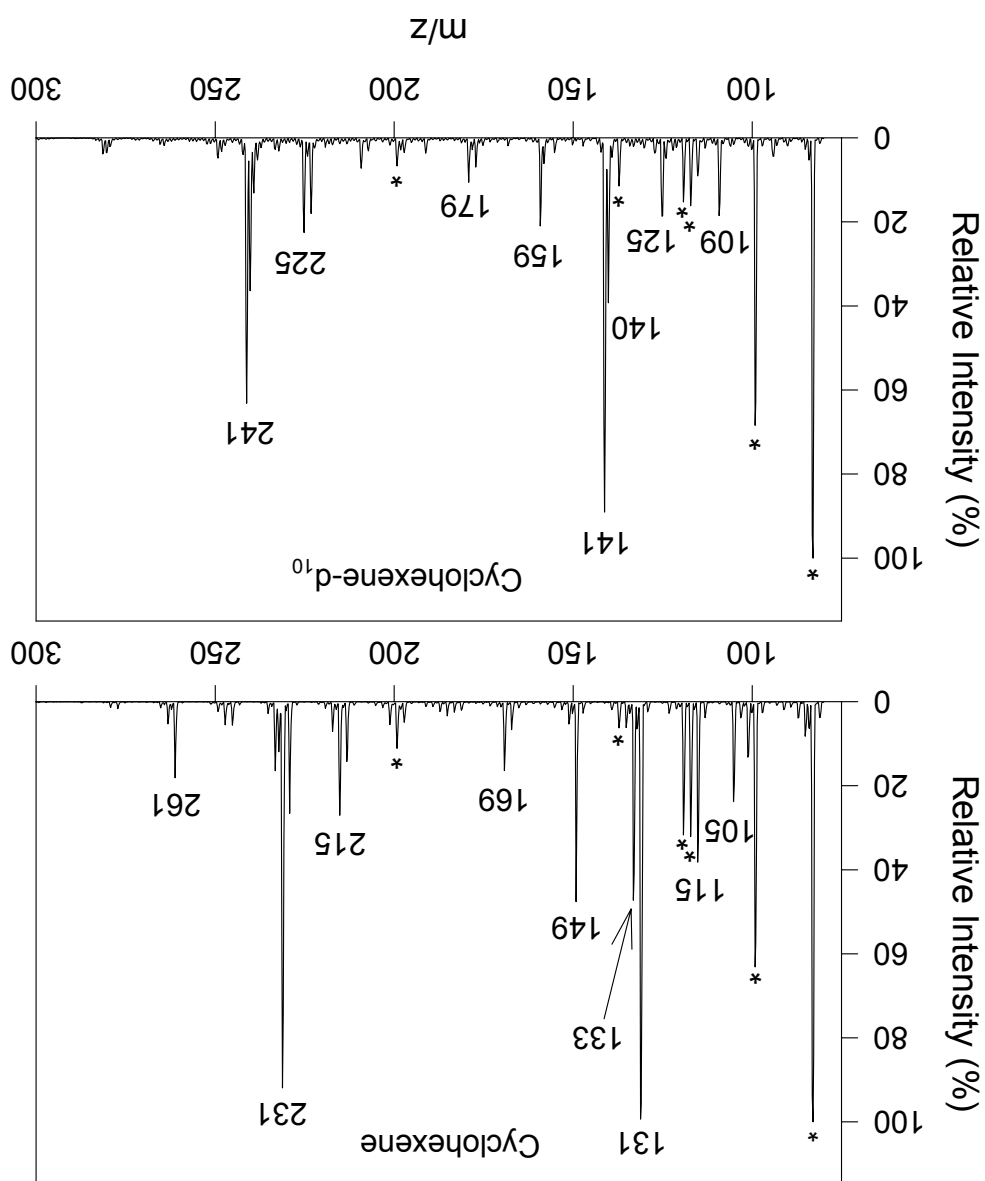


Table 10. Mass spectral evidence for products formed from the gas-phase reactions of O₃ with cyclohexene and cyclohexene-d₁₀ in the presence of an OH radical scavenger

O ₃ + Cyclohexene		O ₃ + Cyclohexene-d ₁₀	
Product (MW)	API ^a (see Figure 29)	Product (MW)	API ^b (see Figure 29)
Pentanal (86) CH ₃ CH ₂ CH ₂ CH ₂ CHO	[M+H] ⁺ = 87 [M+H+H ₂ O] ⁺ = 105	Pentanal-d ₁₀ (96) CD ₃ CD ₂ CD ₂ CD ₂ CDO	[M+H] ⁺ = 97 [M+H+H ₂ O] ⁺ = 115
Glutaraldehyde (100) HC(O)(CH ₂) ₃ CHO	[M+H] ⁺ = 101 ^c	Glutaraldehyde-d ₈ (108) DC(O)CD ₂ CD ₂ CD ₂ CDO	[M+H] ⁺ = 109
Adipaldehyde (114) HC(O)(CH ₂) ₄ CHO	[M+H] ⁺ = 115	Adipaldehyde-d ₁₀ (124) DC(O)(CD ₂) ₄ CDO	[M+H] ⁺ = 125
Secondary ozonide (130) C ₆ H ₁₀ O ₃	[M+H] ⁺ = 131 ^d [M+H+H ₂ O] ⁺ = 149	Secondary ozonide (140) C ₆ D ₁₀ O ₃	[M+H] ⁺ = 141 ^d [M+H+H ₂ O] ⁺ = 159
C ₆ H ₁₀ O ₃ (130) ^e		C ₆ D ₁₀ O ₃ (140)	
Peracid (132) C ₅ H ₇ O ₂ (OOH)	[M+H] ⁺ = 133 ^f	Peracid (139) C ₅ D ₇ O ₂ (OOH) ^g	[M+H] ⁺ = 140 ^f
Hydroxydicarbonyl (130) HC(O)(CH ₂) ₃ CH(OH)CHO ^h		Hydroxydicarbonyl (139)	
Hydroxycarbonyl or oxo-acid (116)		Hydroxycarbonyl or oxo-acid (123)	

^aThe high mass peaks in Figure 3 (top) are those of homo- and hetero-dimers. For example, 261 = 130+130+H; 215 = 114+100+H; 231 = 130+100+H; 169 = 100+86+H-H₂O. Note that the major products from the cyclohexane scavenger reaction with the OH radical are cyclohexanone (MW 98) and cyclohexanol (MW 100) and these may participate in the formation of heterodimers.

^bThe high mass peaks in Figure 3 (bottom) are those of homo- and hetero-dimers. For example, 225 = 124+100+H; 241 = 140+100+H; 179 = 100+96+H-H₂O. Note that the major products from the cyclohexane scavenger reaction with the OH radical are cyclohexanone (MW 98) and cyclohexanol (MW 100) and these participate in the formation of heterodimers.

^cSee text for discussion of reaction with cyclohexane-d₁₂ which allowed unambiguous identification of glutaraldehyde.

^dSee Figure 30 for CAD spectra.

^ePossibly the secondary ozonide which was sampled by the SPME, with decomposition on the fiber to form an oxo-acid which was then derivatized and analyzed as its oxime (see text).

^fSee Figure 31 for CAD spectra.

^gOD/OH exchange occurs, presumably with water in the chamber.

^hTentative identification (see Figure 34).

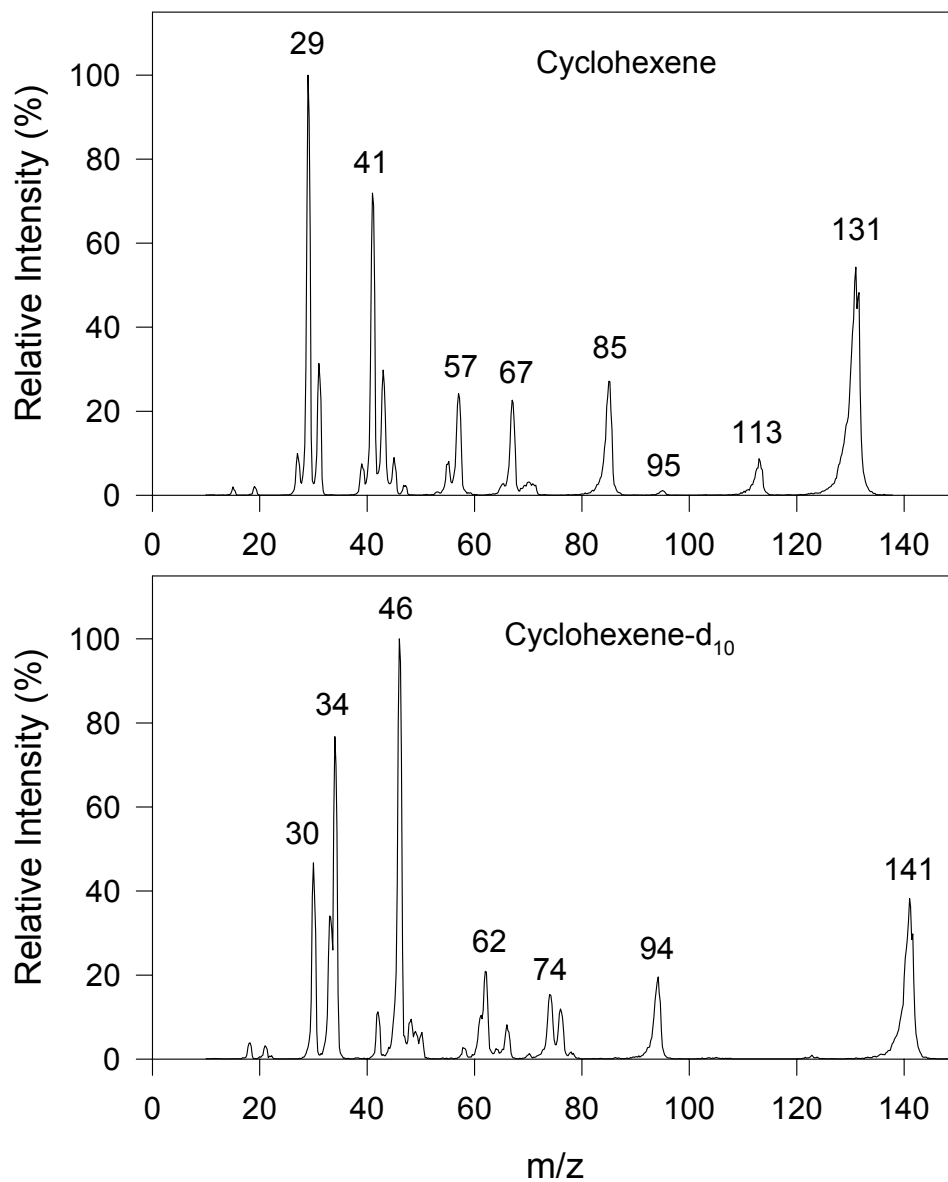


Figure 30. API-MS/MS CAD “product ion” spectra (using $\text{H}_3\text{O}^+(\text{H}_2\text{O})_n$ as the reagent ion) of the 131 and 141 u ion peaks observed in the reactions of O_3 with cyclohexene and cyclohexene-d₁₀ reactions, respectively. Cyclohexane was present to scavenge OH radicals.

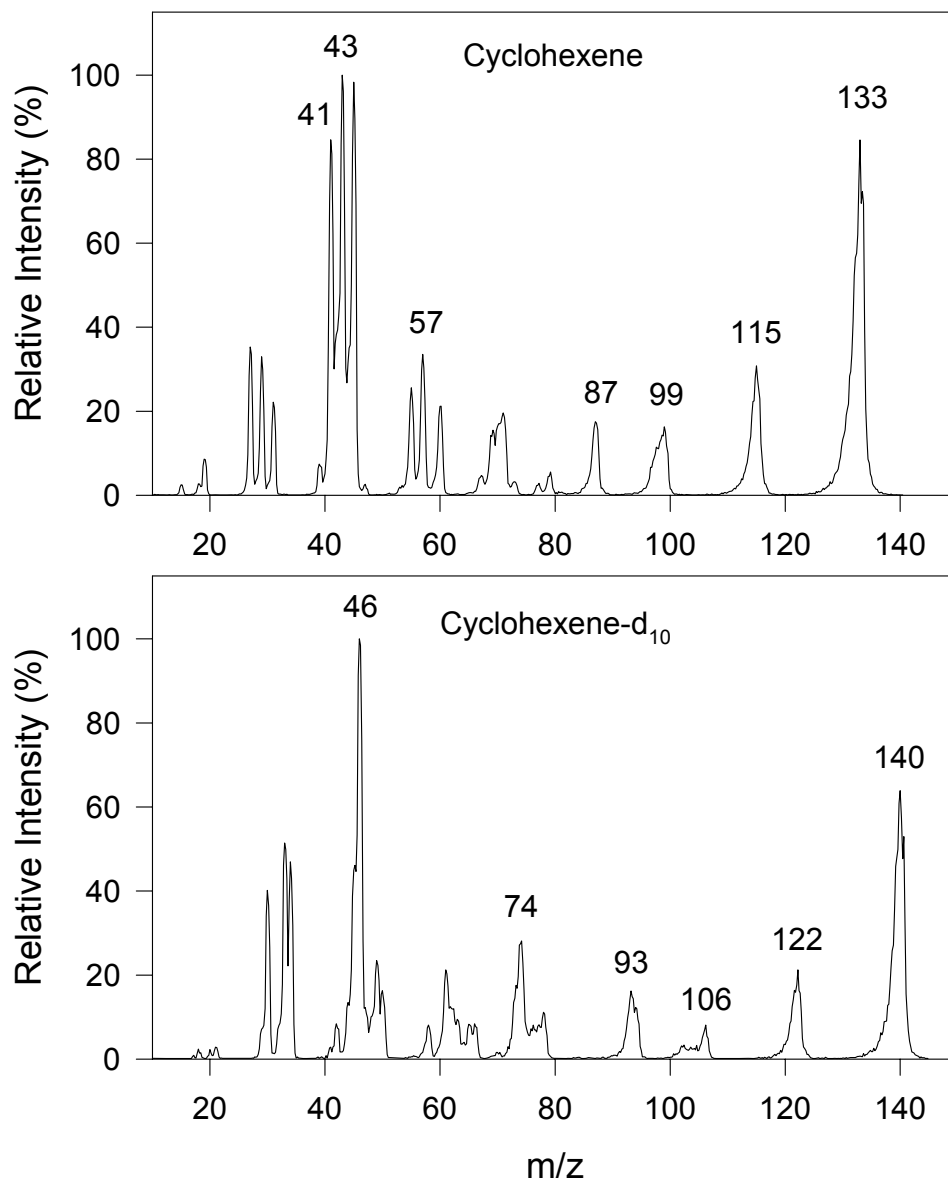
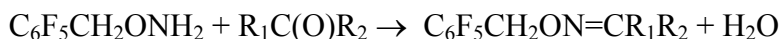


Figure 31. API-MS/MS CAD “product ion” spectra (using $\text{H}_3\text{O}^+(\text{H}_2\text{O})_n$ as the reagent ion) of the 133 and 140 u ion peaks observed in the reactions of O_3 with cyclohexene and cyclohexene- d_{10} reactions, respectively. Cyclohexane was present to scavenge OH radicals. Note the presence of fragment ions at 99 and 106 u from the cyclohexene and cyclohexene- d_{10} reactions, respectively, indicating a loss of H_2O_2 in both cases.

have formula of C₅H₇O₂(OOH) and C₅D₇O₂(OOH), respectively.

Addition of butanal to the reactant mixtures resulted in changes in the post-reaction API-MS spectra. However, at least qualitatively these changes were due to the formation of hetero-dimers of protonated butanal and the protonated butanal dimer with reaction products. Thus, for example, in a reacted O₃ – cyclohexene – cyclohexane – butanal – air mixture compared to a reacted O₃ – cyclohexene – cyclohexane – air mixture the ion peaks of the molecular weight 114 and 130 products (which are believed to involve reactions of the thermalized Criegee intermediate; see below) and their protonated homo- and hetero-dimers at 115, 131, 149, 215, 231 and 261 u (see Table 10) decreased in the presence of butanal and were replaced (at least in part) by ion peaks at 217 u ([114+butanal+H]⁺) and 275 u ([131+butanal+butanal+H]⁺) in the presence of butanal in the reactant mixture. In particular, no evidence for any significant formation of the secondary ozonide arising from reaction of the Criegee intermediate HC(O)CH₂CH₂CH₂CH₂CHOO (and its deuterated analog) with butanal was observed (the protonated secondary ozonides being at 203 and 213 u, respectively).

GC-MS Analyses of PFBHA Derivatives. In two experiments, PDMS/DVB SPME fibers pre-coated with PFBHA were exposed in the chamber to cyclohexene and cyclohexene-d₁₀ reaction products. Oxime derivatives are formed from carbonyl-containing compounds through the reaction.



Utilizing GC-MS with isobutane chemical ionization, generally intense protonated molecules [M+H]⁺ and small adduct ions at [M+41]⁺ are observed, where the molecular mass, M, of the oxime is 195 mass units greater than the weight of the carbonyl, or in the case of a dicarbonyl forming a di-oxime, 390 mass units higher. Note that *Z* and *E* configurations are sometimes present and resolved.

Pentanal and glutaraldehyde were identified based on matching the GC retention times and mass spectra with those of authentic standards. Note that two isomers of the oxime from pentanal were formed and both carbonyls in glutaraldehyde were derivatized, with only a trace of the singly derivatized compound oxime being observed. The corresponding peaks from the cyclohexene-d₁₀ reaction eluted from the GC column a few seconds earlier than the cyclohexene products. The presence of the apparent molecular ion of glutaraldehyde-d₈ at 500 u rather than the predicted 499 u, with an ion peak also observed at 501 u must be attributed to H/D exchange in the ion trap source, which is subject to secondary ion-molecule reactions (Yu *et al.*, 1995).

The SPME analysis confirmed the presence of two carbonyl groups in the molecular weight 114 compound attributed to adipaldehyde in the API analyses. A large oxime peak corresponding to a molecular weight 130 compound was also observed from the cyclohexene reaction and, in contrast to the oximes of pentanal, glutaraldehyde and adipaldehyde which showed almost no fragmentation, the base peak in the spectrum was due to a loss of H₂CO₂ from the [M+H]⁺ molecular ion. The corresponding peak from the cyclohexene-d₁₀ reaction suggested 10 deuteriums and a base peak due to loss of HDCO₂ from the [M+H]⁺ ion (or loss of D₂CO₂ from the [M+D]⁺ ion). It is possible that this oxime peak is due to SPME sampling of the secondary ozonide, with decomposition of the secondary ozonide on the SPME fiber to an oxo-acid which was then derivatized and analyzed as its oxime.

Significantly smaller peaks corresponding to two carbonyl-containing compounds of molecular weight 116 and 130 were also observed in the SPME analysis. For the molecular weight 130 product, both mono- and di-oxime derivatives were observed, indicating a

dicarbonyl. The oximes gave fragments corresponding to a loss of H₂O and, in the cyclohexene-d₁₀ reaction, a loss of H₂O and HDO, suggesting that this product is a hydroxydicarbonyl and possibly that shown in Figure 34 [HC(O)CH₂CH₂CH₂CH(OH)CHO]. For the molecular weight 116 carbonyl-containing product only a mono-oxime derivative was observed. The oxime gave a fragment corresponding to a loss of H₂O and, in the cyclohexene-d₁₀ reaction, a loss of H₂O and HDO, suggesting that this product is a hydroxycarbonyl or possibly an oxo-acid (without standards no conclusive identification is possible).

The presence of a small hydroxydicarbonyl of molecular weight 130 (as noted, possibly HC(O)CH₂CH₂CH₂CH(OH)CHO) is not inconsistent with the API-MS/MS data shown in Figures 30 and 31. In Figure 30 (top) the [M+H]⁺ = 131 u ion peak from the cyclohexene reaction may be attributed primarily to the protonated secondary ozonide plus a small amount of the protonated hydroxydicarbonyl, while the [M+H]⁺ = 141 u ion peak (Figure 30, bottom) from the cyclohexene-d₁₀ reaction is solely due to the protonated secondary ozonide-d₁₀. In Figure 31 (top) the [M+H]⁺ = 133 u ion peak from the cyclohexene reaction may be attributed solely to the protonated peracid, while the [M+H]⁺ = 140 u ion peak (Figure 31, bottom) from the cyclohexene-d₁₀ reaction is due primarily to the protonated peracid-d₇ plus a small amount of the protonated hydroxydicarbonyl-d₉.

3.1.4. Discussion

Based on our GC-FID, GC-MS, API-MS and FT-IR analyses, the gas-phase products observed from the reaction of O₃ with cyclohexene in the presence of an OH radical scavenger are pentanal (23.6 ± 1.8%), OH radicals (54 ± 8%), formic acid (3.5% initial yield), glutaraldehyde [HC(O)CH₂CH₂CH₂CHO], adipaldehyde [HC(O)CH₂CH₂CH₂CH₂CHO], a C₆H₁₀O₃ product which is attributed to the secondary ozonide, a C₅H₇O₂(OOH) product, a hydroxydicarbonyl of molecular weight 130 (possibly HC(O)CH₂CH₂CH₂CH(OH)CHO) and a hydroxycarbonyl or possibly oxo-acid of molecular weight 116. As evident from Table 9, the OH radical formation yield measured here from the cyclohexene reaction is in excellent agreement with the value of Fenske *et al.* (2000b). Furthermore, our present OH radical formation yields from the reactions of O₃ with propene, α-pinene and 2,3-dimethyl-2-butene are in good agreement with recent literature data (Paulson *et al.*, 1998, 1999b; Rickard *et al.*, 1999; Neeb and Moortgat, 1999; Fenske *et al.*, 2000b,c; Siese *et al.*, 2001; Orzechowska and Paulson, 2002) (Table 9), indicating that 2,3-butanediol can be used to determine OH radical yields from the amounts of 3-hydroxy-2-butanone formed.

The deuterium isotope ratios, k_H/k_D, for the OH (or OD) radical yields from the reactions of O₃ with propene and cyclohexene are 1.48 ± 0.31 and 1.08 ± 0.22, respectively. These are fairly close to unity (especially for the cyclohexene reaction) and presumably reflect the fractions of the Criegee intermediates formed in the *syn*-configuration (see below) together with the effect of deuterium substitution on the branching ratios for the various reaction channels.

Our pentanal yield from cyclohexene (23.6 ± 1.8%) is a factor of 1.5 higher than the yield reported by Grosjean *et al.* (1996) of 15.6 ± 0.4%. A similar discrepancy occurs for the reaction of O₃ with cyclopentene where we previously measured a butanal yield of 19.5 ± 2.7% (Atkinson *et al.*, 1995c), compared to the yield of 12.0 ± 0.1% reported by Grosjean and Grosjean (1996). Pentanal yields have also been reported by Hatakeyama *et al.* (1985) (17.2 ± 1.7% relative to the amount of cyclohexene consumed in the absence of an OH radical scavenger; this corresponds to a pentanal yield from the O₃ reaction with cyclohexene of 26.5 ± 4.7% assuming that all of the OH radicals formed reacted with the cyclohexene and did not lead to pentanal formation, in

agreement with our pentanal yield) and by Kalberer *et al.* (2000) ($17.0 \pm 9.4\%$, in the presence of an OH radical scavenger).

Our yield of HC(O)OH from the reaction of O₃ with cyclohexene of 2.5-3.2% in the absence of an OH radical scavenger is similar to that of 3.7% calculated from the spectrum shown by Niki *et al.* (1983), but is significantly lower than the yield of $12 \pm 1\%$ reported by Hatakeyama *et al.* (1985). In agreement with previous studies (Hatakeyama *et al.*, 1985; Niki *et al.*, 1983), HCHO was not detected as a reaction product. In the presence of sufficient cyclohexane to scavenge >95% of the OH radicals formed, the HC(O)OH yield from the cyclohexene reaction was initially 3.5%, increasing to 4.4% after 17 min (note that the O₃ was consumed after 4 min), while the yield of DC(O)OH [which, because of rapid OD/OH exchange, could have been formed as DC(O)OD] from the cyclohexene-d₁₀ reaction was initially 1.6%, increasing to 2.2% after 10 min. There therefore appears to be a significant deuterium isotope effect on the formic acid yield, of a factor of ~2.0-2.2.

The initial reaction of cyclohexene with O₃ forms the primary ozonide which rapidly decomposes to an energy-rich Criegee intermediate, which theoretical studies show to be a carbonyl oxide and which can exist in a *syn*- or *anti*-configuration [see, for example, Fenske *et al.* (2000a) and Kroll *et al.* (2001a,b)].



As shown in Figure 32 (in which identified products are shown in boxes), this Criegee intermediate can be collisionally stabilized, decompose to form CO₂ plus pentanal (possibly through the ester channel), and, for the *syn*-intermediate, isomerize to a hydroperoxide which then eliminates an OH radical (Atkinson, 1997a, 2000; Calvert *et al.*, 2000; Fenske *et al.*, 2000a; Kroll *et al.*, 2001a,b). The recent studies of Kroll *et al.* (2001a,b) and Fenske *et al.* (2000a) show that thermalized Criegee intermediates can also undergo isomerization with subsequent decomposition to form an OH radical (plus organic radical co-product), as also indicated in Figure 32 for the *syn*-intermediate.

The thermalized Criegee intermediate may also react with water vapor present to form an α -hydroxyhydroperoxide, which may be thermally stable or decompose to either 6-oxohexanoic acid [HC(O)CH₂CH₂CH₂CH₂C(O)OH] plus H₂O or to adipaldehyde [HC(O)CH₂CH₂CH₂CH₂CHO] plus H₂O₂ (Figure 33) (Winterhalter *et al.*, 2000; Baker *et al.*, 2002). Our product data indicate that decomposition and/or isomerization of the Criegee intermediate to form pentanal (plus CO₂) and an OH radical plus organic radical co-product account for $78 \pm 9\%$ of the reaction pathways. Adipaldehyde can be formed from reaction of the thermalized Criegee intermediate (presumably the *anti*-intermediate, with the *syn*-intermediate decomposing to an OH radical) with water vapor (Figure 33). The product of molecular weight 130 from cyclohexene and 140 from cyclohexene-d₁₀ observed by API-MS (and possibly by SPME after decomposition) is consistent with this product being the secondary ozonide formed by re-cyclization of the Criegee intermediate (Figure 32).

Addition of $\sim 2.4 \times 10^{13}$ molecule cm⁻³ of butanal to the reactant mixture resulted in no marked changes in the products formed, as deduced from the API-MS spectra. In particular, no secondary ozonide arising from reaction of butanal with the Criegee intermediate was observed. The kinetic data reported by Tobias and Ziemann (2001) for reactions of the CH₃(CH₂)₁₁CHOO intermediate with water and formaldehyde shows that formaldehyde is factor of 2700 more

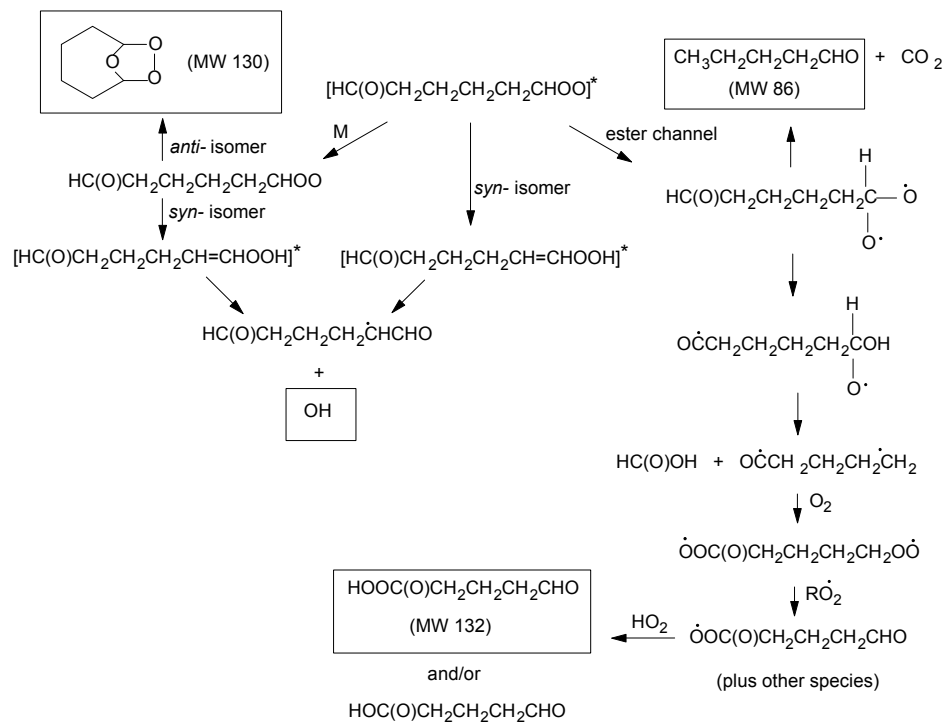


Figure 32. Reaction scheme for reaction of O_3 with cyclohexene.

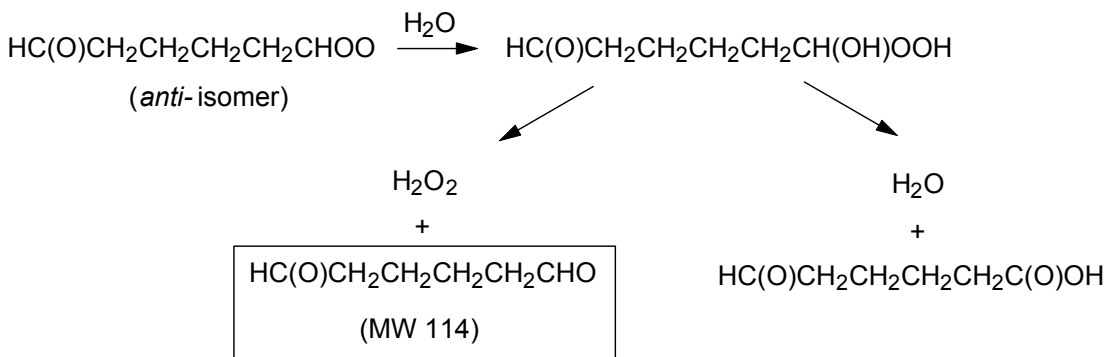


Figure 33. Reaction of the stabilized Criegee intermediate with water vapor.

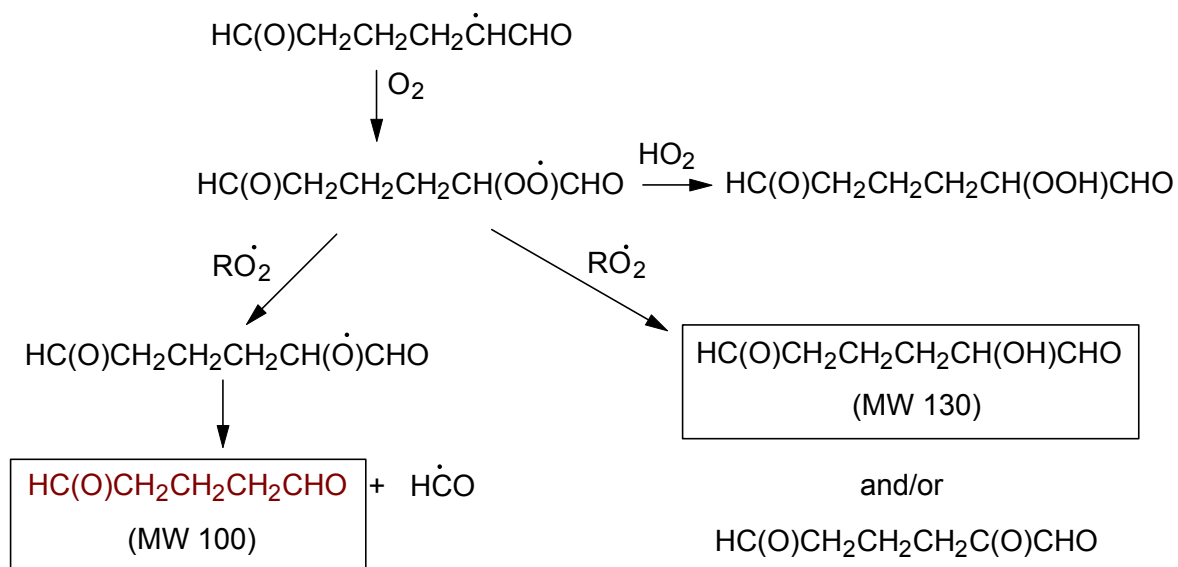


Figure 34. Possible reactions of the radical co-product to the OH radical.

reactive than water vapor. Assuming that the relative reactivities of butanal and water vapor towards the $\text{HC(O)CH}_2\text{CH}_2\text{CH}_2\text{CH}_2\text{CHOO}$ intermediate are the same as those of formaldehyde and water vapor towards the $\text{CH}_3(\text{CH}_2)_{11}\text{CHOO}$ intermediate, then for the water vapor and butanal concentrations used here ($\sim 3.4 \times 10^{16}$ molecule cm^{-3} and 2.4×10^{13} molecule cm^{-3} , respectively) reaction of the $\text{HC(O)CH}_2\text{CH}_2\text{CH}_2\text{CH}_2\text{CHOO}$ intermediate with butanal would be only a factor of ~ 2 faster than with water vapor. Use of higher concentrations of butanal was precluded because the API-MS spectrum was then dominated by ions arising from protonated butanal and its protonated dimer, trimer and tetramer.

The organic co-product to the OH radical, anticipated to be the $\text{HC(O)CH}_2\text{CH}_2\text{CH}_2\text{C}^\bullet\text{HCHO}$ radical (Figure 34) will add O_2 and the resulting peroxy radical will react with HO_2 and organic peroxy (RO_2^\bullet) radicals as shown in Figure 34 (Atkinson, 1997a, 2000), leading to the formation of a series of multifunctional products (Figure 34), including glutaraldehyde and the hydroxydicarbonyl $\text{HC(O)CH}_2\text{CH}_2\text{CH}_2\text{CH(OH)CHO}$.

The formation route to the observed product of formula $\text{C}_5\text{H}_7\text{O}_2(\text{OOH})$ [molecular weight 132] is less obvious. Based on the observed formation of exclusively ^{18}O -labeled $\text{HC}(^{18}\text{O})^{18}\text{OH}$ from the reaction of $^{18}\text{O}_3$ with cyclohexene (in the absence of an OH radical scavenger), Hatakeyama *et al.* (1985) postulated that HC(O)OH arises through the reaction sequence involving the $\text{HC(O)CH}_2\text{CH}_2\text{CH}_2\text{CH}_2\text{CH}(\text{O}^\bullet)\text{O}^\bullet$ and $^\bullet\text{OCCH}_2\text{CH}_2\text{CH}_2\text{CH}_2\text{CH(OH)O}^\bullet$ species (i.e, via the ester channel pathway in Figure 32). The co-product to HC(O)OH is then postulated⁵ to be the $^\bullet\text{OCCH}_2\text{CH}_2\text{CH}_2\text{C}^\bullet\text{H}_2$ biradical which reacts, as proposed by Jenkin *et al.* (2000), to form the $^\bullet\text{OOC(O)CH}_2\text{CH}_2\text{CH}_2\text{CHO}$ species (Figure 32), then leading to the molecular weight 132 peracid $\text{HOOC(O)CH}_2\text{CH}_2\text{CH}_2\text{CHO}$. The corresponding products in the cyclohexene- d_{10} reaction will then be (after OOD/OOH exchange) the molecular weight 139 peracid $\text{HOOC(O)CD}_2\text{CD}_2\text{CD}_2\text{CDO}$. Clearly, the specific identify and formation route of the observed molecular weight 132 $\text{C}_5\text{H}_7\text{O}_2(\text{OOH})$ product shown in Figure 32 is speculative, but the number of other possibilities seems limited. This pathway would also lead to 5-oxopentanoic acid of molecular weight 116, which may possibly be the product of this molecular weight observed in the SPME analysis. It should also be noted that the formic acid formation yield was observed to increase somewhat with increasing extent of reaction, suggesting in addition to a “prompt” formation route the existence of a slow secondary formation pathway for formic acid.

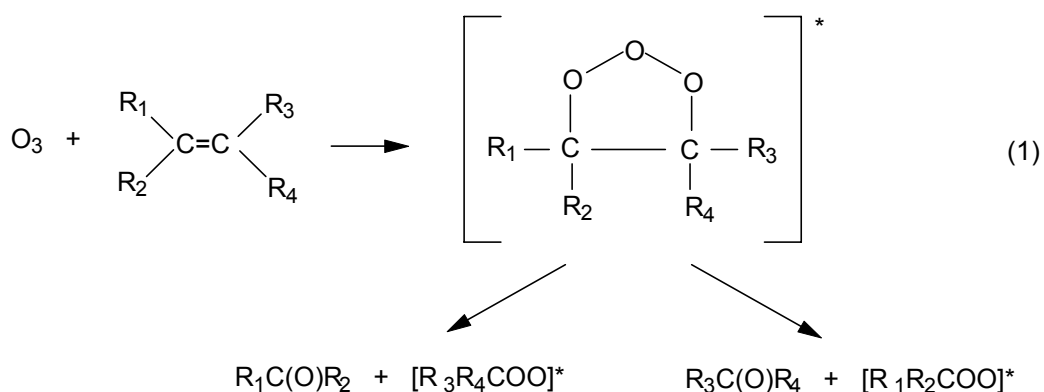
The gas-phase products observed here are consistent with the aerosol-phase products observed by Ziemann (2002). In particular, Ziemann (2002) observed aerosol-phase products attributed to diacyl peroxides formed from reactions of peroxyacyl radicals of structure $\text{HC(O)(CH}_2)_n\text{C(O)OO}^\bullet$ and $\text{HOC(O)(CH}_2)_n\text{C(O)OO}^\bullet$, where $n = 3$ and 4, consistent with our observation of the molecular weight 132 product suggested to be the peracid $\text{HOOC(O)CH}_2\text{CH}_2\text{CH}_2\text{CHO}$ and formed from the acyl peroxy radical $\text{HC(O)(CH}_2)_3\text{C(O)OO}^\bullet$ (Figure 32).

3.2. OH Radical Formation from Reaction of O₃ with Alkenes: Effects of Water Vapor and 2-Butanol

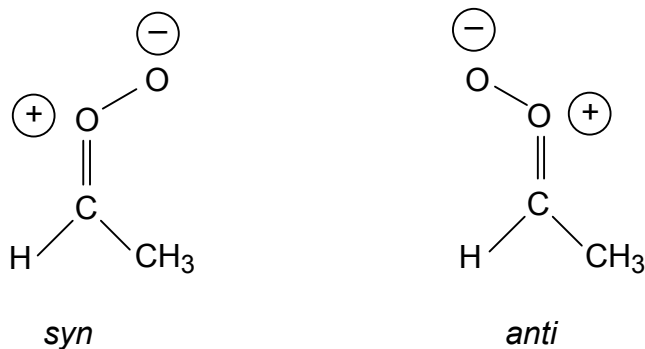
3.2.1. Introduction

Alkenes are an important component of volatile non-methane organic compounds emitted into the atmosphere from anthropogenic and biogenic sources (Calvert *et al.*, 2000). In the atmosphere, alkenes react with OH radicals, NO₃ radicals and O₃ (Atkinson, 1997a, 2000; Atkinson and Arey, 2003), with the O₃ reactions often being an important atmospheric transformation process (Atkinson, 1997a, 2000; Atkinson and Arey, 2003).

The reactions of O₃ with alkenes proceed by initial addition of O₃ across the C=C unsaturated bond to form an energy-rich primary ozonide, which then decomposes to two sets of carbonyl plus chemically-activated “Criegee” intermediate (Gutbrod *et al.*, 1996, 1997; Fenske *et al.*, 2000a,b,c; Kroll *et al.*, 2001a,b, 2002; Zhang and Zhang, 2002), as shown below for R₁-R₄ = H or alkyl.



Theoretical calculations indicate that the Criegee intermediate is a carbonyl oxide (Cremer *et al.*, 1993; Gutbrod *et al.*, 1996, 1997), which for mono-substituted intermediates may be formed in either the *syn* or *anti* configuration (shown below for R = CH₃).

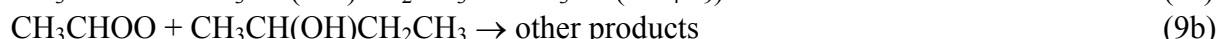


Under atmospheric conditions, the chemically-activated carbonyl oxides (hereafter denoted as Criegee intermediates) are proposed to undergo a number of possible reactions, as shown below for the initially-formed $[\text{CH}_3\text{CHOO}]^*$ intermediate (Sauer *et al.*, 1999; Alvarado *et al.*, 1998; Winterhalter *et al.*, 2000; Fenske *et al.*, 2000a; Hasson *et al.*, 2001a,b, 2003; Kroll *et al.*, 2001a,b, 2002; Baker *et al.*, 2002; Zhang and Zhang, 2002; Atkinson and Arey, 2003):

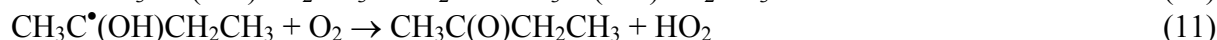


The relative importance of “prompt” (from the chemically-activated intermediates) vs “slow” (from thermalized Criegee intermediates) OH radical formation at atmospheric pressure of air is not totally understood (Fenske *et al.*, 2000a; Kroll *et al.*, 2001a,b; Johnson *et al.*, 2001; Aschmann *et al.*, 2002c; Hasson *et al.*, 2003). However, theoretical calculations show that chemically-activated dialkyl-substituted Criegee intermediates and *syn*- monoalkyl-substituted Criegee intermediates lead to OH radical formation, while the *anti*- substituted monoalkyl-substituted intermediates are mainly collisionally stabilized (but can form OH radicals in small yield (Kroll *et al.*, 2002), and that thermalized *syn*- (but not *anti*-) intermediates can lead to OH radical formation (Kroll *et al.*, 2002).

In addition to reactions (2) through (7), under laboratory conditions the stabilized Criegee intermediates may react with other species, including carbonyl compounds (to form secondary ozonides) (Winterhalter *et al.*, 2000) and added OH radical scavengers such as 2-butanol (Neeb *et al.*, 1996; Tobias and Ziemann, 2001)



The OH radicals generated in reactions (3) and (5), and possibly from the vinoxy ($\bullet\text{CH}_2\text{CHO}$) radical formed from CH_3CHOO intermediates (Atkinson, 1997a), react with the alkene and reaction products or with an added OH radical scavenger. In this work, 2-butanol was used as one of the OH radical scavengers (Chew and Atkinson, 1996), leading to the formation of 2-butanone in $69 \pm 6\%$ yield (Aschmann *et al.*, 2002c) through the reactions



Based on the reactions listed above, variation of water vapor concentration could affect (a) the OH radical yield because of competition of reactions (5) and (6) involving the stabilized Criegee intermediate, and (b) the formation yield of the primary carbonyl (CH_3CHO in the case of an alkene forming the $[\text{CH}_3\text{CHOO}]^*$ intermediate) because of the occurrence of reaction (6) followed by reaction (7b) in competition with reactions (8) and (9). Hence an increase in water

vapor concentration may be expected to result in a decrease in OH radical yield and an increase in the “primary” carbonyl yield.

Use of an alcohol such as 2-butanol to scavenge OH radicals could also result in scavenging the stabilized Criegee intermediate and lead to a reduction in the OH radical yield [because of competition of reaction (9) with reaction (5)] and in the “primary” carbonyl yield [because of competition of reaction (9) with reaction (6) followed by reaction (7b)].

Previous studies (Atkinson *et al.*, 1992; Atkinson and Aschmann, 1993; Johnston *et al.*, 2001; Baker *et al.*, 2002; Aschmann *et al.*, 2002c, Hasson *et al.*, 2003) have shown for ethene propene, *trans*-2-butene, 2-methyl-2-butene and a number of monoterpenes that variation of the water vapor concentration (from 0-5% relative humidity to 50-65% relative humidity) has no effect on the OH radical yield. Furthermore, Johnston *et al.* (2001) showed that addition of species which are known to react with the stabilized Criegee intermediate (SO₂, acetic acid and 2-butanone) also had no effect on the OH radical yield from the 2-methyl-2-butene reaction. Baker *et al.* (2002) observed no effect on the pinonaldehyde yield from α -pinene or of 2,7-octanedione from 1,2-dimethyl-1-cyclohexene (these being the “primary” carbonyls from these reactions) when the OH radical scavenger was changed from cyclohexane to 2-butanol.

In this work, we have investigated the effects of water vapor and 2-butanol concentrations on the OH radical and “primary” carbonyl formation yields from the reactions of O₃ with sabinene, α -pinene and 7-tetradecene. A complicating factor arises for slowly reacting alkenes where, when reactions are carried out with additions of ozone to excess concentrations of the alkene, the ozone is not removed rapidly by reaction. In these cases the use of 2-butanol as an OH radical scavenger has been shown to lead to OH radical formation, presumably from the presence of small amounts of reactive impurities in the 2-butanol or possibly from a slow (wall) reaction of O₃ with 2-butanol. (Chew and Atkinson, 1996).

3.2.2. Experimental Methods

Experiments were carried out at 296 ± 2 K and 740 Torr of purified air at relative humidities (RH) of ≤ 5 to 61% (corresponding to water vapor concentrations of $\leq 3.4 \times 10^{16}$ molecule cm⁻³ to 4.2×10^{17} molecule cm⁻³) in a ~7000 liter Teflon chamber equipped with a Teflon-coated fan to ensure rapid mixing of reactants during their introduction into the chamber. Experiments were carried out in the presence of 2-butanol, cyclohexane or *n*-octane to act as an OH radical scavenger. The initial concentrations (in molecule cm⁻³ units) were: α -pinene, $(1.82-2.90) \times 10^{13}$, sabinene, $(1.56-2.83) \times 10^{13}$, or 7-tetradecene, $(1.15-3.00) \times 10^{13}$; 2-butanol, $(4.4-132) \times 10^{15}$, cyclohexane $(7.5-11.3) \times 10^{16}$ or *n*-octane, 7.4×10^{15} ; and 3 or 4 additions of O₃ in O₂ diluent (each O₃/O₂ addition corresponding to $\sim 5 \times 10^{12}$ molecule cm⁻³ of O₃ in the chamber) were made to the chamber during an experiment. The concentrations of alkene, selected products (pinonaldehyde from α -pinene, sabinaketone from sabinene and heptanal from 7-tetradecene), and 2-butanone were measured during the experiments by gas chromatography with flame ionization detection (GC-FID). Gas samples of 100 cm³ volume were collected from the chamber onto Tenax-TA solid adsorbent for subsequent thermal desorption at ~ 250 °C onto a 30 m DB-1701 megabore column held at 0 °C and then temperature programmed at 8 °C min⁻¹. The GC-FID response factors for the alkenes, 2-butanone and 2-butanol were determined by introducing measured amounts of the liquid compounds from a 1-liter Pyrex bulb into the chamber by flowing N₂ gas through the bulb, and conducting several replicate GC-FID analyses (the chamber volume was determined by introducing a measured amount of *trans*-2-butene and analyzing its concentration using a pre-calibrated GC). The GC-FID response factors for the

pinonaldehyde, sabinaketone and heptanal were calculated by combining the measured GC-FID response factors for α -pinene, sabinene and 7-tetradecene with the estimated Effective Carbon Numbers (ECNs) for the alkene and its respective carbonyl product (Scanlon and Willis, 1985). We have previously (Alvarado *et al.*, 1998; Baker *et al.*, 2002; Aschmann *et al.*, 2002b) shown that such estimated FGC-FID response factors for pinonaldehyde and sabinaketone are in good agreement (within 10%) with measured response factors.

The chemicals used, and their stated purities, were: 2-butanol (99.5%), 2-butanone (99+%), α -pinene (99+%) and sabinene (99%), Aldrich Chemical Company; cyclohexane (HPLC grade), Fisher Scientific; and 7-tetradecene, TCI Americas. O₃ in O₂ diluent was prepared as needed using a Welsbach T-408 ozone generator.

3.2.3. Results and Discussion

In agreement with previous studies of the α -pinene and sabinene reactions (Hakola *et al.*, 1994; Chew and Atkinson, 1996; Baker *et al.*, 2002), 2-butanone was observed to be formed from all three reactions, together with pinonaldehyde from α -pinene and sabinaketone from sabinene. 2-Butanone and heptanal were observed from the 7-tetradecene reaction. The measured 2-butanone yields (when 2-butanol was present as the OH radical scavenger) have been combined with our previously measured yield of 2-butanone from the OH radical-initiated reaction of 2-butanol ($69 \pm 6\%$ (Aschmann *et al.*, 2002c) to obtain the OH radical formation yields from the O₃ reactions (Chew *et al.*, 1996; Aschmann *et al.*, 2002c). The results are discussed below.

Sabinene. In the majority of experiments, 2-butanol was used as the OH radical scavenger, thereby allowing the OH radical formation yield to be determined from the amounts of 2-butanone formed. The 2-butanol concentrations were varied from 4.4×10^{15} molecule cm⁻³ to 6.6×10^{16} molecule cm⁻³. At the lower concentrations of added 2-butanol (4.4×10^{15} molecule cm⁻³), in the initial stages of the reaction 8% of the OH radicals formed would not be scavenged by 2-butanol (rather reacting with sabinene). Hence for these experiments, the measured OH radical yields are ~10% too low; the effect on the sabinaketone yield is <3% (because the OH radical formation yield is ~0.3). In those experiments where 2-butanol was not added, cyclohexane or *n*-octane were used to scavenge $\geq 95\%$ of the OH radicals formed.

Sabinaketone is both a “primary” carbonyl and can be formed from reaction of the C₉-Criegee intermediates with water vapor. As evident from Figure 35, the sabinaketone yield increased with relative humidity (relative humidity from $\leq 5\%$ to 61% [$\leq 3.4 \times 10^{16}$ to 4.2×10^{17} molecule cm⁻³]). This is consistent with reaction of the C₉-Criegee intermediate with water vapor to form sabinaketone [reaction (6) followed by (7b)] being in competition with reaction of the Criegee intermediate with other species, presumably mainly carbonyls (including formaldehyde) to form secondary ozonides [reaction (8)]. This behavior is analogous to that observed by Winterhalter *et al.* (2000) and Hasson *et al.* (2001b) for the β -pinene reaction and by Hasson *et al.* (2001b) for the methylene cyclohexane reaction (β -pinene, sabinene and methylene cyclohexane all have an exo-cyclic =CH₂ group). Interestingly, the sabinaketone yield also increases with increasing concentration of 2-butanol (2-butanol varied from none present (cyclohexane or *n*-octane then being present to scavenge OH radicals) to 6.6×10^{16} molecule cm⁻³, with the water vapor concentration being $\leq 3.4 \times 10^{16}$ molecule cm⁻³), suggesting that 2-butanol behaves like water vapor and reacts with the C₉-Criegee intermediate to form sabinaketone.

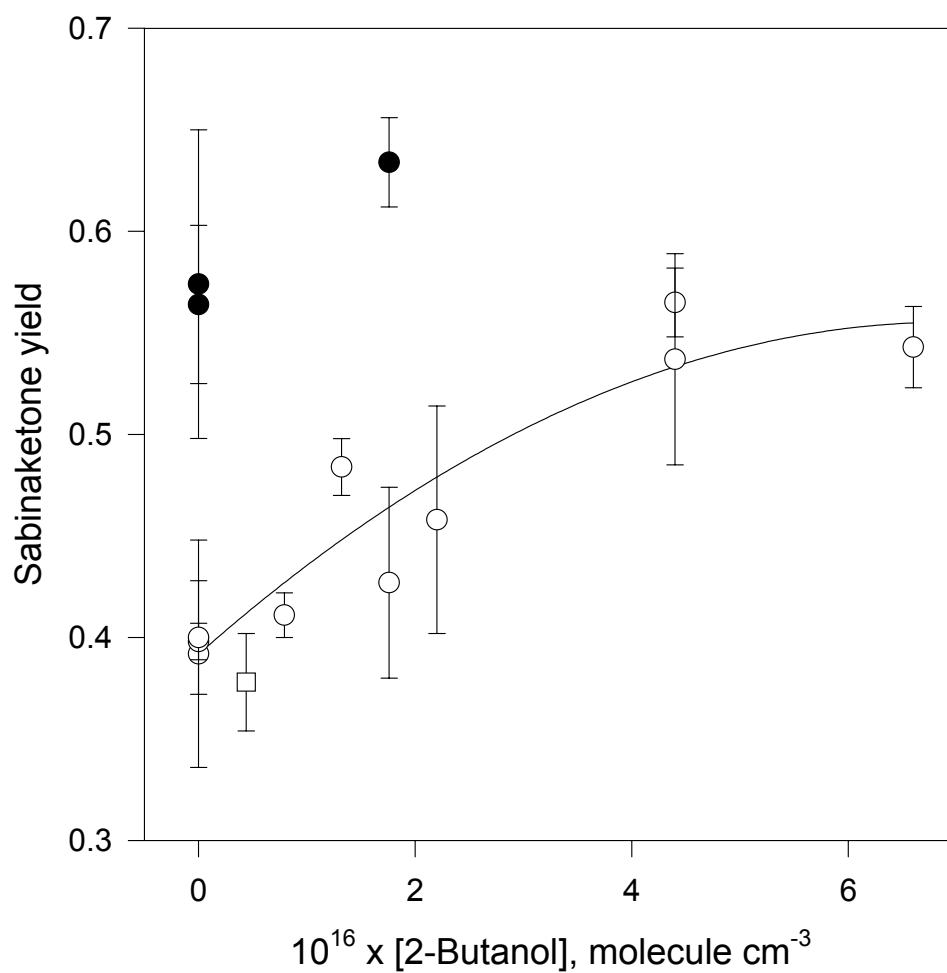


Figure 35. Plot of the sabinaketone yield from the reaction of O_3 with sabinene against the 2-butanol concentration at: \circ ~5% relative humidity; \bullet ~60% relative humidity.

As shown in Figure 36, the OH radical formation yield, as derived from 2-butanone formation, was independent of water vapor concentration ($\leq 3.4 \times 10^{16}$ molecule cm^{-3} to 4.2×10^{17} molecule cm^{-3}), but increased from ~ 0.28 to ~ 0.40 as the 2-butanol concentration increased.

As noted above, the measured OH radical formation yields at the lowest added 2-butanol concentration is slightly low because of incomplete scavenging of OH radicals, and the real increase in OH radical yield with increasing 2-butanol is from 0.30 to 0.40. This observed increase in OH yield (derived from the 2-butanone formation yields) may be due to artifact formation of 2-butanone from 2-butanol in the presence of O_3 , either from a slow O_3 reaction with 2-butanol (homo- or heterogeneous) or from reactive impurities in the 2-butanol, both becoming more important at higher 2-butanol concentrations.

α -Pinene. For the α -pinene reaction, pinonaldehyde can only arise from reaction of the Criegee intermediate(s) with water vapor [reaction (6) followed by (7b)]. The measured pinonaldehyde yield was independent of both water vapor ($\leq 3.4 \times 10^{16}$ molecule cm^{-3} to 4.0×10^{17} molecule cm^{-3}) and 2-butanol (0 - 1.32×10^{17} molecule cm^{-3}) concentration (Figure 37), with an average value of 0.15 ± 0.02 , where the indicated errors are two least-squares standard deviations combined with an estimated uncertainty in the GC-FID response factor for pinonaldehyde relative to that for α -pinene of $\pm 10\%$. These observations are in agreement with our previous data showing no dependence on the pinonaldehyde yield with water vapor nor on changing from cyclohexane to 2-butanol as the OH radical scavenger (Baker *et al.*, 2002).

The OH formation yield, as derived from the 2-butanone formation, was independent of water vapor concentration (relative humidity 5%-59%) but increased with 2-butanol concentration (Figure 38), analogous to the OH yield derived from 2-butanone formation in the sabinene reaction (see above).

7-Tetradecene. Heptanal is a primary carbonyl as well as potentially being formed from the Criegee intermediate via reaction (6) followed by (7b). The heptanal yield was independent of 2-butanol concentration, but increased slightly with increasing water vapor concentration (relative humidity 5%-60%), as shown in Figure 39. The OH radical yield, as derived from the 2-butanone formation yield, was either invariant of 2-butanol or decreased slightly with increasing 2-butanol concentration (from 25% to 20% for 2-butanol concentrations of 4.3×10^{15} molecule cm^{-3} to 6.6×10^{16} molecule cm^{-3}), and appeared to decrease slightly (from 25% to 20%) as the relative humidity increased from 5% to 60% (Figure 40). Note that 7-tetradecene is expected to be significantly more reactive towards O_3 than are sabinene and α -pinene, and hence 2-butanol would be exposed to much less ozone in this reaction system than in the sabinene and α -pinene reactions, with less artifact formation of 2-butanone (as observed).

Our data provide no convincing evidence that reaction (5) is in competition with reactions (6) through (9), except possibly in the 7-tetradecene reaction. The invariance of the pinonaldehyde yield from α -pinene with the 2-butanol concentration shows that reactions (8) and (9) do not compete with reaction (6) followed by (7b) [the only reaction leading to pinonaldehyde] unless reaction (9) also leads to pinonaldehyde. The minor effect of water vapor and, for the 7-tetradecene reaction, of 2-butanol on the OH radical yields suggests that formation of OH radicals from the activated Criegee intermediates [reaction (3)] dominates.

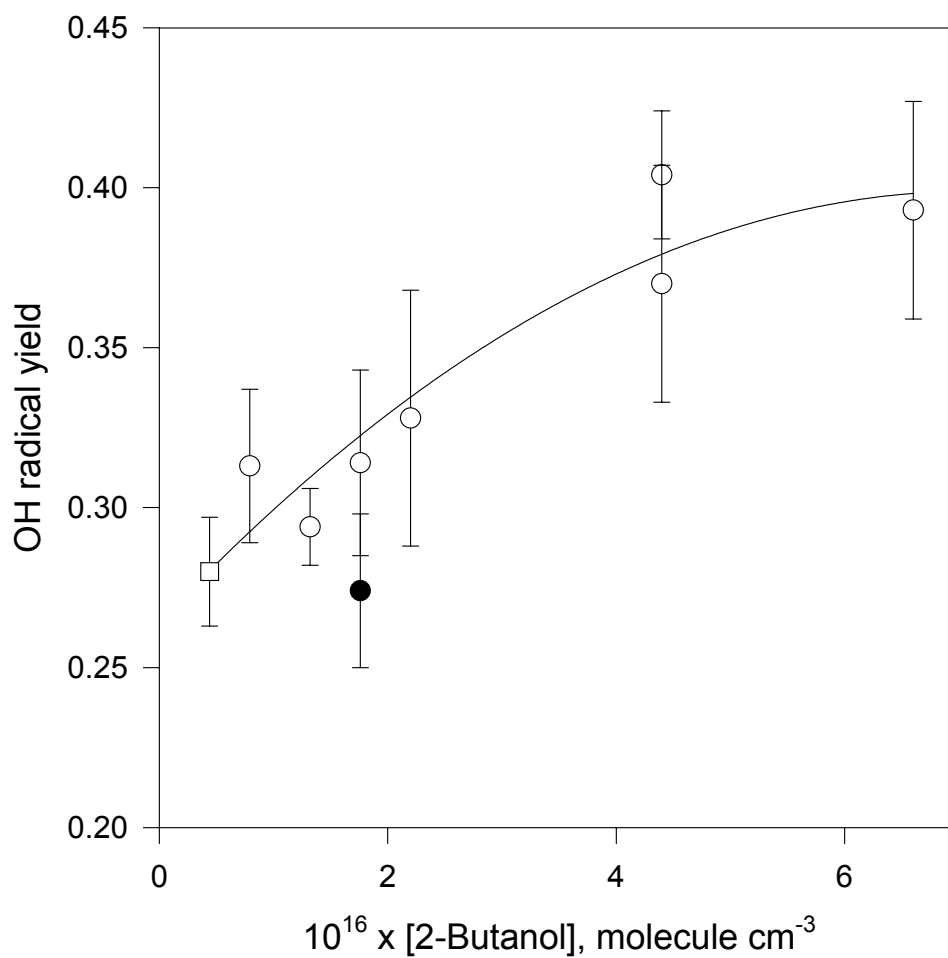


Figure 36. Plot of the OH radical formation yield from the reaction of O_3 with sabinene, as derived from the 2-butanone yield (see text), against the 2-butanol concentration at: \circ ~5% relative humidity; \bullet ~60% relative humidity.

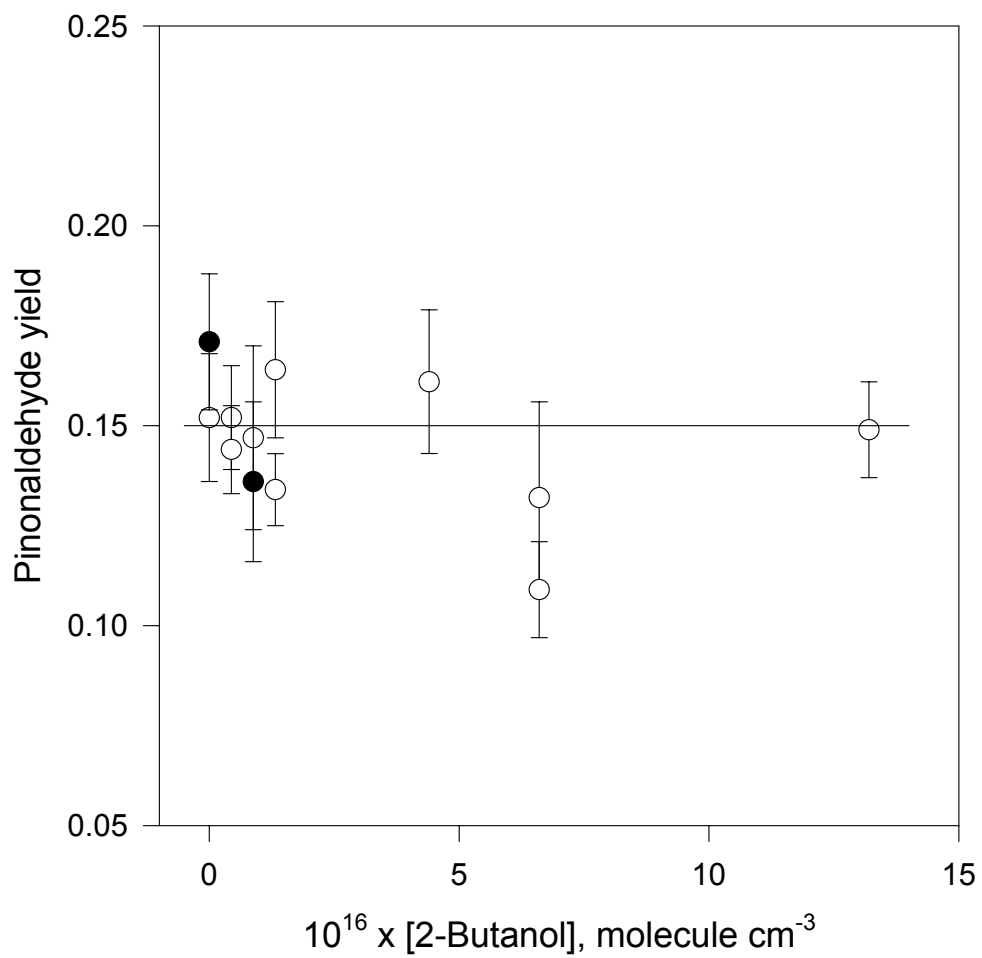


Figure 37. Plot of the pinonaldehyde yield from the reaction of O_3 with α -pinene against the 2-butanol concentration at: \circ ~5% relative humidity; \bullet ~60% relative humidity.

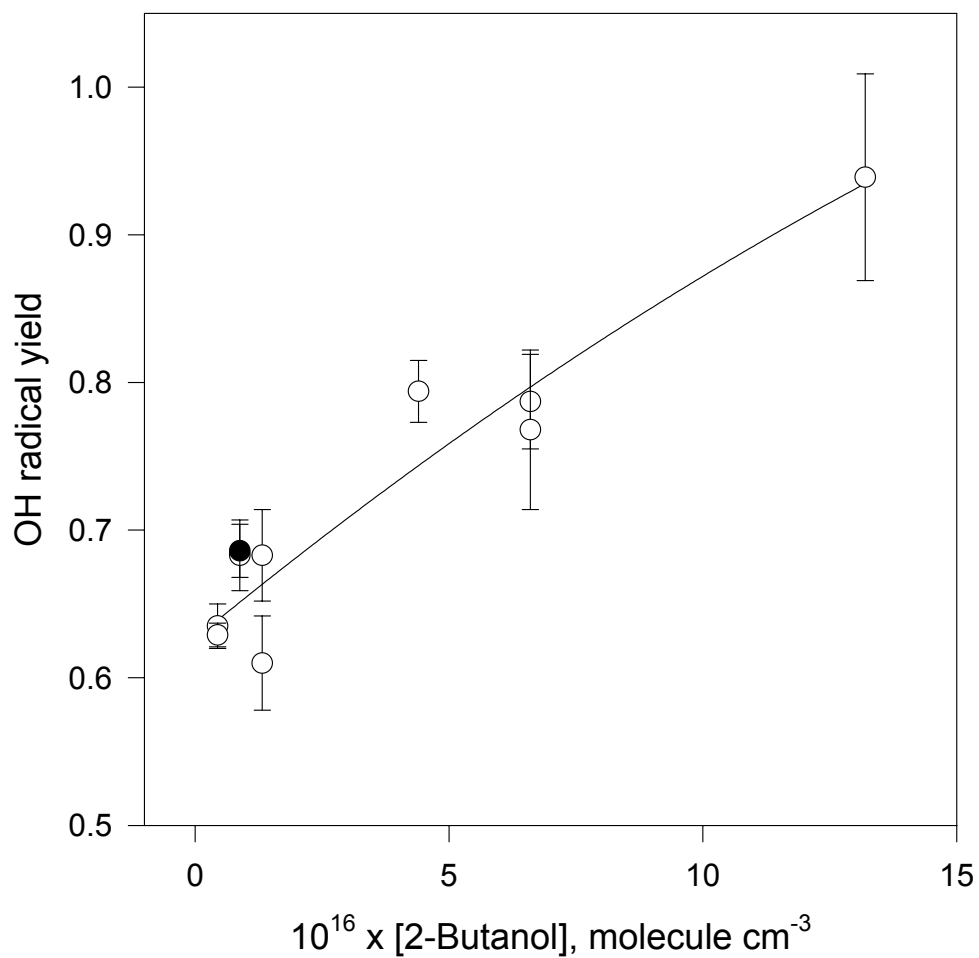


Figure 38. Plot of the OH radical formation yield from the reaction of O_3 with α -pinene, as derived from the 2-butanone yield (see text), against the 2-butanol concentration at: o ~5% relative humidity; • ~60% relative humidity.

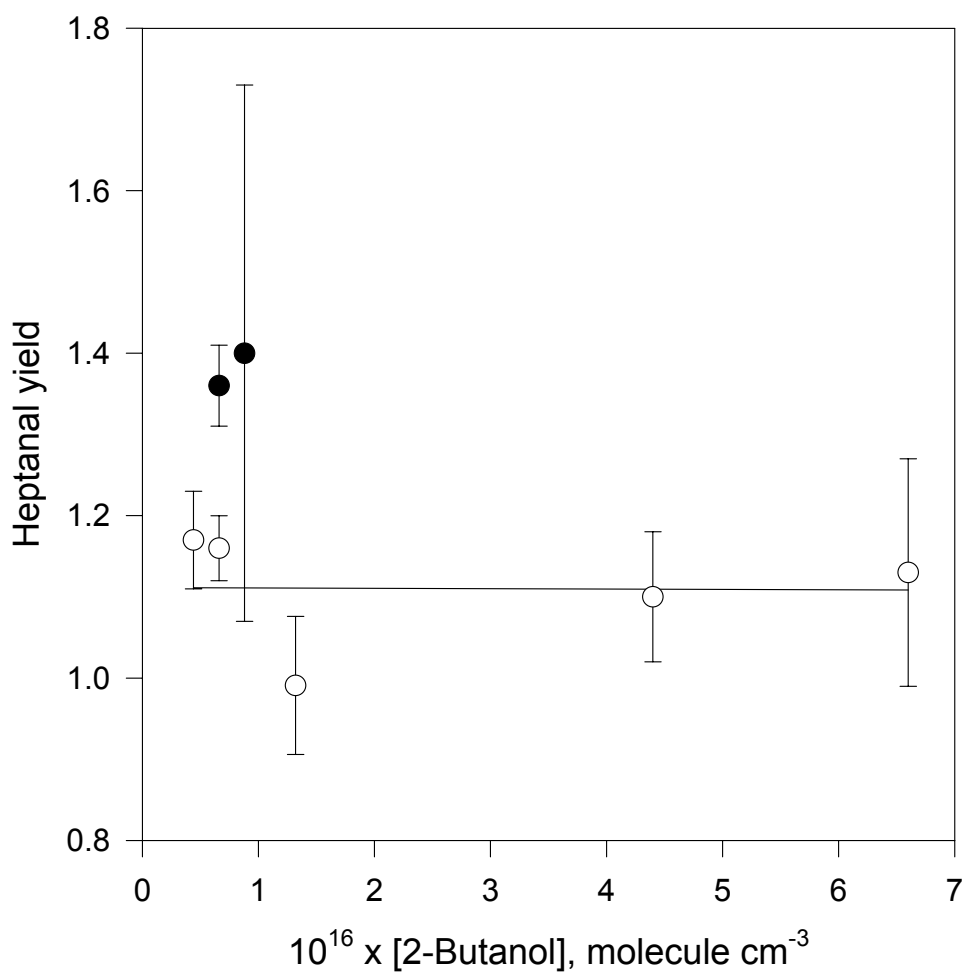


Figure 39. Plot of the heptanal yield from the reaction of O_3 with 7-tetradecene against the 2-butanol concentration at: \circ ~5% relative humidity; \bullet ~60% relative humidity.

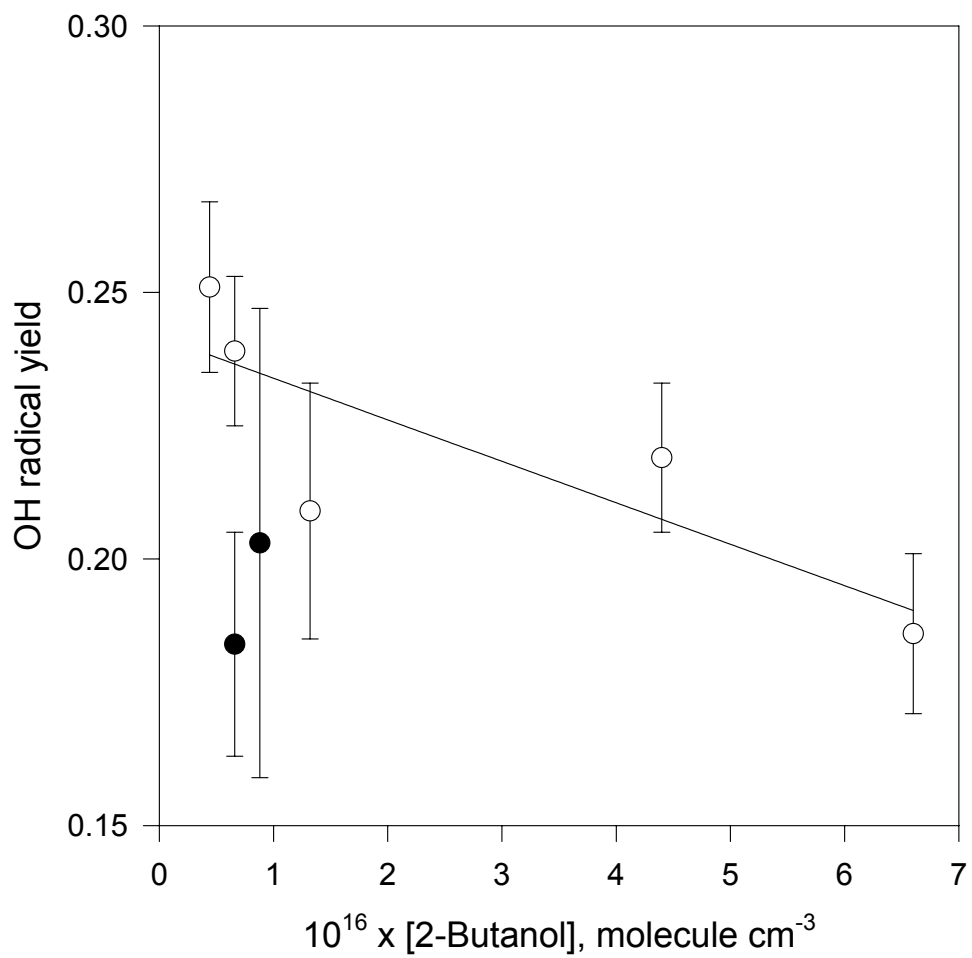


Figure 40. Plot of the OH radical formation yield from the reaction of O_3 with 7-tetradecene, as derived from the 2-butanone yield (see text), against the 2-butanol concentration at: \circ ~5% relative humidity; \bullet ~60% relative humidity.

4. STUDIES OF PAH CHEMISTRY

4.1. Methyl- and Dimethyl-/Ethyl- Nitronaphthalenes Measured in Ambient Air In Southern California

4.1.1. Introduction

Methylnaphthalenes (MNs), dimethylnaphthalenes (DMNs) and ethylnaphthalenes (ENs) are semi-volatile polycyclic aromatic hydrocarbons (PAHs) emitted into the atmosphere from a variety of incomplete combustion sources, including diesel engines (Williams *et al.*, 1986; Nelson, 1989; Zielinska *et al.*, 1996; Marr *et al.*, 1999). Unburned diesel fuel PAHs are likely to contribute significantly to the alkylnaphthalenes observed in urban areas (Williams *et al.*, 1986; Tancell *et al.*, 1995). The MNs, ENs and 9 of the 10 isomers of DMNs have been measured in ambient air [1,8-DMN is not present in ambient air (Phouongphouang and Arey, 2002; 2003a) nor in diesel fuel (Bundt *et al.*, 1991)]. Table 11 gives the ambient concentrations of the volatile PAHs measured in this study and shows for comparison, an analysis of a diesel fuel sample. In both the ambient morning and diesel fuel samples, 2MN is about twice 1MN and the ethylnaphthalenes are about 20% of the DMNs. The relative abundances of the individual DMNs in the ambient samples also closely match that of the diesel fuel. At ambient temperatures, these alkylnaphthalenes exist primarily in the gas-phase and their major atmospheric loss process is by daytime gas-phase reaction with the hydroxyl (OH) radical (Atkinson, 2000). Previous studies reported atmospheric lifetimes of the alkylnaphthalenes due to the gas-phase reactions with the OH radical of about 2 h for the DMNs and 3-4 h for the MNs and ENs (Phouongphouang and Arey, 2002). The products of PAH atmospheric reactions include mutagenic nitrated derivatives (Arey *et al.*, 1992; Sasaki *et al.*, 1995; Gupta *et al.*, 1996; Ciccio *et al.*, 1996; Arey, 1998; Cecinato *et al.*, 2001; Feilberg *et al.*, 2002). All 14 isomers of methylnitronaphthalenes (MNNs) have been reported in ambient air samples (Arey and Zielinska, 1989; Zielinska *et al.*, 1989; Gupta *et al.*, 1996), but dimethylnitronaphthalenes (DMNNs) and ethylnitronaphthalenes (ENNs) have not previously been reported.

We report here on environmental chamber reactions simulating ambient photooxidation of volatilized diesel fuel PAHs and demonstrate for the first time that DMNNs and/or ENNs identified as formed from the OH radical-initiated reactions of alkyl-PAHs present in diesel fuel are also present in ambient air.

4.1.2. Experimental

PAHs were separated from whole diesel fuel using a Silica open column and typically 200 mg were volatilized into the 7000 L all-Teflon environmental chamber. Simulated atmospheric reactions of the diesel fuel PAHs with OH radicals were carried out as described previously using photolysis of CH₃ONO as the OH radical source (Arey *et al.*, 1992; Sasaki *et al.*, 1995). After reaction, the chamber contents were sampled onto polyurethane foam plugs (PUFs), followed by Soxhlet extraction in dichloromethane and fractionation by high performance liquid chromatography (HPLC) using a Silica column (Arey *et al.*, 1992; Sasaki *et al.*, 1995). The HPLC fraction containing the nitro-PAHs was analyzed by gas chromatography/mass spectrometry (GC/MS) on a DB-5MS column with negative ion methane chemical ionization and selected ion monitoring (NCI-SIM).

Ambient measurements were carried out in Southern California, U.S.A. during the summer of 2002 in Los Angeles (an urban site) and Riverside (a downwind receptor site). Four time intervals per day (07:00-10:30, 11:00-14:30, 15:00-18:30 and 19:00-6:30) were sampled for

Table 11. Volatile PAHs measured on Tenax-TA solid adsorbent tubes in Los Angeles during morning sampling (7:00-10:30) and midday sampling (11:00-14:30), August 12-16, 2002. Shown for comparison is an analysis of a diesel fuel sample (data from Rhead and Hardy, 2003)

PAH	Los Angeles Aug. 12-16, 2002 ave. 7:00-10:30 (ng/m ³)	Los Angeles Aug. 12-16, 2002 ave. 11:00-14:30 (ng/m ³)	A2 Diesel Fuel (ppm) ± std (Rhead and Hardy, 2003)
Naphthalene	389	152	1292 ± 13
2-Methylnaphthalene	166	48	4035 ± 52
1-Methylnaphthalene	69	17	2749 ± 34
Ratio 2MN/1MN	2.4	2.8	1.5
2-Ethylnaphthalene	4.8	1.5	
1-Ethylnaphthalene	1.3	0.5	
Σ 1 + 2-Ethylnaphthalene	6.1	2.0	1668 ± 31
Σ ENs/ Σ DMNs	0.2	0.4	0.15
2,6 + 2,7-DMNs	8.9 (32%)^a	1.8 (32%)^a	3356 ± 47 (30%)^a
1,3 + 1,7-DMNs	9.3 (33%) ^a	1.6 (29%) ^a	
1,6-Dimethylnaphthalene	5.0 (18%) ^a	1.0 (18%) ^a	
Σ 1,3+1,6+1,7 – DMNs	14.3 (51%)^a	2.6 (46%)^a	3631 ± 34 (32%)^a
1,4-Dimethylnaphthalene	0.9 (3%) ^a	0.3 (5%) ^a	
1,5 + 2,3-DMNs	2.2 (8%) ^a	0.5 (9%) ^a	
Σ 1,4+1,5+2,3 – DMNs	3.1 (11%)^a	0.8 (14%)^a	2385 ± 29 (21%)^a
1,2-Dimethylnaphthalene	1.6 (6%)^a	0.4 (7%)^a	1874 ± 23 (17%)^a
Σ Dimethylnaphthalenes	27.9	5.6	11,246

^aPercent of total dimethylnaphthalenes.

one 5-day period each in Los Angeles (12-16 August 2002) and Riverside (26-30 August 2002). Samples of volatile PAHs were collected onto replicate Tenax-TA solid adsorbent cartridges at 200 cm³ min⁻¹ for the daytime samples and 100 cm³ min⁻¹ for the nighttime samples. Semi-volatile PAHs and nitro-PAHs were collected onto PUFs at a flow rate of ~0.6 m³ min⁻¹. Following spiking with naphthalene-d₈ and 1-methylnaphthalene-d₁₀ to serve as internal standards, the Tenax samples were thermally desorbed onto a DB-1701 column and analyzed by electron impact (EI) GC/MS-SIM (Phousongphouang and Arey, 2002). Each of the 8 Tenax samples per day were analyzed individually, while the PUFs were composited according to time interval prior to analysis. The PUFs were spiked with 1-nitronaphthalene-d₇ as an internal standard and then extracted, fractionated by HPLC, and analyzed by GC/MS-NCI as described above for the chamber reactions.

The instrumentation used was: Hewlett-Packard (HP) 1050 HPLC, HP-5971A-MSD for EI GC/MS and an Agilent 5973-MSD for GC/MS-NCI.

4.1.3. Results and Discussion

The top panels of Figures 41 and 42 show mass chromatograms for the MNNs (m/z 187) and DMNNs and/or ENNs (m/z 201), respectively, from the OH radical-initiated reaction of the volatilized diesel fuel PAHs. The pattern of MNNs formed (see Figure 41 for identification of the 11 individual peaks observed) matches what has previously been observed from the OH radical-initiated reactions of 1-MN and 2-MN [with initial 2-MN concentrations twice that of 1-MN, reflecting typical ambient air measurements (Gupta *et al.*, 1996; Arey, 1998)]. The identity of the diesel fuel product peaks in Figure 42 (top) as DMNNs and/or ENNs is based upon the selectivity provided by HPLC fractionation and GC/MS-NCI analysis, and was further confirmed from additional chamber reactions of volatilized diesel fuel PAHs with the nitrate radical in which full EI mass spectra showing abundant molecular ions and characteristic fragmentation patterns (Arey and Zielinska, 1989) were obtained (Reisen *et al.*, in preparation).

Similar to the diesel fuel PAH reactions, the ambient samples (see middle and bottom mass chromatograms on figures) also show 11 MNN peaks and about 30 peaks in the m/z 201 mass chromatograms (from a possible 56 isomers of DMNNs and ENNs). The alkylnitronaphthalenes observed in these ambient samples can be rationalized based on the gas-phase chemistry of the alkylnaphthalenes emitted from vehicles at this heavily traffic impacted site.

Table 11 gives the averaged naphthalene and alkylnaphthalenes concentrations for the two sampling intervals shown in Figures 41 and 42. The site in Los Angeles was near the intersection of the 10 and 110 freeways and it is likely that the PAHs measured are almost entirely the result of vehicle emissions. The relative abundances of the alkylnaphthalenes found in the ambient samples were similar to the diesel fuel PAHs with 2-MN > 1-MN, and with 1,6-, 1,7-, 2,6- and 2,7-DMNs among the most abundant DMN isomers (see Table 11). Thus the patterns of the nitro-alkyl-PAHs formed from the chamber reaction (top mass chromatograms in figures) should be similar to those of the ambient samples (lower mass chromatograms) if the major source of the nitro-alkyl-PAHs is gas-phase OH radical-initiated reactions of diesel-derived alkyl-PAHs. Data from Table 11 can be used to verify that, as anticipated, ambient OH radical reactions of the gas-phase PAHs occurred in Los Angeles. While the decrease in the PAH concentrations during the 11-14:30 samples relative to the early morning samples will reflect dilution from an increasing mixing height, it will also reflect atmospheric reactions during this period of highest OH radical concentration (George *et al.*, 1999). Indeed the relative decreases measured during the 11-14:30 samples generally follow the OH radical rate constants of the PAHs, being lowest for naphthalene (~60% decrease) and greatest for the DMNs (~80% decrease), the most reactive of the alkyl-PAHs measured (Phouongphouang and Arey, 2002). The increased ratio of the nitro-PAHs to the parent PAHs during the 11-14:30 samples is also consistent with the nitro-PAHs being formed by OH radical-initiated reactions, with the percent formation of the DMNNs + ENNs reaching over 1% in the midday samples (see Table 12). The samples collected at the downwind Riverside site had consistently higher nitro-PAH/PAH ratios reflecting formation of nitro-PAHs during transport (Reisen *et al.*, in preparation).

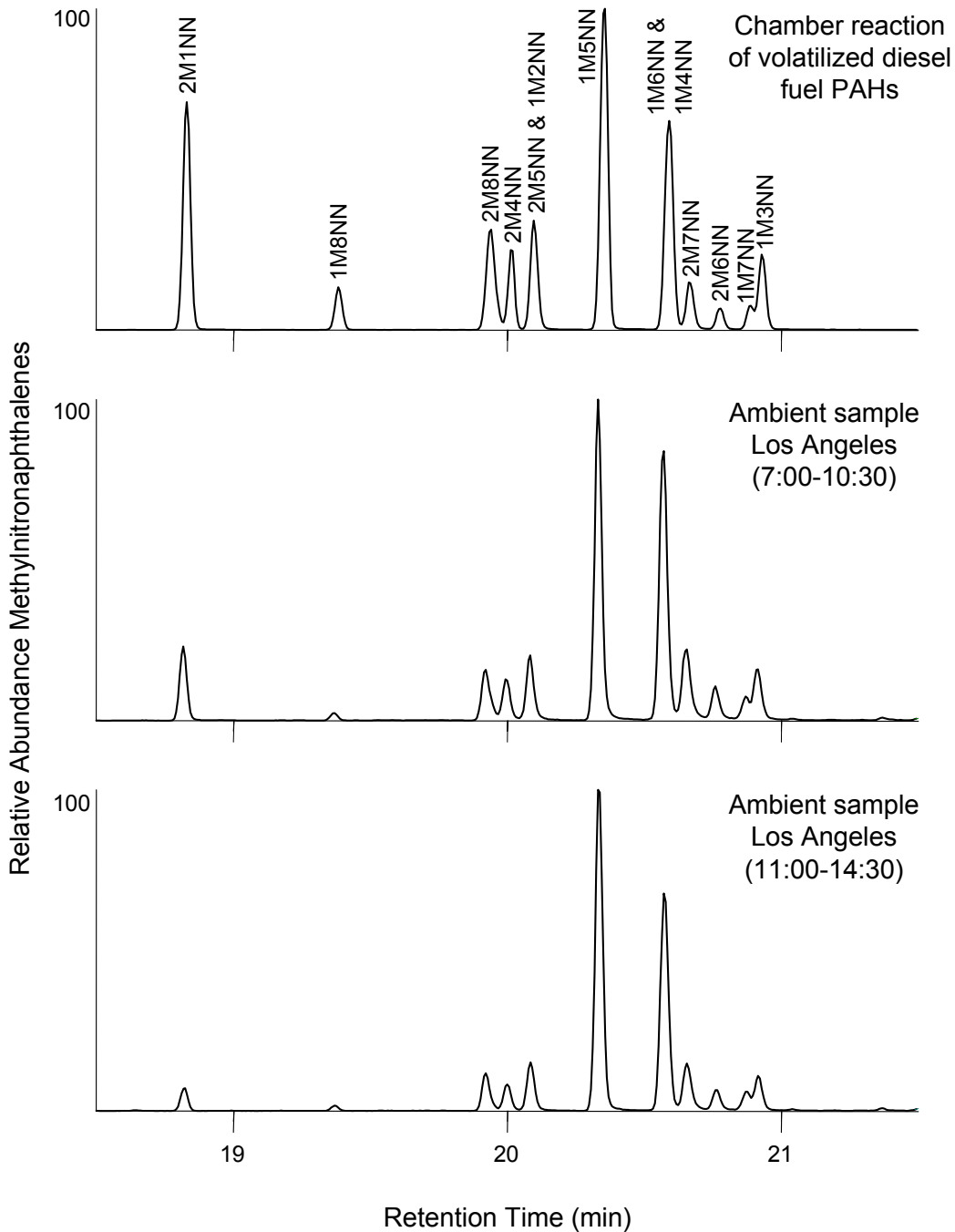


Figure 41. Mass chromatograms for the methylnitronaphthalenes (m/z 187) observed by GC/MS NCI-SIM analysis of: (top) Sample from the OH radical-initiated chamber reaction of the PAHs present in volatilized diesel fuel; (center) Composite of early morning (7-10:30) ambient air samples collected in Los Angeles during August 12-16, 2002; (bottom) Composite of mid-day (11-14:30) ambient air samples collected in Los Angeles during August 12-16, 2002.

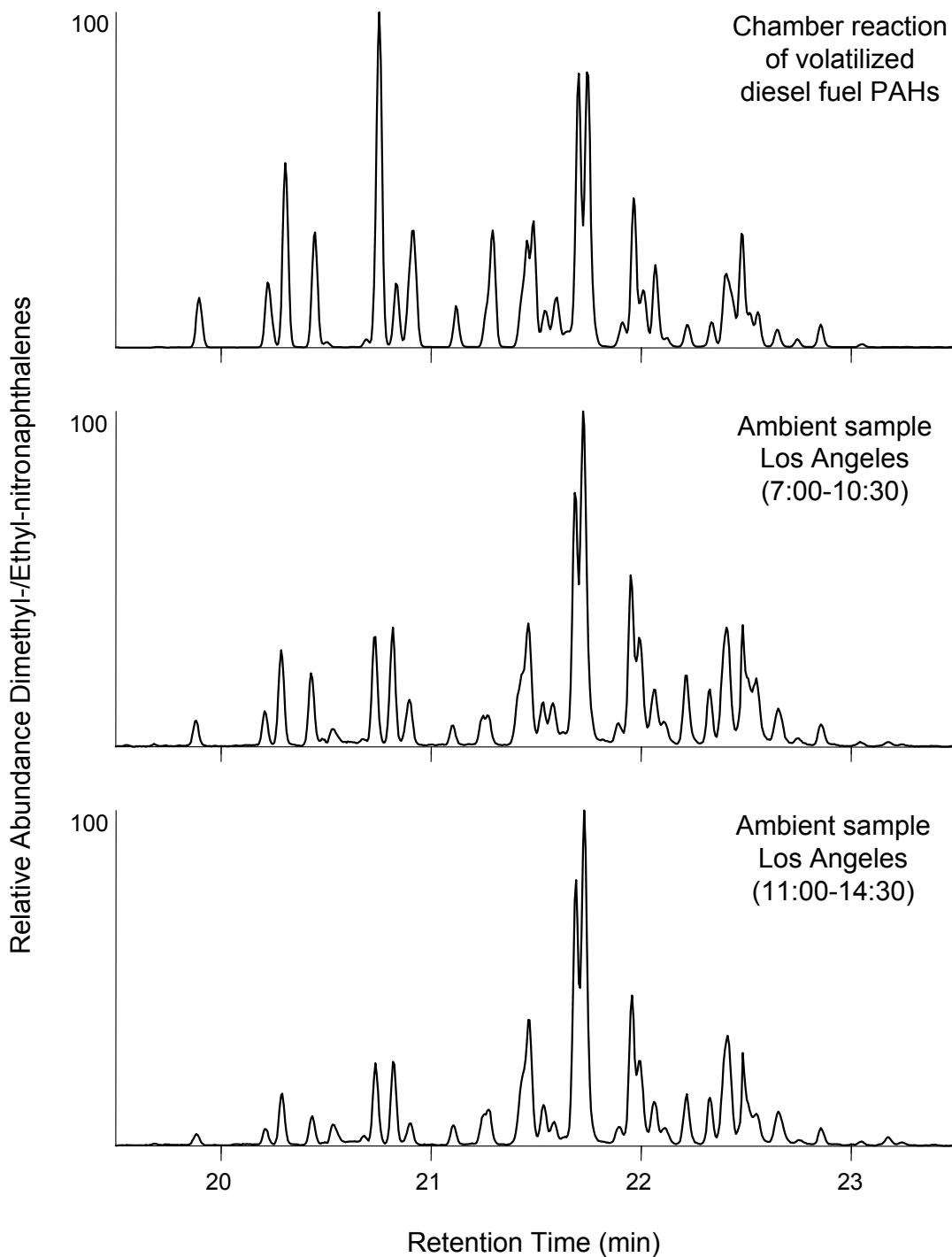


Figure 42. Mass chromatograms for the dimethylnitronaphthalenes and/or ethylnitronaphthalenes (m/z 201) observed by GC/MS NCI-SIM analysis of: (top) Sample from the OH radical-initiated chamber reaction of the PAHs present in volatilized diesel fuel; (center) Composite of early morning (7-10:30) ambient air samples collected in Los Angeles during August 12-16, 2002; (bottom) Composite of mid-day (11-14:30) ambient air samples collected in Los Angeles during August 12-16, 2002.

Table 12. Percent of Nitrated Parent PAH for Samples Collected August 12-16, 2002 in Los Angeles, California, U.S.A.

	Sampling times	
	07:00-10:30	11:00-14:30
% nitrated		
%NNs ^a	0.13	0.32
%MNNs ^b	0.10	0.36
%(DMNNs + ENNs) ^c	0.38	1.29

^a $\Sigma(1\text{-NN} + 2\text{-NN})/\text{Naphthalene}$.

^b $\Sigma(14 \text{ isomers of } x\text{M}_y\text{NN})/\Sigma(1\text{-MN} + 2\text{-MN})$, assumes NCI response of all $x\text{M}_y\text{NN}$ isomers is similar to that of 2M1NN.

^c $\Sigma(\text{isomers of DMNNs and/or ENNs})/\Sigma(9 \text{ isomers of DMNs} + 1\text{-EN} + 2\text{-EN})$, assumes NCI response of all nitro-isomers of 201 daltons is similar to that of 2M1NN.

Looking in detail at the specific MNN isomer distributions, it is clear that 2M1NN and 1M8NN (Figure 41) are significantly lower in the ambient samples than seen from the chamber reactions. The photolysis rates of several MNNs have recently been measured and the photolysis lifetimes of 2M1NN and 1M8NN estimated at 10 and 8 min, respectively, in comparison with 22-133 min for the other MNNs (Phouongphouang and Arey, 2003b). Because of the short reaction times, photolysis of the MNNs during the chamber reactions in which they were produced was negligible (Phouongphouang and Arey, 2002; 2003b). Thus the differences in the profile of the MNN chamber reaction products and the MNNs in the ambient samples can be attributed to ambient photolysis, which is their major atmospheric loss process (Phouongphouang and Arey, 2003b).

For the molecular weight 201 species, the obvious difference between the chamber reaction products and the ambient samples is the lower abundances of peaks in the early portion of the ambient sample chromatograms (see Figure 42). For the MNNs and nitronaphthalenes, photolysis rates showed a distinct trend with ortho- (2M1NN) and peri- (1M8NN) substituted MNNs having the highest rates and with MNNs with NO₂ on the α -carbon of the naphthalene structure being more reactive than those with the NO₂ group on the β -carbon (Feilberg *et al.*, 1999; Phouongphouang and Arey, 2003b). As may be seen from the MNN chromatogram in Figure 41, elution is earliest for ortho- and peri- substituted isomers and latest for isomers with the NO₂ on the β -carbon (e.g., 1M3NN and 1M7NN). Therefore, it is likely that ambient photolysis of DMNNs and/or ENNs also accounts for the differences between the chamber 201 m/z mass chromatograms and those of the ambient samples.

To our knowledge, this is the first time that DMNNs and ENNs have been reported in ambient air, and we attribute their presence in Los Angeles air samples mainly to OH radical-initiated formation from the parent alkyl-PAHs. Nitrate radical reactions may also produce nitro-PAHs (Ciccioli *et al.*, 1996; Arey, 1998), but at the Los Angeles sampling site the rapid reaction of NO₃ radical with NO emissions from vehicles (as well as daytime NO₃ radical photolysis) will preclude NO₃ radical reactions.

NNs and MNNs are bacterial and human cell mutagens (Gupta *et al.*, 1996; Sasaki *et al.*, 1997; 1999), and it is expected that DMNNs and ENNs will also be mutagens. It should be noted that although the DMNs/ENs concentrations are lower than those of naphthalene and the MNs (see Table 12), the relative abundances of the nitro-derivatives were more similar. During this study in Los Angeles, nitronaphthalene concentrations ranged from ~200-500 pg/m³, methylnitronaphthalene concentrations from ~100-250 pg/m³ and dimethyl- and ethyl-nitronaphthalene concentrations from ~50-150 pg/m³. Therefore, further work is warranted to identify the specific DMNN/ENN isomers present in ambient air, their concentrations in other urban areas, their gas/particle partitioning and their potential health effects.

5. STUDIES OF THE CHEMISTRY OF OXYGENATED VOCs

5.1. Kinetics and Products of the Reactions of OH Radicals with 2-Methyl-2-pentanol and 4-Methyl-2-pentanol

5.1.1. Introduction

Volatile organic compounds (VOCs) emitted into the atmosphere can undergo photolysis and reaction with OH radicals, NO₃ radicals, and O₃ (Atkinson, 2000), with the OH radical reaction being an important, and often dominant, atmospheric loss process (Atkinson, 2000). For saturated aliphatic compounds such as alkanes, alcohols, and ethers, these OH radical-initiated reactions proceed by initial H-atom abstraction from the various C-H bonds and, to a much lesser extent, from the O-H bond(s) in alcohols (Atkinson, 2000). The subsequent reactions involve the intermediary of organic peroxy (RO₂[•]) and alkoxy (RO[•]) radicals, with alkoxy radicals being the key intermediate species in the presence of sufficient NO that peroxy radicals react dominantly with NO rather than with HO₂ or organic peroxy radicals (Atkinson, 2000). Under atmospheric conditions, alkoxy radicals decompose, isomerize (through a six-membered transition state) and/or react with O₂ (Atkinson, 1997a,b; Aschmann and Atkinson, 1999). To date, there have been relatively few absolute rate measurements of the rate constants for the reactions of alkoxy radicals with O₂ (Hein *et al.*, 1998, 1999, 2000; Fittschen *et al.*, 1999; Deng *et al.*, 2000, 2001; IUPAC, 2003), or of alkoxy radical decomposition (Hein *et al.*, 1998, 2000; Blitz *et al.*, 1999; Devolder *et al.*, 1999; Caralp *et al.*, 1999; Fittschen *et al.*, 2000; IUPAC, 2003) or isomerization (Hein *et al.*, 1999). Additionally, these studies involve only ≤C₅ alkoxy radicals formed from alkanes, and several of the decomposition and isomerization rate constants are at 37.5 Torr total pressure (Hein *et al.*, 1998, 1999, 2000) and because of falloff effects may not be applicable to atmospheric conditions. Furthermore, the measured room temperature rate constants for the reactions of O₂ with 2-butoxy (Hein *et al.*, 1998; Deng *et al.*, 2000) and 3-pentoxy (Hein *et al.*, 2000; Deng *et al.*, 2001) each disagree by a factor of ~2. Therefore, at present the database concerning alkoxy radical reactions consists largely of relative rate measurements obtained from product studies (Atkinson, 1997a,b).

To obtain additional information concerning the reactions of alkoxy and substituted alkoxy radicals under atmospheric conditions, in this work we have investigated the OH radical-initiated reactions of 2-methyl-2-pentanol [(CH₃)₂C(OH)CH₂CH₂CH₃] and 4-methyl-2-pentanol [CH₃CH(OH)CH₂CH(CH₃)₂]. Specifically, we used a relative rate method to measure rate constants for the gas-phase reactions of 2-methyl-2-pentanol and 4-methyl-2-pentanol with OH radicals at 298 ± 2 K, and investigated the products formed from these reactions using gas chromatography with flame ionization detection (GC-FID), combined gas chromatography-mass spectrometry (GC-MS), and *in situ* atmospheric pressure ionization mass spectrometry (API-MS). These VOCs were chosen because many of the products predicted to be formed from the reactions of the intermediate alkoxy radicals are commercially available and can be readily analyzed by gas chromatography, therefore allowing the relative importance of the various alkoxy radical reactions and the partial rate constants for H-atom abstraction by the OH radical from the various CH₃, CH₂ and CH groups to be determined.

5.1.2. Experimental

Experiments were carried out in 7500 liter Teflon chambers, equipped with two parallel banks of blacklamps for irradiation, at 298 ± 2 K and 740 Torr total pressure of purified air at ~5% relative humidity. Each chamber is fitted with a Teflon-coated fan to ensure rapid mixing of reactants during their introduction into the chamber.

Kinetic Studies. Rate constants for the OH radical reactions were measured using a relative rate method in which the relative disappearance rates of the methylpentanols and a reference compound, whose OH radical reaction rate constant is reliably known, were measured in the presence of OH radicals. Providing that the methylpentanols and the reference compound reacted only with OH radicals, then,

$$\ln \left(\frac{[\text{pentanol}]_{t_0}}{[\text{pentanol}]_t} \right) = \frac{k_1}{k_2} \ln \left(\frac{[\text{reference compound}]_{t_0}}{[\text{reference compound}]_t} \right) \quad (I)$$

where $[\text{pentanol}]_{t_0}$ and $[\text{reference compound}]_{t_0}$ are the concentrations of the methylpentanol and reference compound, respectively, at time t_0 , $[\text{pentanol}]_t$ and $[\text{reference compound}]_t$ are the corresponding concentrations at time t , and k_1 and k_2 are the rate constants for reactions (1) and (2), respectively.



OH radicals were generated by the photolysis of methyl nitrite (CH_3ONO) in air at wavelengths >300 nm, and NO was added to the reactant mixtures to suppress the formation of O_3 and hence of NO_3 radicals. The initial reactant concentrations (in molecule cm^{-3} units) were: CH_3ONO , $\sim 2.4 \times 10^{14}$; NO, $\sim 2.4 \times 10^{14}$; 2-methyl-2-pentanol $(2.18\text{-}3.06) \times 10^{13}$ [or 4-methyl-2-pentanol, $(2.44\text{-}2.56) \times 10^{13}$], and *n*-octane (the reference compound), $\sim 2.4 \times 10^{13}$. Irradiations were carried out for 10-45 min (2-methyl-2-pentanol) and 7-24 min (4-methyl-2-pentanol), resulting in up to 45% and 59% reaction of the initially present 2-methyl-2-pentanol and 4-methyl-2-pentanol, respectively.

The concentrations of 2- and 4-methylpentanol and *n*-octane were measured during the experiments by gas chromatography with flame ionization detection (GC-FID). For the analysis of 2- and 4-methylpentanol, their reaction products (see below), and *n*-octane, 100 cm^3 volume gas samples were collected from the chamber onto Tenax-TA solid adsorbent, with subsequent thermal desorption at ~ 250 °C onto a 30 m DB-1701 megabore column held at -40 °C and then temperature programmed to 200 °C at 8 °C min^{-1} . Based on replicate analyses in the dark, the GC-FID measurement uncertainties for 2- and 4-methylpentanol and *n*-octane were $\leq 3\%$. GC-FID response factors for 2- and 4-methylpentanol and products were determined by introducing measured amounts of the chemicals into the 7500 liter chamber and conducting several replicate GC-FID analyses. On a relative basis, the measured GC-FID response factors agreed to within $\pm 13\%$ with those calculated using the Effective Carbon Number concept (Scanlon and Willis, 1985). NO and initial NO_2 concentrations were measured using a Thermo Environmental Instruments, Inc., Model 42 chemiluminescent NO- NO_x analyzer.

Product Studies. Products were identified and quantified from the reactions of the OH radical with 2- and 4-methylpentanol, both during the kinetic experiments (see above) and from additional irradiated CH_3ONO - NO - 2-methyl-2-pentanol (or 4-methyl-2-pentanol) - air

mixtures by GC-FID and GC-MS. The initial CH₃ONO and NO concentrations in the irradiated CH₃ONO - NO - methylpentanol - air mixtures and the GC-FID analysis procedures were similar to those employed in the kinetic experiments described above, and the initial 2-methyl-2-pentanol and 4-methyl-2-pentanol concentrations were in the range (2.30-2.36) x 10¹³ and (2.32-2.56) x 10¹³ molecule cm⁻³, respectively. To verify the product identities, gas samples were collected onto Tenax-TA solid adsorbent for GC-MS analyses, with subsequent thermal desorption onto a 30 m DB-1701 fused silica capillary column in a HP 5890 GC interfaced to a HP 5971 Mass Selective Detector operated in the scanning mode. Additionally, for one 2-methyl-2-pentanol reaction, products were sampled onto a 65 μm PDMS/DVB Solid Phase MicroExtraction (SPME) fiber coated with *O*-(2,3,4,5,6-pentafluorobenzyl)hydroxylamine hydrochloride (Koziel *et al.*, 2001) to analyze for carbonyl products as their oxime derivatives. The fiber was thermally desorbed onto a 30 m DB-1701 fused silica capillary column in a Varian 2000 GC-MS operated in the chemical ionization (CI) mode with isobutane as the CI gas to provide molecular weight information on any carbonyl products.

CH₃ONO - NO - methylpentanol - air irradiations were also carried out in a 7500 liter Teflon chamber interfaced to a PE SCIEX API III MS/MS direct air sampling, atmospheric pressure ionization tandem mass spectrometer (API-MS). The chamber contents were sampled through a 25 mm diameter x 75 cm length Pyrex tube at ~20 liter min⁻¹ directly into the API mass spectrometer source. The operation of the API-MS in the MS (scanning) and MS/MS [with collision activated dissociation (CAD)] modes has been described previously (Aschmann *et al.*, 1997; Arey *et al.*, 2001). Use of the MS/MS mode with CAD allows the “product ion” or “precursor ion” spectrum of a given ion peak observed in the MS scanning mode to be obtained (Aschmann *et al.*, 1997; Arey *et al.*, 2001).

Both positive and negative ion modes were used in this work. In the positive ion mode, protonated water hydrates (H₃O⁺ (H₂O)_n) generated by the corona discharge in the chamber diluent air were responsible for the protonation of analytes (Aschmann *et al.*, 1997; Arey *et al.*, 2001). In the negative ion mode, adducts were formed between molecules and the negative ions generated by the negative corona around the discharge needle. The superoxide ion (O₂⁻), its hydrates [O₂(H₂O)_n]⁻, and O₂ clusters [O₂(O₂)_n]⁻ are the major reagent negative ions in the chamber pure air. Other reagent ions, for example, NO₂⁻ and NO₃⁻, are formed through reactions between the primary reagent ions and neutral molecules such as NO₂. Ions are drawn by an electric potential from the ion source through the sampling orifice into the mass-analyzing first quadrupole or third quadrupole. In these experiments the API-MS instrument was operated under conditions that favored the formation of dimer ions in the ion source region (Aschmann *et al.*, 1997; Arey *et al.*, 2001). Neutral molecules and particles are prevented from entering the orifice by a flow of high-purity nitrogen (“curtain gas”), and as a result of the declustering action of the curtain gas on the hydrated ions, the ions that are mass analyzed are mainly protonated molecules ([M + H]⁺) and their protonated homo- and hetero-dimers (Aschmann *et al.*, 1997; Arey *et al.*, 2001) in the positive ion mode and mainly O₂⁻ or NO₂⁻ adducts in the negative ion mode (Arey *et al.*, 2001). Because NO₂ is generated from the oxidation of NO during the reactions (by HO₂ and organic peroxy radicals), it is preferable in the negative ion mode to measure the products as NO₂⁻ adducts (Arey *et al.*, 2001). Therefore, sufficient NO₂ was added to the chamber after the irradiations (with NO₂ concentrations ≥(2-3) x 10¹³ molecule cm⁻³) so that NO₂⁻ adducts of the hydroxycarbonyls and hydroxynitrates dominated over the corresponding O₂⁻ adducts (Arey *et al.*, 2001). The C₄-hydroxynitrate

CH₃CH(OH)CH(ONO₂)CH₃ was formed *in situ* from the OH radical-initiated reaction of *cis*-2-butene (Muthutamu *et al.*, 1993; O'Brien *et al.*, 1998) as an internal standard for the quantification of hydroxynitrates (Arey *et al.*, 2001).

Chemicals. The chemicals used, and their stated purities, were: acetone (HPLC grade), Fisher Scientific; *n*-octane (99+%), acetaldehyde (99.5+%), 4-methyl-2-pentanone (99+%), 2-methylpropanal (99+%), 2-methyl-2-pentanol (99%), 4-methyl-2-pentanol (99%), propanal (99+%), 2-pentanone (99+%) and 4-hydroxy-4-methyl-2-pentanone (99%), Aldrich Chemical Company; and *cis*-2-butene (≥95%) and NO (≥99.0%), Matheson Gas Products. Methyl nitrite was prepared as described previously (Taylor *et al.*, 1980) and stored at 77 K under vacuum.

5.1.3. Results

OH Radical Reaction Rate Constants

A series of CH₃ONO - NO - 2-methyl-2-pentanol (or 4-methyl-2-pentanol) - *n*-octane - air irradiations were carried out, and the data obtained are plotted in accordance with Equation (I) in Figure 43. Good straight-line plots are observed, and the rate constant ratios k_1/k_2 obtained from least-squares analyses of these data are given in Table 13. These rate constant ratios are placed on an absolute basis by use of a rate constant k_2 for reaction of the OH radical with *n*-octane at 298 K of $8.71 \times 10^{-12} \text{ cm}^3 \text{ molecule}^{-1} \text{ s}^{-1}$ (Atkinson, 1997a), and the resulting rate constants k_1 are also given in Table 13.

OH Radical Reaction Products; GC Analyses

GC-MS and GC-FID analyses of irradiated CH₃ONO - NO - 2-methyl-2-pentanol (or 4-methyl-2-pentanol) - air and CH₃ONO - NO - 2-methyl-2-pentanol (or 4-methyl-2-pentanol) - *n*-octane - air mixtures showed the formation of several products from each alcohol. By comparison of the GC retention times and mass spectra with those of authentic standards, the products identified from 2-methyl-2-pentanol were acetaldehyde, propanal, acetone, 2-pentanone and 4-hydroxy-4-methyl-2-pentanone, and from 4-methyl-2-pentanol were acetaldehyde, acetone, 2-methylpropanal and 4-methyl-2-pentanone. These products also react with the OH radical, and their measured concentrations were corrected for secondary reactions with the OH radical as discussed previously (Atkinson *et al.*, 1982), using the OH reaction rate constants measured here for the methylpentanols and those for the products recommended by Atkinson (1994) of (in units of $10^{-12} \text{ cm}^3 \text{ molecule}^{-1} \text{ s}^{-1}$): acetaldehyde, 15.8; propanal, 19.6; acetone, 0.219; 2-methylpropanal, 26.3; and 4-methyl-2-pentanone, 14.1. The multiplicative correction factors F to account for secondary reactions with the OH radical increase with increasing rate constant ratio $k(\text{OH} + \text{product})/k(\text{OH} + \text{methylpentanol})$ and with increasing extent of reaction (Atkinson *et al.*, 1982), and the calculated maximum values of F are given in Tables 14 and 15. In addition to removal by secondary reaction with OH radicals, certain of the observed products are formed from other products in these secondary reactions. Thus, reaction of OH radicals with propanal leads to the formation of acetaldehyde (Atkinson, 1994, 2000) in 100% yield in the presence of sufficient NO that the CH₃CH₂C(O)OO• radical reacts with NO rather than with NO₂; reaction of OH radicals with 2-pentanone leads to the formation of propanal (19%) and acetaldehyde (51%) (Atkinson *et al.*, 2000); reaction of OH radicals with 2-methylpropanal is assumed to lead to the formation of acetone in 100% yield (Atkinson, 1994); and reaction of OH radicals with 4-methyl-2-pentanone leads to the formation of acetone (78%) and 2-methylpropanal (7.1%) (Atkinson and Aschmann, 1995). Therefore, in addition to correcting for losses of products by reaction with the OH radicals (note that photolysis of the products was of

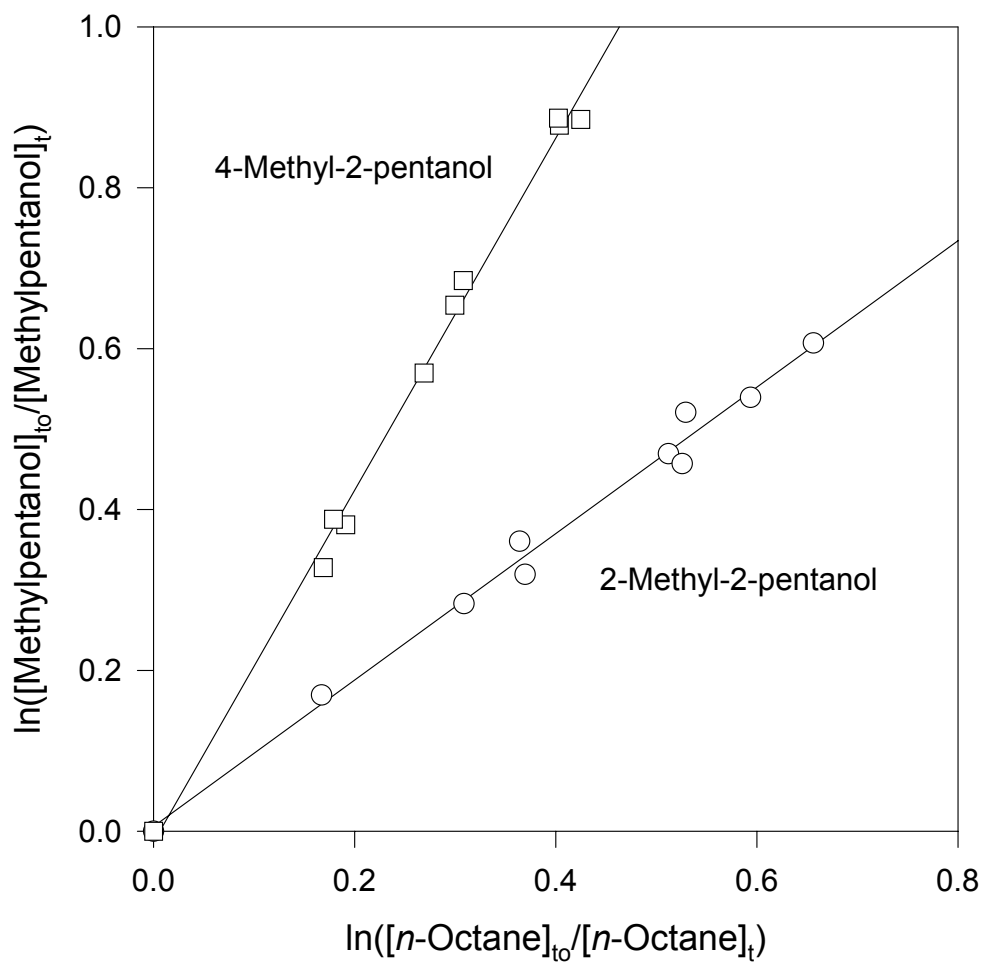


Figure 43. Plots of Equation (I) for the gas-phase reactions of OH radicals with 2-methyl-2-pentanol and 4-methyl-2-pentanol, with *n*-octane as the reference compound.

Table 13. Rate constant ratios k_1/k_2 and rate constants k_1 for the gas-phase reactions of OH radicals with 2-methyl-2-pentanol and 4-methyl-2-pentanol at 298 ± 2 K.

Alcohol	k_1/k_2^a	$10^{12} \times k_1$ (cm ³ molecule ⁻¹ s ⁻¹) ^b	
		This work	Estimated ^c
2-Methyl-2-pentanol	0.910 ± 0.066	7.93 ± 0.58	5.15
4-Methyl-2-pentanol	2.19 ± 0.11	19.1 ± 1.0	13.1

^a*n*-Octane used as the reference compound. The indicated errors are two least-squares standard deviations.

^bPlaced on an absolute basis by use of a rate constant of $k_2(n\text{-octane}) = 8.71 \times 10^{-12}$ cm³ molecule⁻¹ s⁻¹ at 298 K (Atkinson, 1997a). The indicated errors do not include the estimated overall uncertainty in the rate constant k_2 (estimated to be ~10%).

^cCalculated using the estimation method of Kwok and Atkinson (1995) as revised by Bethel *et al.* (2001).

no importance for the light intensity and irradiation periods used here), corrections were also made for secondary formation from other products (Tables 14 and 15). As evident from Tables 14 and 15, the corrected data for the formation of acetaldehyde from the 2-methyl-2-pentanol reaction and of acetone from the 4-methyl-2-pentanol reaction are subject to significant uncertainties.

Plots of the amounts of products formed, corrected for reaction with the OH radical and for secondary formation from other products (when applicable; see above), against the amounts of 2-methyl-2-pentanol and 4-methyl-2-pentanol reacted are shown in Figures 44 and 45, respectively. Reasonably good straight-line plots are observed, and the product formation yields obtained from least-squares analyses of these data are given in Tables 14 (2-methyl-2-pentanol) and 15 (4-methyl-2-pentanol).

The GC-MS analysis of the *O*-(2,3,4,5,6-pentafluoro)benzyl hydroxylamine coated SPME fiber exposed to the 2-methyl-2-pentanol reaction products showed a product peak whose mass spectrum corresponded to the oxime of a molecular weight 102 carbonyl product, which is attributed to the predicted 1,3-hydroxycarbonyl product $\text{CH}_3\text{C}(\text{O})\text{CH}_2\text{CH}(\text{OH})\text{CH}_3$ (see Figure 49). However, no peak attributable to this product was observed in GC-MS analyses of gas samples collected onto Tenax solid adsorbent (note that 1,3-hydroxyketones appear to be amenable to gas chromatography without prior derivatization), and hence this hydroxycarbonyl product could not be quantified.

OH Radical Reaction Products; API-MS Analyses

Analyses of irradiated $\text{CH}_3\text{ONO} - \text{NO} - 2\text{-methyl-2-pentanol}$ (or 4-methyl-2-pentanol) – air mixtures were also carried out with *in situ* API-MS analyses. In the positive ion mode, using protonated water clusters as the reagent ion, API-MS and API-MS/MS analyses of the 2-methyl-2-pentanol reaction showed the presence of products of molecular weight 58 (attributed to

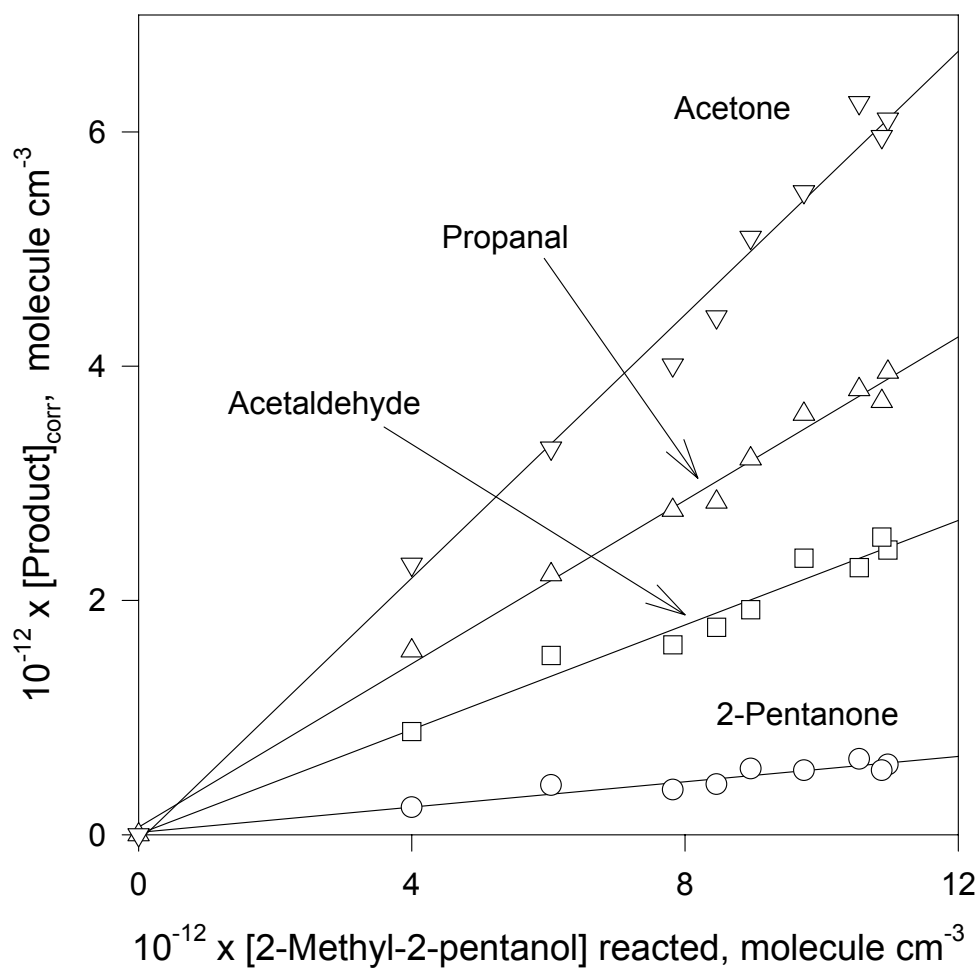


Figure 44. Plots of the amounts of acetaldehyde, propanal, acetone and 2-pentanone formed, corrected for reaction with OH radicals, against the amounts of 2-methyl-2-pentanol reacted with the OH radical.

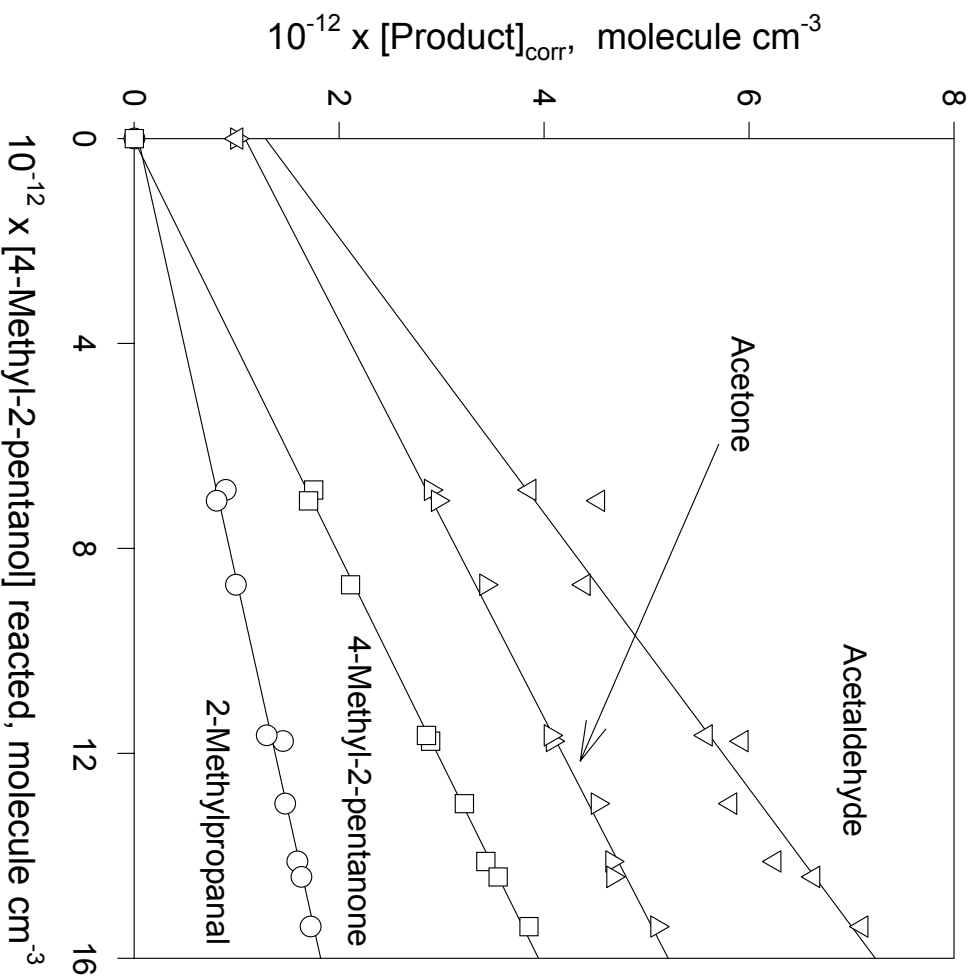


Figure 45. Plots of the amounts of acetaldehyde, acetone, 2-methylpropanal and 4-methyl-2-pentanone formed, corrected for reaction with OH radicals, against the amounts of 4-methyl-2-pentanol reacted with the OH radical. The data for acetaldehyde and acetone have been displaced vertically by 1.0×10^{12} molecule cm^{-3} for clarity.

Table 14. Formation yields of selected products from the gas-phase reactions of the OH radical with 2-methyl-2-pentanol at 296 ± 2 K

Product	Molar yield ^a	Maximum value of factor F to account for reaction with OH radicals ^b	Maximum correction for secondary formation from other products ^c
Acetaldehyde	0.22 ± 0.03	1.86	48%
Propanal	0.35 ± 0.04	2.12	<1%
Acetone	0.56 ± 0.06	1.01	d
2-Pentanone	0.054 ± 0.011	1.23	d
4-Hydroxy-2-pentanone	observed ^e		
4-Hydroxy-4-methyl-2-pentanone	<0.04	1.19	d
MW 163 hydroxynitrate	0.058^f		
MW 179 hydroxynitrate	0.023^f		

^aIndicated errors are two least-squares standard deviations combined with estimated overall uncertainties in the GC-FID response factors for 2-methyl-2-pentanol and products of $\pm 5\%$ each.

^bSee text.

^cSee text.

^dNo formation from other products.

^eFrom GC-MS analysis of *O*-(2,3,4,5,6-pentafluoro)benzyl hydroxylamine coated SPME fiber (see text).

^fEstimated to be uncertain to a factor of ~ 2 .

Table 15. Formation yields of selected products from the gas-phase reactions of the OH radical with 4-methyl-2-pentanol at 296 ± 2 K

Product	Molar yield ^a	Maximum value of factor F to account for reaction with OH radicals ^b	Maximum correction for secondary formation from other products ^c
Acetaldehyde	0.37 ± 0.06	1.55	d
Acetone	0.26 ± 0.03	1.01	33%
2-Methylpropanal	0.111 ± 0.012	2.02	5%
4-Methyl-2-pentanone	0.25 ± 0.02	1.49	d
MW 163 hydroxynitrate	0.055^e		
MW 179 hydroxynitrate	0.018^e		

^aIndicated errors are two least-squares standard deviations combined with estimated overall uncertainties in the GC-FID response factors for 4-methyl-2-pentanol and products of $\pm 5\%$ each.

^bSee text.

^cSee text.

^dNo formation from other products.

^eEstimated to be uncertain to a factor of ~ 2 .

propanal and/or acetone), 86 (attributed to 2-pentanone), 163 and 179 (note that the potential product $\text{CH}_3\text{C}(\text{O})\text{CH}_2\text{CH}(\text{OH})\text{CH}_3$ (see above and Discussion below) has the same molecular weight as 2-methyl-2-pentanol and therefore could not be observed by these analyses). API-MS/MS “product ion” spectra of the protonated hetero-dimers of 2-methyl-2-pentanol with the molecular weight 163 and 179 products (*i.e.*, of the ion peaks at 266 and 282 u, respectively) showed the presence of fragment ions at 46 u (NO_2^+). The products of molecular weight 163 and 179 are therefore identified as organic nitrates. Analogous analyses of the 4-methyl-2-pentanol reaction showed the presence of products of molecular weight 58 (attributed to acetone), 100 (attributed to 4-methyl-2-pentanone), 163 and 179, with the latter two products again being attributed to organic nitrates (as discussed below, to hydroxy- and dihydroxy-nitrates).

In the negative ion mode in the presence of $\sim 2.4 \times 10^{13}$ molecule cm^{-3} of NO_2 , API-MS analyses of both the 2-methyl-2-pentanol and 4-methyl-2-pentanol reactions showed the presence of NO_2^- adduct peaks at 209 and 225 u, as shown in Figure 46 for experiments which included *cis*-2-butene in the reactant mixture to form *in situ* the molecular weight 135 hydroxynitrate $\text{CH}_3\text{CH}(\text{OH})\text{CH}(\text{ONO}_2)\text{CH}_3$ (seen as the NO_2^- adduct at 181 u in Figure 46) as an internal standard (Muthuramu *et al.*, 1993; O’Brien *et al.*, 1998). As noted in the Experimental section, because NO_2 is present after reaction, and the hydroxynitrates will form O_2^- , NO_2^- (and smaller amounts of NO_3^-) adducts, additional NO_2 was added to minimize the O_2^- adducts, thus maximizing sensitivity and simplifying quantification.

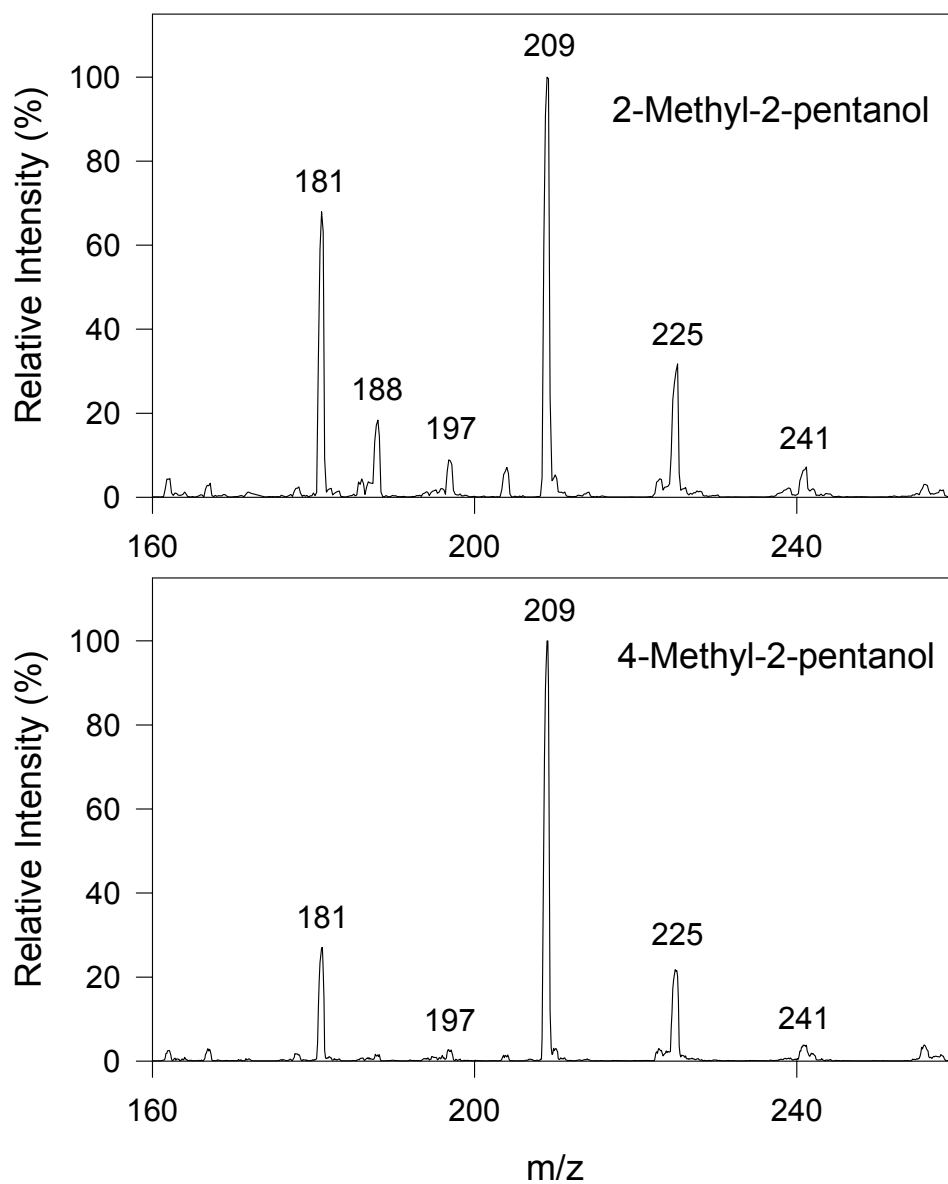


Figure 46. API-MS negative ion spectra of irradiated $\text{CH}_3\text{ONO} - \text{NO} - 2\text{-methyl-2-pentanol} - \text{air}$ and $\text{CH}_3\text{ONO} - \text{NO} - 4\text{-methyl-2-pentanol} - \text{air}$ mixtures, using NO_2^- ions as the reagent ions.

As seen from Figure 46, the major ion peaks observed are those at 181, 209 and 225 u, which are interpreted as the NO₂⁻ adducts of hydroxynitrates of molecular weight 135, 163 and 179. However, under our experimental conditions NO₃⁻ adducts of these products are also present (as evident from the 197 u ion peak for the molecular weight 135 hydroxynitrate CH₃CH(OH)CH(ONO₂)CH₃ seen in Figure 46). Unfortunately, the NO₃⁻ adduct of the molecular weight 163 product cannot be differentiated from the NO₂⁻ adduct of the molecular weight 179 product, both being at 225 u. Therefore, a reacted mixture was diluted with purified air until the dominant ion peaks were the O₂⁻ adducts, i.e., until the molecular weight 135 hydroxynitrate appeared exclusively at 167 u. Then assuming that the signal intensities of the O₂⁻ adducts were proportional to the amounts of hydroxynitrates present, the ratios of the products were determined as the ratio of their O₂⁻ adducts. This ratio was then applied to the yield measurements obtained by summing the 209, 225 and 241 u ion peaks for the NO₂⁻ and NO₃⁻ adducts of the two organic nitrate products relative to the sum of the NO₂⁻ and NO₃⁻ adducts of the internal standard. Using a formation yield of CH₃CH(OH)CH(ONO₂)CH₃ from the OH radical-initiated reaction of *cis*-2-butene of 3.55% (Muthuramu *et al.*, 1993; O'Brien *et al.*, 1998), the formation yields of the molecular weight 163 and 179 hydroxynitrates obtained from three experiments each for 2-methyl-2-pentanol and for 4-methyl-2-pentanol are listed in Tables 14 and 15. As in previous studies (Arey *et al.*, 2001; Aschmann *et al.*, 2001a), these derived formation yields for the molecular weight 163 and 179 hydroxynitrates are estimated to be uncertain to a factor of ~2 (the individual measurements of the formation yields of the molecular weight 163 product from 2-methyl-2-pentanol were 8.1%, 3.8% and 5.5%, and from 4-methyl-2-pentanol were 4.7%, 7.4% and 4.6%).

In addition to these hydroxynitrates, ion peaks were also observed at 148 and 188 u. API-MS/MS “product ion” spectra showed the 148 u ion peak to be an NO₂⁻ adduct of a molecular weight 102 species (presumably the starting methylpentanols), with the 188 u ion peak being an NO₃⁻ adduct of a molecular weight 125 species observed in all reaction systems containing NO₂ (presumably [HNO₃•NO₃]).

5.1.4. Discussion

These are the first measurements of rate constants for reaction of the OH radical with 2-methyl-2-pentanol and 4-methyl-2-pentanol. Room temperature rate constants calculated using the estimation method of Kwok and Atkinson (1995), as revised by Bethel *et al.* (2001) are compared with our measured values in Table 13. The estimated rate constants are seen to be a factor of ~1.5 lower than the measured values, this being considered to be reasonably good agreement (Kwok and Atkinson, 1995). The OH radical reactions with 2- and 4-methyl-2-pentanol proceed by H-atom abstraction from the various C-H bonds and, to a much lesser extent, from the O-H bond (Atkinson, 1989, 1994; Kwok and Atkinson, 1995), and the estimation method of Kwok and Atkinson (1995) [as revised by Bethel *et al.* (2001)] can be used to calculate the fractions of the overall reaction occurring by H-atom abstraction from the various CH₃, CH₂, CH and OH groups. The resulting radicals (apart from α-hydroxyalkyl radicals; see below) then rapidly add O₂ to form organic peroxy radicals (Atkinson, 2000).

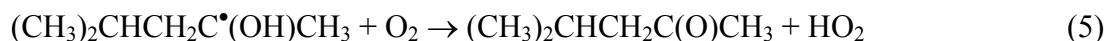


In the presence of NO, these organic peroxy radicals react with NO to form either an organic nitrate (a molecular weight 163 hydroxynitrate in this case) or a hydroxyalkoxy radical plus NO₂.



Clearly, the molecular weight 163 nitrates observed in the API-MS analyses and quantified as their NO_2^- adducts are the hydroxynitrates [for example, $(\text{CH}_3)_2\text{C}(\text{OH})\text{CH}(\text{ONO}_2)\text{CH}_2\text{CH}_3$ and isomers formed from 2-methyl-2-pentanol and $\text{CH}_3\text{CH}(\text{OH})\text{CH}(\text{ONO}_2)\text{CH}(\text{CH}_3)_2$ and isomers from 4-methyl-2-pentanol] formed from reaction (4a). Under atmospheric conditions, alkoxy radicals can react with O_2 , decompose and isomerize through a 6-membered transition state (Atkinson, 1997a,b), noting that not all of these reaction pathways may be feasible for a given alkoxy radical.

Under atmospheric conditions, it appears that α -hydroxyalkyl radicals react rapidly, and solely, with O_2 to form a carbonyl plus HO_2 radical (Atkinson, 1994); for example:



In the following sections, the expected reactions of 2- and 4-methyl-2-pentanol are discussed, based on our current knowledge of the atmospheric chemistry of volatile organic compounds, and compared with the products identified and quantified here. Reaction rates of alkoxy radicals (by reaction with O_2 , decomposition and isomerization) are estimated as described by Atkinson (1997a,b) and Aschmann and Atkinson (1999).

2-Methyl-2-pentanol. The percentage of the overall OH radical reaction occurring by H-atom abstraction from the C-H bonds at the various carbon atoms in $(\text{CH}_3)_2\text{C}(\text{OH})\text{CH}_2\text{CH}_2\text{CH}_3$ are calculated (Kwok and Atkinson, 1995; Bethel *et al.*, 2001) to be: from the two equivalent CH_3 groups at the 1-position, 14%; from the CH_2 group at the 3-position, 58%; from the CH_2 group at the 4-position, 22%; from the CH_3 group at the 5-position, 3%; and from the OH group, 3%. As noted above, the initially formed alkyl-type radicals add O_2 and then react with NO to form hydroxynitrates [mainly $(\text{CH}_3)_2\text{C}(\text{OH})\text{CH}(\text{ONO}_2)\text{CH}_2\text{CH}_3$ and $(\text{CH}_3)_2\text{C}(\text{OH})\text{CH}_2\text{CH}(\text{ONO}_2)\text{CH}_3$] of molecular weight 163. The expected reactions of the alkoxy radicals estimated to be formed in significant yield are shown in Figures 47-49. In these reaction schemes, the intermediate alkyl and alkyl peroxy radicals are generally omitted for clarity. Based on the estimation method of Atkinson (1997a,b), as revised by Aschmann and Atkinson (1999) and Bethel *et al.* (2001) [see Supplementary Material in Aschmann *et al.* (2001b)] and using thermochemical data from compilations (Kerr and Stocker, 1999/2000; Atkinson *et al.*, 2000b) and the NIST estimation program (National Institute of Standards and Technology, 1994), reaction pathways which are estimated to be of minor or negligible importance (<1% of the overall reaction rate) are denoted by dashed arrows, and if a reaction pathway is estimated to dominate over other pathways by a factor of >10, it is shown as a bold arrow. The observed products are shown in boxes and the possible structures for the molecular weight 179 dihydroxynitrates are shown underlined on the schemes. The detailed reactions of ethyl radicals, 1-propyl radicals and $(\text{CH}_3)_2\text{C}(\text{OH})\text{C}^\bullet\text{H}_2$ radicals are not shown, because under atmospheric conditions these lead to the formation of acetaldehyde, propanal, and acetone + HCHO, respectively (Atkinson, 1994, 1997a,b). The alkoxy radical $(\text{CH}_3)_2\text{C}(\text{O}^\bullet)\text{CH}_2\text{CH}_2\text{CH}_3$ formed after H-atom abstraction from the OH group is calculated (Atkinson, 1997a) to mainly isomerize to ultimately form $(\text{CH}_3)_2\text{C}(\text{OH})\text{CH}_2\text{CH}_2\text{CHO}$.

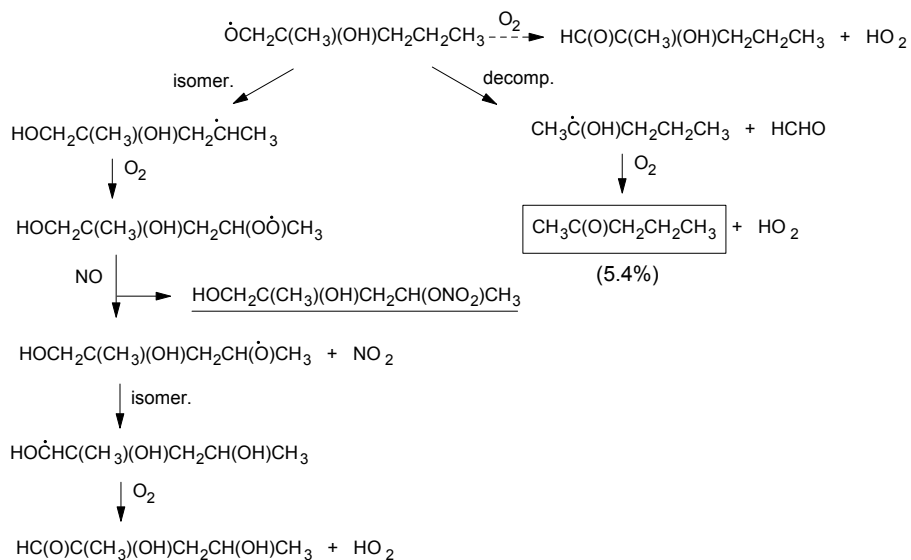


Figure 47. Reactions of the $\dot{\text{O}}\text{CH}_2\text{C}(\text{CH}_3)(\text{OH})\text{CH}_2\text{CH}_2\text{CH}_3$ radical.

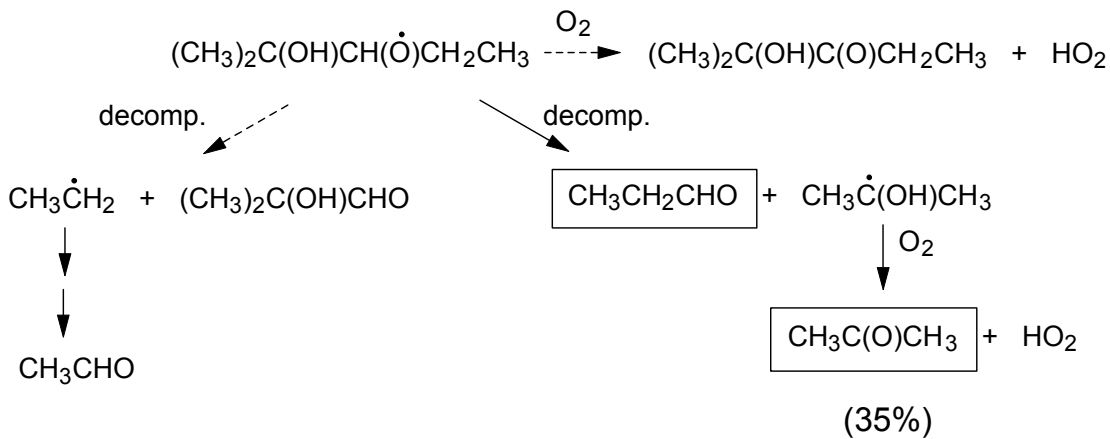


Figure 48. Reactions of the $(\text{CH}_3)_2\text{C}(\text{CH}_3)(\text{OH})\text{CH}(\text{O}\dot{\text{O}})\text{CH}_2\text{CH}_3$ radical.

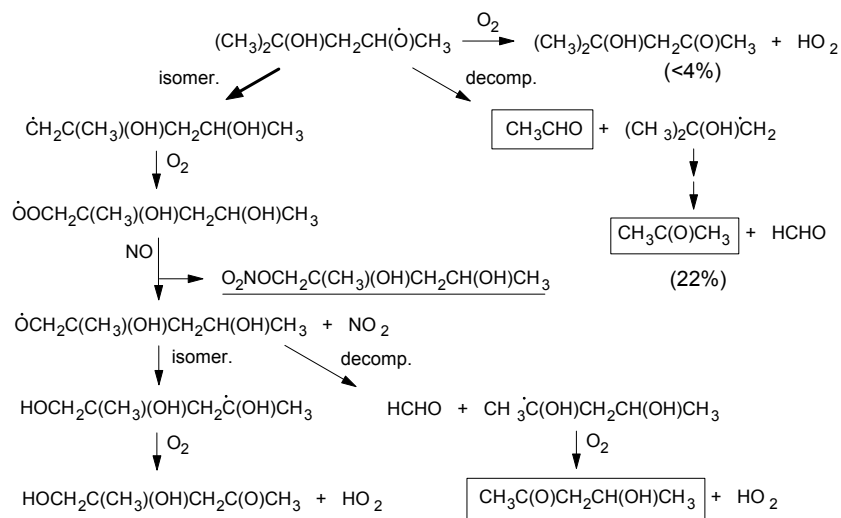


Figure 49. Reactions of the $(\text{CH}_3)_2\text{C}(\text{CH}_3)(\text{OH})\text{CH}_2\text{CH}(\text{O}\cdot)\text{CH}_3$ radical.

These predictions are in general accord with our product data (Table 14). The molecular weight 163 organic nitrates are the hydroxynitrates formed from the $\text{ROO}\cdot + \text{NO}$ reactions, and the expected products from the alkoxy radicals are acetaldehyde + acetone from the $(\text{CH}_3)_2\text{C}(\text{OH})\text{CH}_2\text{CH}(\text{O}\cdot)\text{CH}_3$ radical (Figure 49), acetone + propanal from the $(\text{CH}_3)_2\text{C}(\text{OH})\text{CH}(\text{O}\cdot)\text{CH}_2\text{CH}_3$ radical (Figure 48), and 2-pentanone from the $\cdot\text{OCH}_2\text{C}(\text{CH}_3)(\text{OH})\text{CH}_2\text{CH}_2\text{CH}_3$ radical (Figure 47). The product yields given in Table 14 are in agreement with the expectation (see sentence above) that the acetone yield ($56 \pm 6\%$) is equal to the sum of the formation yields of acetaldehyde plus propanal ($57 \pm 5\%$). Our product yield data indicate that the $(\text{CH}_3)_2\text{C}(\text{OH})\text{CH}(\text{O}\cdot)\text{CH}_2\text{CH}_3$ radical is formed in $35 \pm 4\%$ yield (from the propanal yield), significantly lower than predicted from the calculated percentage of H-atom abstraction from the 3-position CH_2 group (58%), noting that hydroxynitrate formation from the $(\text{CH}_3)_2\text{C}(\text{OH})\text{CH}(\text{OO}\cdot)\text{CH}_2\text{CH}_3$ radical occurs to a small extent. The observed lack of formation of 4-hydroxy-4-methyl-2-pentanone ($<4\%$ yield) is consistent with expectations (Figure 49); however, the sum of the yields of acetaldehyde and acetone arising from reaction of the $(\text{CH}_3)_2\text{C}(\text{OH})\text{CH}_2\text{CH}(\text{O}\cdot)\text{CH}_3$ radical ($22 \pm 3\%$, based on the acetaldehyde yield), is higher than expected because the $(\text{CH}_3)_2\text{C}(\text{OH})\text{CH}_2\text{CH}(\text{O}\cdot)\text{CH}_3$ radical is estimated to dominantly isomerize rather than decompose or react with O_2 (Figure 49) and the calculated percentage of H-atom abstraction at the 4-position CH_2 group is 22% . Our observation of a molecular weight 102 carbonyl, assumed to be 4-hydroxy-2-pentanone, indicates that the isomerization of the $(\text{CH}_3)_2\text{C}(\text{OH})\text{CH}_2\text{CH}(\text{O}\cdot)\text{CH}_3$ radical competes with decomposition. The presence of molecular weight 179 organic nitrates (predicted to be $\text{O}_2\text{NOCH}_2\text{C}(\text{CH}_3)(\text{OH})\text{CH}_2\text{CH}(\text{OH})\text{CH}_3$ and/or $\text{HOCH}_2\text{C}(\text{CH}_3)(\text{OH})\text{CH}_2\text{CH}(\text{ONO}_2)\text{CH}_3$; see Figures 49 and 47, respectively) also shows that isomerization of certain of the alkoxy radicals must occur.

4-Methyl-2-pentanol. The percentage of the overall OH radical reaction occurring by H-atom abstraction from the C-H bonds at the various carbon atoms in $\text{CH}_3\text{CH}(\text{OH})\text{CH}_2\text{CH}(\text{CH}_3)_2$ are

calculated to be: from the CH₃ group at the 1-position, 3%; from the CH group at the 2-position, 53%; from the CH₂ group at the 3-position, 23%; from the CH group at the 4-position, 18%; from the two equivalent CH₃ groups at the 5-positions, 3%; and from the OH group, 1%. As for 2-methyl-2-pentanol, the initially-formed alkyl radicals will solely add O₂ [reaction (3)] and then react with NO [reactions (4a, 4b)] (apart from the CH₃C[•](OH)CH₂CH(CH₃)₂ α-hydroxy radical which reacts with O₂ as shown in reaction (5) to form 4-methyl-2-pentanone). Figures 50 and 51 show the expected reactions of the CH₃CH(OH)CH(O[•])CH(CH₃)₂ and CH₃CH(OH)CH₂C(O[•])(CH₃)₂ radicals, with the same format as mentioned above for 2-methyl-2-pentanol. In addition to the molecular weight 163 hydroxynitrates (primarily expected to be CH₃CH(OH)CH(ONO₂)CH(CH₃)₂ and CH₃CH(OH)CH₂C(ONO₂)(CH₃)₂), the expected products are 4-methyl-2-pentanone from the CH₃C[•](OH)CH₂CH(CH₃)₂ radical, acetaldehyde plus 2-methylpropanal from the CH₃CH(OH)CH(O[•])CH(CH₃)₂ radical (Figure 50), and acetaldehyde plus acetone from the CH₃CH(OH)CH₂C(O[•])(CH₃)₂ radical (Figure 51). It should be noted that isomerization of this latter radical is predicted to dominate over the decomposition to form acetaldehyde plus acetone. The measured product yields are in semi-quantitative accord with these predictions, with the acetaldehyde yield (37 ± 6%) being equal to the sum of the acetone plus 2-methylpropanal yields (37 ± 4%). The measured formation yield of 4-methyl-2-pentanone of 25 ± 2% is a factor of 2 lower than the estimated fraction of the overall OH radical reaction proceeding by H-atom abstraction from the 2-position CH group (53%). Similarly, the 2-methylpropanal yield of 11.1 ± 1.2% is a factor of 2 lower than the calculated percentage of the overall OH radical reaction proceeding by H-atom abstraction from the 3-position CH₂ group (23%), recognizing that some hydroxynitrate formation will occur from the ROO[•] + NO reaction. The yield of acetaldehyde plus co-product acetone of 26 ± 3% (based on the acetone yield) is higher than anticipated because decomposition of the CH₃CH(OH)CH₂C(O[•])(CH₃)₂ radical to form acetone plus acetaldehyde is predicted to be somewhat less important than isomerization (by a factor of 2.5) and the percentage of H-atom abstraction from the 4-position CH groups is calculated to be 18%. Again, the presence of molecular weight 179 organic nitrates (predicted to be mainly O₂NOCH₂CH(OH)CH₂C(OH)(CH₃)₂; see Figures 47, 49 and 51) shows that isomerization of certain of the alkoxy radicals must occur.

5.1.5. Conclusions

Comparison of the experimental kinetic and product data obtained here for the reactions of OH radicals with 2-methyl-2-pentanol and 4-methyl-2-pentanol with predictions based on structure-reactivity relationships shows that we have a qualitative (or semi-quantitative) understanding of the initial rate of reaction and of the detailed subsequent reactions. For both reactions, we can account for ~70% of the reaction products and pathways. However, for both 2- and 4-methylpentanol, using the estimation method (Kwok and Atkinson, 1995; Bethel *et al.*, 2001) to calculate the overall reaction rate constant and the partial rate constants (*i.e.*, the rate constants for H-atom abstraction from the various CH, CH₂, CH₃ and OH groups) and hence the fraction of the overall OH radical reaction proceeding by H-atom abstraction from the various groups (see Table 16), we overestimate the fraction of the overall reaction occurring from C-H bonds on the carbon atom adjacent to that to which the OH group is attached and, in the case of 4-methyl-2-pentanol, at the CH group to which the OH group is attached. In contrast, we appear to

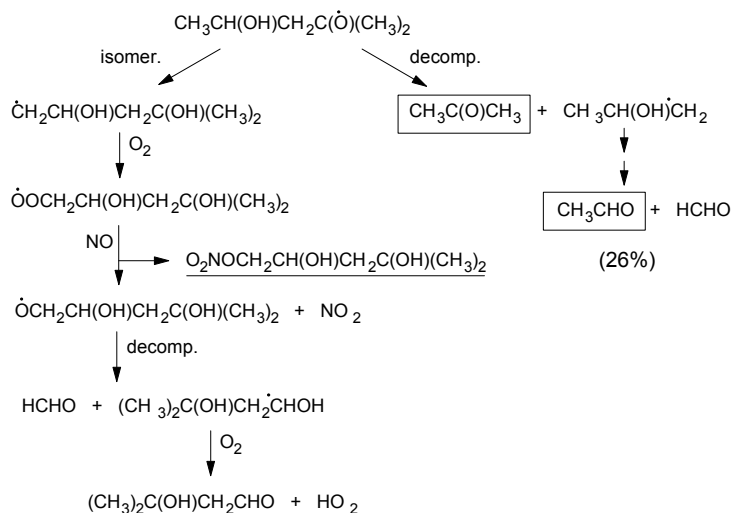


Figure 51. Reactions of the $\text{CH}_3\text{CH}(\text{OH})\text{CH}_2\text{C}(\text{O}^\bullet)(\text{CH}_3)_2$ radical.

underestimate the fraction of the overall reaction occurring from C-H bonds on carbon atoms 2-removed from that to which the OH group is attached (*i.e.*, the γ carbon). However, the calculated partial rate constants for H-atom abstraction from the C-H bond of the CH(OH) group (2-position in 4-methyl-2-pentanol) and of the CH_2 groups adjacent to the carbon to which the OH group is attached (the 3-position CH_2 group in both 2- and 4-methyl-2-pentanol) are in reasonable agreement with the values obtained from our product data (Table 16), as is the partial rate constant for H-atom abstraction from the 1-position CH_3 groups in 2-methyl-2-pentanol. However, the calculated partial rate constants for H-atom abstraction from the 4-position CH_2 or CH groups are much lower (by a factor of ~ 2 or more) than the values obtained from our product analyses. Clearly, the activating effects of the OH group are transmitted far down the carbon chain from the carbon atom to which the OH group is attached, as previously concluded by Wallington *et al.* (1988) and Nelson *et al.* (1990).

Table 16. Comparison of measured and calculated partial rate constants ($\text{cm}^3 \text{ molecule}^{-1} \text{ s}^{-1}$) for H-atom abstraction by OH radicals from the various CH_3 , CH_2 and CH groups

Methylpentanol and group	$10^{12} \times k_{\text{exp}}$	$10^{12} \times k_{\text{calc}}^{\text{a}}$
2-Methyl-2-pentanol		
CH_3 at 1-position	≥ 0.214	0.354
CH_2 at 3-position	2.78	2.99
CH_2 at 4-position	> 1.74	1.15
CH_3 at 5-position		0.167
4-Methyl-2-pentanol		
CH_3 at 1-position		0.354
CH at 2-position	4.78	6.92
CH_2 at 3-position	2.12	2.99
CH at 4-position	> 4.97	2.39
CH_3 at 5- position		0.167

^aUsing the estimation method of Kwok and Atkinson (1995) as revised by Bethel *et al.* (2001).

5.2. Hydroxycarbonyl Products of the Reactions of Selected Diols with the OH Radical

5.2.1. Introduction

Volatile organic compounds present in the atmosphere can undergo photolysis and chemical reaction with OH radicals, NO₃ radicals, and O₃ (Atkinson, 2000), with the OH radical reaction being an important, and often dominant, atmospheric loss process (Atkinson, 2000). Diols are used as solvents (Howard, 1990), and can also be formed in the atmosphere from the OH radical-initiated reactions of alkenes under low-NO_x conditions (Atkinson, 1997a, 2000; Ruppert and Becker, 2000; Aschmann *et al.*, 2000b). To date, room temperature rate constants have been reported for the gas-phase reactions of OH radicals with 1,2-ethanediol (Wiedlemann and Zetzsch, 1982; Neavyn *et al.*, 1994; Aschmann and Atkinson, 1998), 1,2-propanediol (Wiedlemann and Zetzsch, 1982; Aschmann and Atkinson, 1998), 2-methyl-2,4-pentanediol (Bethel *et al.*, 2001) and 1,2-, 1,3- and 2,3-butanediol (Bethel *et al.*, 2001). During our previous kinetic and product study of the reactions of OH radicals with 2-methyl-2,4-pentanediol and 1,2-, 1,3- and 2,3-butanediol (Bethel *et al.*, 2001), we identified and quantified hydroxyketone products formed from these reactions and, because hydroxyaldehyde products also expected from certain of these reactions were not observed, concluded that without derivatization hydroxyaldehydes would not elute from the gas chromatographic columns used.

In this study, we have further investigated the products formed from the reactions of OH radicals with 2-methyl-2,4-pentanediol and 1,2-, 1,3- and 2,3-butanediol, using Solid Phase Micro Extraction (SPME) fibers (Pawliszyn, 1997) coated with *O*-(2,3,4,5,6-pentafluorobenzyl)hydroxylamine hydrochloride (Koziel *et al.*, 2001) for on-fiber derivatization of carbonyl compounds, with subsequent gas chromatographic analyses of their oxime derivatives.

5.2.2. Experimental Methods

All experiments were carried out in a 7500 liter Teflon chamber, equipped with two parallel banks of blacklamps for irradiation, at 296 ± 2 K and 740 Torr total pressure of purified air at ~5% relative humidity. This chamber is fitted with a Teflon-coated fan to ensure the rapid mixing of reactants during their introduction into the chamber. OH radicals were generated by the photolysis of methyl nitrite (CH₃ONO) in air at wavelengths >300 nm, and NO was added to the reactant mixtures to suppress the formation of O₃ and hence of NO₃ radicals. The initial reactant concentrations (molecule cm⁻³) were: CH₃ONO, $\sim 4.8 \times 10^{13}$; NO, $\sim 4.8 \times 10^{13}$; and diol, $\sim 1.2 \times 10^{13}$. Irradiations were carried out for 1.5-5 min, resulting in up to 61% consumption of the initially present diol.

The concentrations of the diols were measured during the experiments by gas chromatography with flame ionization detection (GC-FID) (Bethel *et al.*, 2001). Gas samples of 100 cm³ volume were collected from the chamber onto Tenax-TA solid adsorbent, with subsequent thermal desorption at ~225 °C onto a 30 m DB-1701 megabore column held at 0 °C and then temperature programmed to 200 °C at 8 °C min⁻¹. Based on replicate analyses in the dark, the GC-FID measurement uncertainties for the diols were in the range 1-5%, except for 1,3-butanediol for which the uncertainties were in the range 4-9%. The hydroxyaldehyde and hydroxyketone products were sampled using a 65 μm poly(dimethylsiloxane)/divinylbenzene SPME fiber. The fiber was coated prior to use with *O*-(2,3,4,5,6-pentafluorobenzyl)hydroxylamine hydrochloride (PFBHA) for on-fiber derivatization of carbonyl compounds. The derivatization reagent was loaded onto the SPME fiber for one hour using headspace extraction from a 20 mg ml⁻¹ PFBHA solution immediately before sampling in

the chamber. The coated fiber was inserted into the chamber and exposed to the chamber contents for 5 minutes with the chamber mixing fan on. The fiber was then removed and introduced into the inlet port of the GC-FID with subsequent thermal desorption at 250 °C onto a 30 m DB-1701 megabore column held at 40 °C and then temperature programmed to 260 °C at 8 °C min⁻¹. Identification was carried out by gas chromatography-mass spectrometry (GC-MS), using a Varian 2000 MS/MS with isobutane chemical ionization and a DB-1701 column, using a similar procedure to that for the GC-FID analyses. GC retention times and mass spectra were previously obtained for a number of standard hydroxyketones (Reisen *et al.*, 2003). In addition, an irradiation of a CH₃ONO – NO – 2-methyl-3-buten-2-ol – air mixture was carried out, with similar initial reactant concentrations as used in the diol experiments, to obtain GC retention times and mass spectra of the oximes of glycolaldehyde [HOCH₂CHO], a known product of the OH radical-initiated reaction of 2-methyl-3-buten-2-ol (Ferronato *et al.*, 1998; Alvarado *et al.*, 1999).

The chemicals used, and their stated purities, were: 1,2-butanediol (99%), 1,3-butanediol (99+%), 2,3-butanediol (98%), 1-hydroxy-2-butanone (95%), 3-hydroxy-2-butanone, 4-hydroxy-4-methyl-2-pentanone (99%), 2-methyl-2,4-pentanediol (99%), *O*-(2,3,4,5,6-pentafluorobenzyl)hydroxylamine hydrochloride (98+%), and 2-methyl-3-buten-2-ol (98%), Aldrich Chemical Company; 4-hydroxy-2-butanone (95+%), TCI America; and NO (≥99.0%), Matheson Gas Products. Methyl nitrite was prepared and stored as described previously (Bethel *et al.*, 2001).

5.2.3. Results

GC-MS analyses of irradiated CH₃ONO – NO – diol – air mixtures, using the SPME fiber coated with derivatizing reagent to sample the chamber contents, showed the formation of a number of oximes from each diol (Table 17). The hydroxyketones previously identified and quantified (Bethel *et al.*, 2001) were identified as their oxime derivatives from comparison of the GC retention times and mass spectra with those of the oximes of authentic standards. The oximes gave strong [M+H]⁺ ions with minor [M+41]⁺ adduct ions, where the value of M is 195 mass units above the molecular weight of the carbonyl product (note that asymmetric carbonyls may produce *Z*- and *E*- forms of the oximes). Glycolaldehyde was shown to be formed from the reactions of 1,2- and 1,3-butanediol (Table 17) by comparison with GC-FID and GC-MS analyses, using the same coated SPME fiber method, of an irradiated CH₃ONO – NO – 2-methyl-3-buten-2-ol – air mixture which is known to form glycolaldehyde as a reaction product (Ferronato *et al.*, 1998; Alvarado *et al.*, 1999).

Additional oxime products were observed in the GC-FID and GC-MS analyses and, based on their molecular weights, the fact that they must be hydroxyaldehydes (i.e., they were not observed without derivatization) and consistency with the reaction pathways discussed below, were assigned the structures listed in Table 17. The oximes of the molecular weight 74 product(s) observed from the 1,3-butanediol, 2,3-butanediol and 2-methyl-2,4-pentanediol reactions had identical GC retention times and mass spectra, indicating that the same carbonyl-containing product is formed from each of these diols. From consideration of the likely reaction schemes (see below), this molecular weight 74 product is attributed to the hydroxyaldehyde CH₃CH(OH)CHO. The products (other than the hydroxyketones) of molecular weight 88 observed in the 1,2- and 1,3-butanediol reactions are attributed to the hydroxyaldehydes CH₃CH₂CH(OH)CHO and CH₃CH(OH)CH₂CHO, respectively.

Table 17. Hydroxycarbonyl products predicted and observed, and their predicted and measured yields, from the gas-phase reactions of the OH radical with diols at $296 \pm 2\text{K}$

Diol	Product	Molar Formation Yield (%)		
		Tenax ^a	SPME ^b	Est. ^c
CH ₃ CH ₂ CH(OH)CH ₂ OH	CH ₃ CH ₂ C(O)CH ₂ OH ^d	66 ± 11		64
	CH ₃ CH ₂ CH(OH)CHO		27	25
	HOCH ₂ CHO ^e		10 ± 4	9
	HOCH ₂ CH ₂ CH(OH)CHO			<1
CH ₃ CH(OH)CH ₂ CH ₂ OH	CH ₃ C(O)CH ₂ CH ₂ OH ^d	50 ± 9		40
	CH ₃ CH(OH)CH ₂ CHO		15	19
	CH ₃ CH(OH)CHO ^f		0.7	3
	HOCH ₂ CHO ^e		10 ± 4	34
CH ₃ CH(OH)CH(OH)CH ₃	HOCH ₂ CH(OH)CH ₂ CHO			2
	CH ₃ C(O)CH(OH)CH ₃ ^d	89 ± 9		97
	CH ₃ CH(OH)CHO ^f		2.0	2
	(CH ₃) ₂ C(OH)CH ₂ CH(OH)CH ₃	(CH ₃) ₂ C(OH)CH ₂ C(O)CH ₃ ^d	47 ± 9	
(CH ₃) ₂ C(OH)CH ₂ CH(OH)CH ₃	CH ₃ CH(OH)CHO ^f		24	43
	(CH ₃) ₂ C(OH)CH ₂ CHO		observe d	2
	HOCH ₂ C(OH)(CH ₃)CH ₂ C(O)CH ₃			7

^aFrom Bethel *et al.* (2001) with products sampled on Tenax adsorbent. Indicated errors are two least-squares standard deviations combined with estimated overall uncertainty in the GC-FID response factors for the diols and hydroxyketones of $\pm 5\%$ each.

^bThis work; see text for details of how these yields are obtained. The estimated overall uncertainties are a factor of ~ 2 , except for HOCH₂CHO where the indicated errors are two standard deviations (including the uncertainties in the measured formation yields (Bethel *et al.*, 2001) for the reference hydroxyketone CH₃CH₂C(O)CH₂OH or CH₃C(O)CH₂CH₂OH).

^cEstimated based on the predicted percentages of the initial OH radical reaction proceeding by H-atom abstraction from the various CH, CH₂, CH₃ and OH groups (Kwok and Atkinson, 1995; Bethel *et al.*, 2001) and the estimated reaction rates of the intermediate alkoxy radicals (Atkinson, 1997a,b; Aschmann and Atkinson, 1999; Aschmann *et al.*, 2001b), assuming that all α -hydroxy radicals react solely with O₂ (Atkinson, 1994) and neglecting organic nitrate formation from reaction 7b and analogous reactions.

^dIdentification based on matching of GC retention times and mass spectra with those of authentic standards.

^eIdentification based on comparison of GC retention times and mass spectra of the oximes from reactions of 1,2- and 1,3-butanediol with OH radicals with those from reaction of OH radicals with 2-methyl-3-buten-2-ol (Ferronato *et al.*, 1998; Alvarado *et al.*, 1999).

^fIdentical oximes were formed from the reactions of OH radicals with 1,3- and 2,3-butanediol and 2-methyl-2,4-pentanediol, and this identical molecular weight 74 product is attributed to CH₃CH(OH)CHO from consideration of the likely reaction mechanisms (see text).

We have recently measured GC-FID response factors for the oximes of 30 aldehydes, ketones and hydroxycarbonyls (Reisen *et al.*, 2003). In these experiments, two or three carbonyl compounds were introduced into the chamber at a concentration of $\sim(2.4-7.2) \times 10^{12}$ molecule cm^{-3} each and sampled with the coated SPME fiber, with subsequent GC-FID analysis of the oximes. We therefore have relative response factors (see Table 18) for SPME/GC-FID analyses of the oximes of 1-hydroxy-2-butanone, 4-hydroxy-2-butanone, 3-hydroxy-2-butanone, 4-hydroxy-4-methyl-2-pentanone, and glycolaldehyde. The response factor for glycolaldehyde was obtained from the OH radical-initiated reaction of 2-methyl-3-buten-2-ol, using a glycolaldehyde formation yield of 58% (Alvarado *et al.*, 1999), and taking into account the small loss of glycolaldehyde (<4%) due to its secondary reaction with OH radicals. Based on the measured relative response factors, it is predicted that the response factor for an hydroxyaldehyde or hydroxyketone is a factor of 5.1 higher (with an uncertainty of a factor of ~ 2) than that of the corresponding aldehyde or ketone with the -OH group replaced by a methyl group (Reisen *et al.*, 2003). For example, the response factor for the sum of the oximes of $\text{CH}_3\text{CH}(\text{OH})\text{CHO}$ is estimated to be a factor of 5.1 higher than for the oximes of $(\text{CH}_3)_2\text{CHCHO}$. The relative response factors for the 30 carbonyl compounds studied were all ≤ 23 (Reisen *et al.*, 2003), with the highest response factors being for hexanal (22.3), glycolaldehyde (18.8), pentanal (16.0) and 5-hydroxy-2-pentanone (15.0). Based on the response factors for straight-chain aldehydes, 2-ketones and 3-ketones (Reisen *et al.*, 2003), that for 5-hydroxy-2-pentanone is expected to be a factor of ~ 1.8 higher than the value of 12.5 measured for 4-hydroxy-2-butanone (Reisen *et al.*, 2003), suggesting there is a maximum value of the response factor of $\sim 15-25$ for the SPME sampling and analysis procedure used here. Therefore, because the estimated response factors (relative to that for the oximes of 3-pentanone) for $\text{CH}_3\text{CH}_2\text{CH}(\text{OH})\text{CHO}$, $\text{CH}_3\text{CH}(\text{OH})\text{CH}_2\text{CHO}$ and $\text{CH}_3\text{CH}(\text{OH})\text{CHO}$ are >25 , we use a constant value of 25 for all three of these hydroxyaldehydes (Table 18).

The GC-FID measurements provide the peak areas for the various oximes of the carbonyl-containing compounds, and Figure 52 shows a plot of the peak areas of the oximes of the hydroxyketones and hydroxyaldehydes observed from the 1,3-butanediol reaction against the percentage reaction for three replicate experiments with the same initial 1,3-butanediol concentrations. The hydroxyaldehyde and hydroxyketone products also react with OH radicals, and the decreases in yield with increasing percentage of reaction are evident in Figure 52.

We have previously measured the hydroxyketone formation yields (for example, of 4-hydroxy-2-butanone in the case of the 1,3-butanediol reaction) (Bethel *et al.*, 2001) and here we have used these hydroxyketones as internal standards. For example, the ratio of the hydroxyaldehyde oxime peak areas to that of the oximes of the hydroxyketone product as a function of the percent of 1,3-butanediol reacted is shown in Figure 53. The decrease in the ratio of the GC-FID peak areas of the hydroxyaldehydes relative to 4-hydroxy-2-butanone with increasing extent of reaction shows that $\text{CH}_3\text{CH}(\text{OH})\text{CH}_2\text{CHO}$ and $\text{CH}_3\text{CH}(\text{OH})\text{CHO}$ are more reactive towards OH radicals than is $\text{CH}_3\text{C}(\text{O})\text{CH}_2\text{CH}_2\text{OH}$. Using the fraction of the initial diol reacted (determined from the Tenax/GC-FID analyses) and the known (Aschmann *et al.*, 2000a; Bethel *et al.*, 2001) or estimated (Kwok and Atkinson, 1995; Bethel *et al.*, 2001) rate constants for reaction of the diols and hydroxycarbonyl products with OH radicals listed in Table 18, the hydroxyaldehyde/hydroxyketone GC-FID peak area ratios were corrected to take into account secondary reactions with OH radicals. As expected, the corrected GC-FID peak area ratios do not vary with extent of reaction (filled symbols in Figure 53) and the averages of the individual ratios were used (dashed lines in Figure 53). The GC-FID response factors for the oximes of the various hydroxycarbonyls, relative to that for the oximes of 3-pentanone, obtained using the

Table 18. Analytical relative response factors for the oximes of the products observed, and OH radical reaction rate constants for the diols and products.

Reactant or product	SPME/GC-FID Response factor relative to 3-pentanone	$10^{12} \times k_{\text{OH}}$ ($\text{cm}^3 \text{ molecule}^{-1} \text{ s}^{-1}$)
$\text{CH}_3\text{CH}_2\text{CH}(\text{OH})\text{CH}_2\text{OH}$		$27.0 \pm 1.4^{\text{a}}$
$\text{CH}_3\text{CH}(\text{OH})\text{CH}_2\text{CH}_2\text{OH}$		$33.2 \pm 1.1^{\text{a}}$
$\text{CH}_3\text{CH}(\text{OH})\text{CH}(\text{OH})\text{CH}_3$		$23.6 \pm 4.2^{\text{a}}$
$(\text{CH}_3)_2\text{C}(\text{OH})\text{CH}_2\text{CH}(\text{OH})\text{CH}_3$		$27.7 \pm 2.4^{\text{a}}$
$\text{CH}_3\text{CH}_2\text{C}(\text{O})\text{CH}_2\text{OH}$	5.6^{b}	$7.7 \pm 0.8^{\text{c}}$
$\text{CH}_3\text{C}(\text{O})\text{CH}_2\text{CH}_2\text{OH}$	12.5^{b}	$8.1 \pm 0.8^{\text{c}}$
$\text{CH}_3\text{C}(\text{O})\text{CH}(\text{OH})\text{CH}_3$	7.3^{b}	$10.3 \pm 0.5^{\text{c}}$
$(\text{CH}_3)_2\text{C}(\text{OH})\text{CH}_2\text{C}(\text{O})\text{CH}_3$	3.1^{b}	$4.0 \pm 0.9^{\text{c}}$
HOCH_2CHO	18.8^{d}	13^{e}
$\text{CH}_3\text{CH}_2\text{CH}(\text{OH})\text{CHO}$	25^{f}	30^{g}
$\text{CH}_3\text{CH}(\text{OH})\text{CH}_2\text{CHO}$	25^{f}	30^{g}
$\text{CH}_3\text{CH}(\text{OH})\text{CHO}$	25^{f}	30^{g}

^aFrom Bethel *et al.* (2001). The indicated uncertainties do not take into account the uncertainties in the rate constant for the reaction of OH radicals with the reference compound *n*-octane.

^bFrom Reisen *et al.* (2003). The estimated overall uncertainties in these relative response factors are $\sim\pm 20\%$.

^cFrom Aschmann *et al.* (2000a). The indicated uncertainties do not take into account the uncertainties in the rate constant for the reaction of OH radicals with the reference compound *n*-octane.

^dObtained from coated SPME/GC-FID analysis of 3 irradiated $\text{CH}_3\text{ONO} - \text{NO} - 2\text{-methyl-3-buten-2-ol} - \text{air}$ mixtures, with 4-hydroxy-3-hexanone and (in one experiment) 1-hydroxy-2-butanone added after the irradiation as an internal standard(s) and using our previously measured glycolaldehyde formation yield of $58 \pm 4\%$ [a weighted average of the measured formation yields of glycolaldehyde and its co-product acetone (Alvarado *et al.*, 1999)] and taking into account the small loss of glycolaldehyde ($<4\%$) due to its secondary reaction with OH radicals. The estimated overall uncertainty in this relative response factor is $\pm 20\%$.

^eFrom IUPAC (2003).

^fEstimated from the measured relative response factors for $(\text{CH}_3)_2\text{CHCHO}$, $\text{CH}_3\text{CH}_2\text{CH}(\text{CH}_3)\text{CHO}$ and $(\text{CH}_3)_2\text{CHCH}_2\text{CHO}$; see text and Reisen *et al.* (2003). Estimated overall uncertainties in these relative response factors are a factor of ~ 2 .

^gEstimated. While the rate constants calculated as described in Bethel *et al.* (2001) are (in units of $10^{-11} \text{ cm}^3 \text{ molecule}^{-1} \text{ s}^{-1}$): $\text{CH}_3\text{CH}(\text{OH})\text{CHO}$, 4.95; $\text{CH}_3\text{CH}_2\text{CH}(\text{OH})\text{CHO}$, 5.8; and $\text{CH}_3\text{CH}(\text{OH})\text{CH}_2\text{CHO}$, 4.7, the literature database suggests that these estimated OH radical reaction rate constants for hydroxyaldehydes are too high (Bethel *et al.*, 2001). Accordingly, an approximate rate constant of $3.0 \times 10^{-11} \text{ cm}^3 \text{ molecule}^{-1} \text{ s}^{-1}$ was used for all three hydroxyaldehydes.

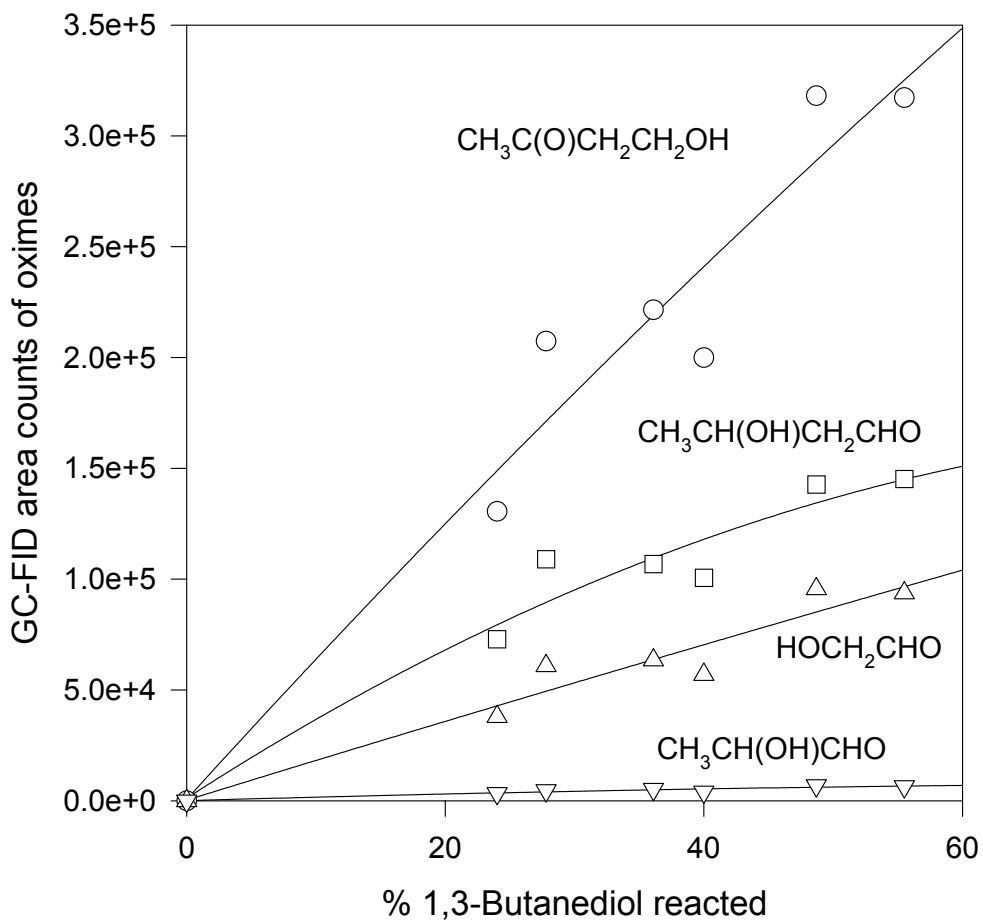


Figure 52. Plot of the GC-FID peak areas for the oximes of the hydroxycarbonyls observed, against the percentage of 1,3-butanediol reacted with the OH radical. The measured initial concentrations of 1,3-butanediol in the three experiments were the same, within the measurements uncertainties of $\pm 5-9\%$ (see text).

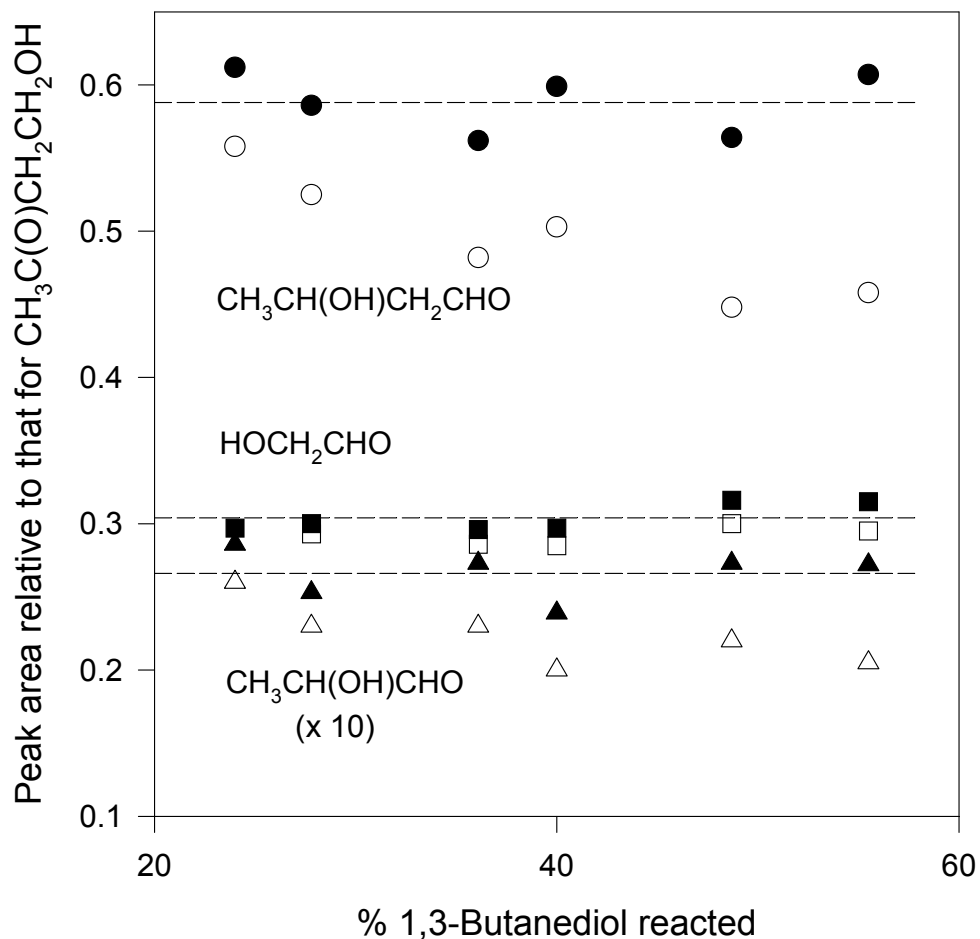


Figure 53. Plots of the GC peak areas (see Figure 52) of the oximes of the hydroxyaldehydes $\text{CH}_3\text{CH}(\text{OH})\text{CH}_2\text{CHO}$, HOCH_2CHO and $\text{CH}_3\text{CH}(\text{OH})\text{CHO}$ ratioed to the peak area of the oximes of the hydroxyketone $\text{CH}_3\text{C}(\text{O})\text{CH}_2\text{CH}_2\text{OH}$. o, □, Δ – Experimental data; •, ■, ▲ - experimental data corrected for reactions of $\text{CH}_3\text{CH}(\text{OH})\text{CH}_2\text{CHO}$, HOCH_2CHO , $\text{CH}_3\text{CH}(\text{OH})\text{CHO}$ and $\text{CH}_3\text{C}(\text{O})\text{CH}_2\text{CH}_2\text{OH}$ with OH radicals; (---) - ratios obtained by averaging the corrected data.

coated SPME fiber for sample collection and on-fiber derivatization (Reisen *et al.*, 2003), are also given in Table 18. These relative response factors were then combined with the corrected hydroxyaldehyde/hydroxyketone GC-FID peak area ratios and with the hydroxyketone formation yields previously determined by Bethel *et al.* (2001) to obtain the hydroxyaldehyde formation yields. The resulting hydroxyaldehyde yields for each diol studied are given in Table 17.

5.2.4. Discussion

As previously discussed by Bethel *et al.* (2001), H-atom abstraction from the C-H bonds of the CH and/or CH₂ groups to which the OH group is attached is predicted to be important in the reactions of OH radicals with the four diols studied here, with the rapid reaction of the resulting α -hydroxyalkyl radicals with O₂ forming hydroxyketone or hydroxyaldehyde products. Taking the 1,2-butanediol reaction as an example, the reactions,



followed by reactions of the α -hydroxyalkyl radicals with O₂ (Atkinson, 1994),



result in the formation of 1-hydroxy-2-butanone and 2-hydroxybutanal from 1,2-butanediol. Analogous reactions lead to the formation of 3-hydroxy-2-butanone from 2,3-butanediol, 4-hydroxy-2-butanone and 3-hydroxybutanal from 1,3-butanediol, and 4-hydroxy-4-methyl-2-pentanone from 2-methyl-2,4-pentanediol. As indicated in Table 17, several other hydroxycarbonyls were observed in addition to these major products, and the formation routes to these compounds are discussed below.

1,2-Butanediol

H-atom abstraction from the C-H bonds at the 2-position CH(OH) group and the 1-position CH₂OH group lead to the formation of CH₃CH₂C(O)CH₂OH and CH₃CH₂CH(OH)CHO, respectively, by reactions 1-4. H-atom abstraction from the 3-position CH₂ group leads to formation of the 1,2-hydroxyalkoxy radical CH₃CH(O[•])CH(OH)CH₂OH (reaction 7a) and a small amount of a nitrate (reaction 7b).



The 1,2-hydroxyalkoxy radical is predicted (Atkinson, 1997a,b; Aschmann and Atkinson, 1999; Aschmann *et al.*, 2001b), using listed or estimated heats of formation for the various species from National Institute of Standards and Technology (1994), Kerr and Stocker (1999/2000) and Atkinson *et al.*, 2000b), to dominantly decompose rather than react with O₂



with the α -hydroxy radical reacting with O₂ to form glycolaldehyde. It should be noted that CH₃CHO could not be quantified using SPME due to background interferences.



By analogous reactions to reactions 5-7, H-atom abstraction from the 4-position CH_3 group, which is predicted to account for <1% of the overall OH radical reaction (Kwok and Atkinson, 1995; Bethel *et al.*, 2001), leads to the alkoxy radical $^\bullet\text{OCH}_2\text{CH}_2\text{CH}(\text{OH})\text{CH}_2\text{OH}$ which is predicted (Atkinson, 1997a,b; Aschmann and Atkinson, 1999; Aschmann *et al.*, 2001b) to dominantly isomerize through a 6-membered transition state to ultimately form $\text{HOCH}_2\text{CH}_2\text{CH}(\text{OH})\text{CHO}$.

The hydroxycarbonyls observed (Table 17) are in accord with the expected reactions, and our measured yields are in good agreement with predictions made using the estimation method of Kwok and Atkinson (1995) and Bethel *et al.* (2001) to calculate the percentages of the overall OH radical reaction occurring at the various C-H bonds, combined with estimates of the fates of the various hydroxyalkoxy radicals (as discussed above and shown in Table 17).

1,3-Butanediol

H-atom abstraction from the C-H bonds of the 3-position $\text{CH}(\text{OH})$ and 1-position CH_2OH groups leads to formation of $\text{CH}_3\text{C}(\text{O})\text{CH}_2\text{CH}_2\text{OH}$ and $\text{CH}_3\text{CH}(\text{OH})\text{CH}_2\text{CHO}$, respectively (see above). H-atom abstraction from the 2-position CH_2 group leads, by reactions analogous to reactions 5-7, to the hydroxyalkoxy radical $\text{CH}_3\text{CH}(\text{OH})\text{CH}(\text{O}^\bullet)\text{CH}_2\text{OH}$, which is predicted (Atkinson, 1997a,b; Aschmann and Atkinson, 1999; Aschmann *et al.*, 2001b) to dominantly decompose, mainly (~93%) by the pathway,



with the alternative decomposition pathway 10b being minor, and with the α -hydroxy radicals $\text{CH}_3\text{C}^\bullet\text{HOH}$ and $\text{C}^\bullet\text{H}_2\text{OH}$ reacting with O_2 (Atkinson, 1994) to form CH_3CHO and HCHO , respectively (not quantified here due to background interferences).



H-atom abstraction from the 4-position CH_3 group, which is expected to account for ~2% of the overall OH radical reaction (Kwok and Atkinson, 1995; Bethel *et al.*, 2001), leads to the hydroxyalkoxy radical $^\bullet\text{OCH}_2\text{CH}(\text{OH})\text{CH}_2\text{CH}_2\text{OH}$ which is predicted (Atkinson, 1997a,b; Aschmann and Atkinson, 1999; Aschmann *et al.*, 2001b) to mainly isomerize to ultimately form $\text{HOCH}_2\text{CH}(\text{OH})\text{CH}_2\text{CHO}$.

Again as shown in Table 17, the hydroxycarbonyls observed are in accord with the expected reactions, and our measured yields are in reasonable agreement with predictions.

2,3-Butanediol

H-atom abstraction from the two equivalent $\text{CH}(\text{OH})$ groups leads to the formation of $\text{CH}_3\text{C}(\text{O})\text{CH}(\text{OH})\text{CH}_3$. H-atom abstraction from the two equivalent CH_3 groups leads, after reactions analogous to reactions 5-7, to formation of the hydroxyalkoxy radical $^\bullet\text{OCH}_2\text{CH}(\text{OH})\text{CH}(\text{OH})\text{CH}_3$, which is predicted (Atkinson, 1997a,b; Aschmann and Atkinson, 1999; Aschmann *et al.*, 2001b) to decompose and isomerize at approximately similar rates. Isomerization is expected to lead to formation of $\text{HOCH}_2\text{CH}(\text{OH})\text{CH}(\text{OH})\text{CHO}$, while decomposition forms HCHO plus $\text{CH}_3\text{CH}(\text{OH})\text{CHO}$. As shown in Table 17, the dominant product observed was $\text{CH}_3\text{C}(\text{O})\text{CH}(\text{OH})\text{CH}_3$ together with a minor amount of $\text{CH}_3\text{CH}(\text{OH})\text{CHO}$.

2-Methyl-2,4-pentanediol

H-atom abstraction from the 4-position CH(OH) group leads to formation of 4-hydroxy-4-methyl-2-pentanone, (CH₃)₂C(OH)CH₂C(O)CH₃ (Table 17). The other major initial reaction involves H-atom abstraction from the 3-position CH₂ group, leading (after reactions analogous to reactions 5-7) to the hydroxyalkoxy radical (CH₃)₂C(OH)CH(O•)CH(OH)CH₃, which is predicted (Atkinson, 1997a,b; Aschmann and Atkinson, 1999; Aschmann *et al.*, 2001b) to dominantly decompose by the pathway



followed by reaction of CH₃C•(OH)CH₃ with O₂ to form CH₃C(O)CH₃ plus HO₂.

The minor initial reaction pathways involving H-atom abstraction from the CH₃ groups (predicted to account for <10% of the overall reaction) are expected to lead to formation of (CH₃)₂C(OH)CH₂CHO plus HCHO after H-atom abstraction from the 5-position CH₃ group and HOCH₂C(OH)(CH₃)CH₂C(O)CH₃ after H-atom abstraction from the two equivalent 1-position CH₃ groups followed by isomerization of the initially-formed alkoxy radical. The major hydroxycarbonyls observed here were those expected, with the (CH₃)₂C(OH)CH₂CHO product predicted to be formed in ~2% yield (see Table 17) being observed in the GC-MS analysis, but too minor for GC-FID quantification. No oxime attributable to the dihydroxyketone was observed.

5.2.5. Conclusion

The predicted hydroxycarbonyls and their associated yields, obtained from estimates of the percentages of the OH radical reaction proceeding by H-atom abstraction from the various C-H groups combined with estimates of the reaction rates of the intermediate alkoxy radicals, are given in Table 17 (H-atom abstraction from the O-H bonds is expected to account for <1% of the overall reactions in all cases and is neglected here). Using SPME sampling with on-fiber derivatization, we have been able to observe the hydroxycarbonyls predicted to be formed in >1-2% yield (the predicted dihydroxycarbonyl HOCH₂C(OH)(CH₃)CH₂C(O)CH₃ was not observed). Taking into account the likely uncertainties in the hydroxyaldehyde quantifications, the predicted formation yields are in generally reasonable agreement with the measured yields, and we can account for 71-103% of the reaction pathways occurring. Clearly, the use of coated SPME fibers with on-fiber derivatization and GC-MS and GC-FID analyses can provide qualitative and quantitative information concerning the formation of hydroxyaldehydes which was not available using earlier sampling techniques.

5.3. H-atom Abstraction from Selected C-H Bonds in 2,3-Dimethylpentanal, 1,4-Cyclohexadiene and 1,3,5-Cycloheptatriene

5.3.1. Introduction

For many volatile organic compounds (VOCs) emitted into the atmosphere, daytime reaction with the OH radical is an important, and often dominant, transformation process (Atkinson, 2000). For alkanes, alkenes, aromatic hydrocarbons and oxygenated compounds, these OH radical reactions proceed by H-atom abstraction from C-H and O-H bonds, OH radical addition to the carbon atoms of C=C bonds and by OH radical addition to the carbon atoms of aromatic rings (Atkinson, 1994, 1997a, 2000; Kwok and Atkinson, 1995; Calvert *et al.*, 2000, 2002). While the overall rate constants for the gas-phase reactions of OH radicals with over 500 VOCs have been measured (Kwok and Atkinson, 1995), the partial rate constants for H-atom abstraction from the various C-H (or O-H) bonds are known only for a small sub-set of these VOCs. These partial rate data have been obtained from, for example, kinetic studies of alkanes (Droege and Tully, 1986a,b; Tully *et al.*, 1986; Atkinson, 1989), alcohols (Hess and Tully, 1988; McCaulley *et al.*, 1989; Dunlop and Tully, 1993), methyl hydroperoxide (Vaghjiani and Ravishankara, 1989) and toluene (Tully *et al.*, 1981), using partially- and fully-deuterated VOCs or using ^{16}OH and ^{18}OH radicals, and from product studies of a number of VOCs [for example, of 1,3- and 1,4-cyclohexadiene (Ohta, 1984), *n*-pentane (Atkinson *et al.*, 1995a), diethyl ether (Atkinson, 1994), methyl *tert*-butyl ether (Atkinson, 1994), and selected diols (Bethel *et al.*, 2001; see also Section 5.2) and alcohols (Chew and Atkinson, 1996; Baxley and Wells, 1998; Cavalli *et al.*, 2000, 2002)].

The major focus of this study was to investigate the importance of H-atom abstraction from sites in an aliphatic aldehyde other than from the CHO group. For the reaction of OH radicals with acetaldehyde the major reaction pathway involves H-atom abstraction from the CHO group (Cameron *et al.*, 2002),



and it is generally accepted that H-atom abstraction from the CHO group dominates for higher aldehydes such as propanal and butanal (Kwok and Atkinson, 1995), although no data are presently available to confirm this. The potential mechanisms of a number of commercially available aldehydes were reviewed, using empirical predictive methods (Atkinson, 1997b; Aschmann *et al.*, 2001b), to assess which aldehyde(s) could lead to a product or products which would be unique to H-atom abstraction from C-H bond(s) other than that on the CHO group. 2,3-Dimethylpentanal [$\text{CH}_3\text{CH}_2\text{CH}(\text{CH}_3)\text{CH}(\text{CH}_3)\text{CHO}$] appeared to fit this criteria, with H-atom abstraction from the 2-position CH group being predicted methods (Atkinson, 1997b; Aschmann *et al.*, 2001b) to lead only to formation of 3-methyl-2-pentanone, a product which is predicted not to be formed to any significant extent after H-atom abstraction from any other C-H bond in 2,3-dimethylpentanal. Accordingly, in this work we have investigated the kinetics and products of the reaction of OH radicals with 2,3-dimethylpentanal. In addition, we have investigated the importance of H-atom abstraction by OH radicals from the allylic C-H bonds in 1,4-cyclohexadiene and 1,3,5-cycloheptatriene by measuring the formation yields of benzene from 1,4-cyclohexadiene and of tropone (2,4,6-cycloheptatrienone) from 1,3,5-cycloheptatriene, noting that Ohta (1984) previously observed the formation of benzene from the OH radical-initiated reaction of 1,4-cyclohexadiene in 15% yield (and from 1,3-cyclohexadiene in 7% yield).

5.3.2. Experimental Methods

Experiments to measure the rate constant for the reaction of OH radicals with 2,3-dimethylpentanal and to investigate the formation of selected products from the OH radical-initiated reactions of 2,3-dimethylpentanal, 1,4-cyclohexadiene and 1,3,5-cycloheptatriene were carried out at 298 ± 2 K and 740 Torr total pressure of synthetic air (80% N₂ + 20% O₂) in a 5870 liter evacuable, Teflon-coated chamber equipped with an *in situ* multiple-reflection optical system interfaced to a Mattson Galaxy 5020 FT-IR spectrometer. Irradiation was provided by a 24-kW xenon arc lamp, with the light being filtered through a 6 mm thick Pyrex pane to remove wavelengths <300 nm. The chamber is fitted with two Teflon-coated fans to ensure rapid mixing of reactants during their introduction into the chamber. IR spectra were recorded with 32 scans per spectrum (corresponding to 1.2 min averaging time), a full-width-at-half-maximum resolution of 0.7 cm⁻¹ and a path length of 62.9 m.

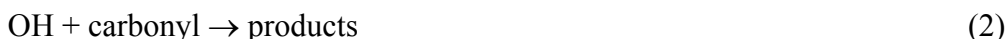
Preliminary experiments on the OH radical-initiated reactions of 2,3-dimethylpentanal and 1,3,5-cycloheptatriene and experiments to measure the rate constants for the reactions of OH radicals with 3-methyl-2-pentanone and tropone and to determine the formation yield of benzene from 1,4-cyclohexadiene were carried out at 298 ± 2 K and 740 Torr total pressure of purified air (at ~5% relative humidity) in a 7000 liter Teflon chamber equipped with two parallel banks of blacklamps for irradiation and a Teflon-coated fan to ensure rapid mixing of reactants during their introduction into the chamber. Analyses were by gas chromatography with flame ionization detection (GC-FID). For these GC-FID analyses, 100 cm³ volume gas samples were collected from the chamber either onto Tenax-TA solid adsorbent with subsequent thermal desorption at ~250 °C onto a 30 m DB-1701 megabore column held at -40 °C and then temperature programmed at 8 °C min⁻¹ to 200 °C (solid adsorbent/thermal desorption procedure), or were collected in an all-glass, gas-tight syringe with subsequent transfer via a 1 cm³ gas sampling valve onto a 30 m DB-5 megabore column held at -25 °C and then temperature programmed at 8 °C min⁻¹ to 200 °C (gas transfer/gas sampling valve procedure).

Kinetic Studies

Rate constants for the reactions of OH radicals with 2,3-dimethylpentanal, 3-methyl-2-pentanone and tropone were determined using a relative rate technique, in which the relative decays of the carbonyl compound and a reference compound, whose OH radical reaction rate constant is reliably known, were measured in the presence of OH radicals. Provided that the carbonyls and the reference compound reacted only with OH radicals, then,

$$\ln\left(\frac{[\text{carbonyl}]_{t_0}}{[\text{carbonyl}]_t}\right) = \frac{k_2}{k_3} \ln\left(\frac{[\text{reference compound}]_{t_0}}{[\text{reference compound}]_t}\right) \quad (\text{I})$$

where [carbonyl]_{t₀} and [reference compound]_{t₀} are the concentrations of 2,3-dimethylpentanal, 3-methyl-2-pentanone or tropone and reference compound at time t₀, respectively, [carbonyl]_t and [reference compound]_t are the corresponding concentrations at time t, and k₂ and k₃ are the rate constants for reactions (2) and (3), respectively.



Hydroxyl radicals were generated in the presence of NO by the photolysis of CH₃ONO in air at wavelengths >300 nm.

The initial reactant concentrations for the experiments involving 2,3-dimethylpentanal carried out in the evacuable chamber were (in molecule cm⁻³): CH₃ONO, 2.46 x 10¹⁴; NO, 2.46 x 10¹⁴; 2,3-dimethylpentanal, (2.36-2.41) x 10¹⁴; and 2-methylpropene (the reference compound), (1.84-2.46) x 10¹⁴. Irradiations were carried out intermittently in 6 min periods, with IR spectra being recorded during the dark periods and with total irradiation times of 18 min.

For experiments carried out in the Teflon chamber, the initial reactant concentrations (molecule cm⁻³) were: CH₃ONO, ~2.4 x 10¹⁴; NO, ~2.4 x 10¹⁴; 3-methyl-2-pentanone or tropone, ~2.4 x 10¹³; and *n*-octane or methyl vinyl ketone (the reference compounds), ~2.4 x 10¹³. Irradiations were carried out for 3-45 mins, resulting in the reaction of up to 39-73% of the carbonyls or reference compounds. The concentrations of 3-methyl-2-pentanone, tropone, *n*-octane and methyl vinyl ketone were measured by GC-FID using the solid adsorbent/thermal desorption procedure.

Product Studies

Experiments in the Teflon chamber with GC analyses were conducted as described above for the kinetic experiments, with similar initial reactant concentrations and GC-FID analysis procedures, except that no reference compound was present.

For the experiments conducted in the evacuable chamber with *in situ* FT-IR analyses, the initial reactant concentrations (in molecule cm⁻³) were: CH₃ONO, 2.46 x 10¹⁴; NO, 2.46 x 10¹⁴; 2,3-dimethylpentanal, (2.35-2.41) x 10¹⁴, 1,4-cyclohexadiene, 3.69 x 10¹⁴ (including the benzene impurity initially present), or 1,3,5-cycloheptatriene, 2.46 x 10¹⁴. 2-Methylpropene was present in two of the three 2,3-dimethylpentanal experiments at an initial concentration of (1.84-2.46) x 10¹⁴ molecule cm⁻³. For 2,3-dimethylpentanal, the three experiments involved intermittent irradiation (6-10 min duration each) with IR spectra being recorded during the dark periods and with total irradiation times of 18-28 min. For 1,3,5-cycloheptatriene, one experiment was carried out with intermittent irradiation (1-5 min duration) for a total irradiation time of 20 min. For 1,4-cyclohexadiene, one irradiation was carried out with continuous irradiation for 15 min.

Because of the difficulties in quantifying the carbonyl products from the 2,3-dimethylpentanal reaction solely by FT-IR spectroscopy, concurrent GC-FID analyses using the solid adsorbent/thermal desorption procedure were carried out. These GC-FID analyses for specific carbonyl products were used as a basis for subtracting the spectral contributions of these compounds from the total product spectra (see below), thus facilitating the FT-IR analyses of other species, including the parent compound.

Chemicals

The sources and stated purities of the chemicals used were: 2,3-dimethylpentanal (93%), Chemsampco; 1,4-cyclohexadiene (97%), 1,3,5-cycloheptatriene (90%), tropone (97%), 2-butanone (99%), 3-methyl-2-pentanone (99%), and acetaldehyde (99.5+%), Aldrich Chemical Company; benzene (99.9+%), American Burdick and Jackson; and NO (≥99.0%), Matheson Gas Products. All of the above compounds were used as received, except for 2,3-dimethylpentanal which was fractionated in a vacuum line with a middle fraction being collected and used for the experiments. Methyl nitrite was prepared as described by Taylor *et al.* (1980) and stored under vacuum at 77 K.

5.3.3. Results

1,4-Cyclohexadiene

Preliminary experiments in the Teflon chamber with analyses by GC-FID using the solid adsorbent/thermal desorption procedure showed significant artifact formation of benzene from 1,4-cyclohexadiene during the sampling and analysis procedure. However, GC-FID analyses involving transfer of gas samples onto the GC column via a gas sampling valve showed no evidence for such artifact benzene formation (although benzene was observed to be present in the 1,4-cyclohexadiene sample used, at levels of 2.6% and 6.3% in the two independent sets of experiments conducted using GC-FID analyses). Two sets of experiments were carried out, with independent calibrations of the GC-FID response factors for 1,4-cyclohexadiene and benzene, and plots of the amounts of benzene formed against the amounts of 1,4-cyclohexadiene reacted are shown in Figure 54. Corrections for secondary reaction of benzene with OH radicals were negligible (<1%). The benzene formation yields obtained from least-squares analyses of the data from these two sets of experiments were $12.7 \pm 2.4\%$ and $12.6 \pm 1.5\%$, where the indicated errors are two least-squares standard deviations combined with estimated overall uncertainties in the GC-FID response factors for 1,4-cyclohexadiene and benzene of $\pm 5\%$ each.

A vapor sample of 1,4-cyclohexadiene introduced into the evacuable chamber initially contained 7.1% benzene, as analyzed by *in situ* FT-IR spectroscopy. The sharp Q-branch of benzene at 674 cm^{-1} and the series of sharp peaks of 1,4-cyclohexadiene at around $\sim 960\text{ cm}^{-1}$ were used for IR analyses. Irradiation of a $\text{CH}_3\text{ONO} - \text{NO} - 1,4\text{-cyclohexadiene} - \text{air}$ mixture resulted in a benzene yield of $12.2 \pm 2.2\%$ (see the plot in Figure 54), where the indicated error is two least-squares standard deviations combined with $\pm 4\%$ and $\pm 7\%$ estimated uncertainties in the IR analyses of 1,4-cyclohexadiene and benzene, respectively.

1,3,5-Cycloheptatriene

Preliminary experiments in the Teflon chamber with analyses by GC-FID using the solid adsorbent/thermal desorption procedure showed significant artifact formation of tropone from cycloheptatriene during the sampling and analysis procedure. Furthermore, tropone could not be analyzed by GC-FID involving transfer of gas samples onto the GC column via a gas sampling valve. It was hence not possible to investigate the formation of tropone from the OH radical-initiated reaction of cycloheptatriene using GC for analysis, and experiments were therefore carried out in the evacuable chamber with analyses by *in situ* FT-IR spectroscopy.

However, tropone could be reliably analyzed in the absence of cycloheptatriene by GC-FID using the solid adsorbent/thermal desorption procedure. Accordingly, the rate constant for the reaction of OH radicals with tropone was measured using the relative rate method, with methyl vinyl ketone as the reference compound. The data obtained from three experiments are plotted in accordance with Equation (I) in Figure 55, and a least-squares analysis yields the rate constant ratio k_2/k_3 and rate constant k_2 given in Table 19.

In the experiments with *in situ* FT-IR spectroscopic analyses, after subtraction of IR absorption bands of the remaining cycloheptatriene and CH_3ONO and of the photooxidation products NO_2 , HCHO , HC(O)OH , HNO_3 and CH_3ONO_2 , no evidence for the formation of tropone or of its isomer benzaldehyde was obtained. The IR analyses of cycloheptatriene, tropone and benzaldehyde were based on their distinct peaks at 709 , 1656 , and 688 cm^{-1} , respectively. After taking into account secondary reactions of tropone and benzaldehyde with OH radicals, using rate constants for the reactions of OH radicals with cycloheptatriene, tropone and benzaldehyde (in units of $10^{-11}\text{ cm}^3\text{ molecule}^{-1}\text{ s}^{-1}$) of 9.95 (Atkinson, 1997a), 4.2 (Table 19) and 1.6 (Atkinson, 1994), respectively, upper limits to the formation yields of tropone and benzaldehyde from cycloheptatriene of $<1.2\%$ and $<0.7\%$, respectively, were obtained.

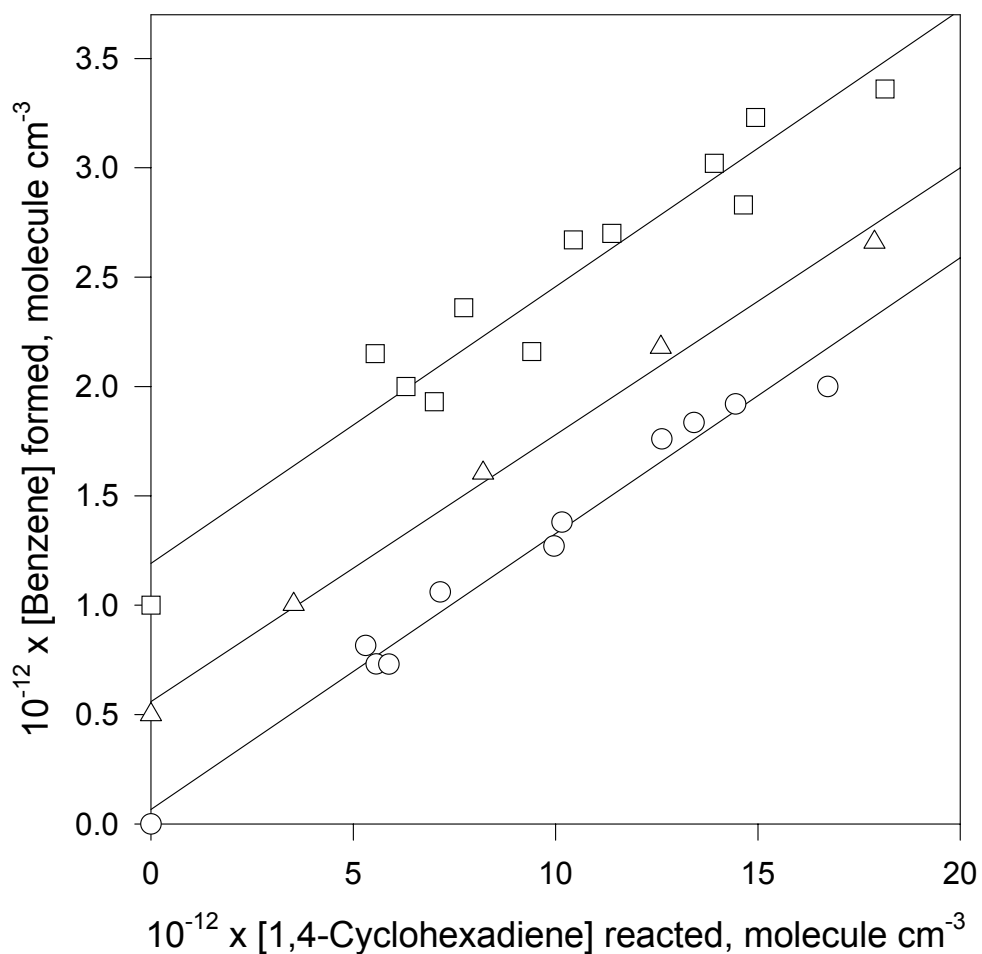


Figure 54. Plots of the amounts of benzene formed against the amounts of 1,4-cyclohexadiene reacted with the OH radical. □, o - Analyses by GC-FID (two independent sets of experiments with three experiments per set); Δ - analyses by *in situ* FT-IR spectroscopy from a single experiment. Data with □ and Δ symbols have been displaced vertically by 1.0 and 0.5 units, respectively, for clarity.

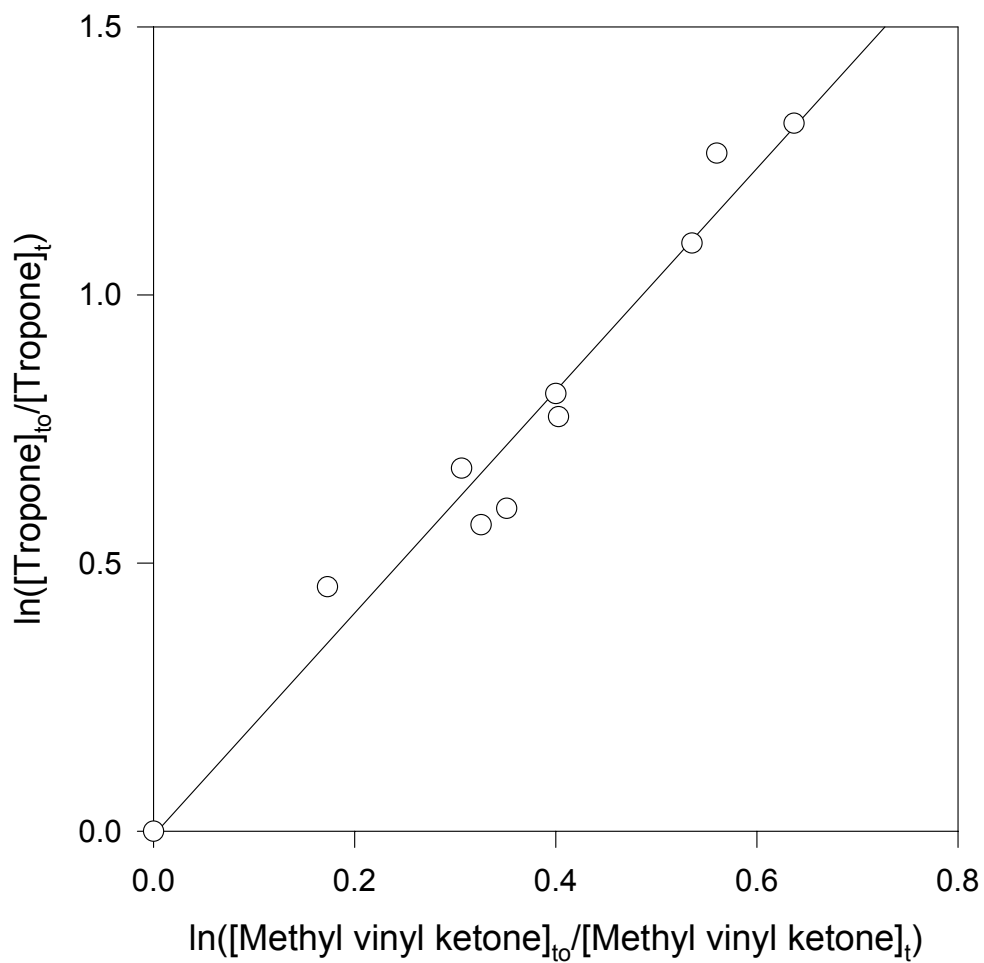


Figure 55. Plot of Equation (I) for the reaction of OH radicals with tropone, with methyl vinyl ketone as the reference compound. Analyses were by GC-FID.

Table 19. Rate constant ratios k_2/k_3 and rate constants k_2 ($\text{cm}^3 \text{ molecule}^{-1} \text{ s}^{-1}$) for the gas-phase reactions of OH radicals with tropone, 2,3-dimethylpentanal and 3-methyl-2-pentanone at $298 \pm 2 \text{ K}$

carbonyl	reference compound	k_2/k_3 ^a	$10^{12} \times k_2$ ^{a,b}
tropone	methyl vinyl ketone	2.07 ± 0.29	42 ± 6
2,3-dimethylpentanal	2-methylpropene	0.82 ± 0.13	42 ± 7
3-methyl-2-pentanone	<i>n</i> -octane	0.789 ± 0.009	6.87 ± 0.08

^aIndicated uncertainties are two least-squares standard deviations, except for 2,3-dimethylpentanal where an additional $\pm 15\%$ uncertainty in k_2/k_3 (0.815 ± 0.032 with two least-squares uncertainties) has been included to account for possible additional errors in the subtraction procedure.

^bPlaced on an absolute basis by use of rate constants k_3 ($\text{cm}^3 \text{ molecule}^{-1} \text{ s}^{-1}$) at 298 K of k_3 (methyl vinyl ketone) = 2.01×10^{-11} (IUPAC, 2003), k_3 (2-methylpropene) = 5.14×10^{-11} (Atkinson, 1997a), and k_3 (*n*-octane) = 8.71×10^{-12} (Atkinson, 1997a). The cited rate constants k_2 do not include the uncertainties (estimated to be $\sim \pm 10\%$) in the rate constants k_3 .

2,3-Dimethylpentanal

Initial GC-FID analyses of 2,3-dimethylpentanal using the Tenax/thermal desorption procedure showed no analytical problems in the absence of NO_x , with no decrease in the 2,3-dimethylpentanal concentration in the dark over a period of several hours. However, in the presence of NO_x , the 2,3-dimethylpentanal GC peak area was observed to decrease with time, gradually leveling off after ~ 4 hrs to a value 40-45% lower than the initial analysis, with a concurrent increase in the GC-FID peak area of 2-butanone (but not of 3-methyl-2-pentanone) over this time period. Because analogous experiments with *in situ* FT-IR analysis did not show this behavior, it appears that degradation of 2,3-dimethylpentanal occurs in the presence of NO_x , presumably due to reaction with NO_2 on the Tenax solid adsorbent during sampling and/or thermal desorption.

Therefore experiments to measure the rate constant for the reaction of OH radicals with 2,3-dimethylpentanal and to investigate the products formed were carried out in the evacuable chamber with *in situ* FT-IR analyses of 2,3-dimethylpentanal (and certain other species). In these experiments the infrared analyses involved subtraction of absorption bands by the unreacted CH_3ONO and its photolysis products in the presence of NO (*i.e.*, HCHO, CH_3ONO_2 , HNO_3 , HONO, HCOOH, H_2O , and NO_2). The analysis of 2,3-dimethylpentanal utilized its strongest band at 1743 cm^{-1} but required prior subtraction of overlapped absorption bands by 2-butanone, 3-methyl-2-pentanone, and acetaldehyde, as well as by acetone when 2-methylpropene was a component of the irradiated mixture. Subtraction of the CH_3CHO absorption bands was based on its sharp absorption feature at 1352 cm^{-1} . Subtractions of the absorption bands by 2-butanone and 3-methyl-2-pentanone using calibrated spectra were based on their concurrent analyses by GC-FID. 2-Methylpropene, used as the reference compound in the kinetic experiments, was analyzed by its weak, but sharp, peak at 890 cm^{-1} , while the absorption bands of its main oxidation product $\text{CH}_3\text{C}(\text{O})\text{CH}_3$ (along with HCHO) were subtracted based on its distinct band at 1365 cm^{-1} .

Rate constants for the reactions of OH radicals with 2,3-dimethylpentanal and 3-methyl-2-pentanone were measured using the relative rate method, with 2-methylpropene and *n*-octane as the reference compounds, respectively. Data from CH₃ONO – NO – 2,3-dimethylpentanal – 2-methylpropene – air irradiations carried out in the evacuable chamber with *in situ* FT-IR analyses and from CH₃ONO – NO – 3-methyl-2-pentanone – *n*-octane – air irradiations carried out in the Teflon chamber with GC-FID analyses are plotted in accordance with Equation (I) in Figure 56. The rate constant ratios k_2/k_3 and rate constants k_2 obtained from these data by least-squares analyses are given in Table 19.

Products of the reaction of OH radicals with 2,3-dimethylpentanal were also identified and quantified in the two CH₃ONO – NO – 2,3-dimethylpentanal – 2-methylpropene – air irradiations and in an additional CH₃ONO – NO – 2,3-dimethylpentanal – air irradiation. As noted above, the concentrations of 2,3-dimethylpentanal during the experiments were measured by FT-IR spectroscopy, and the concentrations of 2-butanone and 3-methyl-2-pentanone were measured by GC-FID. The acetaldehyde concentrations were determined by both FT-IR and GC-FID in one experiment and by GC-FID in the other two experiments, noting that both FT-IR and GC-FID have relatively low sensitivity for acetaldehyde. Figure 57 illustrates the spectra obtained from the irradiated CH₃ONO – NO – 2,3-dimethylpentanal – air mixture with 31% of the initial 2.35×10^{14} molecule cm⁻³ of 2,3-dimethylpentanal reacting after a total irradiation time of 18 min, and with corresponding amounts (in units of 10^{13} molecule cm⁻³) of 2-butanone, 3-methyl-2-pentanone and acetaldehyde of 1.75, 0.44 and 4.82, respectively, being formed.

The products also react with OH radicals, and their secondary reactions were taken into account as described previously (Atkinson *et al.*, 1982), using the rate constants measured here for 2,3-dimethylpentanal and 3-methyl-2-pentanone and the recommended values (IUPAC, 2003) for acetaldehyde and 2-butanone. Corrections for secondary reactions were <1% for 2-butanone, <5% for 3-methyl-2-pentanone, and <11% for acetaldehyde. Plots of the amounts of acetaldehyde, 2-butanone and 3-methyl-2-pentanone formed, corrected for reaction with OH radicals, against the amounts of 2,3-dimethylpentanal reacted with OH radicals are shown in Figures 58 (acetaldehyde and 2-butanone) and 59 (3-methyl-2-pentanone). The formation yields of acetaldehyde and 2-butanone decrease with increasing extent of reaction (see Discussion below), and were uniformly lower during the two experiments with 2-methylpropene present. This behavior suggests that at least part of the acetaldehyde and 2-butanone observed arise from reactions involving an acylperoxy radical precursor(s) [see below and Atkinson and Aschmann (1995)]. In contrast, the plot (Figure 59) for 3-methyl-2-pentanone is a good straight line with no evidence for curvature, and hence no evidence for the intermediary of an acylperoxy radical. The formation yields for 3-methyl-2-pentanone and (based on the initial slopes obtained from a second-order regression) for acetaldehyde and 2-butanone are given in Table 20.

The residual IR spectra (see Figure 57C) showed a set of absorption bands at 795, 1299, 1736, and 1825 cm⁻¹ and another set at 856, 1284, and 1651 cm⁻¹, which can be attributed to the generalized products RC(O)OONO₂ and RONO₂, respectively. After the first 8 min irradiation period in the experiment without 2-methylpropene, which consumed ~17% of the initial 2.35×10^{14} molecule cm⁻³ of 2,3-dimethylpentanal, the remaining NO (~ 1.0×10^{14} molecule cm⁻³) was sufficiently high that the thermal decay of RC(O)OONO₂ (Atkinson, 1994, 2000) during an ensuing 69 min dark period caused spectral differences that allowed separate spectra to be “synthesized” for the RC(O)OONO₂ and RONO₂ species. On the basis of the derived spectra and the common integrated absorption coefficient applicable to the bands at ~1290 cm⁻¹ (Tuazon and Atkinson, 1990), the concentrations of RONO₂ were calculated for the three irradiation periods of this experiment and resulted in an estimated yield of $12 \pm 4\%$ for RONO₂. The yield

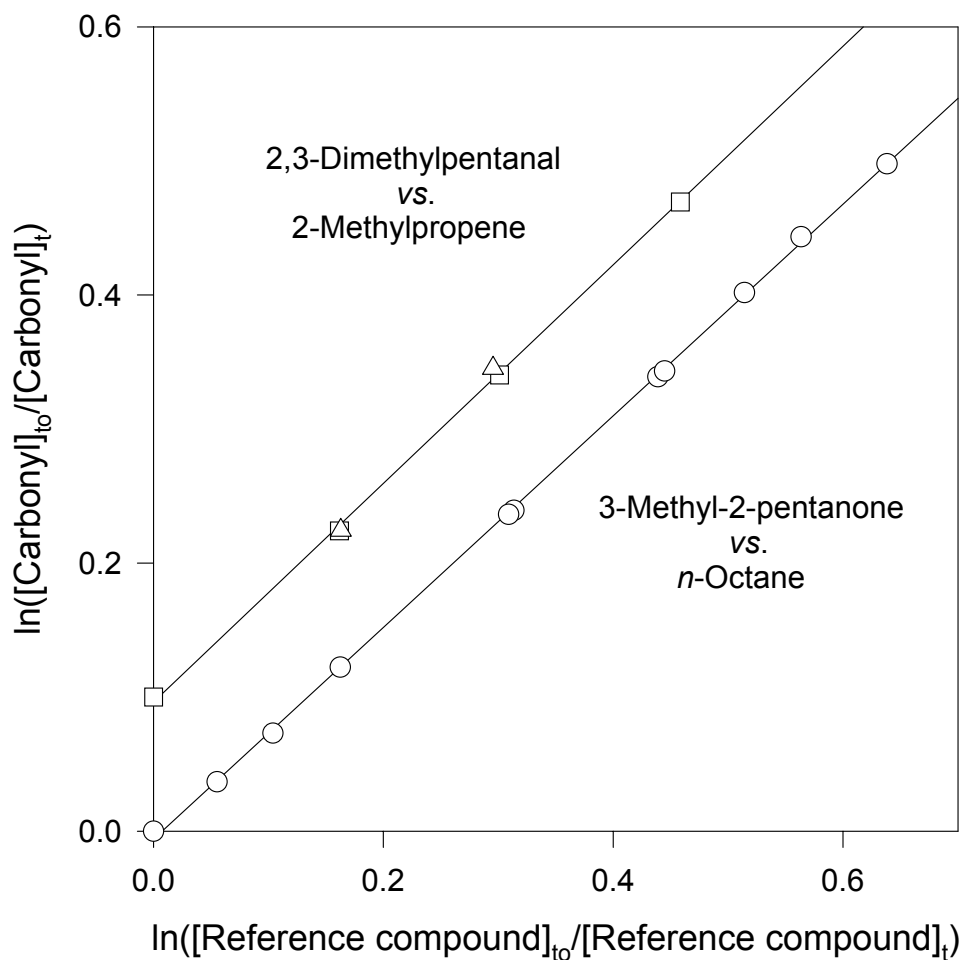


Figure 56. Plots of Equation (I) for the reactions of OH radicals with 3-methyl-2-pentanone and 2,3-dimethylpentanal, with *n*-octane and 2-methylpropene as the reference compounds, respectively. Analyses of 3-methyl-2-pentanone and *n*-octane were by GC-FID, and of 2,3-dimethylpentanal and 2-methylpropene were by *in situ* FT-IR spectroscopy. Data for the 2,3-dimethylpentanal reaction are displaced vertically by 0.1 unit for clarity and the differing symbols for this reaction denote the individual experiments.

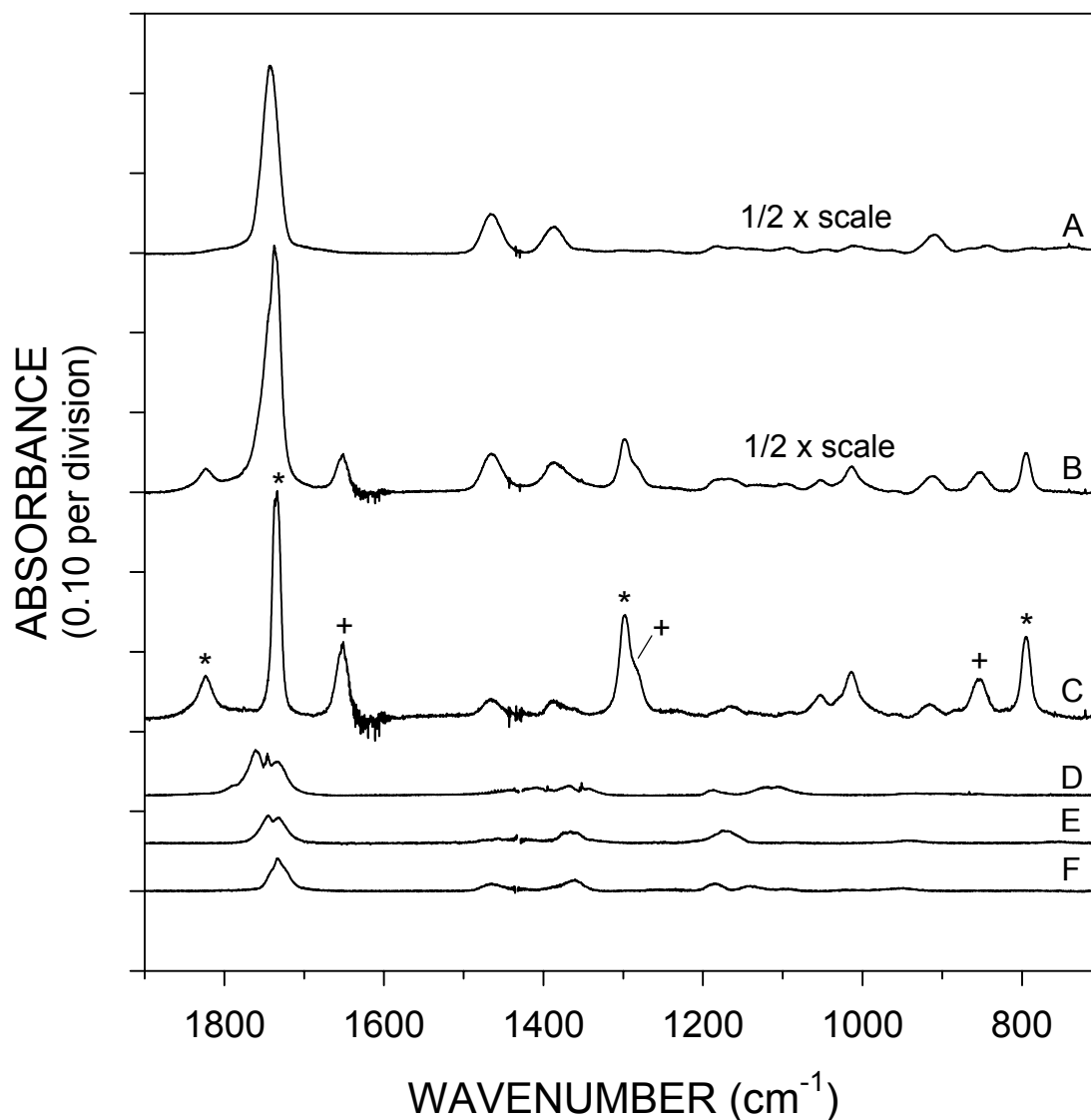


Figure 57. Infrared spectra from a $\text{CH}_3\text{ONO} - \text{NO} - 2,3\text{-dimethylpentanal} - \text{air}$ irradiation (concentrations are in molecule cm^{-3}). (A) Initial 2,3-dimethylpentanal (2.35×10^{14}). (B) Irradiated mixture, with 31% of 2,3-dimethylpentanal reacted, after subtraction of unreacted CH_3ONO and its photolysis products in the presence of NO . (C) From (B) after subtraction of unreacted 2,3-dimethylpentanal and its known carbonyl products acetaldehyde, 2-butanone and 3-methyl-2-pentanone (see text). Peaks marked with + and * are attributed to the products RONO_2 and RC(O)OONO_2 , respectively. (D) CH_3CHO reference (4.92×10^{13}). (E) 2-Butanone reference (2.46×10^{13}). (F) 3-Methyl-2-pentanone reference (2.46×10^{13}).

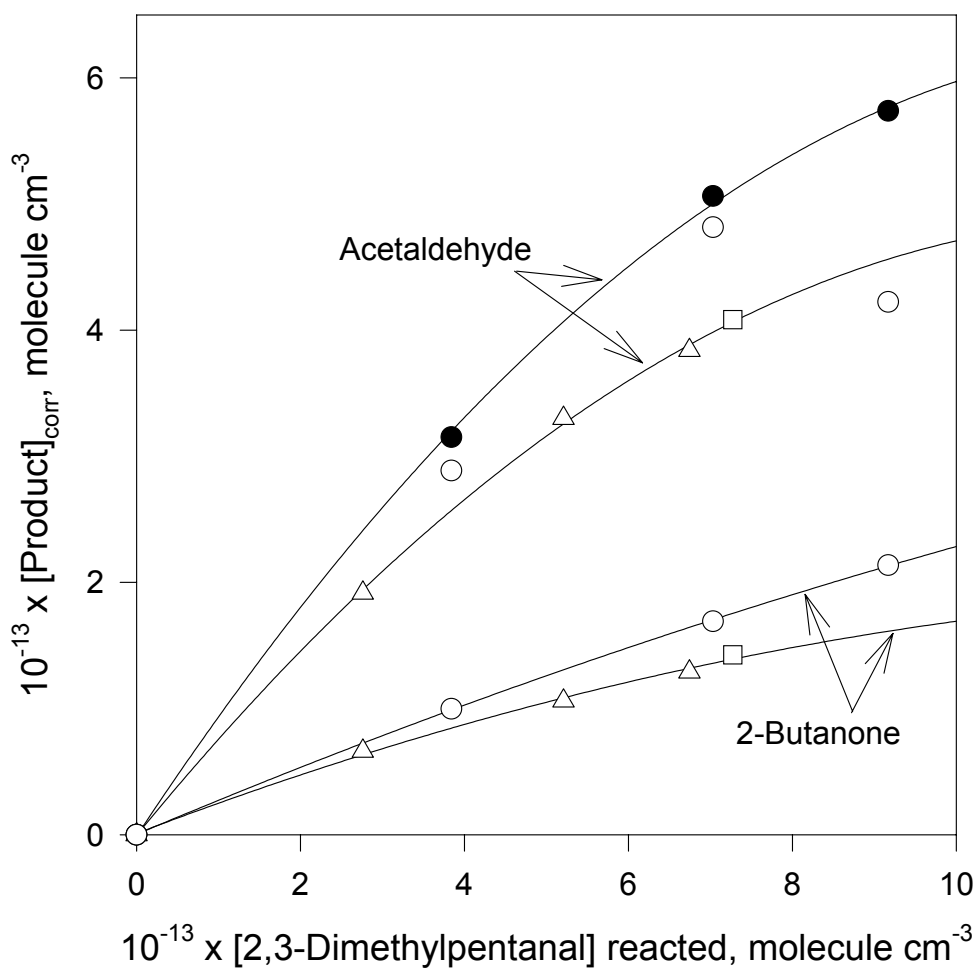


Figure 58. Plots of the amounts of acetaldehyde and 2-butanone formed (corrected for secondary reactions, see text) against the amounts of 2,3-dimethylpentanal reacted with the OH radical. Δ , \square - experiments with 2-methylpropene present, analyses of acetaldehyde and 2-butanone by GC-FID. \circ , \bullet - experiment with no 2-methylpropene present, analyses of products by: \circ - GC-FID, \bullet - *in situ* FT-IR spectroscopy. The lines are from second-order regressions (for acetaldehyde using only the FT-IR data in the experiment without 2-methylpropene).

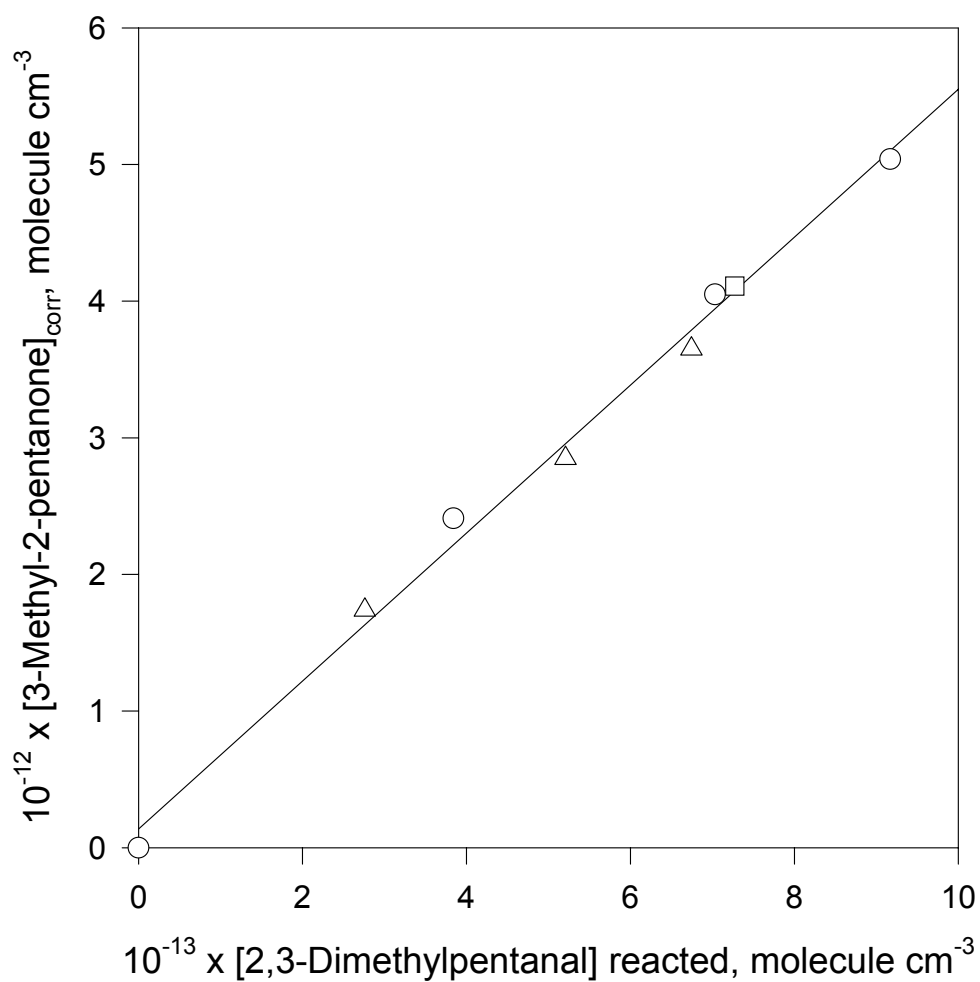


Figure 59. Plot of the amounts of 3-methyl-2-pentanone formed (corrected for secondary reactions, see text) against the amounts of 2,3-dimethylpentanal reacted with the OH radical. Analysis of 3-methyl-2-pentanone by GC-FID and of 2,3-dimethylpentanal by *in situ* FT-IR spectroscopy. Symbols are as in Figure 58.

Table 20. Products observed, and their molar yields, from the reaction of OH radicals with 2,3-dimethylpentanal in the presence of NO

product ^a	molar yield	molar yield at first data point ^b
acetaldehyde	0.98 ^{b,c} 0.80 ^{c,d}	0.82
2-butanone	0.27 ^{b,c} 0.25 ^{c,d}	0.26
3-methyl-2-pentanone	0.054 ± 0.010 ^e	0.054 ± 0.010
RC(O)OONO ₂		0.28
RONO ₂	0.12 ± 0.04 ^b	0.12 ± 0.04

^a2,3-Dimethylpentanal, organic nitrates (RONO₂), acylperoxy nitrates (RC(O)OONO₂) and, in the experiments without 2-methylpropene, acetaldehyde were measured by FT-IR spectroscopy, and acetaldehyde, 2-butanone and 3-methyl-2-butanone were measured by GC-FID. The measured concentrations of acetaldehyde, 2-butanone and 3-methyl-2-butanone have been corrected for secondary reactions with OH radicals (see text)

^bExperiment without 2-methylpropene present (see text).

^cInitial slope of second-order regression (Figure 58).

^dExperiments with 2-methylpropene present.

^eFrom all three experiments. Indicated error is two least-squares standard deviations of the plot shown in Figure 6 combined with estimated overall uncertainties in the FT-IR analyses for 2,3-dimethylpentanal of ±15% and in the GC-FID response factor for 3-methyl-2-pentanone of ±5%.

of RC(O)OONO₂ for the first irradiation period was estimated as ~28%, but its concentration could not be followed meaningfully for the other irradiation periods due to its thermal decay.

5.3.4. Discussion

H-atom abstraction from 1,4-cyclohexadiene and 1,3,5-cycloheptatriene

In agreement with the previous study of Ohta (1984), we observed benzene to be formed from the reaction of OH radicals with 1,4-cyclohexadiene, and our benzene formation yield of 12.5 ± 1.2% (weighted average, two standard deviation) is in reasonable agreement with those of Ohta (1984) of 15.4 ± 0.3% from CH₃ONO – 1,4-cyclohexadiene – N₂ – O₂ (with ≥100 Torr of O₂) irradiations and 15.1 ± 0.3% from H₂O₂ – 1,4-cyclohexadiene – N₂ – O₂ irradiations (both at a total pressure of one atmosphere). As discussed by Ohta (1984), benzene formation is consistent with the reaction of cyclohexadienyl radicals with O₂ proceeding by H-atom abstraction to form benzene rather than by addition to form the C₆H₇O₂[•] peroxy radical, as shown in Figure 60.

It is also possible that the reaction of O₂ with the cyclohexadienyl radical proceeds by initial addition of O₂ followed by elimination of HO₂. Therefore, H-atom abstraction from the allylic C-H bonds in cyclohexadiene accounts for 12-15% of the overall OH radical reaction, with the remainder proceeding by OH radical addition to form the 1-hydroxycyclohex-4-en-2-yl radical. The C-H bond dissociation energy of the allylic C-H bonds in cyclohexadiene is 76.3 kcal mol⁻¹,

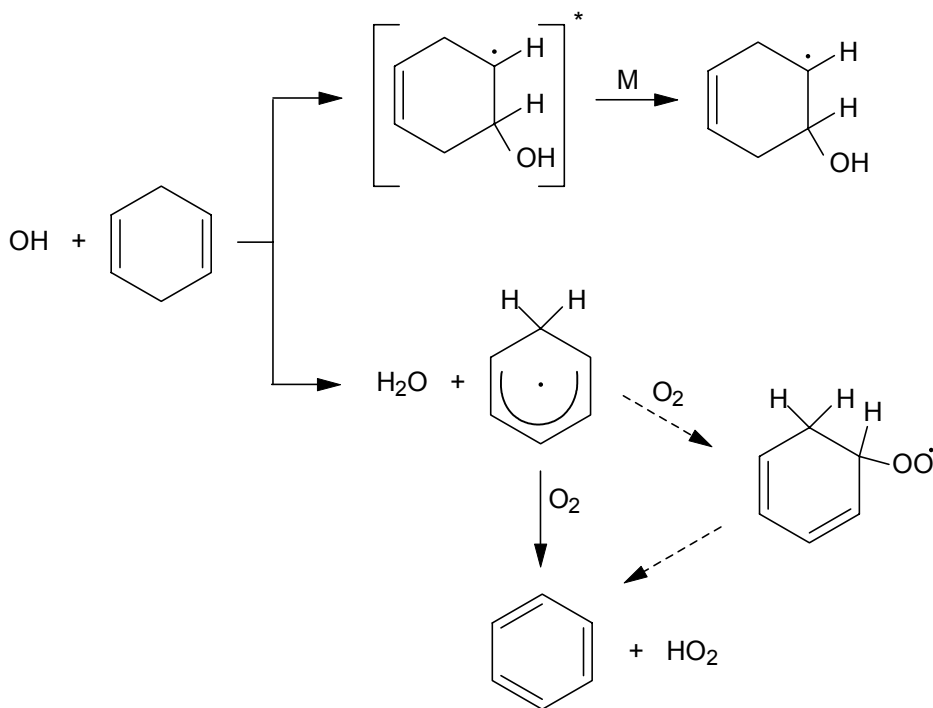


Figure 60. Reaction scheme for reaction of OH radicals with 1,4-cyclohexadiene.

based on the heats of formation of 1,4-cyclohexadiene (National Institute of Standards and Technology, 1994) and the cyclohexadienyl radical (Tsang, 1986; National Institute of Standards and Technology, 1994).

The C-H bond dissociation energy of the allylic C-H bonds in cycloheptatriene is similar, being in the range $73.2 \text{ kcal mol}^{-1}$ (McMillen and Golden, 1982; National Institute of Standards and Technology, 1994) to $75.6 \text{ kcal mol}^{-1}$ (National Institute of Standards and Technology, 1994; Smith and Hall, 1997), yet we observed no formation of tropone ($<1.2\%$) from the reactions shown in Figure 61, nor of benzaldehyde ($<0.7\%$) [the product arising after any isomerization of tropylium radicals to benzyl radicals (Atkinson, 1994)]. Clearly, either H-atom abstraction is negligible ($<2\%$) or the expected cycloalkoxy radical (A in Figure 61) must decompose rather than reacting with O₂. By analogy with the HOCH₂C(CH₃)=CHCH₂O• radical formed from the reaction of OH radicals with isoprene (Lei and Zhang, 2001; Dibble, 2002), decomposition of the cycloalkoxy radical (A) to form the conjugated vinyl radical HC(O)CH=CHCH=CHCH=C•H is expected to be slow. It therefore appears that for cycloheptatriene H-atom abstraction is of no importance.

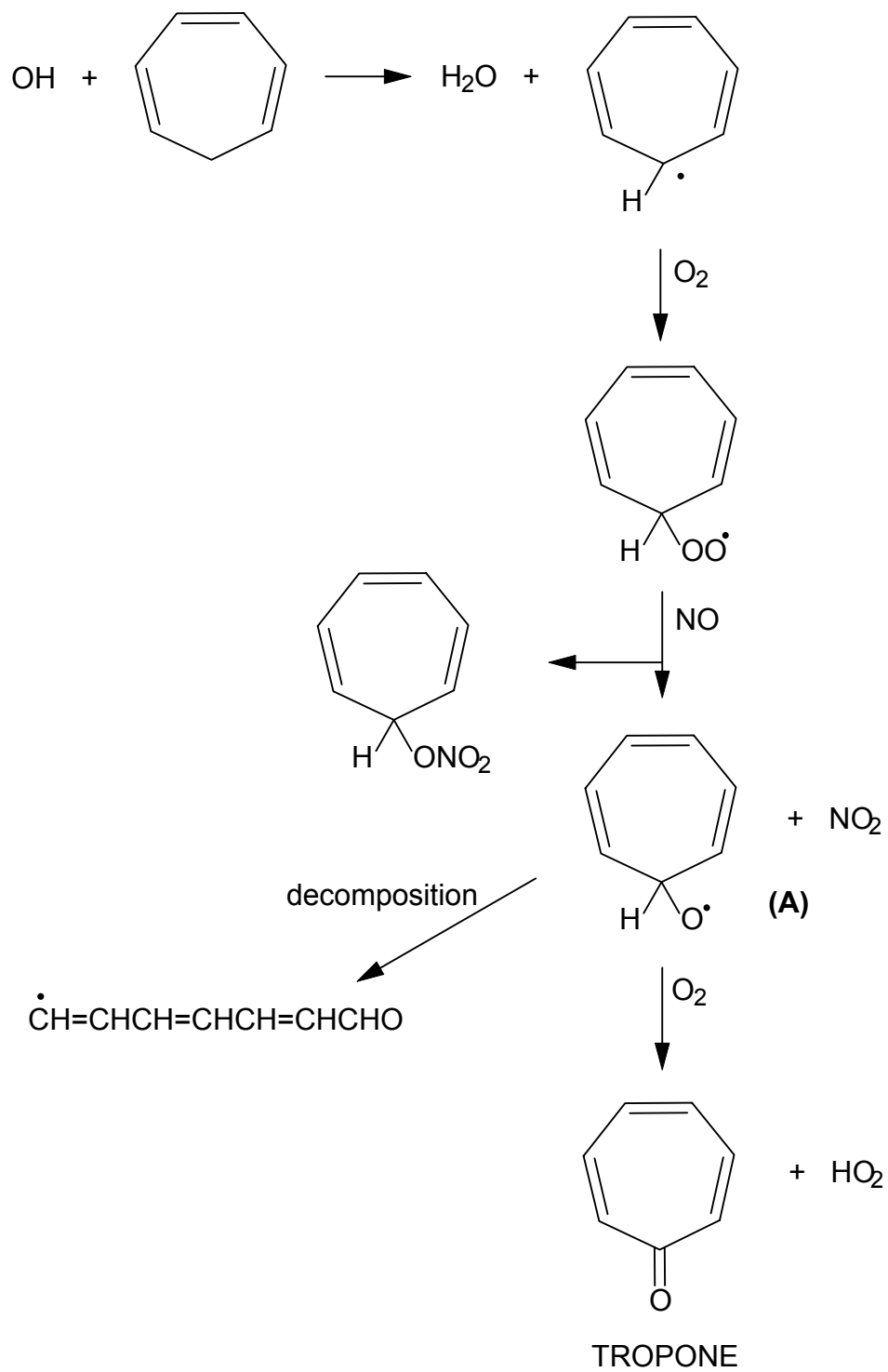


Figure 61. Reaction scheme for the reaction of OH radicals with 1,3,5-cycloheptatriene.

H-atom abstraction from the 2-position CH group in 2,3-dimethylpentanal

The reaction of OH radicals with 2,3-dimethylpentanal proceeds by H-atom abstraction from the various C-H bonds, with H-atom abstraction from the C-H bond in the CHO group being predicted to be dominant and H-atom abstraction from the C-H bonds in the three CH₃ groups being minor (Kwok and Atkinson, 1995). Figures 62-65 show predicted reaction schemes after H-atom abstraction from the C-H bonds at the CHO group, the 2-position CH group, the 3-position CH group, and the 4-position CH₂ group, respectively, where a bold arrow indicates a predicted dominant pathway (by a factor of 5) and a dashed arrow indicates a pathway predicted to account for <4% of the overall alkoxy radical reaction rate. The rates of the various alkoxy radical reactions were estimated as described by Atkinson (Atkinson, 1997a,b) and Aschmann *et al.* (2001b), using thermochemical data from the NIST program (National Institute of Standards and Technology, 1994) and IUPAC (2003).

Figures 62-65 show that the expected products are: acetaldehyde plus 2-butanone or 3 molecules of acetaldehyde after H-atom abstraction from the CHO group; 3-methyl-2-pentanone after H-atom abstraction from the 2-position CH group; 2-butanone plus acetaldehyde after H-atom abstraction from the 3-position CH group; and 3 molecules of acetaldehyde after H-atom abstraction from the 4-position CH₂ group. Acyl peroxy radicals, RC(O)OO•, occur as intermediates after H-atom abstraction from the CHO group (Figure 62) and, if an alkoxy radical isomerization occurs, after H-atom abstraction from the 4-position CH₂ group (Figure 65). The intermediary of these acyl peroxy radicals (forming acyl peroxy nitrates RC(O)OONO₂ as a temporary “reservoir” species which, as noted above, were observed by FT-IR spectroscopy) accounts for the decreasing yield of acetaldehyde and 2-butanone with increasing extent of reaction. This occurs (Atkinson and Aschmann, 1995) because the NO₂/NO concentration ratio increases as the reaction proceeds (from photolysis of methyl nitrite which has an overall reaction of CH₃ONO + hv (+ O₂) → HCHO + OH + NO₂ and from conversion of NO to NO₂ by HO₂ and organic peroxy radicals), leading to a longer effective lifetime of the RC(O)OONO₂ species. Furthermore, more rapid NO to NO₂ conversion would occur in the experiments with 2-methylpropene present because of the higher reactivity of 2-methylpropene and the higher organic/NO_x ratio, leading to a higher fraction of the OH radicals reacting with organic compounds in competition with reaction with NO and NO₂. In contrast, no acyl peroxy radical intermediate is involved in the formation of 3-methyl-2-pentanone in Figure 63.

Therefore, 3-methyl-2-pentanone appears to be the sole product formed after initial H-atom abstraction from the 2-position CH group. Formation of 3-methyl-2-pentanone after initial H-atom abstraction from the CHO group (Figure 62) is predicted to account for ≤3% of the products of this pathway and involves the intermediary of an acylperoxy radical. As noted above, we observe no evidence for an acylperoxy radical intermediate in the formation of 3-methyl-2-pentanone (Figure 59). Our measured 3-methyl-2-pentanone formation yield of 5.4 ± 1.0% (plus any formation of the organic nitrate CH₃CH₂CH(CH₃)C(ONO₂)(CH₃)CHO; see Figure 65) is therefore the percentage of the overall OH radical reaction with 2,3-dimethylpentanal proceeding by H-atom abstraction from the 2-position CH group.

The product yields given in Table 20 indicate that at the first measurement time in the experiment without added 2-methylpropene ~90% of the reaction products and pathways are accounted for, assuming that acetaldehyde is a co-product to the 2-butanone formed after H-atom abstraction from the CHO group and the 3-position CH group, and that 3 molecules of acetaldehyde are formed after H-atom abstraction from the CHO group (the alternate products

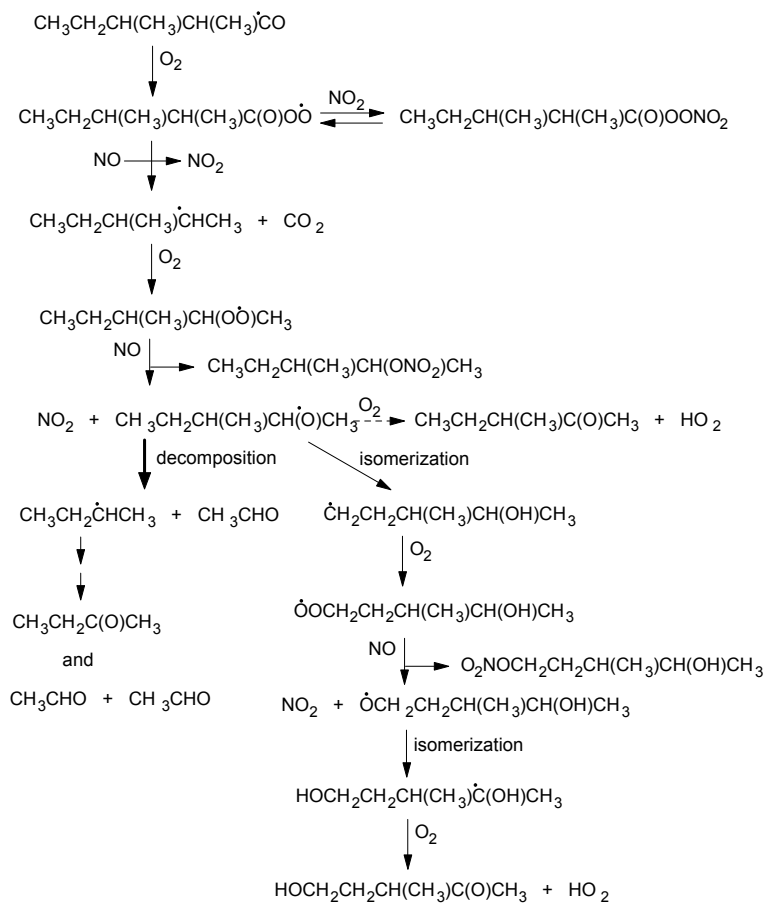


Figure 62. Reactions expected after H-atom abstraction from the CHO group in 2,3-dimethylpentanal.

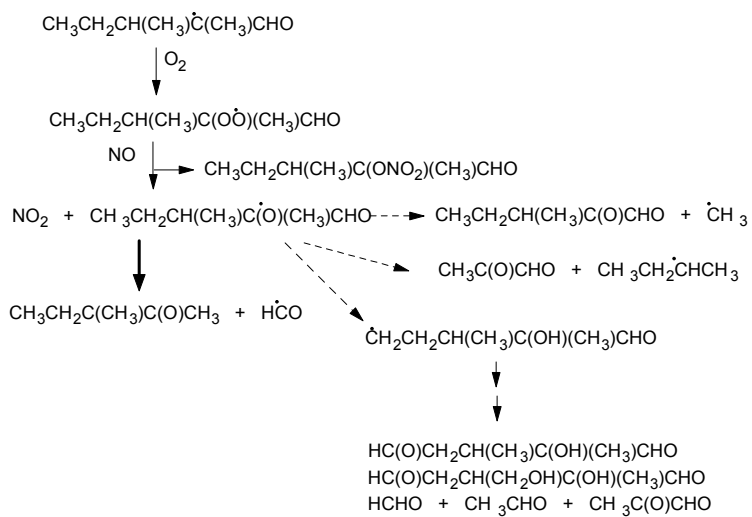


Figure 63. Reactions expected after H-atom abstraction from the 2-position C-H bond in 2,3-dimethylpentanal.

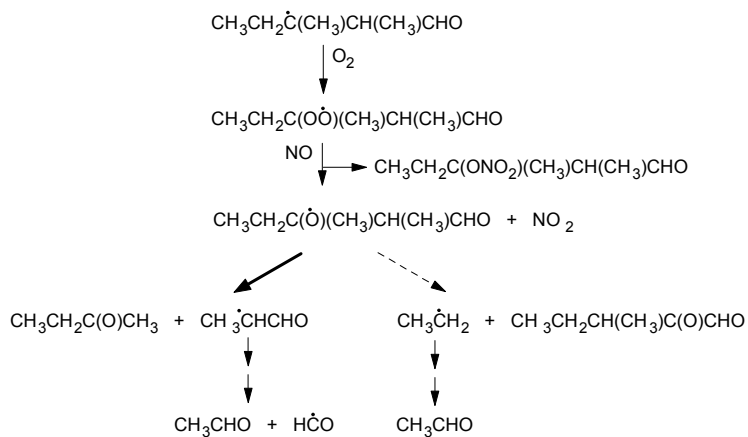


Figure 64. Reactions expected after H-atom abstraction from the 3-position C-H bond in 2,3-dimethylpentanal.

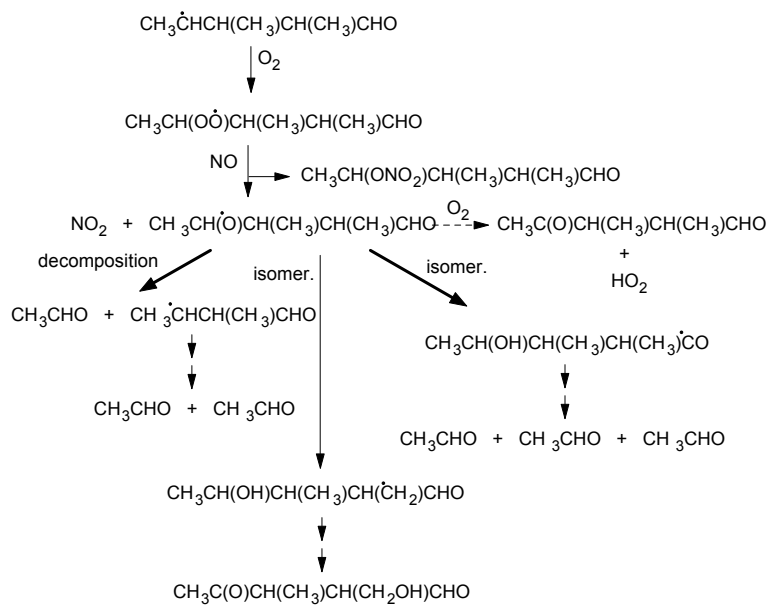


Figure 65. Reactions expected after H-atom abstraction from the 4-position C-H bond in 2,3-dimethylpentanal.

being 2-butanone plus acetaldehyde) and from the 4-position CH₂ group as shown in Figures 62, 64 and 65). The estimation method of Kwok and Atkinson (1995) predicts that the percentages of the overall OH radical reaction proceeding by H-atom abstraction are: from the CHO group, 61%; from the 2-position CH group, 5.3%; from the 3-position CH group, 27%; from the 4-position CH₂ group, 3.4%; and from the three CH₃ groups, 3% (total); and with an overall OH radical reaction rate constant of $3.4 \times 10^{-11} \text{ cm}^3 \text{ molecule}^{-1} \text{ s}^{-1}$ at 298 K. The predicted total OH radical reaction rate constant agrees well with our measured value of $(4.2 \pm 0.7) \times 10^{-11} \text{ cm}^3 \text{ molecule}^{-1} \text{ s}^{-1}$, and the predicted percentage of the overall reaction occurring at the 2-position CH group (5.3%) agrees very well with the measured percentage of $5.4 \pm 1.0\%$. Unfortunately, the same products (2 butanone and/or acetaldehyde) are formed after H-atom abstraction from the CHO, 3-position CH and 4-position CH₂ groups and hence our product data shed no light on the relative importance of these three H-atom abstraction pathways. Until such data become available, in particular confirming or disproving the prediction of the Kwok and Atkinson (1995) estimation method that for aldehydes H-atom abstraction from the CH or CH₂ groups located 2 carbon atoms away from the CHO group (*i.e.*, the 3-position CH group in 2,3-dimethylpentanal) is significantly enhanced over adjacent CH or CH₂ groups, then the Kwok and Atkinson (1995) estimation method appears to offer an approximate means of estimating the relative importance of H-atom abstraction from the various CH, CH₂ and CH₃ groups in aliphatic aldehydes.

6. SUMMARY AND CONCLUSIONS

During this three-year experimental program, we used the facilities and expertise available at the Air Pollution Research Center, University of California, Riverside, to investigate the atmospheric chemistry of selected volatile organic compounds found in California's atmosphere. Experiments were carried out in large volume (5800 to ~7500 liter) chambers with analysis of reactants and products by gas chromatography (with flame ionization and mass spectrometric detection), *in situ* Fourier transform infrared spectroscopy, and *in situ* direct air sampling atmospheric pressure ionization mass spectrometry. The gas chromatographic analyses included the use of Solid Phase MicroExtraction fibers coated with derivatizing agent for on-fiber derivatization of carbonyl-containing compounds, with subsequent gas chromatographic analyses of the carbonyl-containing compounds as their oximes. This research consisted primarily of kinetic and product studies of a number of selected VOCs. The room temperature rate constants measured in this work are listed in Table 21, and the products observed and quantified are listed in Table 22.

Table 21. Room temperature rate constants measured in this work for the reactions of OH radicals, NO₃ radicals and O₃ with selected VOCs

VOC	Rate constant (cm ³ molecule ⁻¹ s ⁻¹) for reaction with		
	OH radicals	NO ₃ radicals	O ₃
2,3,4-trimethylpentane	(6.84 ± 0.12) x 10 ⁻¹²		
5-hydroxy-2-pentanone	(1.6 ± 0.4) x 10 ⁻¹¹		
4,5-dihydro-2-methylfuran	(2.18 ± 0.11) x 10 ⁻¹⁰	(1.68 ± 0.12) x 10 ⁻¹⁰	(3.49 ± 0.24) x 10 ⁻¹⁵
2-methyl-2-pentanol	(7.93 ± 0.58) x 10 ⁻¹²		
4-methyl-2-pentanol	(1.91 ± 0.10) x 10 ⁻¹¹		
2,3-dimethylpentanal	(4.2 ± 0.7) x 10 ⁻¹¹		
3-methyl-2-pentanone	(6.87 ± 0.08) x 10 ⁻¹²		
tropone	(4.2 ± 0.6) x 10 ⁻¹¹		

Table 22. Products identified and quantified in this work from the reactions of OH radicals, NO₃ radicals and O₃ with VOCs

Reaction	Product	Molar yield (%)	Measured by ^a
OH + 2,2,4-trimethylpentane	acetaldehyde	<4	GC
	acetone	54 ± 7	GC and API-MS
	2-methylpropanal	26 ± 3	GC and API-MS
	4-hydroxy-4-methyl-2-pentanone	5.1 ± 0.6	GC and API-MS
	2,2-dimethylpropanal	<1.3	GC
	4,4-dimethyl-2-pentanone	<0.4	GC
	MW 128 product	observed	API-MS
	MW 130 hydroxycarbonyl	~3	API-MS
	C ₄ -hydroxynitrate	observed	API-MS
	MW 144 hydroxycarbonyl	~3	API-MS
	C ₇ -hydroxynitrate	observed	API-MS
	C ₈ -hydroxynitrate	observed	API-MS
OH + 2,3,4-trimethylpentane	acetaldehyde	47 ± 6	GC
	acetone	76 ± 11	GC and API-MS
	3-methyl-2-butanone	41 ± 5	GC and API-MS
	2-propyl nitrate	6.2 ± 0.8	GC
	3-methyl-2-butyl nitrate	1.6 ± 0.2	GC
	C ₈ -alkyl nitrate	~2	GC
	C ₅ -hydroxynitrate	observed	API-MS
	C ₈ -hydroxynitrate	observed	API-MS
OH + <i>n</i> -pentane	5-hydroxy-2-pentanone	observed	SPME/GC-MS
	4-hydroxypentanal	observed	SPME/GC-MS
OH + <i>n</i> -hexane	5-hydroxy-2-hexanone	observed	SPME/GC-MS
	6-hydroxy-3-hexanone	observed	SPME/GC-MS
	4-hydroxyhexanal	observed	SPME/GC-MS
OH + <i>n</i> -heptane	5-hydroxy-2-heptanone	observed	SPME/GC-MS
	6-hydroxy-3-heptanone	observed	SPME/GC-MS
	7-hydroxy-4-heptanone	observed	SPME/GC-MS
	4-hydroxyheptanal	observed	SPME/GC-MS
OH + <i>n</i> -octane	5-hydroxy-2-octanone	observed	SPME/GC-MS
	6-hydroxy-3-octanone	observed	SPME/GC-MS
	7-hydroxy-4-octanone	observed	SPME/GC-MS
	4-hydroxyoctanal	observed	SPME/GC-MS

Table 22. Products identified and quantified in this work from the reactions of OH radicals, NO₃ radicals and O₃ with VOCs (continued)

Reaction	Product	Molar yield (%)	Measured by ^a
OH + 5-hydroxy-2-pentanone	CH ₃ C(O)CH ₂ CH ₂ CHO	observed	SPME/GC-MS and API-MS
	CH ₃ C(O)CH ₂ CHO	observed	SPME/GC-MS and API-MS
OH + 4,5-dihydro-2-methylfuran	CH ₃ C(O)OCH ₂ CH ₂ CHO	74 ± 19	FT-IR, GC and API-MS
	formaldehyde	5.4-12	FT-IR
	ethene	3.4-4.8	FT-IR
	acetic acid	<2	FT-IR
NO ₃ + 4,5-dihydro-2-methylfuran	CH ₃ C(O)OCH ₂ CH ₂ CHO	5.4-12	FT-IR
	MW 100 epoxide	observed	FT-IR and API-MS
O ₃ + 4,5-dihydro-2-methylfuran	CH ₃ C(O)OCH ₂ CH ₂ CHO	23	FT-IR and API-MS
	formaldehyde	28	FT-IR
	methanol	9.5	FT-IR
	formic acid	2.1	FT-IR
	ketene	2.1	FT-IR
	ethene	6.6	FT-IR
	CO	20	FT-IR
	CO ₂	47	FT-IR
O ₃ + cyclohexene	OH	54 ± 8	GC
	pentanal	23.6 ± 1.8	GC, SPME/GC-MS and API-MS
	formic acid	3.5	FT-IR
	glutaraldehyde	observed	SPME/GC-MS and API-MS
	adipaldehyde	observed	SPME/GC-MS and API-MS
	MW 130 secondary ozonide	observed	API-MS
	MW 132 peracid	observed	API-MS
	MW 116 hydroxycarbonyl or oxo-acid	observed	SPME/GC-MS

Table 22. Products identified and quantified in this work from the reactions of OH radicals, NO₃ radicals and O₃ with VOCs (continued)

Reaction	Product	Molar yield (%)	Measured by ^a
O ₃ + cyclohexene-d ₁₀	OH/OD	50 ± 7	GC
	pentanal-d ₁₀	16.4 ± 1.4	GC, SPME/GC-MS and API-MS
	formic acid-d ₁ (DC(O)OH)	1.6	FT-IR
	glutaraldehyde-d ₈	observed	SPME/GC-MS and API-MS
	adipaldehyde-d ₁₀	observed	SPME/GC-MS and API-MS
	MW 140 secondary ozonide	observed	API-MS
	MW 139 peracid	observed	API-MS
	MW 123 hydroxycarbonyl or oxo-acid	observed	SPME/GC-MS
O ₃ + propene	OH	40 ± 6	GC
O ₃ + propene-d ₆	OH/OD	27 ± 4	GC
O ₃ + α-pinene	OH	86 ± 13	GC
	OH	~65	GC
	pinonaldehyde	15 ± 2	GC
O ₃ + 2,3-dimethyl-2-butene	OH	107 ± 16	GC
O ₃ + sabinene	OH	~30	GC
	sabinaketone	~40 at 5% RH ^b ~55 at 50% RH ^b	GC
O ₃ + <i>trans</i> -7-tetradecene	OH	~24 at 5% RH ^b ~19 at 50% RH ^b	GC
	heptanal	~110 at 5% RH ^b ~135 at 50% RH ^b	GC
OH + 2-methyl-2-pentanol	acetaldehyde	22 ± 3	GC
	propanal	35 ± 4	GC
	acetone	56 ± 6	GC
	2-pentanone	5.4 ± 1.1	GC
	4-hydroxy-2-pentanone	observed	SPME/GC-MS
	4-hydroxy-4-methyl-2-pentanone	<4	GC
	MW 163 hydroxynitrate	~5.8	API-MS
	MW 179 dihydroxynitrate	~2.3	API-MS

Table 22. Products identified and quantified in this work from the reactions of OH radicals, NO₃ radicals and O₃ with VOCs (continued)

Reaction	Product	Molar yield (%)	Measured by ^a
OH + 4-methyl-2-pentanol	acetaldehyde	37 ± 6	GC
	acetone	26 ± 3	GC
	2-methylpropanal	11.1 ± 1.2	GC
	4-hydroxy-2-pentanone	25 ± 2	GC
	MW 163 hydroxynitrate	~5.5	API-MS
	MW 179 dihydroxynitrate	~1.8	API-MS
1,2-butanediol	2-hydroxybutanal	27	SPME/GC
	glycolaldehyde	10 ± 4	SPME/GC
1,3-butanediol	3-hydroxybutanal	15	SPME/GC
	2-hydroxypropanal	0.7	SPME/GC
	glycolaldehyde	10 ± 4	SPME/GC
2,3-butanediol	2-hydroxypropanal	2.0	SPME/GC
2-methyl-2,4-pentanediol	2-hydroxypropanal	24	SPME/GC
	3-hydroxy-3-methylbutanal	observed	SPME/GC-MS
1,4-cyclohexadiene	benzene	12.5 ± 1.2	GC and FT-IR
1,3,5-cycloheptatriene	tropone	<1.2	FT-IR
	benzaldehyde	<0.7	FT-IR
2,3-dimethylpentanal	acetaldehyde	80-98 (initial)	GC and FT-IR
	2-butanone	26	GC
	3-methyl-2-pentanone	5.4 ± 1.0	GC

^aGC, gas chromatography; API-MS, atmospheric pressure ionization mass spectrometry; FT-IR, Fourier transform infrared spectroscopy; SPME, Solid Phase MicroExtraction with on-fiber derivatization.

^bRH, relative humidity.

The research carried out during this Contract has finally elucidated the atmospheric chemistry of alkanes, which comprise ~50% of the non-methane organic compounds observed in ambient air in urban areas, and shown that 1,4-hydroxycarbonyls are major products of the long-chain alkanes and, to a lesser extent, of branched alkanes. Our data show that isomerization of the alkoxy radicals formed after the initial OH radical reaction dominates for the larger ($>C_4$) *n*-alkanes, leading to formation of 1,4-hydroxycarbonyls and 1,4-hydroxynitrates. Because the rates of decomposition of branched alkoxy radicals are significantly higher than the decomposition rates of linear alkoxy radicals, alkoxy radical isomerization plays a lesser role in the chemistry of branched alkanes, and therefore more carbonyl compounds, and less hydroxycarbonyls, are formed from branched alkanes. We have investigated the atmospheric reactions of 5-hydroxy-2-pentanone, the only commercially available 1,4-hydroxycarbonyl (and the major product formed from *n*-pentane). In addition to measuring its rate constant for reaction with OH radicals and the products of that reaction, we observed that 5-hydroxy-2-pentanone cyclizes with loss of water to form the unsaturated and highly reactive compound 4,5-dihydro-2-methylfuran. For 5-hydroxy-2-pentanone, cyclization to form the dihydrofuran occurs in dry air, but the presumed equilibrium lies in favor of 5-hydroxy-2-pentanone for ~5% or higher relative humidity at room temperature. However, given the high reactivity of 4,5-dihydro-2-methylfuran towards OH radicals, NO₃ radicals and O₃ (with an estimated lifetime in the atmosphere of an hour or less, based on our measured rate constants), 4,5-dihydro-2-methylfuran may well play an important role in the atmospheric chemistry of *n*-pentane, even for the high water vapor concentrations in the typical lower atmosphere. Our initial results concerning the reactions of larger 1,4-hydroxycarbonyls formed from *n*-hexane through *n*-octane suggest that the dihydrofurans formed by cyclization and loss of water from the larger 1,4-hydroxycarbonyls are more important at higher relative humidities, and maybe up to ~50% relative humidity. This body of work on alkane chemistry both places previous predictions (for example, the formation of 1,4-hydroxycarbonyls) on a firm basis as well as discovering that a class of new and potentially important products (the dihydrofurans) are formed in the atmospheric photooxidation of alkanes. These data will need to be incorporated into chemical mechanisms used in modeling photochemical air pollution and ozone formation from alkanes. Further work is, however, needed to better assess the formation of the dihydrofurans as a function of water vapor concentration, recognizing that the effects of water vapor on the formation of the dihydrofurans or the equilibrium between the dihydrofurans and the 1,4-hydroxycarbonyls may depend on the specific 1,4-hydroxycarbonyl/dihydrofuran.

Our work on alkene chemistry focused on the reactions of alkenes with O₃. We have shown that measurements of OH radical formation yields from the reactions of O₃ with alkenes are not affected to any significant extent by water vapor, and hence that laboratory studies conducted in the absence of water vapor, or at low water vapor concentrations, are applicable to atmospheric conditions. Our results on the effects of water vapor and 2-butanol (a potential scavenger of Criegee intermediates, the key intermediate species in these O₃-alkene reactions) on these reactions aids in the elucidation of the overall reaction mechanisms, and suggests (in agreement with other recent literature data) that the formation routes to the OH radical and to other products can be viewed as parallel reaction pathways, independent of water vapor concentration. This finding is important for chemical mechanism development.

Research into the formation of volatile nitro-PAH and their presence in the Los Angeles atmosphere shows that alkylnaphthalenes are a significant fraction of the naphthalene concentrations in ambient air, and that alkyl-nitronaphthalenes are formed from the OH radical-initiated reactions of their precursor alkylnaphthalenes. Methyl-nitronaphthalenes and dimethyl- and ethyl- nitronaphthalenes were observed in ambient air samples collected in the Los Angeles air basin. This observation of dimethyl- and ethyl- nitronaphthalenes is the first report of the presence of these potentially toxic air pollutants in the atmosphere.

Our studies of the kinetics and products of selected oxygenated organic compounds (in addition to those of 1,4-hydroxycarbonyls and dihydrofurans mentioned above) have included the use of Solid Phase MicroExtraction fibers for on-fiber derivatization to identify and quantify hydroxycarbonyls (primarily hydroxyaldehydes) which otherwise cannot be readily analyzed. Our studies of the products formed from 2- and 4-methyl-2-pentanol, a series of diols, and 2,3-dimethylpentanal allow reasonably detailed reaction mechanisms for the reactions of OH radicals (the dominant atmospheric loss process for these oxygenated compounds) to be derived. These data expand the database concerning the details of VOC atmospheric reactions, which can be used to either refine present empirical estimation methods and to test new estimation and/or *ab-initio* theoretical calculational methods for the reactions of the key intermediate alkoxy radicals, and hence provide the ability to predict reaction products and their yields under atmospheric conditions.

7. REFERENCES

- Aelterman, W.; De Kimpe, N.; Kalinin, V. (1997) *J. Nat. Prod.*, **60**, 385.
- Alvarado, A.; Tuazon, E. C.; Aschmann, S. M.; Atkinson, R.; Arey J. (1998) *J. Geophys. Res.*, **103**, 25541.
- Alvarado, A.; Tuazon, E. C.; Aschmann, S. M.; Arey, J.; Atkinson, R. (1999) *Atmos. Environ.*, **33**, 2893.
- Arey, J.; Zielinska, B. (1989) *J. High Res. Chromat.*, **12**, 101.
- Arey, J.; Harger, W. P.; Helmig, D.; Atkinson, R. (1992) *Mutat. Res.*, **281**, 67.
- Arey, J. (1998) *Atmospheric Reactions of PAHs Including Formation of Nitroarenes in PAHs and Related Compounds*, Ed. Neilson, A. H., The Handbook of Environmental Chemistry, 3.I, Series Ed. Hutzinger, O., Springer, Berlin, pp. 347-385.
- Arey, J.; Aschmann, S. M.; Kwok, E. S. C.; Atkinson, R. (2001) *J. Phys. Chem. A*, **105**, 1020.
- Aschmann, S. M.; Chew, A. A.; Arey, J.; Atkinson, R. (1997) *J. Phys. Chem. A*, **101**, 8042.
- Aschmann, S. M.; Reissell, A.; Atkinson, R.; Arey, J. (1998) *J. Geophys. Res.*, **103**, 25553.
- Aschmann, S. M.; Atkinson, R. (1998) *Int. J. Chem. Kinet.*, **30**, 533.
- Aschmann, S. M.; Atkinson, R. (1999) *Int. J. Chem. Kinet.*, **31**, 501.
- Aschmann, S. M.; Arey, J.; Atkinson, R. (2000a) *J. Phys. Chem. A*, **104**, 3998.
- Aschmann, S. M.; Arey, J.; Atkinson, R. (2000b) *Environ. Sci. Technol.*, **34**, 1702.
- Aschmann, S. M.; Arey, J.; Atkinson, R. (2001a) *J. Phys. Chem. A*, **105**, 7598.
- Aschmann, S. M.; Martin, P.; Tuazon, E. C.; Arey, J.; Atkinson, R. (2001b) *Environ. Sci. Technol.*, **35**, 4080.
- Aschmann, S. M.; Atkinson, R.; Arey, J. (2002a) *J. Geophys. Res.*, **107 (D14)**, ACH 6-1.
- Aschmann, S. M.; Arey, J.; Atkinson, R. (2002b) *Environ. Sci. Technol.*, **36**, 625.
- Aschmann, S. M.; Arey, J.; Atkinson, R. (2002c) *Atmos. Environ.*, **36**, 4347.
- Aschmann, S. M.; Arey, J.; Atkinson, R. (2003) *J. Atmos. Chem.*, **45**, 289.

- Atkinson, R.; Carter, W. P. L.; Winer, A. M.; Pitts, J. N., Jr. (1981) *J. Air Pollution Control Assoc.*, **31**, 1090.
- Atkinson, R.; Aschmann, S. M.; Carter, W. P. L.; Winer, A.M.; Pitts, J. N., Jr. (1982) *J. Phys. Chem.*, **86**, 4563.
- Atkinson, R.; Aschmann, S. M.; Carter, W. P. L.; Winer, A. M.; Pitts, J. N., Jr. (1984a) *Int. J. Chem. Kinet.*, **16**, 1085.
- Atkinson, R.; Plum, C. N.; Carter, W. P. L.; Winer, A. M.; Pitts, J. N., Jr. (1984b) *J. Phys. Chem.*, **88**, 1210.
- Atkinson, R.; Aschmann, S. M.; Pitts, J. N., Jr. (1988) *J. Phys. Chem.*, **92**, 3454.
- Atkinson, R. (1989) *J. Phys. Chem. Ref. Data*, **Monograph 1**, 1.
- Atkinson, R. (1991) *J. Phys. Chem. Ref. Data*, **20**, 459.
- Atkinson, R.; Aschmann, S. M.; Arey, J.; Shorees, B. (1992) *J. Geophys. Res.*, **97**, 6065.
- Atkinson, R.; Aschmann, S. M. (1993) *Environ. Sci. Technol.*, **27**, 1357.
- Atkinson, R. (1994) *J. Phys. Chem. Ref. Data*, **Monograph 2**, 1.
- Atkinson, R.; Arey, J. (1994) *Environ. Health Perspect.*, **102(Suppl 4)**, 117.
- Atkinson, R.; Aschmann, S. M. (1994) *Int. J. Chem. Kinet.*, **26**, 929.
- Atkinson, R.; Aschmann, S. M. (1995) *Int. J. Chem. Kinet.*, **27**, 261.
- Atkinson, R.; Kwok, E. S. C.; Arey, J.; Aschmann, S. M. (1995a) *Faraday Discuss.*, **100**, 23.
- Atkinson, R.; Tuazon, E. C.; Aschmann, S. M. (1995b) *Environ. Sci. Technol.*, **29**, 1674.
- Atkinson, R.; Tuazon, E. C.; Aschmann, S. M. (1995c) *Environ. Sci. Technol.*, **29**, 1860.
- Atkinson, R. (1997a) *J. Phys. Chem. Ref. Data*, **26**, 215.
- Atkinson, R. (1997b) *Int. J. Chem. Kinet.*, **29**, 99.
- Atkinson, R. (2000) *Atmos. Environ.*, **34**, 2063.
- Atkinson, R.; Tuazon, E. C.; Aschmann, S. M. (2000a) *Environ. Sci. Technol.* **34**, 623.
- Atkinson, R.; Baulch, D. L.; Cox, R. A.; Hampson, R. F., Jr.; Kerr, R. A.; Rossi, M. J.; Troe, J. (2000b) *J. Chem. Phys. Ref. Data*, **29**, 167.
- Atkinson, R.; Arey, J. (2002) *Chem. Rev.*, **103**, 4605.

- Atkinson, R. (2003) *Atmos. Chem. Phys.*, **3**, 2233.
- Baker, J.; Aschmann, S. M.; Arey, J.; Atkinson, R. (2002) *Int. J. Chem. Kinet.*, **34**, 73.
- Baxley, J. S.; Wells, J. R. (1998) *Int. J. Chem. Kinet.*, **30**, 745.
- Bethel, H. L.; Atkinson, R.; Arey, J. (2001) *Int. J. Chem. Kinet.*, **33**, 310.
- Bethel, H. L.; Atkinson, R.; Arey, J. (2000) *J. Phys. Chem. A*, **104**, 8922.
- Bidleman, T. F. (1988) *Environ. Sci. Technol.*, **22**, 361.
- Blitz, M.; Pilling, M. J.; Robertson, S. H.; Seakins, P. W. (1999) *Phys. Chem. Chem. Phys.*, **1**, 73.
- Bundt, J.; Herbel, W.; Steinhart, H.; Franke, S.; Francke, W. (1991) *J. High Res. Chromat.*, **14**, 91.
- Calvert, J. G.; Atkinson, R.; Kerr, J. A.; Madronich, S.; Moortgat, G. K.; Wallington, T. J.; Yarwood, G. (2000) *The Mechanisms of Atmospheric Oxidation of the Alkenes*, Oxford University Press, New York, NY.
- Calvert, J. G.; Atkinson, R.; Becker, K. H.; Kamens, R. M.; Seinfeld, J. H.; Wallington, T. J.; Yarwood, G. (2002) *The Mechanisms of Atmospheric Oxidation of Aromatic Hydrocarbons*, Oxford University Press, New York, NY.
- Cameron, M.; Sivakumaran, V.; Dillon, T. J.; Crowley, J. N. (2002) *Phys. Chem. Chem. Phys.*, **4**, 3628.
- Caralp, F.; Devolder, P.; Fittschen, C.; Gomez, N.; Hippler, H.; Méreau, R.; Rayez, M. T.; Striebel, F.; Viskolcz, B. (1999) *Phys. Chem. Chem. Phys.*, **1**, 2935.
- Carter, W. P. L.; Atkinson, R. (1989) *J. Atmos. Chem.*, **8**, 165.
- Cavalli, F.; Barnes, I.; Becker, K. H. (2000) *Environ. Sci. Technol.*, **34**, 4116.
- Cavalli, F.; Geiger, H.; Barnes, I.; Becker, K. H. (2002) *Environ. Sci. Technol.*, **36**, 1263.
- Cecinato, A.; Mabilia, R.; Brachetti, A.; Di Filippo, P.; Liberti, A. (2001) *Anal. Lett.*, **34**, 927.
- Chew, A. A.; Atkinson, R. (1996) *J. Geophys. Res.*, **101**, 28649.
- Chew, A. A.; Atkinson, R.; Aschmann, S. M. (1998) *J. Chem. Soc. Faraday Trans.* **94**, 1083.

- Ciccioli, P.; Cecinato, A.; Brancaleoni, E.; Frattoni, M.; Zacchei, P.; Miguel, A. H.; de Castro Vasconcellos, P. (1996) *J. Geophys. Res.*, **101**, 19567.
- Cremer, D.; Gauss, J.; Kraka, E.; Stanton, J. F.; Bartlett, R. J. (1993) *Chem. Phys. Lett.*, **209**, 547.
- Deng, W.; Wang, C.; Katz, D. R.; Gawinski, G. R.; Davis, A. J.; Dibble, T. S. (2000) *Chem. Phys. Lett.*, **330**, 541.
- Deng, W.; Davis, A. J.; Zhang, L.; Katz, D. R.; Dibble, T. S. (2001) *J. Phys. Chem. A*, **105**, 8985.
- Devolder, P.; Fittschen, Ch.; Frenzel, A.; Hippler, H.; Poskrebyshev, G.; Striebel, F.; Viskolcz, B. (1999) *Phys. Chem. Chem. Phys.*, **1**, 675.
- Dibble, T. S. (2002) *J. Phys. Chem. A*, **106**, 6643.
- Droege, A. T.; Tully, F. P. (1986a) *J. Phys. Chem.*, **90**, 1949.
- Droege, A. T.; Tully, F. P. (1986b) *J. Phys. Chem.*, **90**, 5937.
- Dunlop, J. R.; Tully, F. P. (1993) *J. Phys. Chem.*, **97**, 6457.
- Eberhard, J.; Müller, C.; Stocker, D. W.; Kerr, J. A. (1995) *Environ. Sci. Technol.*, **29**, 232.
- Feilberg, A.; Kamens, R. M.; Strommen, M. R.; Nielsen, T. (1999) *Atmos. Environ.*, **33**, 1231.
- Feilberg, A.; Nielsen, T.; Binderup, M.-L.; Skov, H.; Poulsen, M. W. B. (2002) *Atmos. Environ.*, **36**, 4617.
- Fenske, J. D.; Hasson, A. S.; Ho, A. W.; Paulson, S. E. (2000a) *J. Phys. Chem. A*, **104**, 9921.
- Fenske, J. D.; Kuwata, K. T.; Houk, K. N.; Paulson, S. E. (2000b) *J. Phys. Chem. A*, **104**, 7246.
- Fenske, J. D.; Hasson, A. S.; Paulson, S. E.; Kuwata, K. T.; Ho, A.; Houk, K. N. (2000c) *J. Phys. Chem. A*, **104**, 7821.
- Ferronato, C.; Orlando, J. J.; Tyndall, G. S. (1998) *J. Geophys. Res.*, **103**, 25,579.
- Fittschen, C.; Frenzel, A.; Imrik, K.; Devolder, P. (1999) *Int. J. Chem. Kinet.*, **31**, 860.
- Fittschen, C.; Hippler, H.; Viskolcz, B. (2000) *Phys. Chem. Chem. Phys.*, **2**, 1677.
- George, L. A.; Hard, T. M.; O'Brien, R. J. (1999) *J. Geophys. Res.*, **104**, 11643.
- Grosjean, E.; Grosjean, D. (1996) *Environ. Sci. Technol.*, **30**, 1321.

- Grosjean, E.; Grosjean, D; Seinfeld, J. H. (1996) *Environ. Sci. Technol.*, **30**, 1038.
- Grosjean, E.; Grosjean, D. (1999) *J. Atmos. Chem.*, **32**, 205.
- Guenther, A.; Hewitt, C. N.; Erickson, D.; Fall, R.; Geron, C.; Graedel, T.; Harley, P.; Klinger, L.; Lerdau, M.; Mackay, W. A.; Pierce, T.; Scholes, B.; Steinbrecher, R.; Tallamraju, R.; Taylor, J.; Zimmerman, P. (1995) *J. Geophys. Res.*, **100**, 8873.
- Guenther, A.; Geron, C.; Pierce, T.; Lamb, B.; Harley, P.; Fall, R. (2000) *Atmos. Environ.*, **34**, 2205.
- Gupta, P.; Harger, W. P.; Arey, J. (1996) *Atmos. Environ.*, **30**, 3157.
- Gutbrod, R.; Schindler, R. N.; Kraka, E.; Cremer, D. (1996) *Chem. Phys. Lett.*, **252**, 221.
- Gutbrod, R.; Kraka, E.; Schindler, R. N.; Cremer, D. (1997) *J. Am. Chem. Soc.*, **119**, 7330.
- Harner, T.; Bidleman, T. F. (1998) *Environ. Sci. Technol.*, **32**, 1494.
- Harris, S. J.; Kerr, J. A. (1989) *Int. J. Chem. Kinet.*, **20**, 939.
- Hasson, A. S.; Orzechowska, G.; Paulson, S. E. (2001a) *J. Geophys. Res.*, **106**, 34131.
- Hasson, A. S.; Ho, A. W.; Kuwata, K. T.; Paulson, S. E. (2001b) *J. Geophys. Res.*, **106**, 34143.
- Hasson, A. S.; Chung, M. Y.; Kuwata, K. T.; Converse, A. D.; Krohn, D.; Paulson, S. E. (2003) *J. Phys. Chem. A*, **107**, 6176.
- Hatakeyama, S.; Tanonaka, T.; Weng, J.; Bandow, H.; Takagi, H.; Akimoto, H. (1985) *Environ. Sci. Technol.*, **19**, 935.
- Hein R.; Crutzen, P. J.; Heimann, M. (1997) *Global Biogeochem. Cycles*, **11**, 43.
- Hein, H.; Hoffmann, A.; Zellner, R. (1998) *Ber. Bunsenges. Phys. Chem.*, **102**, 1840.
- Hein, H.; Hoffmann, A.; Zellner, R. (1999) *Phys. Chem. Chem. Phys.*, **1**, 3743.
- Hein, H.; Somnitz, H.; Hoffmann, A.; Zellner, R. (2000) *Z. Phys. Chem.*, **214**, 449.
- Hess, W. P.; Tully, F. P. (1988) *Chem. Phys. Lett.*, **152**, 183.
- Hoekman, S. K. (1992) *Environ. Sci. Technol.*, **26**, 1206.
- Hoffmann, T.; Odum, J. R.; Bowman, F.; Collins, D.; Klockow, D.; Flagan, R. C.; Seinfeld, J. H. (1997) *J. Atmos. Chem.*, **26**, 189.

- Howard, P. H. (1990) *Handbook of Environmental Fate and Exposure data for Organic Chemicals*, Vol. II, Solvents, Lewis Publishers, Chelsea, MI.
- IARC (1983) *IARC Monographs on the Evaluation of the Carcinogenic Risk of Chemicals to Humans, Polynuclear Aromatic Compounds, Part. 1, Chemical, Environmental and Experimental Data*, Vol. 32, International Agency for Research on Cancer, Lyon, France.
- IARC (1984) *IARC Monographs on the Evaluation of the Carcinogenic Risk of Chemicals to Humans, Polynuclear Aromatic Compounds, Part. 2, Carbon Blacks, Mineral Oils and Some Nitroarenes*, Vol. 33, International Agency for Research on Cancer, Lyon, France.
- IARC (1989) *IARC Monographs on the Evaluation of the Carcinogenic Risk of Chemicals to Humans, Diesel and Gasoline Engine Exhausts and Some Nitroarenes*, Vol. 46, International Agency for Research on Cancer, Lyon, France.
- IUPAC (2003) <http://www.iupac-kinetic.ch.cam.ac.uk/>.
- Jenkin, M. E.; Shallcross, D. E.; Harvey, J. N. (2000) *Atmos. Environ.*, **34**, 2837.
- Johnson, D.; Lewin, A. G.; Marston, G. (2001) *J. Phys. Chem. A*, **105**, 2933.
- Kalberer, M.; Yu, J.; Cocker, D. R.; Flagan, R. C.; Seinfeld, J. H. (2000) *Environ. Sci. Technol.*, **34**, 4894.
- Kerr, J. A.; Stocker, D. W. (1999/2000) *Strengths of Chemical Bonds*, in *The Handbook of Chemistry and Physics*, 80th Ed., Lide, D. R., ed., CRC Press, Boca Raton, FL p. 9-51.
- Knispel, R.; Koch, R.; Siese, M.; Zetsch, C. (1990) *Ber. Bunsenges. Phys. Chem.*, **94**, 1375.
- Koziel, J.A.; Noah, J.; Pawliszyn, J. (2001) *Environ. Sci. Technol.*, **35**, 1481.
- Kramp, F.; Paulson, S. E. (1998) *J. Phys. Chem. A*, **102**, 2685.
- Krol, M.; van Leeuwen, P. J.; Lelieveld, J. (1998) *J. Geophys. Res.* **103**, 10697.
- Kroll, J. H.; Sahay, S. R.; Anderson, J. G.; Demerjian, K. L.; Donahue, N. M. (2001a) *J. Phys. Chem. A*, **105**, 4446.
- Kroll, J. H.; Clarke, J. S.; Donahue, N. M.; Anderson, J. G.; Demerjian, K. L. (2001b) *J. Phys. Chem. A*, **105**, 1554.
- Kroll, J. H.; Donahue, N. M.; Cee, V. J.; Demerjian, K. L.; Anderson, J. G. (2002) *J. Am. Chem. Soc.*, **124**, 8518.
- Kwok, E. S. C.; Atkinson, R. (1995) *Atmos. Environ.*, **29**, 1685.

- Kwok, E. S. C.; Atkinson, R.; Arey, J. (1995) *Environ. Sci. Technol.*, **29**, 2467.
- Kwok, E. S. C.; Aschmann, S. M.; Arey, J.; Atkinson, R. (1996a) *Int. J. Chem. Kinet.*, **28**, 925.
- Kwok, E. S. C.; Arey, J.; Atkinson, R. (1996b) *J. Phys. Chem.*, **100**, 214.
- Le Calvé, S.; Hitier, D.; Le Bras, G.; Mellouki, A. (1998) *J. Phys. Chem. A*, **102**, 4579.
- Lei, W.; Zhang, R. (2001) *J. Phys. Chem. A*, **105**, 3808.
- Logan, J. A. (1985) *J. Geophys. Res.*, **90**, 10463.
- Lurmann, F. W.; Main, H. H. (1992). *Analysis of the Ambient VOC Data Collected in the Southern California Air Quality Study*, Final Report to California Air Resources Board Contract No. A832-130, February.
- Markevich, V. S.; Stepanova, Gg. A.; Nevaeva, V. E.; Rakhmatullina, L. Kh. (1981) *Khim.-Farm. Zh.*, **15**, 64. [CA 95:61884].
- Marr, L. C.; Kirchstetter, T. W.; Harley, R. A.; Miguel, A. H.; Hering, S. V.; Hammond, S. K. (1999) *Environ. Sci. Technol.*, **33**, 3091.
- Martin, P.; Tuazon, E. C.; Aschmann, S. M.; Arey, J.; Atkinson, R. (2002) *J. Phys. Chem. A*, **106**, 11492.
- Martos, P. A.; Pawliszyn, J. (1998) *Anal. Chem.* **70**, 2311.
- McCaulley, J. A.; Kelly, N.; Golde, M. F.; Kaufman, F. (1989) *J. Phys. Chem.*, **93**, 1014.
- McMillen, D. F.; Golden, D. M. (1982) *Ann. Rev. Phys. Chem.*, **33**, 493.
- Mikhlina, E. E.; Yanina, A. D.; Yakhontov, L. N. (1970) *Khim.-Farm. Zh.*, **4**, 26. [CA 73:66358].
- Millikan, R. C.; Pitzer, K. S. (1957) *J. Chem. Phys.*, **27**, 1305.
- Muthuramu, K.; Shepson, P. B.; O'Brien, R. J. (1993) *Environ. Sci. Technol.*, **27**, 1117.
- National Institute of Standards and Technology (1994) *Standard Database 25, Structures and Properties Database and Estimation Program*, Version 2.0, Stein, S. E., Chemical Kinetics and Thermodynamics Division, NIST, Gaithersburg, MD.
- Neavyn, R.; Sidebottom, H.; Treacy, J. (1994) *Reactions of Hydroxyl Radicals with Polyfunctional Group Oxygen-Containing Compounds*, in *The Proceedings of EUROTRAC Symposium '94*, Eds. Borrell, P. M.; Borrell, P.; Cvitaš, T.; Seiler, W., SPB Academic Publishing bv, Den Haag, The Netherlands, pp. 105-109.

- Neeb, P.; Horie, O.; Moortgat, G. K. (1996) *Int. J. Chem. Kinet.*, **28**, 721.
- Neeb, P.; Moortgat, G. K. (1999) *J. Phys. Chem. A*, **103**, 9003.
- Nelson, P. F. (1989) *Fuel*, **68**, 283.
- Nelson, L.; Rattigan, O.; Neavyn, R.; Sidebottom, H.; Treacy, J.; Nielsen, O. J. (1990) *Int. J. Chem. Kinet.*, **22**, 1111.
- Niki, H.; Maker, P. D.; Savage, C. M.; Breitenbach, L. P. (1981) *Chem. Phys. Lett.*, **80**, 499.
- Niki, H.; Maker, P. D.; Savage, C. M.; Breitenbach, L. P. (1983) *Environ. Sci. Technol.*, **17**, 312A.
- O'Brien, J. M.; Czuba, E.; Hastie, D. R.; Francisco, J. S.; Shepson, P. B. (1998) *J. Phys. Chem. A*, **102**, 8903.
- Orlando, J. J.; Tyndall, G. S.; Bilde, M.; Ferronato, C.; Wallington, T. J.; Vereecken, L.; Peeters J. (1998) *J. Phys. Chem. A*, **102**, 8116.
- Ohta, T. (1984) *Int. J. Chem. Kinet.*, **16**, 1495.
- Orzechowska, G.; Paulson, S. E. (2002) *Atmos. Environ.*, **36**, 571.
- Pankow, J. F. (1987) *Atmos. Environ.*, **21**, 2275.
- Pankow, J. F. (1994) *Atmos. Environ.*, **28**, 189.
- Paulson, S. E.; Chung, M.; Sen, A. D.; Orzechowska, G. (1998) *J. Geophys. Res.*, **103**, 25533.
- Paulson, S. E.; Chung, M. Y.; Hasson, A. S. (1999a) *J. Phys. Chem. A*, **103**, 8125.
- Paulson, S. E.; Fenske, J. D.; Sen, A. D.; Callahan, T. W. (1999b) *J. Phys. Chem. A*, **103**, 2050.
- Pawliszyn, J. (1997) *Solid Phase Microextraction: Theory and Practice*, Wiley-VCH, Inc. 247 pp.
- Pouchert, C. J. (1975) *The Aldrich Library of Infrared Spectra*, 2nd ed.; Aldrich Chemical Co., Inc.: pp. 317-366; p. 113.
- Pouchert, C. J. (1989) *The Aldrich Library of FT-IR Spectra*, 1st ed.; Aldrich Chemical Co., Inc. **1989**, Vol. 3, pp. 605-633; pp. 309-310; pp.748-758.
- Phouongphouang, P. T.; Arey, J. (2002) *Environ. Sc. Technol.*, **36**, 1947.

- Phouongphouang, P. T.; Arey, J. (2003a) *Environ. Sci. Technol.*, **37**, 308.
- Phouongphouang, P. T.; Arey, J. (2003b) *J. Photochem. Photobiol. A: Chem.*, **157**, 301.
- Prinn, R. G.; Huang, J.; Weiss, R. F.; Cunnold, D. M.; Fraser, P. J.; Simmonds, P. G.; McCulloch, A.; Harth, C.; Salameh, P.; O'Doherty, S.; Wang, R. H. J.; Porter, L.; Miller, B. R. (2001) *Science*, **292**, 1882.
- Prinn, R. G.; Weiss, R. F.; Miller, B. R.; Huang, J.; Alyea, F. N.; Cunnold, D. M.; Fraser, P. J.; Hartley, D. E.; Simmonds, P. G. (1995) *Science*, **269**, 187.
- Reisen, F.; Aschmann, S. M.; Atkinson, R.; Arey, J. (2003) *Environ. Sci. Technol.*, **37**, 4664.
- Reisen, F.; Aschmann, S. M.; Atkinson, R.; Arey, J. (2004) unpublished data.
- Rhead, M. M.; Hardy, S. A. (2003) *Fuel*, **82**, 385.
- Rickard, A. R.; Johnson, D.; McGill, C. D.; Marston, G. (1999) *J. Phys. Chem. A*, **103**, 7656.
- Ruppert, L.; Becker, K. H. (2000) *Atmos. Environ.*, **34**, 1529.
- Sasaki, J.; Arey, J.; Harger, W. P. (1995) *Environ. Sci. Technol.*, **29**, 1324.
- Sasaki, J.; Arey, J.; Eastmond, D. A.; Parks, K. K.; Grosovsky, A. J. (1997) *Mutat. Res.*, **393**, 23.
- Sasaki, J. C.; Arey, J.; Eastmond, D. A.; Parks, K. K.; Phouongphouang, P. T.; Grosovsky, A. J. (1999) *Mutat. Res.*, **445**, 113.
- Sauer, F.; Schäfer, C.; Neeb, P.; Horie, O.; Moortgat, G. K. (1999) *Atmos. Environ.*, **33**, 229.
- Sawyer, R. F.; Harley, R. A.; Cadle, S. H.; Norbeck, J. M.; Slott, R.; Bravo, H. A. (2000) *Atmos. Environ.*, **34**, 2161.
- Scanlon, J. T.; Willis, D. E. (1985) *J. Chromat. Sci.*, **23**, 333.
- Seila, R. L.; Lonneman, W. A.; Meeks, S. A. (1989) *Determination of C₂ to C₁₂ Ambient Air Hydrocarbons in 39 U.S. Cities, from 1984 through 1986*, U.S. Environmental Protection Agency Report EPA/600/3-89/058, Research Triangle Park, NC, September.
- Siese, M.; Becker, K. H.; Brockmann, K. J.; Geiger, H.; Hofzumahaus, A.; Holland, F.; Mihelcic, D.; Wirtz, K. (2001) *Environ. Sci. Technol.*, **35**, 4660.
- Smith, B. J.; Hall, N. E. (1997) *Chem. Phys. Lett.*, **279**, 165.
- Smith, D. F.; Kleindienst, T. E.; McIver, C. D. (1999) *J. Atmos. Chem.*, **34**, 339.

Streitwieser, A., Jr.; Heathcock, C. H. (1976) *Introduction to Organic Chemistry*, Macmillan, New York, NY, p. 679.

Stephens, E. R. (1964) *Anal. Chem.*, **36**, 928.

Tancell, P. J.; Rhead, M. M.; Pemberton, R. D.; Braven, J. (1995). *Environ. Sci. Technol.*, **29**, 2871.

Taylor, W. D.; Allston, T. D.; Moscato, M. J.; Fazekas, G. B.; Kozlowski, R.; Takacs, G. A. (1980) *Int. J. Chem. Kinet.*, **12**, 231.

Tobias, H. J.; Ziemann, P. J. (2001) *J. Phys. Chem. A*, **105**, 6129.

Tsang, W. (1986) *J. Phys. Chem.*, **90**, 1152.

Tuazon, E. C.; Atkinson, R. (1990) *Int. J. Chem. Kinet.*, **22**, 1221.

Tuazon, E. C.; Aschmann, S. M.; Arey, J.; Atkinson, R. (1998) *Environ. Sci. Technol.*, **32**, 2106.

Tuazon, E. C.; Aschmann, S. M.; Atkinson, R. (1999) *Environ. Sci. Technol.* **33**, 2885.

Tuazon, E. C.; Aschmann, S. M.; Atkinson, R.; Carter, W. P. L. (1998) *J. Phys. Chem. A*, **102**, 2316.

Tully, F. P.; Ravishankara, A. R.; Thompson, R. L.; Nicovich, J. M.; Shah, R. C.; Kreutter, N. M.; Wine, P. H. (1981) *J. Phys. Chem.*, **85**, 2262.

Tully, F. P.; Goldsmith, J. E. M.; Droege, A. T. (1986) *J. Phys. Chem.*, **90**, 5932.

Vaghjiani, G. L.; Ravishankara, A. R. (1989) *J. Phys. Chem.*, **93**, 1948.

Vereecken, L., J. Peeters, J. J. Orlando, G. S. Tyndall, and C. Ferronato (1999). *J. Phys. Chem. A*, **103**, 4693.

Wallington, T. J.; Dagaut, P.; Liu, R.; Kurylo, M. J. (1988) *Int. J. Chem. Kinet.*, **20**, 541.

Wiedemann, A.; Zetzsch, C. (1982) Presented at Bunsentagung, Ulm and Neu-Ulm, Germany, May 20-22; cited in Atkinson (1989).

Williams, P. T.; Bartle, K. D.; Andrews, G. E. (1986) *Fuel*, **65**, 1150.

Wine, P. H.; Astalos, R. J.; Mauldin, R. L., III (1985) *J. Phys. Chem.*, **89**, 2620.

Winterhalter, R.; Neeb, P.; Grossmann, D.; Kolloff, A.; Horie, O.; Moortgat, G. (2000) *J. Atmos. Chem.*, **35**, 165.

- Yokouchi, Y.; Ambe, Y. (1985) *Atmos. Environ.*, **19**, 1271.
- Yu, J.; Jeffries, H. E.; Le Lacheur, R. M. (1995) *Environ. Sci. Technol.*, **29**, 1923.
- Zhang, D.; Zhang, R. (2002) *J. Am. Chem. Soc.*, **124**, 2692.
- Zielinska, B.; Arey, J.; Atkinson, R.; McElroy, P. A. (1989) *Environ. Sci. Technol.*, **23**, 723.
- Zielinska, B.; Sagebiel, J. C.; Harshfield, G.; Gertler, A. W.; Pierson, W. R. (1996) *Atmos. Environ.*, **30**, 2269.
- Ziemann, P. J. (2002) *J. Phys. Chem. A*, **106**, 4390.

8. GLOSSARY

API-MS	Atmospheric pressure ionization mass spectrometry
API-MS/MS	Atmospheric pressure ionization tandem mass spectrometry
DMN	Dimethylnaphthalene
EN	Ethyl naphthalene
F	Multiplicative factor to take into account secondary reactions
FT-IR	Fourier transform infrared
GC-FID	Gas chromatography with flame ionization detection
GC-MS	Combined gas chromatography-mass spectrometry
HO ₂	Hydroperoxyl radical
IR	Infrared
MN	Methylnaphthalene
NCI	Negative chemical ionization
NO	Nitric oxide
NO ₂	Nitrogen dioxide
NO ₃	Nitrate radical
OH	Hydroxyl radical
O ₃	Ozone
PAH	Polycyclic aromatic hydrocarbon
P _L	Liquid phase vapor pressure
R [•]	Alkyl or substituted alkyl radical
RO [•]	Alkoxy radical
ROO [•] or RO ₂ [•]	Alkyl peroxy radical

SIM	Single ion monitoring
SPME	Solid phase micro extraction
VOC	Volatile organic compound

9. PUBLICATIONS ARISING WHOLLY OR IN PART FROM SUPPORT FROM THIS CONTRACT

Reactions of Stabilized Criegee Intermediates formed from the Gas-Phase Reactions of O₃ with Selected Alkenes.

Int. J. Chem. Kinet., **34**, 73-85 (2002).

J. Baker, S. M. Aschmann, J. Arey and R. Atkinson

Products and Mechanism of the Reactions of OH Radicals with 2,2,4-Trimethylpentane in the Presence of NO.

Environ. Sci. Technol., **36**, 625-632 (2002).

S. M. Aschmann, J. Arey and R. Atkinson

Formation and Atmospheric Reactions of 4,5-Dihydro-2-methylfuran.

J. Phys. Chem. A, **106**, 11492-11501 (2002).

P. Martin, E. C. Tuazon, S. M. Aschmann, J. Arey and R. Atkinson

Products of the Gas-Phase Reaction of O₃ with Cyclohexene.

J. Phys. Chem. A, **107**, 2247-2255 (2003).

S. M. Aschmann, E. C. Tuazon, J. Arey and R. Atkinson

Kinetics and Products of the Reactions of OH Radicals with 2-Methyl-2-pentanol and 4-Methyl-2-pentanol.

J. Photochem. Photobiol. A: Chem., **157**, 257-267 (2003).

H. L. Bethel, R. Atkinson and J. Arey

Kinetics and Products of the Gas-Phase Reaction of OH Radicals with 5-Hydroxy-2-pentanone at 296 ± 2 K.

J. Atmos. Chem., **45**, 289-299 (2003).

S. M. Aschmann, J. Arey and R. Atkinson

H-Atom Abstraction from C-H Bonds in 2,3-Dimethylpentanal, 1,4-Cyclohexadiene, and 1,3,5-Cycloheptatriene.

Int. J. Chem. Kinet., **35**, 415-426 (2003).

E. C. Tuazon, S. M. Aschmann, M. V. Nguyen and R. Atkinson

Hydroxycarbonyl Products of the Reactions of Selected Diols with the OH Radical.

J. Phys. Chem. A, **107**, 6200-6205 (2003).

H. L. Bethel, R. Atkinson and J. Arey

Methyl- and Dimethyl-/Ethyl-Nitronaphthalenes Measured in Ambient Air in Southern California.

Atmos. Environ., **37**, 3653-3657

F. Reisen, S. Wheeler and J. Arey

Products and Mechanism of the Reaction of OH Radicals with 2,3,4-Trimethylpentane in the Presence of NO.

Environ. Sci. Technol., submitted for publication,
S. M. Aschmann, J. Arey and R. Atkinson

OH Radical and Carbonyl Formation from Reaction of O₃ with Alkenes: Effects of Water Vapor and 2-Butanol.

Int. J. Chem. Kinet., to be submitted for publication
S. M. Aschmann, J. Arey and R. Atkinson